TITRIMETRIC STUDIES OF THE ION EXCHANGE AND SORPTION PROPERTIES OF INORGANIC ION EXCHANGERS

Thesis submitted to the University of Glasgow

for the degree of Ph.D.

by

STEPHEN GALLAGHER

FACULTY OF SCIENCE

CHEMISTRY DEPARTMENT

August 1992

TABLE OF CONTENTS

Acknowledgements

Declaration

Summary

Chapter 1 General Introduction

References

Chapter 2 Fundamentals of Ion Exchange and Sorption Processes

2.1 Donnan Equilibria

2.2 Ion Exchange Equilibria and Ion Selectivity

2.3 Summary

References

Chapter 3 Automated Multi-Electrode Titration System

Introduction

3.1 Ion Selective Electrodes

3.2 Titration Theory

3.3 Automatic Calibration System

3.4 Automated Calibration of Ion Selective Electrodes

3.5 Performance of Automated Multi-Electrode Potentiometric Titrations

3.6 Processing of Data

3.7 Control Experiments

References

Chapter 4 The Suspension Potential

Introduction

4.1 Origin of the Suspension Potential

4.2 Factors Influencing the Suspension Potential

CONTENTS (contd.)

4.3	Results and Discussion
4.3.1	Method of Correction for the Suspension Potential
4.3.2	Application of Suspension Potential Corrections to Potentiometric Titration Data
4.3.3	Re-analysis of Previously Published Potentiometric Titration Data
	References
Chapter 5	Ion Exchange Properties of Aluminosilicate Materials
	Introduction
5.1	Aluminosilicates as Ion exchangers
5.2	Caesium Ion Selective Electrode
5.3	Sample Preparation
5.4	Procedure for the Study of the Ion Exchange Properties of Alumino-silicate Materials by Potentiometric Titration
5.5	Results and Discussion
5.5.1	Ion Exchange Characteristics of Clay Minerals
5.5.2	Ion Exchange Characteristics of Urban Building Materials
5.6	Conclusions
	References
Chapter 6	Ion Exchange Characteristics of Inorganic Oxides
	(I) Indifferent Electrolyte Sorption
	Introduction
6.1	Mechanisms of Ion Exchange on Inorganic Oxides
6.2	Preparation of Oxides
6.3	Results and Discussion
6.3.1	Ion exchange properties of monoclinic zirconia

6.3.2	Ion exchange properties of silica
6.3.3	Ion exchange properties of γ alumina
6.3.4	Ion exchange properties of titania
6.3.5	Ion exchange properties of α alumina
6.3.6	Ion exchange properties of NASICON
6.3.7	Prediction of Surface Charge of Active Layer Oxides
6.4	Conclusions
	References
Chapter 7	Ion Exchange Characteristics of Inorganic Oxides
	(II) Specific Sorption
	Introduction
7.1	Specifically Sorbed Ions
7.2	Modifications to Uptake Calculations
7.3	Results and Discussion
7.3.1	Calcium Ion Sorption
7.3.2	Sulphate Ion Sorption
7.3.3	Phosphate Ion Sorption
7.3.4	Fluoride Ion Sorption
7.4	Conclusions
	References
Chapter 8	General Conclusions
List of Symbols	
Published papers	

This thesis is dedicated to the memory

of my father, Charles Gallagher.

ACKNOWLEDGEMENTS

I wish to express my gratitude to Dr. Russell Paterson for the guidance, thought-provoking discussion and sustained creative enthusiasm he has provided throughout the course of this research. I am also indebted to my colleagues in the Colloid and Membrane Research Group at Glasgow University for their help and support. Thanks also go to the researchers at E.N.S.C. Montpellier who worked with the Glasgow Group on the ceramic membranes Jumelage research project.

I acknowledge the financial support provided by the Commission of European Communities (Contract No. B16-0270.UK(H)) and by the Science and Engineering Research Council (Contract No. GR/F 64296).

DECLARATION

The research presented in Chapter 5 of this thesis was published in 1991 in a Commission of the European Communities Report EUR 12555 EN pp. 105-142 and in Reactive Polymers Volume 16 pp. 105-114. These publications were made jointly with Dr. Russell Paterson.

The research presented in Chapters 6 and 7 was published in the Proceedings from the 2nd International Conference on Inorganic Membranes (ICIM91) pp. 99-104 and in Ion Exchange Advances: Proceedings of IEX92 pp. 318-325. These publications were made jointly with Dr. Russell Paterson, Prof. Louis Cot, Prof. Andre Larbot and Jocelyn Etienne.

SUMMARY

Research has been performed on the ion exchange and sorption processes which occur on the surfaces and within the pores of inorganic ion exchangers. Exchangers of the aluminosilicate type and inorganic oxide ion exchangers were studied.

Multi-electrode potentiometric titrations of colloidal dispersions of ion exchangers in aqueous media were performed. A computer controlled automated titration system was developed and used in this work, enabling the simultaneous monitoring by ion selective electrodes of the activities of up to four ion species. Up to six titrants could be used in any titration. After activity corrections, solution concentrations of the monitored ions were obtained and the uptake or release by the exchanger of these ions calculated by mass balance. The enhanced precision of the automated titration method enabled exchange capacities of less than 0.1 meq/g to be resolved with confidence.

By performing multi-electrode potentiometric titrations it was shown that suspension potentials may be detected. A method by which suspension potentials could be corrected for was devised and used in this research. Corroborative results were obtained from electrophoretic measurements.

The ion exchange characteristics of a wide range of ion exchangers of the aluminosilicate type (clay minerals, urban building materials) were studied using the potentiometric titration methods. The aim of this work was to identify the urban surfaces which selectively adsorb radiocaesium and to determine the mechanisms of sorption, the total caesium binding capacity and its ease of displacement on these surfaces. An electrode sensitive to caesium ion was developed and tested. Near ideal response was observed in the range 10^{-1} to 10^{-5}M in aqueous caesium ion. The electrode showed good selectivity for caesium over other cations, with the exception of potassium ion. Accordingly this electrode was used

for the titration of samples from which potassium ion had previously been extracted. The caesium ion binding capacities of clay minerals and urban surfaces were characterised using the automated titration method. The mechanism of Cs^+ sorption was shown to be ion exchange with those counterions present in the natural material. The relative selectivities of the exchange sites on clay minerals and building materials were generally $Cs^+ > K^+ > Na^+$, with the magnitude of selectivity varying according to the nature of the material. Cation exchange capacity on a typical clay rooftile was shown to be directly proportional to the total surface area of the tile, enabling the determination of the caesium binding capacity per unit of superficial tile surface.

The ion exchange and sorptive properties of the oxide active layer of ceramic membranes were determined. The ceramic oxides studied were ZrO_2, TiO_2, SiO_2 and γAl_2O_3. Additionally, titrations of dispersions of the three-dimensional cation exchanger NASICON were performed. pH and salt concentration effects were evaluated. The mechanisms of ion exchange were consistent with those of non-calcined oxides such as ZrO_2 and βFeOOH. Anion exchange was shown to be a function of the activity of total acid pA and cation exchange a function of the activity of total base pB. The ion exchange capacity of calcined zirconia was considerably lower than that of its non-calcined analogue. Good agreement was observed when the capacities of each zirconia sample were expressed per unit area.

Ion exchange properties were determined in the presence of a range of ions to which the ceramic membrane may be routinely exposed. Specific sorption of multivalent ions calcium, sulphate and phosphate were observed in titrations of zirconia dispersions in the presence of these ions. Fluoride ions also were specifically adsorbed. A degree of irreversibility was observed in the sorption of sulphate, phosphate and fluoride.

CHAPTER 1

GENERAL INTRODUCTION

Introduction

The research presented in this thesis is concerned primarily with the investigation of the ion exchange and sorption processes which occur on the surfaces of inorganic ion exchangers. The exchangers which were studied fall into two broad categories - fixed charge aluminosilicate ion exchangers (including clay minerals, man-made ceramic urban surfaces and "natural" construction materials) and variable charge inorganic oxides (zirconia, γ alumina, α alumina, silica, titania). Additionally, the ion exchange properties of the three-dimensional cation exchanger, NASICON (Na^+ Super-Ionic Conductor), were examined.

The research on the ion exchange and sorption properties of clay minerals and urban surfaces was funded by the Commission of European Communities as part of a Post-Chernobyl Initiative on the Improvement of Practical Countermeasures Against Nuclear Contamination in the Urban Environment (Contract No. B16-0270.UK(H)).

Studies on the ion exchange characteristics of inorganic oxides were performed as part of two research projects on the fundamentals of ceramic membrane design and performance - a European Community funded joint project (Jumelage) between Ecole Nationale Supérieure de Chimie de Montpellier, Université des Sciences et Techniques du Languedoc and University of Glasgow (Contract No. SC 1 0178-C(EDB)) and a S.E.R.C. funded research project on fouling of ceramic membranes by charged substrates, Contract No. GR/F 64296.

In order to place the presented research in its context, there follows an overview of the aims and objectives of each of these research projects. It is shown in this thesis that these

seemingly diverse research areas are linked by the commonality of the underlying principles which determine the ion exchange and sorptive properties of all the materials investigated.

Background to Research on Ion Exchange Properties of Clay Minerals and Building Materials

In the aftermath of a nuclear accident, the radioactive product which presents the greatest medium and long-term threat to a contaminated urban environment is ^{137}Cs [1,2]. This was confirmed after the Chernobyl accident, when it was found that the most important isotope in terms of its contribution to the total population radiation dose was ^{137}Cs [3]. Consequently, research on the improvement of countermeasures against urban contamination concentrated exclusively on this isotope. Early studies on Chernobyl deposition showed that many urban surfaces, such as rooftiles and concretes, had considerable potential for intercepting and retaining radiocaesium [4,5]. For a realistic assessment of countermeasures against radiocaesium sorption, it was necessary to determine both the total caesium binding capacity and its ease of displacement on a representative range of exposed urban surfaces. It was also necessary to determine the mechanism of sorption and, should it be ion exchange (as was shown in this work), to identify the sites, determine the selectivity coefficients for Cs^+ over naturally occurring counterions (for example, Na^+, K^+) and the ease of displacement of sorbed Cs^+. Therefore a major aim of this research project was to determine the ion exchange and ion sorption properties, with particular reference to caesium ion sorption, of a wide range of construction materials taken from sites throughout the U.K. and Western Europe. Since clays minerals are almost ubiquitously present in urban building materials (even after firing) and since they are well-known as ion exchangers, the research was extended to

assess the caesium ion sorption properties of clay minerals.

Background to Ceramic Membrane Research

Inorganic (ceramic) membranes have numerous advantages over organic counterparts in separation processes. These include resistance to compaction under high pressure, chemical stability at high temperatures (including steam sterilisation procedures), insensitivity to bacterial action and a long operational life.

In the manufacture of ceramic membranes for applications in ultrafiltration (UF) and reverse osmosis (RO), the sol-gel process provides the only generally applicable technique for producing thin ceramic active layers of controlled porosity on a wide range of macroporous substrates [6,7]. The active layer of operational ceramic membranes consists of inorganic oxide particles, typically 3-10μm thick in a commercial membrane.

While it has been known for some time [8] that firing (calcining) results in the loss of much of the ion exchange capacity of inorganic oxides, these "ceramic membrane" oxides (as was shown in this research) still retain some ion exchange characteristics, albeit at reduced capacities relative to unfired oxides. Most oxides are amphoteric and surface and pore charges may be altered and even reversed as the pH of the solution is changed from acidic to alkaline.

The surface charge and ion sorptive properties of the oxides which form the active layers of ceramic membranes have extremely important implications in the design and the efficient use of ceramic membranes. These properties are major contributory factors to membrane fouling by polar or ionic substrates, since surface sorption is often the first

step in fouling leading to pore blocking within the membrane structure. By altering the surface charge density and/or changing its polarity, the opportunity exists for minimising fouling and optimising separation processes.

The importance of these parameters is paramount to the operation of reverse osmosis membranes, in which surface charge plays a dominant role in determining the degree of salt rejection through the Donnan potential.

Consequently, a fundamental understanding of the surface charge and sorptive properties within the pores of the active layers of ceramic membranes is essential to their efficient use. The major aim of this research was to achieve this detailed knowledge of the ion exchange properties of the calcined inorganic oxides which form the active layers of ceramic membranes. This research continued and expanded the work performed in this laboratory on the ion exchange properties of the (non-calcined) inorganic oxide precursors of ceramic membrane materials [9-14].

Commonality of Research Projects

The major research technique employed in this research was applicable to all ion exchangers studied. In all cases, ion exchange processes were studied using a new, fully automated multi-electrode titration system. Supportive research techniques included electrophoretic studies, performed using a Doppler Electrophoretic Light Scattering Analyzer (DELSA).

Fundamental to both these research projects were the principles of ion exchange. This thesis presents the research performed on the ion exchange and ion sorption properties of inorganic ion exchangers - a topic common and central to both research programmes. In the interests of completeness, brief discussions on the "wider picture" - the practical

applications of the current research - will be made at relevant points in the text. However, the central theme of the thesis and the commonality between the two research projects should be evident. There follows a discussion on the underlying theories of ion exchange.

References

[1] G.N. Kelly, Radiation Protection Dosimetry, **21**, No.1-3, 13 (1987)

[2] J.R. Simmonds, S.M. Haywood and G.S. Linsley, Accidental release of radionuclides: a preliminary study of the consequences of land contamination, NRPB-R133, ISBN O 85951 176 6 (1982)

[3] IAEA Safety Series No. 75-INSAG-1, Summary report of the post-accident review meeting on the Chernobyl accident, ISBN 92-0-123186-5

[4] J. Roed, Radiation Protection Dosimetry, **21**, No.1-3, 59 (1987)

[5] F.J. Sandalls, Radiation Protection Dosimetry, **21**, No.1-3, 65 (1987)

[6] L. Cot, Proc. 1st International Conference on Inorganic Membranes, Montpellier, 17 (1989)

[7] A. Larbot, A. Julbe, J. Randon, C. Guizard, L. Cot, Proc. 1st International Conference on Inorganic Membranes, Montpellier, 31 (1989)

[8] K.A. Kraus, H.O. Phillips, T.A. Carlson and J.S. Johnson, Proc. 2nd International Conference on Peaceful Uses of Atomic Energy, **28**, 3 (1958)

[9] R. Paterson, H. Rahman, J. Coll. Int. Sci., **94**, 60 (1983)

[10] R. Paterson, H. Rahman, J. Coll. Int. Sci., **97**, 423 (1984)

[11] R. Paterson, H. Rahman, J. Coll. Int. Sci., **98**, 494 (1985)

[12] R. Paterson, H. Rahman, J. Coll. Int. Sci., **103**, 106 (1985)

[13] R. Paterson, A. Smith, J. Coll. Int. Sci., **124**, 581 (1988)

[14] R. Paterson, Proc. 1st International Conference on Inorganic Membranes, Montpellier, 127 (1989)

CHAPTER 2

FUNDAMENTALS OF ION EXCHANGE AND SORPTION PROCESSES

Introduction

Ion exchangers are insoluble materials which carry a fixed charge on their surfaces or within their pores. The surplus charge is compensated by counterions of the opposite sign - these ions are free to move within the exchanger and may be replaced by a stoichiometrically equivalent amount of ions of the same sign when the exchanger is in contact with an electrolyte solution. Those which carry a net negative charge are cation exchangers, whilst those bearing a net positive charge are anion exchangers. Certain materials, notably many inorganic oxides, have amphoteric properties, behaving as either cation exchangers or anion exchangers depending on the composition of the solution with which it is in contact.

The exchange process between two monovalent cations may represented by eqn. 2.1, whilst monovalent anion exchange is given by eqn. 2.2. Barred species refer to the solid phase, with M representing a structural unit associated with a single fixed charge of the ion exchanger. These expressions are normally an adequate description of the ion exchange process because co-ions (ions bearing the same charge as the exchanger phase) are efficiently excluded (by Donnan exclusion) from an ion exchanger in dilute electrolyte solution. The exchangeable ions (cations in eqn 2.1, anions in eqn. 2.2) are the counterions, whilst the non-participating ions bearing the same charge as the exchanger are co-ions.

$$\overline{M^-A^+}_{(s)} + B^+X^-_{(aq.)} \rightleftharpoons \overline{M^-B^+}_{(s)} + A^+X^-_{(aq.)} \qquad \textbf{(2.1)}$$

$$\overline{M^+X^-}_{(s)} + A^+Y^-_{(aq.)} \rightleftharpoons \overline{M^+Y^-}_{(s)} + A^+X^-_{(aq.)} \qquad \textbf{(2.2)}$$

The general equation for stoichiometric ion exchange reactions between any two ions A^{z_A} and B^{z_B} is given by eqn. 2.3. Co-ions and the structural units of the exchanger have been omitted from this equation.

$$\overline{z_B A^{z_A}} + z_A B^{z_B} \rightleftharpoons \overline{z_A B^{z_B}} + z_B A^{z_A} \qquad (2.3)$$

Electroneutrality in each phase is preserved, so counterions can leave the exchanger only if they are replaced by ions of equivalent charge. The counterion content within the exchanger is termed the ion exchange capacity and is usually expressed as milliequivalents of exchangeable ions per gramme of exchanger. Ion exchangers of the layered alumino-silicate type generally have a constant charge between the layers and on the surface, hence the exchange capacities have a constant value. In contrast, the pore charges and surface charges of inorganic oxides vary as a function of pH and electrolyte concentration, so the exchange capacities vary and can change sign in cases where the material is amphoteric. The mechanisms of ion exchange on these classes of ion exchanger will be discussed in detail in Chapters 5 and 6 respectively.

2.1 Donnan Equilibria

An ion exchanger corresponds to the equivalent of an electrolyte solution in which either the cations or the anions are fixed to a matrix. When such a material is placed in water or in a solution of dilute electrolyte, the ion concentration in the exchanger phase is considerably greater than in the solution phase - for a typical commercial ion exchanger the internal molarity is 3-4M. Under normal circumstances an electrolyte would be free to diffuse throughout the medium but because one of the charged species is fixed on the solid only the counterions are free to diffuse. Diffusion of counterions from the exchanger

to the solution causes charge separation, resulting in the build up of an electrical potential difference (the Donnan Potential) between the two phases. This potential acts to attract counterions back into the ion exchanger and to repel co-ions from the exchanger. The state of equilibrium which is established is a Donnan equilibrium in which the activity gradient between the solid and the liquid phases is balanced by an electrical gradient.

An expression for the Donnan Potential can be obtained from consideration of the electrochemical potential of ion i in the solid phase ($\bar{\tilde{\mu}}_i$) and in the solution phase ($\tilde{\mu}_i$). These are defined in eqns. 2.4. a, b

$$\tilde{\mu}_i = \mu_i^o + RT \ln a_i + z_i F \Psi \qquad (a)$$

$$\bar{\tilde{\mu}}_i = \overline{\mu_i^o} + RT \ln \overline{a_i} + z_i F \overline{\Psi} \qquad (b) \qquad \textbf{(2.4)}$$

where μ_i^o is the chemical potential of ion i in the standard state, z_i is its charge (including sign), F the Faraday constant, Ψ the electrical potential of the phase, R the gas constant, T the temperature and a_i the activity of ion i. Barred species refer to the solid phase.

At equilibrium, the electrochemical potential of ion i is the same in both phases -

$$\bar{\tilde{\mu}}_i = \tilde{\mu}_i \qquad \textbf{(2.5)}$$

Substituting eqns. 2.3 and 2.4 into eqn. 2.5 gives the equilibrium condition -

$$\overline{\mu_i^o} + RT \ln \overline{a_i} + z_i F \overline{\Psi} = \mu_i^o + RT \ln a_i + z_i F \Psi \qquad \textbf{(2.6)}$$

The choice of standard states for each phase is arbitrary. For the solution phase, the standard state is normally defined as a (hypothetical) ideal solution of ion i of unit molarity, at a pressure of 1 atmosphere. All deviations from ideality in the expression of the chemical potential are therefore incorporated in the activity coefficient.

Various choices of standard state for the solid phase have been made by different authors, [1-3]. Some workers chose to incorporate a pressure-volume term [4,5], while others defined the standard state as the homoionic form of the ion exchange material [6]. If these definitions are made the standard states of the solid and solution phases are not equal. In the research presented in this thesis the standard state of the solid phase was defined in the same way as the standard state of the solution phase, giving a common standard state for both phases. By making this choice, the standard states of both phases are equal. (By this definition of the standard state, the activity coefficient for ion i in the solid phase contains not only the coulombic interactions of the ion with its environment but also any pressure-volume terms or complexing terms which may occur within the solid phase.)

Using these definitions, rearrangement of eqn 2.6 gives an expression for the electrical potential difference (the Donnan Potential, E_{DON}) between the two phases -

$$(\overline{\Psi} - \Psi) = -\frac{RT}{z_i F} \ln(\overline{a_i} / a_i) = E_{DON} \qquad (2.7)$$

2.2 Ion Exchange Equilibria and Ion Selectivity

The thermodynamic equilibrium constant K_T for the ion exchange reaction in eqn. 2.3 involving ions A and B, is given by eqn. 2.8. Due to the choice of the same standard states for both phases, this equilibrium constant is defined as unity.

$$K_T = \frac{a_B^{\overline{|z_A|}} \cdot a_A^{|z_B|}}{a_A^{\overline{|z_B|}} \cdot a_B^{|z_A|}} \qquad (2.8)$$

$$= 1$$

The activity a_i of an ion i is related to the ion concentration c_i by introduction of the activity coefficient γ_i

$$a_i = c_i \gamma_i \qquad (2.9)$$

Substitution of eqn. 2.9 (for each ion in each phase) into eqn. 2.8 gives

$$K_T = \frac{c_B^{\overline{|z_A|}} c_A^{|z_B|} \; \gamma_B^{\overline{|z_A|}} \gamma_A^{|z_B|}}{c_A^{\overline{|z_B|}} c_B^{|z_A|} \; \gamma_A^{\overline{|z_B|}} \gamma_B^{|z_A|}} \qquad (2.10)$$

In practical applications considerable use is made of the concentration terms from eqn. 2.10. This parameter - the selectivity coefficient K_A^B - measures the preference shown by the exchanger for ion B over ion A. If K_A^B is greater than unity, the exchanger shows a greater preference for ion B. When K_A^B is equal to unity, the exchanger shows no preference for one or other of the ions. The molar selectivity coefficient is defined by eqn. 2.11. Concentration scales of molality or equivalent ionic fraction may be used analogously, giving the molal and the rational selectivity coefficients respectively. For counterions of equal valence, the numerical values of the molar, the molal and the rational selectivity coefficients are equivalent. In this research, selectivity coefficients were calculated for monovalent exchange processes only.

$$K_A^B = \frac{c_B^{\overline{|z_A|}} c_A^{|z_B|}}{c_A^{\overline{|z_B|}} c_B^{|z_A|}} \qquad (2.11)$$

Since the equilibrium constant is defined as unity, the magnitude of the selectivity coefficient is equal to the reciprocal of the activity term in eqn. 2.10. This term may change at different fractional loadings, so the selectivity coefficient is not constant over the whole exchange isotherm.

In some applications, equilibrium is most conveniently expressed in terms of distribution coefficients of the counterions. This is defined as the ratio of the concentrations of the counterion in the exchanger and in the solution. The distribution coefficient is commonly used when the ion species is a trace component.

2.3 Summary

The principles presented in this Chapter are generally applicable to all of the exchange processes studied in this research. The following Chapter presents a methodology, based on multi-electrode potentiometric titration of colloidal dispersions of ion exchangers, by which detailed study of these reactions may be made. The commonality of the discussed principles enabled the method to be applied to practically any class of ion exchanger.

References

[1] L.W. Holm, Arkiv Kemi, **10**, 151 (1956)
[2] L.W. Holm, Arkiv Kemi, **10**, 445 (1956)
[3] L.W. Holm, Arkiv Kemi, **10**, 461 (1956)
[4] H.P. Gregor, J. Am. Chem. Soc., **70**, 1293 (1948)
[5] H.P. Gregor, J. Am. Chem. Soc., **73**, 642 (1951)
[6] G.L. Gaines and H.C. Thomas, J. Chem. Phys., **21**, 714 (1953)

CHAPTER 3

AUTOMATED MULTI-ELECTRODE TITRATION SYSTEM

Introduction

The theories and methods for the determination of ion exchange capacities from potentiometric titrations were originally established for single (pH) electrode studies of the ion exchange properties of some insoluble crystalline inorganic oxide-hydroxides (β FeOOH, α FeOOH and monoclinic zirconia) [1-5]. The research presented in this thesis is a further development from the techniques and methods of these earlier studies.

A major advancement in the methodology was the development of a computer controlled, automated multi-electrode titration system. With this system, it was possible to monitor simultaneously the ion concentrations (and therefore the ion uptake and/or release) of up to four ion species. These multi-electrode titrations provided support and confirmation for the results obtained from single electrode titrations. Furthermore, using several ion selective electrodes it was possible in a single experiment to measure and correct for suspension potentials (Chapter 4) - this cannot be done from single ion selective electrode titrations. Multi-ion selective electrode titration techniques may be applied to any ion exchange system - for example, the study of Cs^+/Na^+ exchange processes on aluminosilicates, as presented in Chapter 5. Another major advantage of the automated titration system was the precise control of electrode stability. The criteria for electrode stability were defined by the user before performing a titration. Using this system, exchange capacities an order of magnitude less than those of the previously studied exchangers could be measured with precision.

3.1 Ion Selective Electrodes

Ion Selective Electrodes (ISEs) are intrinsically thermodynamic devices, responding to activity changes in their selected ion. The electrode potential (E) of an ISE is given by the Nernst Equation, eqn. 3.1.

$$E = E^{\circ} + \frac{RT}{z_i F} \ln a_i \tag{3.1}$$

where E° is the reference potential, a_i is the specific ion activity and z_i its ionic valency, including sign.

The mean activity coefficient $\gamma_{\pm}$ for an electrolyte in aqueous solution at 25°C is given by the Davies equation, (an extended Debye-Hückel equation) eqn. 3.2 [6].

$$-\log \gamma_{\pm} = 0.5 \mid z_+ \mid\mid z_- \mid \left(\frac{\sqrt{I}}{(\sqrt{I}+1)} - 0.3I \right) \tag{3.2}$$

where I is the ionic strength of the solution, defined by

$$I = 0.5 \sum_i c_i z_i^2 \tag{3.3}$$

with c_i the solution concentration of ion i. The Davies equation is valid in media with ionic strength less than 0.2M.

Activity coefficients for single ions γ_i (not separately determinable experimentally) were calculated empirically by

$$-\log\gamma_i = 0.5z_i^2\left(\frac{\sqrt{I}}{(\sqrt{I}+1)}-0.3I\right) \quad \textbf{(3.4)}$$

Ion concentrations c_i in solution were then calculated from

$$a_i = \gamma_i c_i \quad \textbf{(3.5)}$$

Many ISEs obey the Nernst equation closely over a useful range of conditions but all are subject to errors caused by interfering ions or to specific limitations related to their functional chemistry. These limitations are well-documented and understood. Commercial ISEs for Ca^{2+}, Cl^-, K^+, Na^+ and F^- (Orion Research ™ Inc., Boston, USA., Model Nos. 100049, 94-17B, 93-19, 97-11-00, 94-09) and H^+ (Russell Electrodes ™, Auchtermuchty, Scotland) were used in this research. Additionally, an electrode responsive to caesium ion was developed, tested and used in this research (Chapter 5). The lower operational ranges for these electrodes were typically at or close to 10^{-5} M for the selected ion. The exception was the H^+ glass electrode which is viable in the pH range 1-12. For all ion selective electrodes used in this work, the linearity of the Nernst response was good and the theoretical slope of 59.16 mV at 25°C (59.16/2 mV for Ca^{2+}) was achieved to within 95%. At very low concentrations the slopes deviated increasingly and the electrodes were subject to considerable error, determining the lower limits of their use.

3.2 Titration Theory

The method of calculation of ion exchange capacities from potentiometric titrations have been presented previously in papers on the study of the ion exchange properties of β FeOOH and of zirconia [1-5]. The calculations used in this current study were essentially the same as those employed earlier, with some refinements. Firstly, since all ionic species were

monitored by ion selective electrode, it was possible to detect directly the uptake of any ion by the ion exchanger. Secondly, by performing multi-electrode titrations, suspension potential effects can be detected and the titration results corrected for any errors resulting from the occurrence of these effects (Chapter 4). The methods for calculating ion exchange capacity are presented here for the specimen case of the titration of an ion exchanger with acid (HCl), base (NaOH) and salt (NaCl), with the use of electrodes sensitive to H^+, Na^+ and Cl^- ions.

Consider an equilibration of G grammes of ion exchanger in V_o ml distilled water at 25°C. Additions of A, B or S milliequivalents (meq) of acid, base or salt respectively were made using V_a, V_b or V_s ml of the respective titrant. It was assumed that solution volumes were additive, so that the total volume of solution, V, was given by

$$V = V_o + V_a + V_b + V_s \qquad \textbf{(3.6)}$$

Ion activities of all ions in solution (H^+, OH^-, Na^+, Cl^-) were measured directly by the respective ion selective electrodes. The solution concentration of each ion was calculated in the following manner. In the first approximation, activity coefficients were set to unity and concentrations of each ion were estimated in order to obtain a first approximation of ionic strength using eqn. 3.3. This value of ionic strength was used in the calculation of activity coefficients (eqn. 3.4), which were in turn used to give improved estimates of ion concentration using eqn. 3.5. These improved estimates modified the ionic strength. The cycle was repeated until changes in the calculated concentrations were negligible.

Ion uptakes for each ion (in milliequivalents per gramme of exchanger (meq/g)) were calculated from the discrepancy between the amount of ion added to the initial system and the amount measured in the solution phase. For the above equilibration, ion uptakes for each ion (Na_{UPT}, Cl_{UPT} and H_{UPT}) were given by

$$Na^{+}_{UPT} = \frac{[Na^{+}]_o V_o + B + S - [Na^{+}]V}{G} \tag{3.7}$$

$$Cl^{-}_{UPT} = \frac{[Cl^{-}]_o V_o + A + S - [Cl^{-}]V}{G} \tag{3.8}$$

$$H^{+}_{UPT} = \frac{[H^{+}]_o V_o - [OH^{-}]_o V_o + A - B - ([H^{+}]V - [OH^{-}]V)}{G} \tag{3.9}$$

where $[Na^{+}]_o$, $[Cl^{-}]_o$, $[H^{+}]_o$ and $[OH^{-}]_o$ are initial solution concentrations of these ions.

It should be noted at this point that throughout this thesis, the term *uptake* refers to the values as calculated from the above equations. Uptakes are therefore expressed relative to the initial condition. Positive uptake means that the ion is being taken up by the exchanger, while negative uptake means that the ion is being released by the exchanger.

The term *ion exchange capacity*, as used in this thesis, refers (unless otherwise stated) to the absolute ion exchange capacity. Anion exchange capacity is expressed as negative capacity (positive uptake of anion) and cation exchange capacity as positive capacity.

The above theory was central to the titration data processing routines used in the automated titration system described in the following section.

3.3 Automatic Titration System

A fully automated system for performing titrations was developed in the course of this research. This computer-controlled system enabled the performance of multi-ionic titrations with a maximum of six syringes and the simultaneous monitoring of the solution concentrations of up to four different ions using ion-selective electrodes (ISEs). Figure 3.1 shows schematically the connection between the central computer and the titration equipment on one hand and the output devices - VDU, plotter and printer - on the other. The electronic interfacing was achieved using the Biodata "Microlink"™ system.

At the centre of the titration system lies the titration cell (Figure 3.2), which typically contained either a dispersion of the solid under study or a test solution. The titration cell consisted of a standard cylindrical polyethylene container within a 50 ml jacketed beaker, thermostatted at 25°C by recirculated water. The beakers were sealed with a perspex top which could hold up to four electrodes and the medical cannulae through which additions of reagents from the syringes were made. The cell was also fitted with a nitrogen inlet and outlet to maintain a carbon dioxide free system in alkaline conditions.

Micrometer syringes replaced conventional burettes in this system. The micrometers (Agla™) were driven by stepper motors which advanced 1/200 rev per pulse received from the controller. The syringes were calibrated in independent experiments and their calibration parameters entered into controlling computer programmes. The syringe outlet was through a medical cannula of internal diameter 0.03 cm, which was immersed in the titrated solution during use. The very fine capillary excluded the possibility of significant diffusion of reagent into the solution during use. Using this system, volume additions from a 10ml syringe could be made with an accuracy of 2×10^{-5} ml. A schematic representation of the micrometer syringe is shown in Figure 3.3.

The titration system was set up so that the user was able to choose operations from a menu, allowing the system to be used without further programming. In effect, the menu-driven options act as a high-level "language" for titration schemes. Figure 3.4 illustrates the menu choices open to the operator. These figures are directly captured from the VDU display.

3.4 Automated Calibration of Ion Selective Electrodes

Ion concentrations in the titration cell were monitored by ion selective electrodes (ISE). By calculating the ionic strength and the ion activity coefficient, the ion concentration in the cell was determined (eqns. 3.3, 3.4, 3.5). Ion selective electrodes were calibrated before each titration. Calibrations were made by titrating aliquots of the selected ion into a solvent or a solution of supporting electrolyte similar to that to be expected in the subsequent titration. A double junction Ag/AgCl reference electrode (Orion model 90-02) with an outer fill solution of KNO_3 (NaCl outer fill solution when using the potassium ISE) was used in all cases. These calibration techniques were conducted automatically by computer programmes similar to those used for the multi-electrode titrations of dispersions. Standardised solutions were used for calibration.

On selection of the option "Calibrate ISE" from the main menu (Figure 3.4), the menu prompt for automatic calibration was obtained, shown in Figure 3.5. Electrodes could be calibrated in pairs or individually, as required. During calibration, electrodes were automatically read and checked for stability after each addition of reagent. The screen display plotted the measured electrode potential in millivolts against the corresponding p[ion] calculated from the computed concentration of the ion and its activity coefficients obtained from the Davies equation. Figure 3.6 shows the screen display from a dual calibration of Na and Cl ISEs by titration of NaCl into water. Calibration displays were rescaled automatically during the titration.

After the calibration, the titration data were stored on computer disk by filename. They could then be recalled for calculation of calibration constants and a general assessment of the performance of the electrodes. The software offered a curve fit option to obtain the best-fit curve, linear or second order polynomial least-squares curve fit through the data. Emf data (E) and p[ion] (actual) were compared with the estimates obtained by 1st and 2nd order curve fits. The percentage error produced from the 1st and 2nd order estimations was displayed. This is a direct estimate of the error on the ion activity (concentration) calculation, using the curve fit equations. Typical calibration results for the ion selective electrodes used in this research (Na, K, Ca, Cl and F ISEs) are presented in Figures 3.7-3.11. All the ISEs employed in this work generally had errors less than 5% over the range of calibration. These results show that exceptional precision may be obtained using ISEs as concentration measuring devices under these carefully controlled conditions.

Glass pH electrode calibrations were performed using a range of buffers (pH range 1.5-12), made according to standard methods [7]. The collected data were processed by a computer programme in the same manner as other ISE calibration data. The results from a typical pH electrode calibration are shown in Figure 3.12.

3.5 Performance of Automated Multi-Electrode Potentiometric Titrations

As previously constituted, the titration may be performed with up to six titrant solutions and a maximum of four electrodes can be used simultaneously. Selection of the "Perform Titration" option from the main menu enabled the creation of a "command file" containing all the information necessary to perform a titration. This information was entered in response to a series of prompts (Figure 3.13). Firstly, the user entered the information defining the dispersion and titrants to be used - dispersion volume, weight of exchanger in the dispersion and the nature and concentration of titrants. The ion selective electrode data (obtained from calibrations prior to titration) were entered. A command format, defining the manner and range of the titration to be performed was then created. Within this format, the criteria for electrode stability were set, followed by a series of commands for the addition of titrants. Once all the parameters were entered, the titration ran automatically, following exactly the options selected by the user. The raw (emf) data from each of the electrodes and the volumes and concentrations of reagents were collected automatically. Data on ion sorption and ion release, pH and all other vital experimental data were collected, calculated and displayed as the titration proceeded.

A range of screen displays were available during the course of a titration, which were updated automatically as the titration proceeded (Figure 3.14). The selected display options could be altered at any time during the titration, allowing the assessment of all aspects of the titration and computed results at all times during the experiment. Typical screen displays from a titration at various stages of progress are shown in Figures 3.15-3.17.

For the dispersions, titrations were made over predetermined ranges of pH or other p(ion) using acids, bases or salts as required. The major difference between a calibration titration

and that of a dispersion titration is that with the dispersion, the electrode potentials were used to calculate the concentrations of the selected ions free in solution at each stage of the titration. Once these concentrations were known with confidence, the uptake or release of ions by the exchanger were calculated using the principles described previously.

After each addition of reagent, the dispersion was stirred for a specified period, after which electrode reading commenced, each electrode being read in turn. The criteria for electrode stability (standard deviation, number of readings taken, gap between readings) were entirely at the control of the operator. Once the electrode was stable to within its predetermined tolerance (limits of tolerance having been inputted by the user), the reading was accepted. If one or more electrodes did not satisfy the predetermined criteria for its own stability after a set period, a time-out bell was sounded and the titration was allowed to proceed. Unstable electrode data points were marked in the printouts.

3.6 Processing of Data

Although the titration results were available continuously during the experiment, detailed analysis of the titration was available in tabular form by selection of the "Process Data" option from the main menu. Titration information was printed out in a data file, containing details of titrants and their concentrations, exchanger weights, ISE readings (millivolts) and reagent volumes added. For each ISE, a results table was printed containing, for each titration point, p(ion) (as calculated from ISE readings), mmoles of ion added, mmoles of ion in solution as measured by ISE, calculated uptake of ion (in meq/g), pH +pX (or pM + pOH) and ion distribution coefficient (in ml/g). The calculated ionic strength, activity coefficient and charge balance in solid and solution phases were also printed out. An additional option allowing the calculation and correction for suspension potentials by minimisation of charge imbalance was also available (discussed fully in Chapter 4).

Titration results could also be presented graphically as X-Y plots. A number of ranges were available for plotting, as shown in Figure 3.14. Measurement error margins could be set and the resultant error bars on the measured ion uptake could be displayed. As the ISEs used in this work consistently produced measurement errors of less than 5% on estimated concentrations in calibration and test procedures, the error margin was generally a maximum of 5%.

To assess the significance of obtained uptake data of a given ion i, a significance factor $S.F.(\%)$ was introduced, defined as

$$S.F(\%) = \frac{Uptake of i \times wt.of exchanger \times 100}{mmol_i added + mmol_i initially} \qquad \textbf{(3.10)}$$

The significance factor is the percentage by which an electrode would have to be in error in its estimation of concentration to account for the uptake value calculated, in the absence of real sorption effects in the system. For example, if the S.F. were 5% (or less), we may place little or no confidence in the uptake value obtained by that electrode, since this is close to its limits as a concentration measuring device. Should the S.F. be large (80% for example), this far exceeds our confidence limits on the electrode and the result will be highly significant. An estimate of the probable uncertainty of uptake values was obtained from the probable uncertainty in the electrode measurement of concentration. Typically, this was ± 5% or less. The probable uncertainty in the measured uptake i_{UPT} of an ion i, is defined as

$$i_{UPT} = \frac{mmoli initial + mmoli added - mmoli calc. \pm Err\%}{wt.exchanger} \qquad \textbf{(3.11)}$$

where *Err%* is the percentage error on electrode measurement of concentration. As the concentration of the measured ion increases, the probable uncertainty also increases. Consequently the validity of results obtained from ISEs decreases at high concentrations of their selected ions. Application of these criteria was essential in assessing titration data.

3.7 Control Experiments

In order to test the behaviour of ion selective electrodes within the pH range (generally 3-11) and ionic strengths (less than 0.1) encountered in typical titrations and to confirm the validity of the calculations described above, a number of control experiments were performed.

In each case, additions of standardised acid, base or salt titrants were added to a 25ml of stirred, distilled water within the titration cell. Measurements of ion activities in solution were made using ion selective electrodes. Since no exchanger was present in these experiments, the measured ion uptakes should equal zero (within experimental error) in each case. Figure 3.18 shows the measured H^+ uptake for such a null experiment. An initial addition of 0.3ml of 0.1M HCl to 25ml of distilled water was made, reducing the pH to 2.93, followed by titration with 0.1M NaOH to pH 11.02 and back titration with HCl to pH 2.94. Throughout the titration, pH was monitored by electrode and the measured (null) uptake of hydrogen ion calculated by eqn. 3.9. The negligible uptake measured in this titration confirmed the reliability of the pH electrode within the pH range measured. Tests on the response of other ion selective electrodes were performed within the working pH and ionic strength range. Perhaps the most serious electrode error encountered was that observed with sodium ion selective electrodes in acid solution, due to the well-known effect of the glass sodium ISE responding to H^+ in addition to Na^+. In neutral and basic solution, the null effect was observed with the sodium ISE. Less significant acid inter-

ference effects were observed with K^+ and Ca^{2+} ISEs. The chloride ISE demonstrated a null effect throughout the titration range, whilst with the fluoride ISE the major restriction was the necessity to avoid formation of HF in solution, restricting the use of this electrode to pH greater than 5.

To test the calculation of ion uptake, an acid-base titration (HCl and NaOH) was performed after the addition of 3ml 0.1M $Na^+H_2PO_4^-$ (0.3 mmol) to 25ml distilled water. pH and hydrogen ion uptake were monitored by electrode. On addition of $Na^+H_2PO_4^-$ the pH was 4.64. At this pH the only phosphate species in solution in significant quantity was $H_2PO_4^-$. On addition of base, a release of hydrogen ion (relative to the initial condition) was measured as dissociation of $H_2PO_4^-$ took place, with the formation of HPO_4^{2-}. Between pH 9.5 and 10 (at which pH range the only significant phosphate species was HPO_4^{2-}) the release of hydrogen ion (in mmol) was equivalent to the total amount of phosphate ion in solution (0.3 mmol). Above pH 11 further release of hydrogen ion was observed as further dissociation to PO_4^{3-} took place. At pH 11.4 the solution was back-titrated with HCl. The uptake curve for the back-titration was superimposable on the forward titration curve. When the pH of the solution dropped below the initial pH, positive uptake was observed as the undissociated species H_3PO_4 was formed in significant quantities in solution. Hydrogen ion uptakes for forward and back titrations are plotted as a function of pH in Figure 3.19.

References

[1] R. Paterson and H. Rahman, J. Coll. Int. Sci., **94**, 60 (1983)
[2] R. Paterson and H. Rahman, J. Coll. Int. Sci., **97**, 423 (1984)
[3] R. Paterson and H. Rahman, J. Coll. Int. Sci., **98**, 494 (1985)
[4] R. Paterson and H. Rahman, J. Coll. Int. Sci., **103**, 106 (1985)
[5] R. Paterson and A. Smith, J. Coll. Int. Sci., **124**, 581 (1988)

[6] C.W. Davies, Electrochemistry, W. Clowes & Sons, London (1967)

[7] D.D. Perrin and B. Dempsey, Buffers for pH and metal ion control, Chapman & Hall Ltd. (1974)

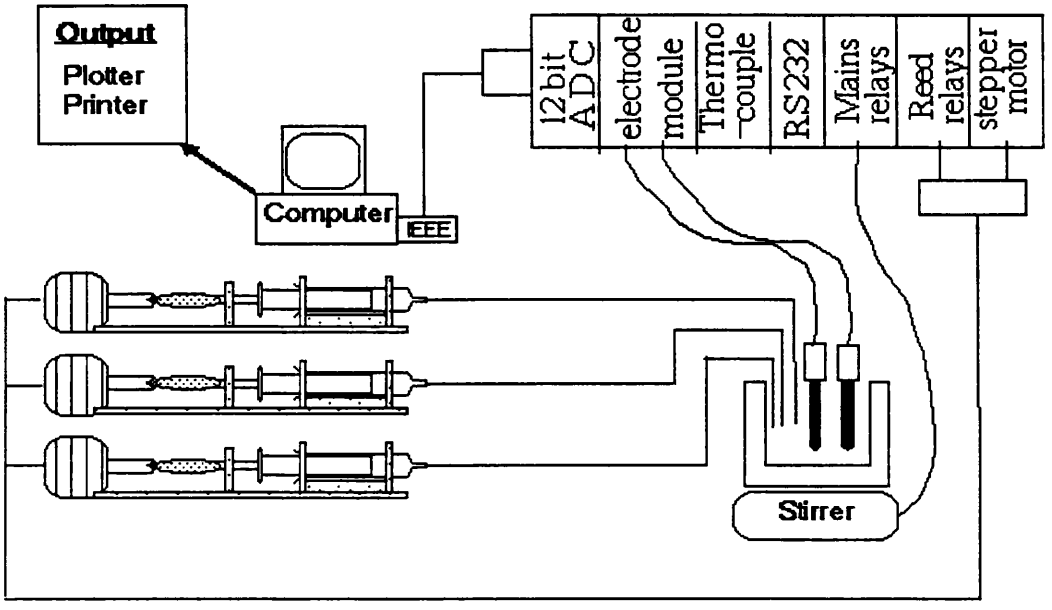

Figure 3.1 : Schematic representation of the automatic titration system.

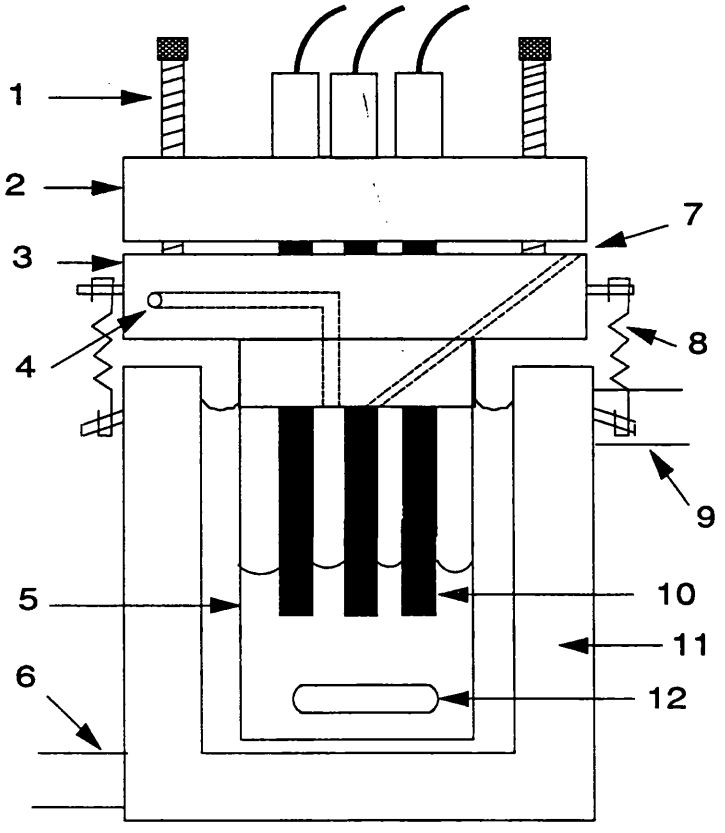

1 Height Adjustment	7 Reagent Inlet Port
2 Electrode Holder	8 Spring
3 Cell Cap	9 Water Outlet
4 Nitrogen Inlet	10 Electrodes (Max. 4)
5 Polypropylene Beaker	11 Double Wall Glass Beaker
6 Water Inlet	12 Stir Bar

Figure 3.2 : Titration cell

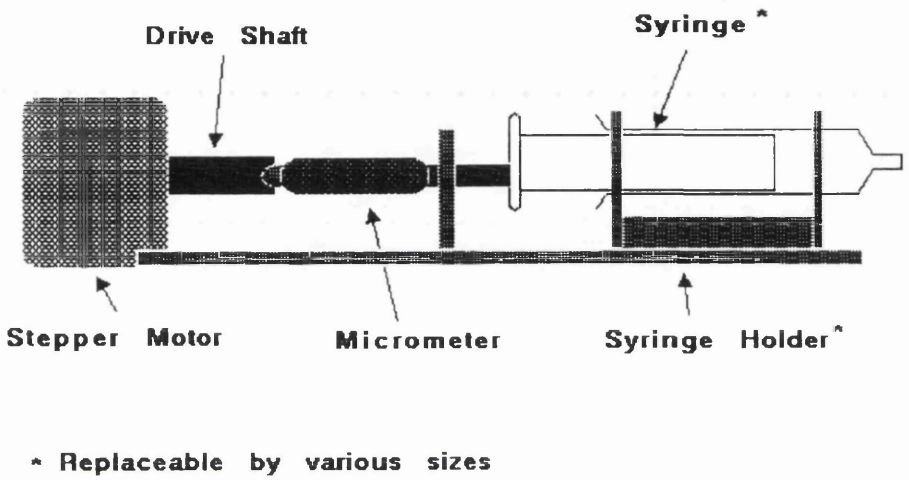

Figure 3.3 : Micrometer syringe

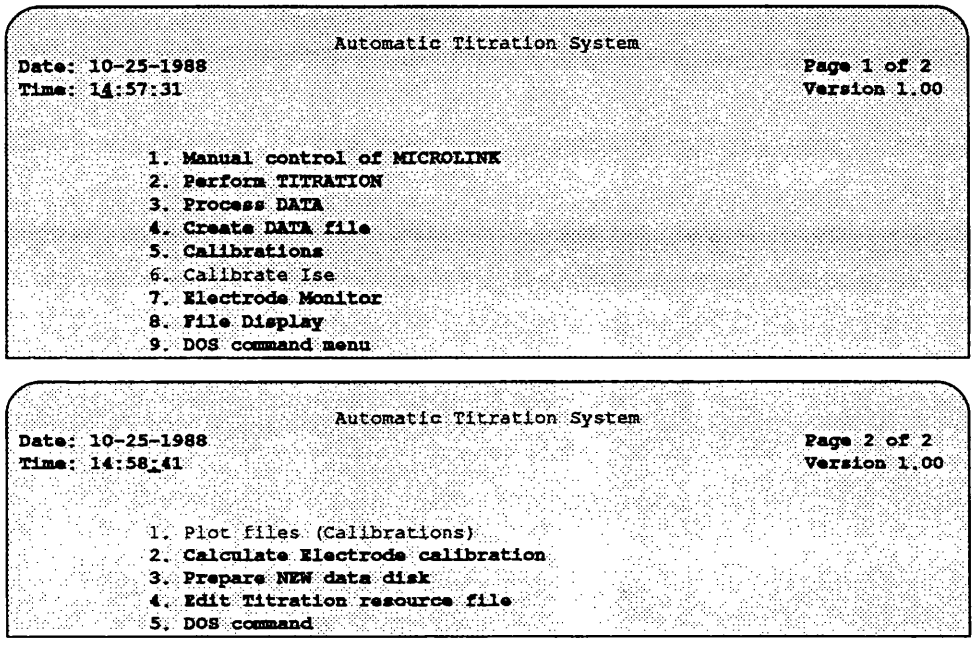

Figure 3.4 : Options menu for the automatic titration system.

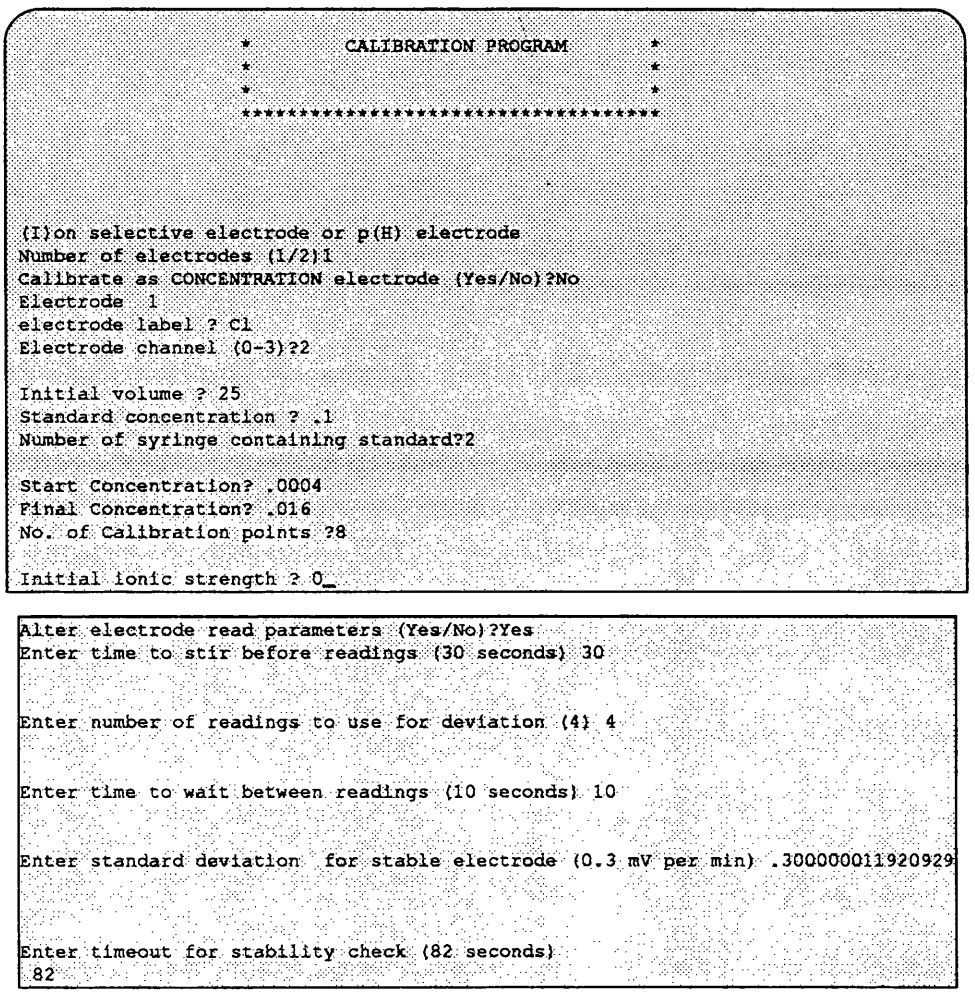

Figure 3.5 : Screen capture of user prompts, with specimen responses, for performing an automated calibration of an ion selective electrode.

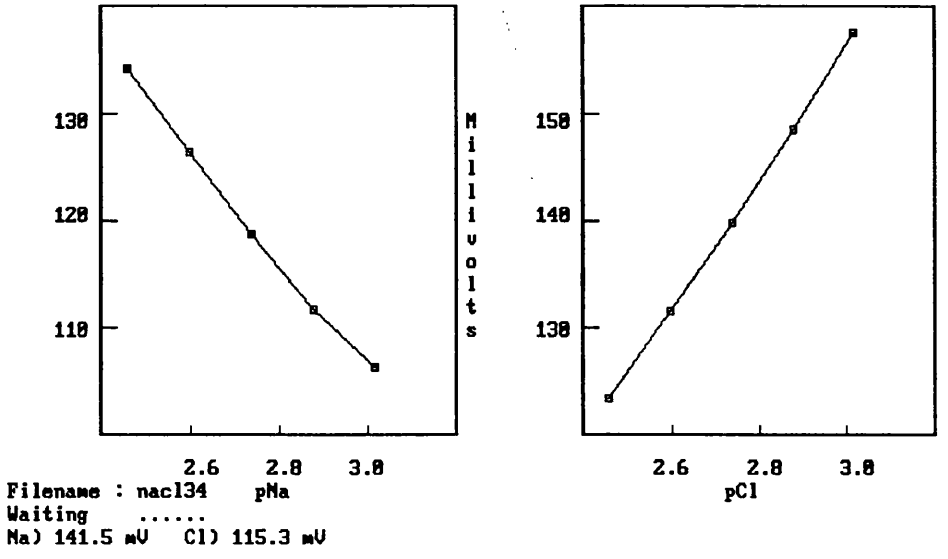

Figure 3.6 : Screen display for a dual calibration of Na and Cl ion selective electrodes by progressive addition of 0.1M NaCl solution to 25ml distilled water.

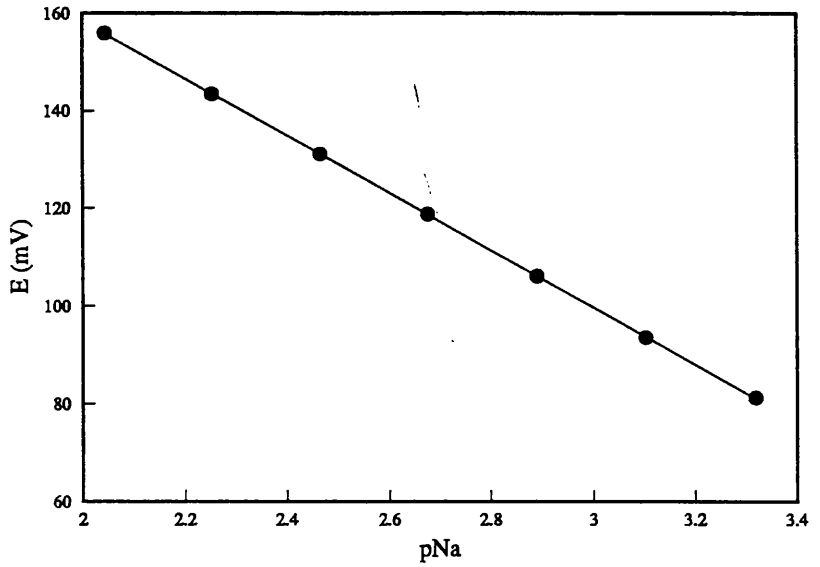

Filename NA133.Na

1st order equation $Y = -58.66X + 275.6$

2nd order equation $Y = -0.5392 X^2 - 61.55X + 279.4$

No.	E (mV)	pNa (actual)	pNa 2nd order	pNa 1st order	% error 2nd order	% error 1st order
1	81.2	3.318	3.317	3.315	0.1	0.6
2	93.6	3.102	3.104	3.104	-0.2	-0.2
3	106.1	2.889	2.889	2.890	-0.1	-0.4
4	118.7	2.675	2.674	2.676	0.3	0.0
5	131.1	2.464	2.463	2.464	0.1	-0.2
6	143.4	2.253	2.255	2.255	-0.4	-0.4
7	155.9	2.044	2.044	2.041	0.1	0.6

(% errors are concentration errors)

Figure 3.7 : Typical calibration of a sodium ion selective electrode.

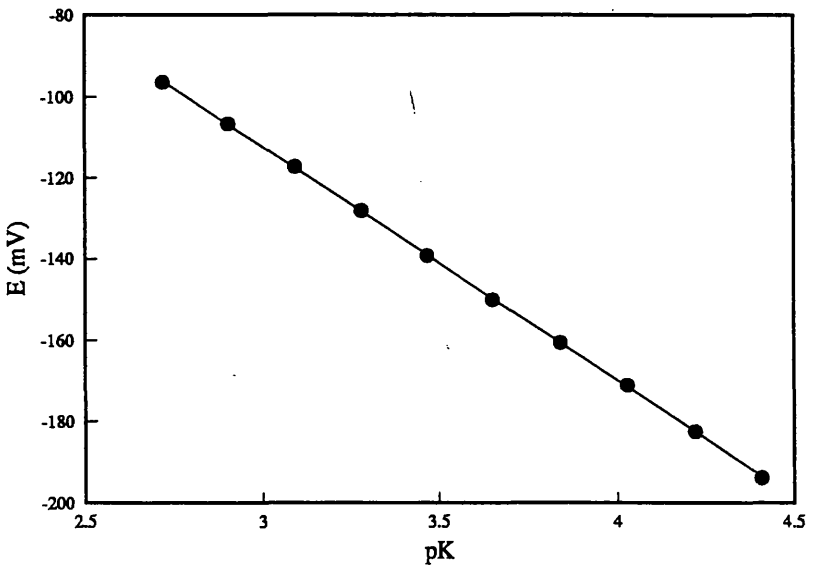

Filename KCL129.K

1st order equation $Y = -57.71X + 60.88$

2nd order equation $Y = -0.462\ X^2 - 54.22X + 55.15$

No.	E (mV)	pK (actual)	pK 2nd order	pK 1st order	% error 2nd order	% error 1st order
1	-193.7	4.406	4.408	4.411	-0.5	-1.2
2	-182.5	4.218	4.216	4.217	0.5	0.2
3	-171.2	4.027	4.022	4.021	1.2	1.3
4	-160.7	3.839	3.841	3.839	-0.5	-0.1
5	-150.0	3.651	3.656	3.654	-1.1	-0.6
6	-139.1	3.464	3.467	3.465	-0.9	-0.4
7	-128.0	3.277	3.274	3.273	0.6	0.9
8	-117.2	3.091	3.086	3.086	1.0	1.2
9	-106.7	2.905	2.903	2.904	0.5	0.3
10	-96.5	2.720	2.724	2.727	-0.8	-1.6

(% errors are concentration errors)

Figure 3.8 : Typical calibration of a potassium ion selective electrode.

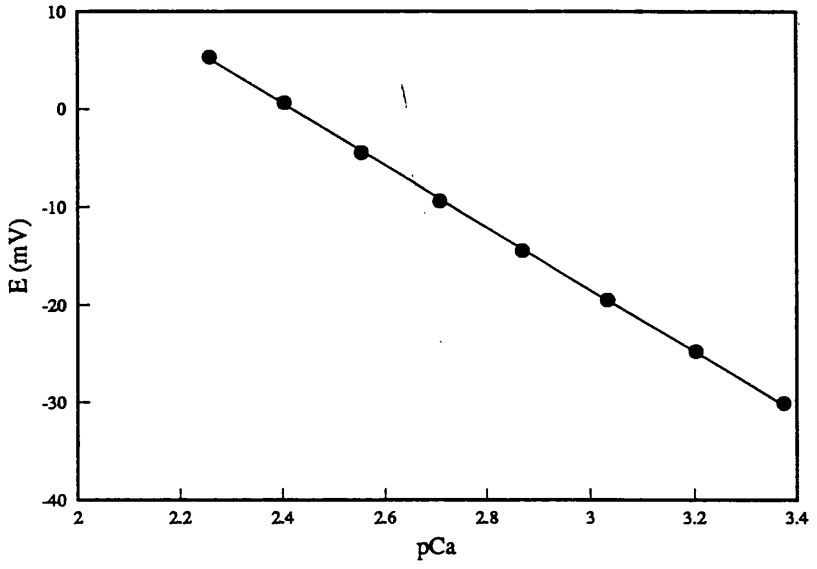

Filename CA32.Ca

1st order equation $Y = -31.65X + 76.52$

2nd order equation $Y = 1.350 X^2 - 39.25X + 87.03$

No.	E (mV)	pCa (actual)	pCa 2nd order	pCa 1st order	% error 2nd order	% error 1st order
1	-30.1	3.375	3.377	3.369	-0.4	1.4
2	-24.8	3.202	3.202	3.201	0.1	0.2
3	-19.5	3.033	3.030	3.034	0.8	-0.1
4	-14.4	2.868	2.867	2.873	0.2	-1.1
5	-9.4	2.708	2.709	2.715	-0.4	-1.6
6	-4.5	2.553	2.557	2.560	-1.0	-1.7
7	0.6	2.403	2.400	2.399	0.5	0.9
8	5.3	2.258	2.258	2.250	0.1	1.9

(% errors are concentration errors)

Figure 3.9 : Typical calibration of a calcium ion selective electrode.

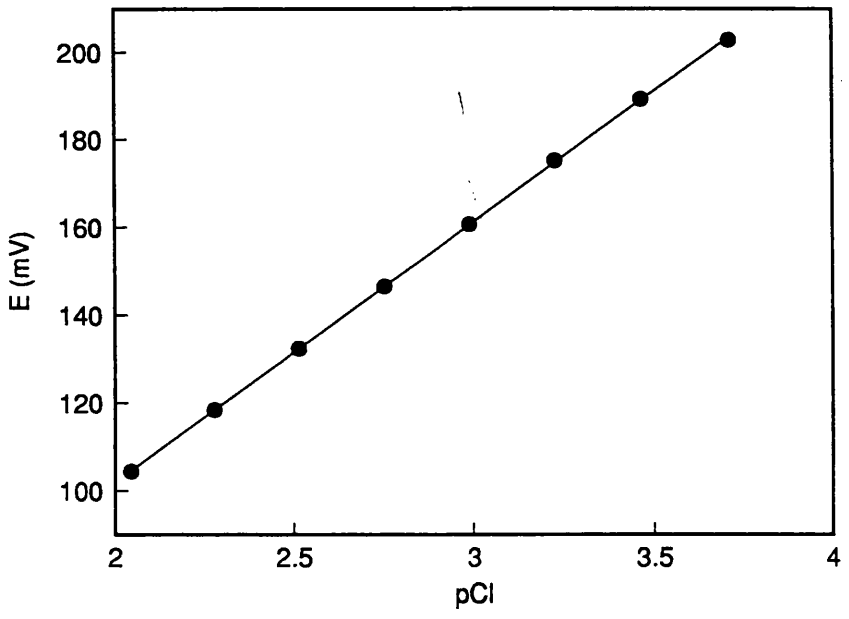

Filename CL141.Cl

1st order equation $Y = 59.40X - 16.91$

2nd order equation $Y = -0.859\ X^2 + 64.34X - 23.75$

No.	E (mV)	pCl (actual)	pCl 2nd order	pCl 1st order	% error 2nd order	% error 1st order
1	202.8	3.709	3.704	3.699	1.0	2.3
2	189.2	3.466	3.471	3.470	-1.1	-0.9
3	175.2	3.227	3.232	3.234	-0.9	-1.5
4	160.7	2.987	2.986	2.990	0.2	-0.7
5	146.5	2.749	2.747	2.751	0.6	-0.4
6	132.3	2.512	2.509	2.512	0.6	0.1
7	118.3	2.277	2.277	2.276	0.1	0.3
8	104.3	2.044	2.046	2.040	-0.5	0.8

(% errors are concentration errors)

Figure 3.10 : Typical calibration of a chloride ion selective electrode.

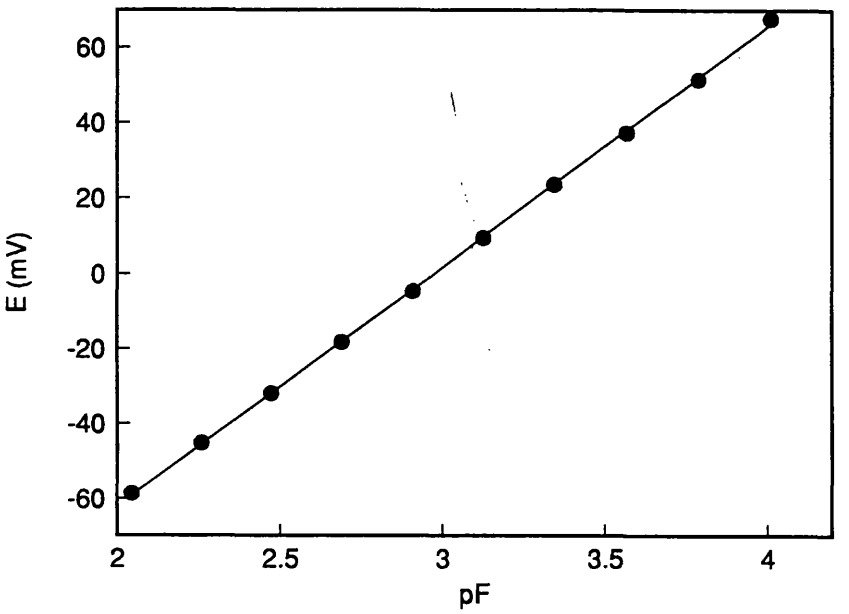

Filename CAL73.F

1st order equation $Y = 63.83X - 189.7$

2nd order equation $Y = 1.340 X^2 + 55.72X - 178$

No.	E (mV)	pF (actual)	pF 2nd order	pF 1st order	% error 2nd order	% error 1st order
1	67.6	4.009	4.019	4.031	-2.3	-5.3
2	51.5	3.785	3.776	3.779	2.1	1.3
3	37.2	3.567	3.558	3.555	2.2	2.7
4	23.6	3.345	3.348	3.342	-0.9	0.5
5	9.5	3.126	3.129	3.121	-0.7	1.2
6	-4.6	2.907	2.908	2.900	-0.4	1.5
7	-18.3	2.689	2.692	2.686	-0.5	0.8
8	-32.0	2.473	2.473	2.471	-0.1	0.3
9	-45.3	2.258	2.259	2.263	-0.3	-1.2
10	-58.7	2.044	2.041	2.053	0.8	-2.0

(% errors are concentration errors)

Figure 3.11 : Typical calibration of a fluoride ion selective electrode.

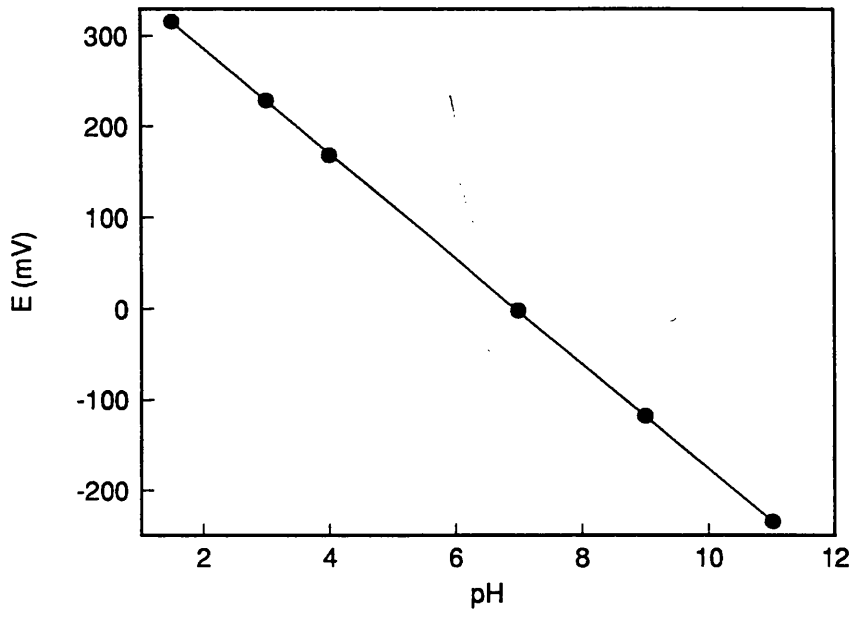

Filename H211.H

1st order equation $Y = -57.75X + 401.5$

2nd order equation $Y = 0.001\ X^2 - 57.77X + 401.5$

No.	E (mV)	pH (actual)	pH 2nd order	pH 1st order	% error 2nd order	% error 1st order
1	315.5	1.5	1.488	1.489	2.7	2.6
2	228.7	3.0	2.991	2.992	2.1	1.9
3	168.2	4.0	4.039	4.039	-9.5	-9.4
4	-1.7	7.0	6.980	6.981	4.4	4.3
5	-117.7	9.0	8.990	8.990	2.2	2.4
6	-234.4	11.0	11.011	11.010	-2.6	-2.4

(% errors are concentration errors)

Figure 3.12 : Typical calibration of a pH electrode.

```
Load a titration command file (Yes/No)?No
pH at the ISOELECTRIC POINT :? 7
Initial Volume :? 25
Exchanger - grams dried weight :? .5

Exchanger - grams effective weight :? .4

Initial Ionic strength :? 0

Enter number of syringes to be used :? 2
Please enter syringe contents using atomic symbols
But omit any stoicionetric coefficients eg CaCl
Enter contents of syringe  1 ? HCl

Concentration of HCl  :? 0.1
Enter contents of syringe  2 ? NaOH

Concentration of NaOH  :? .1002


ENTER NUMBER OF ISE'S RECORDED (1-4) :? 3
FIRST ELECTRODE MUST BE pH

ENTER CALIBRATION INFORMATION
IN THE FORM  Y = A + BX
IN THE FORM  Y = AA + BB(X) + CC(X^2)

PH DATA

A =  :? 482.8234

B =  :? -59.16

AA =  :? 481.4634

BB =  :? -58.84

CC =  :? 0.0003
Use curve fit instead of straight line (Yes/No)?No
Was Electrode calibrated as concentration electrode (Yes/No)?No


Command format either :
set readings [nn] (4) NB. must be the FIRST COMMAND
set timeout [ww] (420)
set stirrer [ON\off] ( during electrode readings )
set stirtime [hh] (60)
set deviation [dd] (0.15)
set readgap [gg] (10)
add [vv] from syringe [ss] for [tt]
add [vv] from syringe [ss] until electrode [ee] reads [< >] [pp]
user add [vv] of syringe [ss]

dd = standard deviation per minute for electrode stability
ee = electrode number which is used to check pH
gg = time in seconds between electrode readings
hh = number of seconds to stir after each addition
nn = number of readings for standard deviation
pp = p[] value calculated from electrode ee
ss = syringe from addition is made
tt = number of additions to be made
vv = volume added at each addition
ww = number of seconds to wait before electrode time-out


type end to finish inputing commands
Command ? add .1 from syringe 1 until electrode 1 reads < 3
Command ? add .15 from syringe 2 until electrode 1 reads > 11
Command ? add .15 from syringe 1 until electrode 1 reads < 3
Command ? end
```

Figure 3.13 : Screen capture of user prompts, with specimen responses, for performing automatic titrations.

```
Which of the following is to be displayed on X axis
1)              p[electrode]
2)              Millimoles of Ion added
3)              volume added
4)              total volume added
5)              BASE-ACID
Select number ? 1
Electrode Label ? H
Which of the following is to be displayed on y axis
1)              p[electrode]
2)              Millivolts
3)              Uptake
4)              Millimoles of Ion measured
5)              Calculated Charge balance
Select number ? 3
Electrode Label ? H
```

Figure 3.14 : On-screen display options available to the user during the course of a titration.

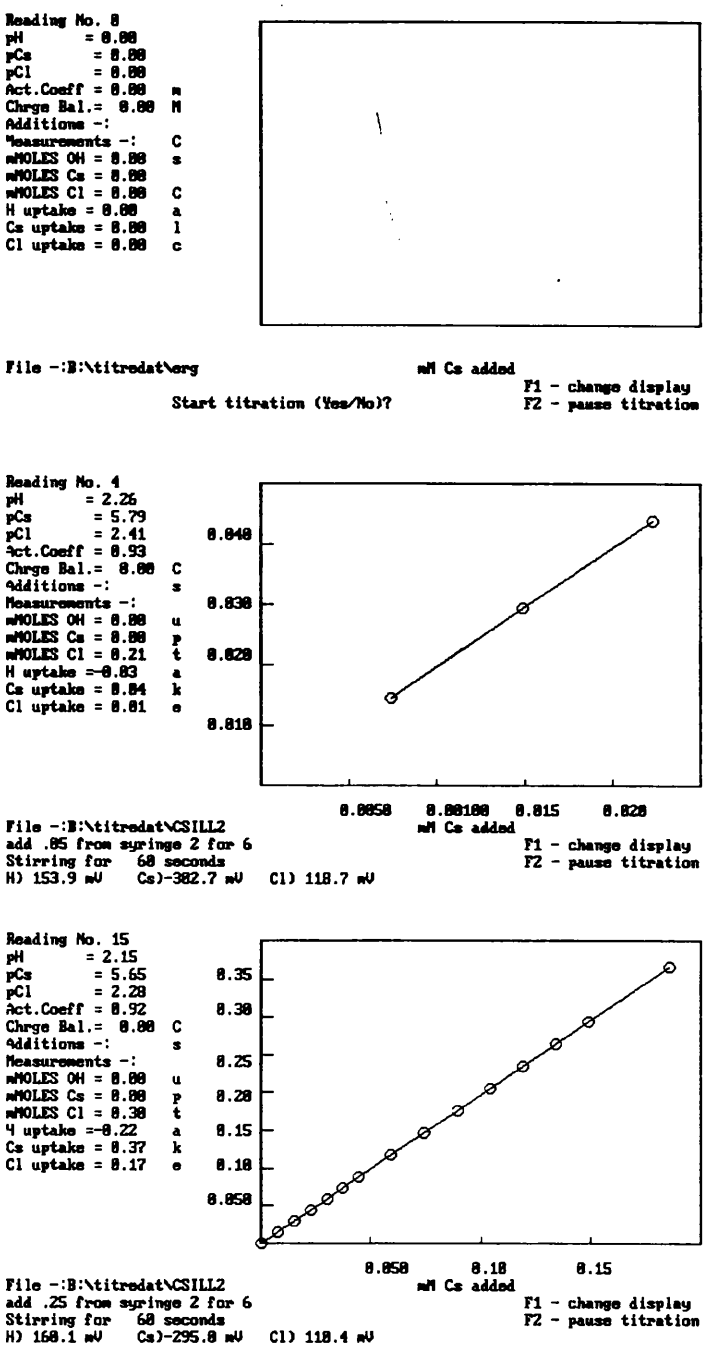

Figures 3.15 to 3.17 : Successive screen displays of a automated titration in progress. Ion activities and uptakes for H^+, Cs^+ and Cl^- were monitored by ISE. The screen display shows uptake of Cs^+ as a function of millimoles of Cs^+ added.

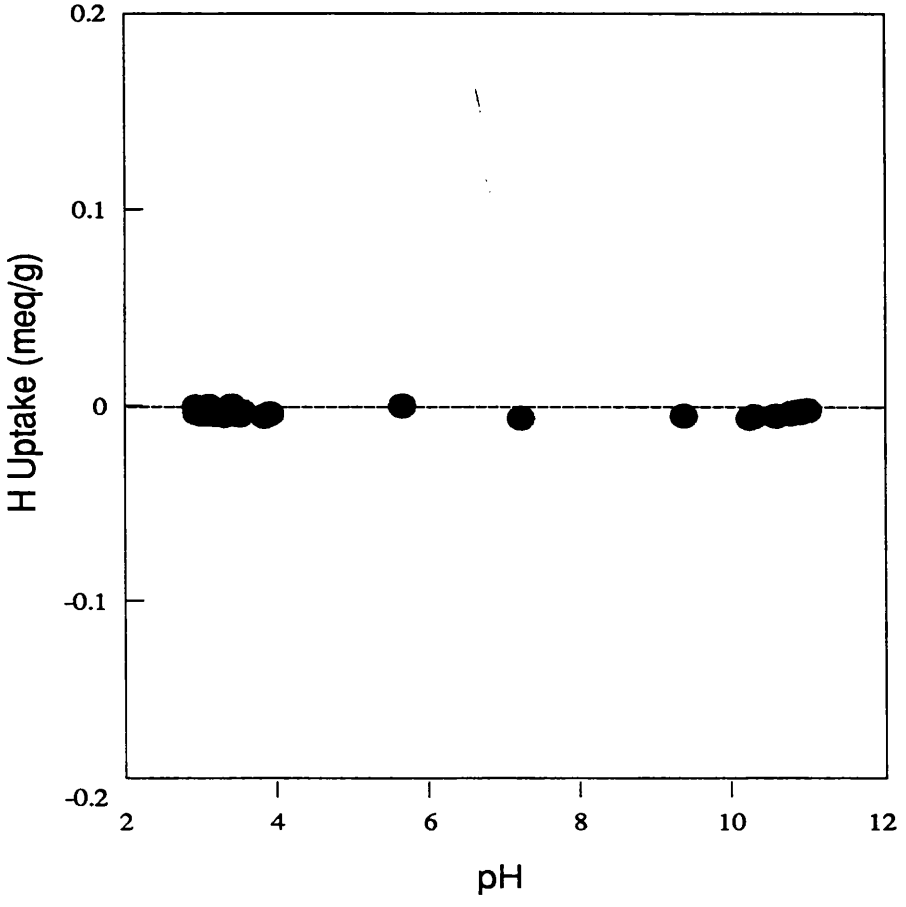

Figure 3.18 : Control experiment to illustrate zero uptake of hydrogen ion. An initial addition of 0.3mls 0.1M HCl to 25ml of distilled water was made, reducing the pH to 2.93, followed by titration with 0.1M NaOH to pH 11.02 and back titration with HCl to pH 2.94. Throughout the titration, pH was monitored by electrode and the measured (null) uptake of hydrogen ion calculated by eqn. 3.9.

Titration file: SYSTEST

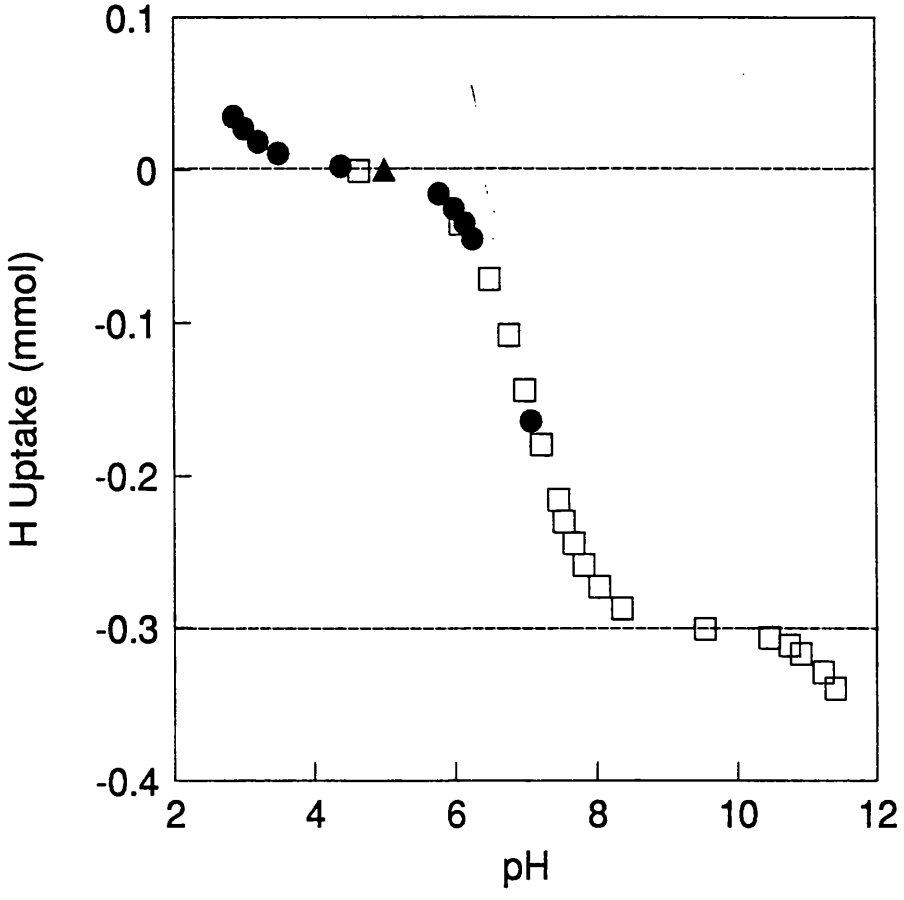

Figure 3.19 : Test of pH electrode uptake system. An addition of 3ml 0.1M $Na^{+}H_2PO_4^{-}$ was made to 25ml distilled water (▲). The solution was then titrated with 0.14M NaOH (□) and 0.1M HCl (●). Apparent uptakes were determined from pH electrode measurements.

Titration File: PBLANK

CHAPTER 4

THE SUSPENSION POTENTIAL

Introduction

A traditional complication in the potentiometric determination of pH or other p(ion) in colloidal solution is the problem of the suspension effect. The effect is particularly apparent in colloidal dispersions of highly charged particles in solutions of low ionic strength. The surface charge on the colloidal particles creates an electrical double layer which, in dilute solutions, extends well out into solution. In the region of the double layer, the activity of counterions exceeds those of co-ions due to the influence of the electrical potential near the surface. In effect the ion exchange properties of the colloid extend into free solution. In a suspension, ion selective electrodes (ISEs) will measure (within their normal limitations) these activities. In consequence, for dispersions in solutions of low ionic strength and high particle charge, significant suspension effects are observed. The effects are particularly apparent when there is a high density of solid particles in the dispersion.

In this Chapter, a discussion of the source of the suspension potential and its implications for the investigation of ion exchange processes by potentiometric titration is followed by a methodology for the measurement and correction for suspension potentials. To illustrate the means of correction and to assess its significance, several examples are given from titrations of colloids inorganic oxides and aluminosilicate clay minerals. This necessitates the introduction in this chapter of information and terms which will be fully discussed in subsequent chapters. Since all subsequent titration data presented in this thesis have been corrected for the suspension potential, a full discussion of the methods of correction have been given here in advance.

4.1 Origin of the Suspension Potential

In colloidal suspensions of charged particles in solutions of low ionic strength, the surface charge of the particles creates an electrical double layer which extends well out into the solution. The electrical potential Ψ decreases with increasing distance from the particle surface, becoming zero in bulk solution. As was shown in Chapter 2, the thermodynamics of equilibrium conditions require that the electrochemical potential $\tilde{\mu}_i$ of an ionic species i is constant at all distances from the colloidal surface. From eqn. 2.4, the electrochemical potential $\tilde{\mu}_{i(x)}$ of ion i at distance x from the particle surface (where x is within the electrical double layer) and the electrochemical potential $\tilde{\mu}_{i(\infty)}$ of ion i in bulk solution are given by

$$\tilde{\mu}_{i(x)} = \mu_i^0 + RT\ln a_{i_{(x)}} + z_i F\Psi_{(x)} \qquad (4.1)$$

$$\tilde{\mu}_{i(\infty)} = \mu_i^0 + RT\ln a_{i_{(\infty)}} + z_i F\Psi_{(\infty)}$$

where $a_{i_{(x)}}$ and $\Psi_{(x)}$ are the activity of ion i and the electrical potential respectively, at distance x from the particle surface. $a_{i_{(\infty)}}$ and $\Psi_{(\infty)}$ are the activity of ion i and the electrical potential respectively, in the bulk solution. Since $\tilde{\mu}_{i(x)}$ is equal to $\tilde{\mu}_{i(\infty)}$, it is readily shown from eqn. 4.1 that

$$\frac{a_{i(\infty)}}{a_{i(x)}} = \exp\left[\frac{z_i F(\Psi_{(x)} - \Psi_{(\infty)})}{RT}\right] \qquad (4.2)$$

$$pI_{(x)} - pI_{(\infty)} = \frac{z_i F}{2.303\,R\,T}(\Psi_{(x)} - \Psi_{(\infty)}) \qquad (4.3)$$

In the bulk solution there is no electrical potential ($\Psi_{(\infty)} = 0$). Consequently electroneutrality is obtained in the bulk solution. Within the double layer there is an electrical potential, so the activity of an ion is greater in the double layer than its activity in the bulk solution if the signs of the ionic charge and electrical potential are opposite (eqn. 4.2). If the charge on an ion has the same sign as the electrical potential, the ion activity in the double layer is less than its activity in bulk solution. Consequently there are deviations from electroneutrality within the double layer.

To illustrate these features, consider a suspension of positively charged particles in acid H^+X^-. Within the electrical double layer, pH and pX are not equivalent. The positive potential results in an increase in pH and a decrease in pX as the particle surface is approached. In the bulk solution pH = pX. These effects are shown diagrammatically in Figure 4.1. (It is worthwhile to note that equilibrium conditions require that pH + pX = constant at all points from $x = 0$ to $x = \infty$.) If pH and pX of the colloid are measured by ion selective electrodes for H^+ and X^- respectively, pH_m will be greater than pX_m (where $p(ion)_m$ is the value measured by ISE). The observed pH and pX represent a "time and space averaged" measure of the pH and pX in the aqueous phase of the suspension. Consequently, pH_m is greater than the pH of the bulk solution, while pX_m is less than pX in the bulk solution.

These effects were demonstrated by the addition of HCl to a dispersion of monoclinic zirconia in distilled water (0.3g in 25 ml). (As is shown in Chapter 6, monoclinic zirconia has anion exchange properties in acid solution (positive surface charge)). pH and pCl were monitored by the respective ion selective electrodes. The only ions present in the suspension were H^+ and Cl^-. In the absence of a suspension potential, the measured pH would necessarily be equal to the measured pCl, within the limits of accuracy of the ISEs. In this

case, pH 3.32 and pCl 3.06 were measured. This result was reproducible and control experiments showed that the discrepancy between measured pH and pCl was not due to electrode errors. The difference in the activities of the ions was due to the positively charged surfaces of the colloidal particles of monoclinic zirconia at this pH. The resultant positive suspension potential results in a lower pCl and higher pH within the electrical double layer (eqn. 4.3).

With a six times more dilute suspension of zirconia in acid solution (0.1g in 50ml), the measured pH and pCl were identical, within the measurement accuracies of the electrodes (3.46 and 3.49 respectively). Since the particle-to-particle distances were greater in this case, the solution volume affected by the electrical double layer was small compared to the main bulk of solution, so the effect of the suspension potential on the electrode response was consequently negligible.

Pore charges, such as those which occur in porous inorganic oxides or in layered clays, do not affect the suspension potential. The measurement of ion exchange processes which occur within the deep pores of such material is unaffected by the presence of suspension potentials. The measurement of the ion exchange processes which occur on the external surface of the ion exchanger are, however, affected by suspension potentials. In the presence of a positive potential, cation uptakes are overestimated and anion uptakes underestimated. (Negative potentials give the converse effect). If the effect of the suspension potential is removed, the total ion exchange capacity (including surface capacity) may be determined.

4.2 Factors Influencing the Suspension Potential

The electrical double layer potential is influenced by the ionic strength of the solution, the surface charge and the valency of the electrolyte. These same factors influence the suspension potential. An increase in the ionic strength (at constant surface potential)

decreases the potential of the electrical layer and thus decreases the suspension potential, at constant suspension density. This effect is shown in Figure 4.2 where the potential in the electrical double layer is plotted for a constant surface potential (20 mV) at various ionic strengths: 0.0001, 0.001, 0.01. The Debye-Hückel approximation has been used for these calculations [1].

If the ionic strength remains constant, an increase in surface potential enhances the electrical double layer potential and therefore increases the suspension potential at constant suspension density. Figure 4.3 displays the potential at various surface potentials when the ionic strength equals 0.001M.

It should be stressed that the current method of analysis for the suspension potential is based entirely on the fundamental thermodynamics of ions in solution. The electrical double layer models are not involved in any part of the calculations and are presented here merely to illustrate the factors which influence the suspension potential.

4.3 Results and Discussion

4.3.1 Method of Correction for the Suspension Potential

Eqn. 4.2 provides a quantitative definition of the variation in the activity of an ion in solution with distance from the surface of a charged particle. The experimental situation of measuring ion activities with ion selective electrodes in a colloidal suspension is more complex, since suspended particles are present in large numbers at time-varying distances from the ISE surface. It is impossible to calculate specific values of electrical potentials at the electrode surface. However, since constant ISE measurements were obtained in these experiments, there is an averaging of these potentials, giving a time-averaged effective suspension potential Ψ_{sp}.

Replacing $p\,I_{(x)}$ with $p\,I_m$ (the value of pI as measured by ISE) and the term $(\Psi_{(x)} - \Psi_{(\infty)})$ by Ψ_{sp} (the effective suspension potential experienced by the ISE), eqn. 4.3 becomes

$$p\,I_m \;-\; p\,I_{(\infty)} \;=\; \frac{z_i F \Psi_{sp}}{2.303\,R\,T} \qquad \textbf{(4.4)}$$

Expressing this equation in terms of ion activity gives

$$\frac{a_{i(\infty)}}{a_{im}} \;=\; \exp\left(\frac{z_i F \Psi_{sp}}{RT}\right) \qquad \textbf{(4.5)}$$

where a_{im} is the activity of ion i measured by ISE.

In the equilibrium bulk solution, there is no suspension potential (since $\Psi = 0$ at infinite separation from the surface) and consequently the electroneutrality criterion is observed ($\Sigma_i z_i c_i = 0$). Calculations using ion selective electrode data, which were available for all ions in solution, showed that electroneutrality was not obtained ($\Sigma_i z_i c_i^m \neq 0$) with measurements from a dispersion of charged colloidal particles in a solution of low ionic strength. The sign of this charge imbalance was opposite to the sign of the surface charge on the solid.

The magnitude of the suspension potential Ψ_{sp} was obtained from consideration of electroneutrality in the equilibrium bulk solution. By successive approximations, a common value of Ψ_{sp} was obtained which, when applied in eqn. 4.5 for each ion in solution, minimized the charge balance. Ion uptakes were recalculated with reference to the calculated ion concentration in the equilibrium bulk solution.

To demonstrate the method of correction for the suspension potential, the following example is presented. An addition of 1.5 ml 0.098M HCl was made to a dispersion of calcined monoclinic zirconia (1.39g in 25ml distilled water). The only ions present in solution after this addition were H^+ and Cl^-. The activities of both these ions were measured by ISE. The electrode calibration data were

$$E_H\,(mV) = -57.01\ pH + 394.2$$

$$E_{Cl}\,(mV) = 60.12\ pCl - 28.08$$

At equilibrium, electrode potentials of 217.3mV and 125.8mV respectively were measured with the H^+ and Cl^- ISEs. Using these potentials in the electrode calibration equations gave an equilibrium pH of 3.10 and pCl 2.56. The measured charge imbalance in solution was negative ($\sum_i z_i c_i = -0.00206$), indicating a positive surface potential. Ion uptakes, calculated by the principles described in Chapter 3, were 0.09 meq/g for H^+ and 0.051 meq/g for Cl^-. By successive approximations, a value of Ψ_{sp} was obtained which, when added to the measured electrode potentials of each ISE, minimized the charge balance. Optimum charge balance was achieved when Ψ_{sp} equalled 15.5 mV, giving both pH and pCl equal to 2.82 ($[H^+] = [Cl^-] = 0.0016M$). These concentrations are the ion concentrations in the equilibrium bulk solution. Ion uptakes, recalculated with respect to the bulk solution concentrations, were calculated as 0.076 meq/g for each ion. Data for this calculation are summarised in Table 4.1.

It should be stressed that in order to perform these corrections, it was necessary to monitor the activities of <u>all</u> ion species by ISE - the method cannot be applied to traditional single (pH) electrode titrations. Furthermore it is clearly of paramount importance that ion selective electrode responses were accurate, reproducible and free from interferences from other ions. Rigourous calibration procedures for all ISEs were therefore of central

importance to this method.

4.3.2 Application of Suspension Potential Corrections to Potentiometric Titration Data

Titration with HCl, KOH and KCl of a dispersion of calcined monoclinic zirconia

The hydrous oxide monoclinic zirconia has amphoteric properties, behaving as an anion exchanger in acid solution and as a cation exchanger in basic solution. Corrections for the suspension potential were performed on ISE data obtained from a titration of a dispersion of calcined monoclinic zirconia (1.39g in 25ml distilled water) with 0.1M HCl, 0.1M KOH and 1M KCl. ISEs for H^+, K^+ and Cl^- were used, with a common reference electrode.

Ion exchange capacities from this titration, before and after correction for the suspension potential, are displayed in Figure 4.4. The corrections have a dual effect - a change in pH (since measured pH is not equal to pH in the bulk solution when there is a suspension potential) and an alteration to the calculated exchange capacity. It is evident that these corrections only have significance at the pH extremes of the titration. The largest effects were observed at the initial titration points (pH 3-4), where the surface charge was relatively high and the ionic strength was low. Under these conditions, relatively large suspension potentials would be expected, as predicted by the Gouy-Chapman model.

Ion uptake data (calculated by mass balance) obtained from H^+, K^+ and Cl^- ISE measurements, are shown in Figure 4.5. There is noticeable deviation from the expected stoichiometry of H^+ and Cl^- uptake in acid solution, while in basic solution the predicted uptake of K^+ is hardly observed at all from the K^+ ISE data. These findings, originally attributed partly to electrode measurement errors and to the difficulty of measuring ion

uptake on low capacity ion exchangers (calcined zirconia capacities are approximately 10 times less than for non-calcined zirconia), can now be explained by the effects of the suspension potential. Ion uptakes from the same titration data, after correction for Ψ_{sp}, are given in Figure 4.6 and in Table 4.2. The stoichiometry of ion uptakes is now clearly observed, with anion exchange occurring in acid solution (H^+ and Cl^- uptake) and cation uptake (K^+ uptake and H^+ release) in base. No K^+ was observed in acid solution and similarly no Cl^- uptake in basic solution. It should be stressed that these corrections were based solely on the criterion of electroneutrality in the bulk solution, with no prior assumptions about the exchange characteristics of monoclinic zirconia. Furthermore, it is evident that the suspension potential results in larger errors in uptake calculations when the monitored ion concentration is high (for this titration, pH >> pK and pCl at all but the initial titration points).

In Figure 4.7 the values of the suspension potential used in the above corrections are plotted against pH for the forward titration with KOH of the zirconia dispersion, after initial addition of HCl. Positive potentials are observed when the exchanger is positively charged (acid solution). The potential reduces to zero at the zero point charge of monoclinic zirconia (pH 7-8) and becomes negative at higher pH.

These results were supported by electrophoretic mobility studies of zirconia particles in solutions of indifferent electrolyte. Measurements were made using a Coulter ™ DELSA 440 (Doppler Electrophoretic Light Scattering Analyzer). Electrophoretic mobilities and zeta potentials were obtained by analysis of the Doppler shifts of laser light scattered by the moving particles. Zeta potentials are presented as a function of pH in Figure 4.8. Results were qualitatively similar to calculated suspension potentials, with positive potentials in acid solution, and negative potentials in basic solution. Since the suspension potential represents the "averaged" potential observed by each ISE, its magnitude is

necessarily considerably less than the zeta potential (the potential at the shear plane). No quantitative comparison between the relative magnitudes of these potentials is attempted here - however the qualitative agreements are good, with the suspension potential and zeta potential having the same sign throughout the pH range.

As shown in Chapter 5, the pH dependent equilibria for the ion exchange processes on monoclinic zirconia (with KCl as the electrolyte) are given by eqns. 4.6 and 4.7. The magnitude and signs of oxide pore charges are sensitive to both pH and the activity of the counterion in solution (here, chloride in acid, potassium in alkaline solution). The mechanisms of are validated by the observations that anion capacity is a single valued function of total acid, pA (= pH + pCl) and cation capacity is a single valued function of total base, pB (= pNa + pOH).

$$\overline{M-OH} + H^+_{aq} + Cl^-_{aq} \rightleftharpoons \overline{M-OH_2^+Cl^-} \qquad \textbf{(4.6)}$$

$$\overline{M-OH} \;+\; OH^-_{aq} \;+\; K^+_{aq} \rightleftharpoons \overline{M-O^-K^+} \;+\; H_2O \qquad \textbf{(4.7)}$$

The effects of suspension potential corrections on pA and pB relationships were investigated by back titration of the zirconia dispersion with HCl, after increasing the salt concentration by addition of 1mmol KCl. Capacities before and after correction are plotted as functions of pA and pB respectively in Figures 4.9 and 4.10. The suspension potential does not lead to an error in the pA or pB measurements, since the parameters pA (= pH + pCl) and pB (=pK + pOH) are constant throughout the solution phase, from the bulk solution through the electrical double layer. The only corrections are the relatively minor effects on the calculation of capacity. These findings demonstrate a major advantage of

multi-electrode titrations - pA and pB may be determined precisely, without subsequent correction, in the presence of a suspension potential. It is not possible to do this with a single pH electrode titration.

Titration with HCl and $Ca(OH)_2$ of a dispersion of non-calcined monoclinic zirconia

Further evidence to support the explanation of Ψ_{sp} in terms of external surface charge was given by the measurements obtained on titration of a dispersion of 0.263g monoclinic zirconia (non-calcined) with $Ca(OH)_2$ and HCl. Solution activities and uptakes of hydrogen, chloride and calcium ions were monitored by ion selective electrode. Exchange capacities before and after correction for the suspension potential are shown in Figure 4.11. In this titration, considerably higher cation exchange capacities were obtained than with monovalent cations at equivalent pH. However, despite the relatively large cation exchange capacities for Ca^{2+}, the measured values of Ψ_{sp} in basic solution were small (Figure 4.12). As shown in Chapter 7, this was interpreted as due to the occurrence of specific sorption of Ca^{2+} leading to a net lowering of surface charge. These findings were supported by electrophoretic studies of this system, relatively small zeta potentials being measured in basic solution, Figure 4.13.

Titration with NaOH of a dispersion of β FeOOH

β FeOOH is a crystalline oxide hydroxide of Fe^{III} with a hollandite structure. Previous studies showed that this oxide had chloride ion exchange capacity within the pH range 3-11 [2,3,6]. The capacity for chloride ion exchange was a function of both hydrogen and chloride ion activity in the solution phase. This relationship was interpreted as due to a pore mechanism, with positive sites being created on the pore walls by protonation and simultaneous uptake of chloride counterion.

Corrections for the suspension potential were performed on data obtained from a titration of β FeOOH (0.337g in 25ml distilled water) with NaOH. The method of preparation was as in [2], producing β FeOOH with chloride ions within the pores. Activities and uptakes

of hydrogen and chloride were monitored by ISE. The effects of correction for suspension potentials are shown in Figure 4.14. As before, the corrections were small and limited to points at which the ionic strength was relatively low and the surface charge high. Values of calculated suspension potentials from this titration are shown in Figure 4.15. Independent electrophoretic studies on dispersions of β FeOOH gave zeta potential measurements which are shown in the same figure. In both sets of data, the measured potential was positive in acidic solution, with a reversal of sign at around pH 8 and negative values at higher pH. The exchange sites on the external surface (those sites which are responsible for the generation of a surface potential) are therefore amphoteric with a point of zero charge at around pH 8, analogous to the exchange sites of α FeOOH [4]. However, there was no measurable cation exchange capacity for β FeOOH. This can be interpreted as due to the exclusion of sodium counterions from the 5Å hollandite pores of β FeOOH by an ion sieve mechanism.

These findings are of particular relevance to the current discussion of the suspension potential since they demonstrate that the suspension potential is entirely due to the external surface charge of the exchanger. The charge within the pores has little if any effect on the surface potential, hence the generation (in this case) of negative suspension potentials when the oxide has anionic capacity. The suspension potential results are supported by observance of the same effects from zeta potential measurements.

Titration of dispersions of clay minerals

Many clay minerals with a layer structure have cation exchange properties. These materials bear a net negative charge due to isomorphic substitution of cations of higher charge by cations of lower charge within its crystal lattice. The overall charge is balanced by cations co-ordinated between the layers. Some or all of the interlayer cations may be

exchangeable with other cations in solution phase. These materials are therefore fixed charge cation exchangers. The ion exchange properties of these materials and of fired building materials containing residual amounts of clay minerals were studied, with particular reference to the sorption of caesium ion from aqueous solution. These results are presented and discussed in Chapter 5.

Corrections for suspension potentials in these titrations could be performed to a lesser degree of precision than with inorganic oxide titrations, since the ionic composition of the dispersion was known with less confidence (due to slight solubility leading to low concentrations of ions such as silicate). Calculations were performed on the basis of there being an initial anionic background equivalent to the initial sodium concentration in the aqueous phase (since the exchanger had previously been converted to the sodium form it was considered reasonable to assume that the dominant cationic species released into the solution phase would be sodium ion). A second assumption was that the degree of dissolution of the solid did not significantly increase in the course of the titration.

The effects of suspension potential calculations on the results from a typical clay mineral titration are illustrated in Figure 4.16. In this titration 0.5g of the clay mineral Fithian illite in the sodium form was titrated with KCl. Sodium and potassium ion activities and uptakes were monitored by ISE. The figure shows that the suspension potential correction had little effect on the measured uptake of potassium ion in the early stages of the titration, with significant effects only observed at higher solution concentration of potassium. Significant corrections to the release of sodium ion from the clay mineral were seen throughout the titration, as a consequence of the higher concentration of sodium ion in the solution phase.

The sign of the suspension potentials for clay mineral dispersions calculated by this method (with the assumptions as stated above) were generally negative, as expected for a fixed charge cation exchanger. These findings were supported by electrophoretic mobility measurements on suspensions of clay minerals performed in the course of this research. A zeta potential of -36mV was measured for a suspension of particles of the clay mineral vermiculite in distilled water.

4.3.3 Re-analysis of Previously Published Potentiometric Titration Data

In the light of the current research, it was considered worthwhile to re-analyse some previous research on the ion exchange properties of inorganic oxides [2-6]. In these original research papers, the ion exchange processes were investigated using a single pH electrode. As shown in the current research, it is not possible to detect suspension effects in pH or any single electrode titrations. The resultant errors caused in previous work were small but significant and limited to a few points in the titration. In particular the deviations from the common capacity versus pA curve, assigned tentatively to surface charges and interpreted as such, were quantitatively in error. Similar data collected in this research showed the same effect and may be used for illustration, Figure 4.17. As before, the initial titration point was obtained after the uncharged zirconia suspension was treated with dilute acid, thereafter the suspension was titrated with base to alkaline pH and back again with acid. As predicted, anion capacities were a single valued function of pA (= pH + pCl), with the exception of the initial point, as before. The solid curve and points on it represent the true capacity/pA curve. The Figure shows clearly the progressive corrections on this stray point and how they are corrected, firstly due to the erroneous assumption (obligatory in a single electrode pH titration) that in the pure dilute hydro-

chloric acid pH = pCl. The second position closer to the curve uses the experimental pCl from a chloride electrode and so the correct value of pA. (For a system at equilibrium the pA value is constant and independent of position, even close to the particle surface, in regions where the electrical (double layer) potential is large.) The final position, in which all errors are corrected and the point lies on the true pA curve, is based on pH and pCl values recalculated at infinity to remove the suspension effect. The earlier analysis which regarded the difference in capacity as due to surface charge was qualitatively correct, since the suspension effect is entirely due to the deviation from electroneutrality in the aqueous solution close to the particles. These findings again demonstrate the necessity of performing multi-electrode titrations when studying the ion exchange properties of charged colloidal materials.

References

1 P.C. Heimenz, Chapter 12 in Principles of Colloid and Surface Chemistry 2nd edition, Marcel Dekker Inc, ISBN 0-8247-7476-0, (1986)
2 R. Paterson and H. Rahman, J. Coll. Int. Sci., **103**, 106 (1985)
3 R. Paterson and H. Rahman, J. Coll. Int. Sci., **94**, 60 (1983)
4 R. Paterson and H. Rahman, J. Coll. Int. Sci., **97**, 423 (1984)
5 R. Paterson and H. Rahman, J. Coll. Int. Sci., **98**, 494 (1984)
6 R. Paterson and A.M. Smith, J. Coll. Int. Sci., **124**, 581 (1988)

Table 4.1 : Calculation and correction for the suspension potential for a dispersion of calcined monoclinic zirconia (1.39g in 25ml distilled water) after an addition of 1.5ml 0.098M HCl. ISEs for H^+ and Cl^- were used.

Electrode Response (mV)		**Measured p(ion)**		**Uptake (meq/g)**			
H	**Cl**	**pH**	**pCl**	**H^+**	**Cl^-**	**$\sum_i z_i c_i$**	**I**
217.7	125.7	3.1	2.56	0.090	0.051	-.00206	0.0019

	Corrected p(ion)		**Uptake (meq/g)**			
Ψ_{sp}	**pH**	**pCl**	**H^+**	**Cl^-**	**$\sum_i z_i c_i$**	**I**
15.5	2.82	2.82	0.076	0.076	0	0.0016

Table 4.2 : pH and H^+ uptake data from a potentiometric titration of a dispersion of calcined monoclinic zirconia with HCl and KOH. Results are presented before and after correction for the suspension potential. The charge balance in the solution phase (as measured from H^+, K^+ and Cl^- ISEs) and the values of Ψ_{sp} applied to minimize the charge balance are given for each titration point.

measured pH	corrected pH	charge balance solution	measured H uptake	corrected H uptake	Ψ_{sp}
6.087	6.087	0.000	0.000	0.000	0
3.096	2.824	-0.054	0.090	0.076	15.5
3.268	3.031	-0.053	0.081	0.073	13.5
3.524	3.322	-0.053	0.071	0.067	11.5
3.871	3.713	-0.050	0.060	0.059	9
4.347	4.231	-0.045	0.047	0.047	6.6
4.892	4.810	-0.038	0.033	0.033	4.7
5.224	5.157	-0.033	0.026	0.026	3.8
5.562	5.504	-0.031	0.019	0.019	3.3
5.966	5.917	-0.028	0.012	0.012	2.8
6.639	6.601	-0.024	0.005	0.005	2.2
6.981	6.950	-0.021	0.001	0.001	1.8
7.453	7.428	-0.016	-0.002	-0.002	1.45
7.799	7.782	-0.011	-0.006	-0.006	0.95
8.376	8.372	-0.002	-0.013	-0.013	0.2
8.742	8.756	0.009	-0.020	-0.020	-0.8
9.000	9.044	0.030	-0.028	-0.028	-2.5
9.086	9.134	0.046	-0.029	-0.029	-2.75
9.660	9.756	0.096	-0.050	-0.049	-5.5
10.265	10.402	0.148	-0.082	-0.081	-7.83
10.654	10.815	0.189	-0.112	-0.107	-9.15

Titration File : ZIR5

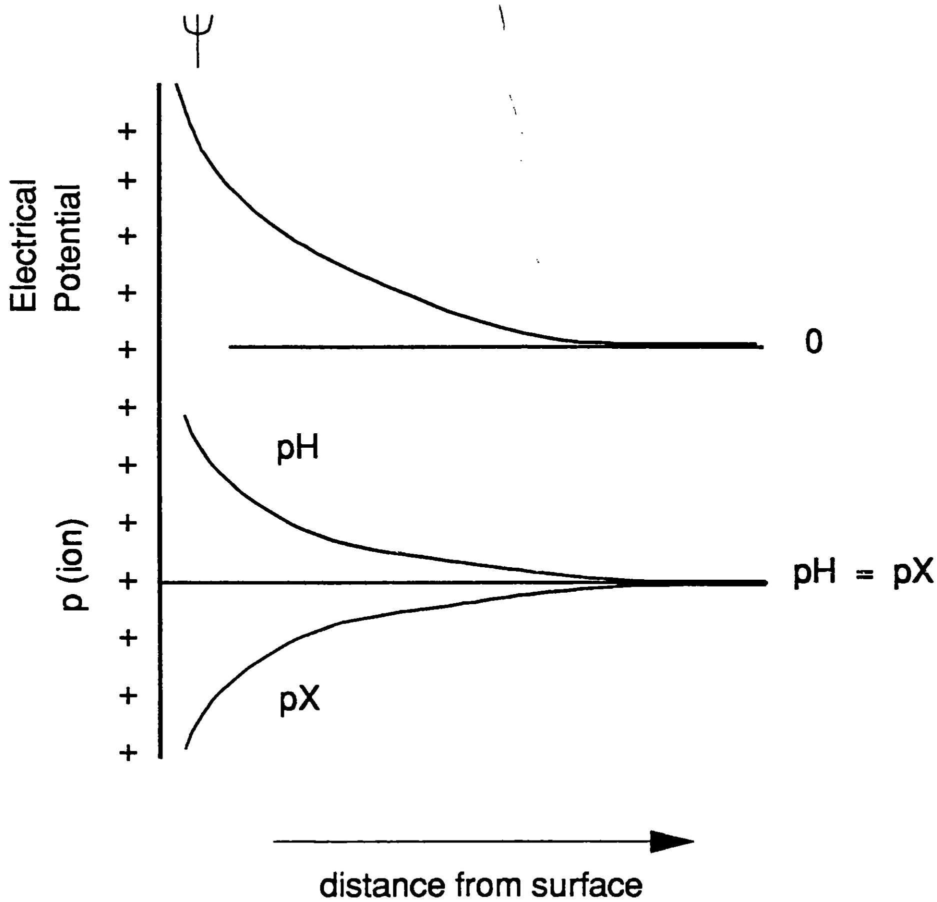

Figure 4.1 : Diagrammatic representation of variation of suspension potential with distance from particle surface for a suspension of positively charged particles in a solution of acid HX. The variation in p(ion) with distance from the particle surface for the ions H^+ and X^- are also shown.

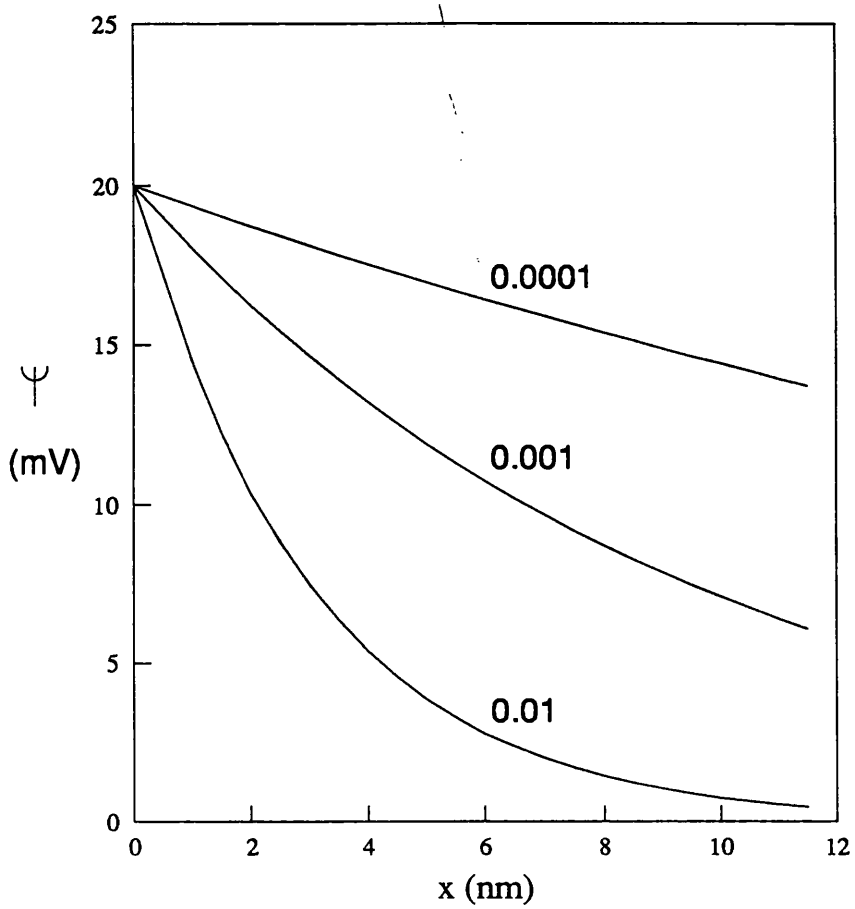

Figure 4.2 : Variation of the potential in the electrical double layer at varying ionic strength (0.0001, 0.001, 0.01M) for a 1:1 electrolyte, as calculated by the Debye-Hückel approximation.

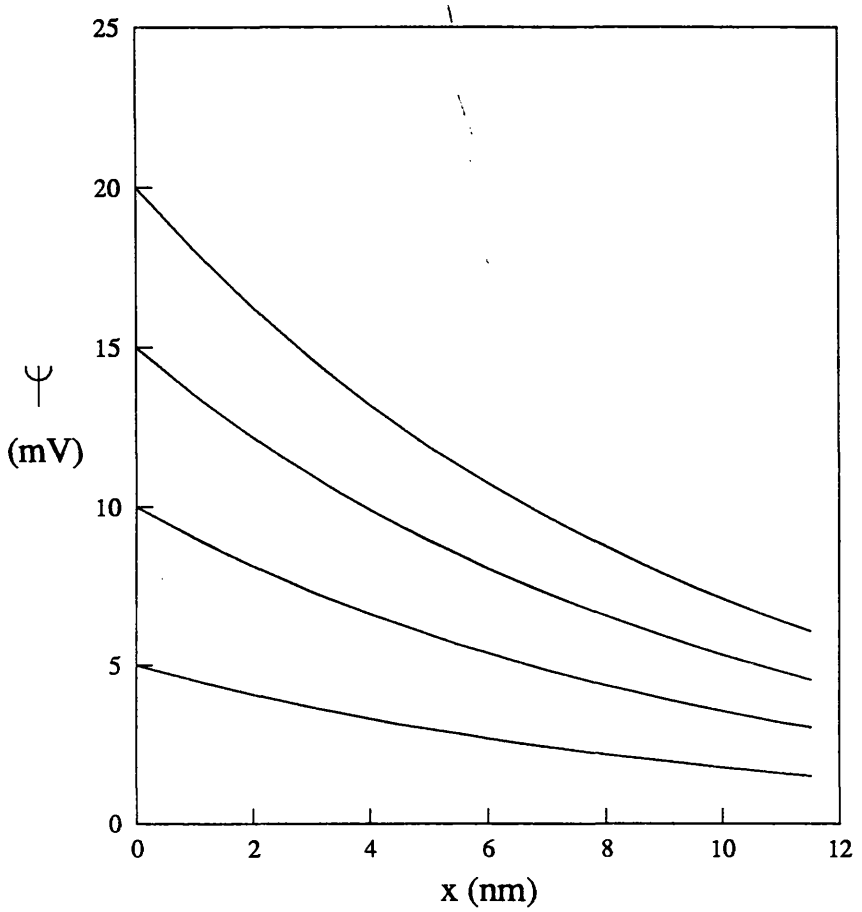

Figure 4.3 : Potential in the electrical double layer for various surface potentials at constant ionic strength of 0.001M (1:1 electrolyte), as calculated by the Debye-Hückel approximation.

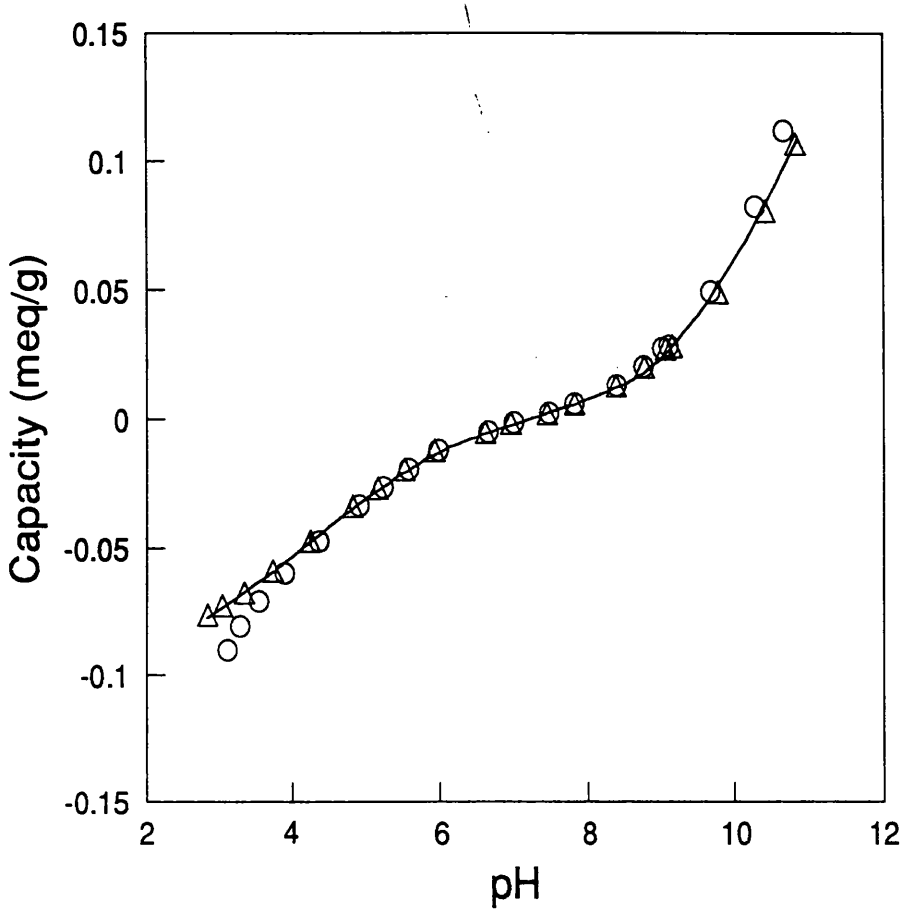

Figure 4.4 : Titration of a dispersion of 1.39g calcined monoclinic zirconia in 25ml distilled water. After an initial addition 1.5ml 0.1M HCl the dispersion was titrated with 0.1M KOH. Ion exchange capacities were calculated from ISE measurements. Results are shown before correction (○) and after correction (△) for Ψ_{sp}.

Titration File: ZIR5

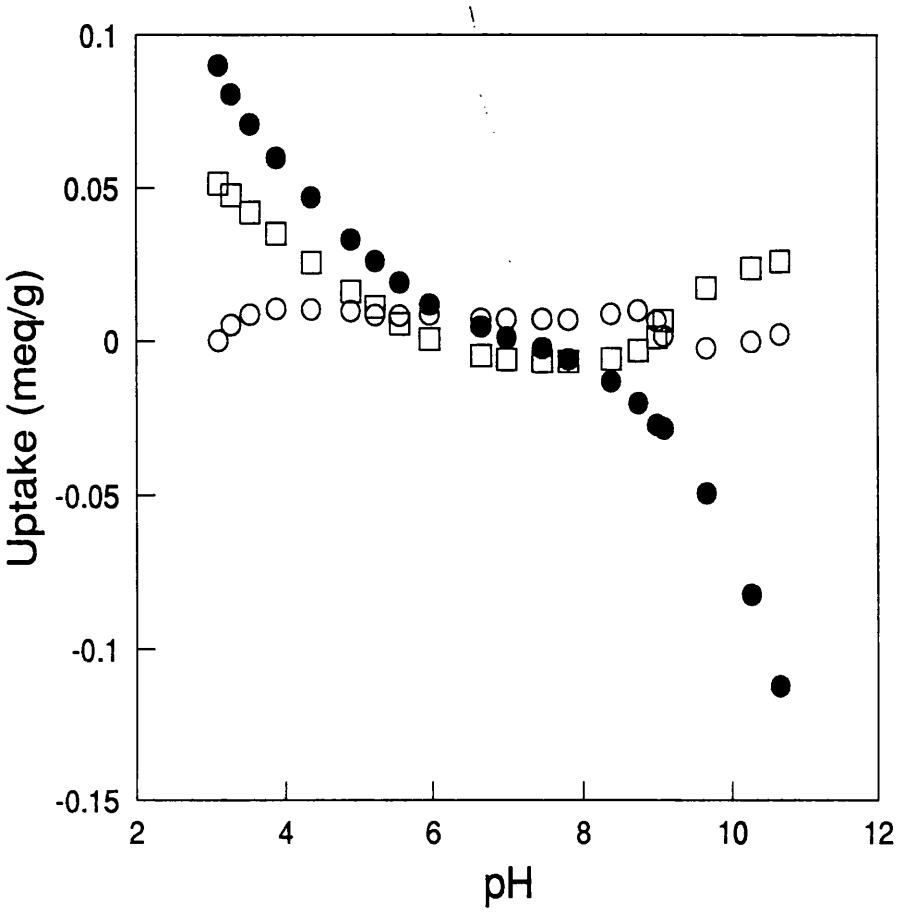

Figure 4.5 : Uptakes of H^+ (●), K^+ (○), Cl^- (□), as calculated by mass balance from ISE data of the titration shown in Figure 4.4. No corrections for the suspension potential have been made.

Titration File: ZIR5

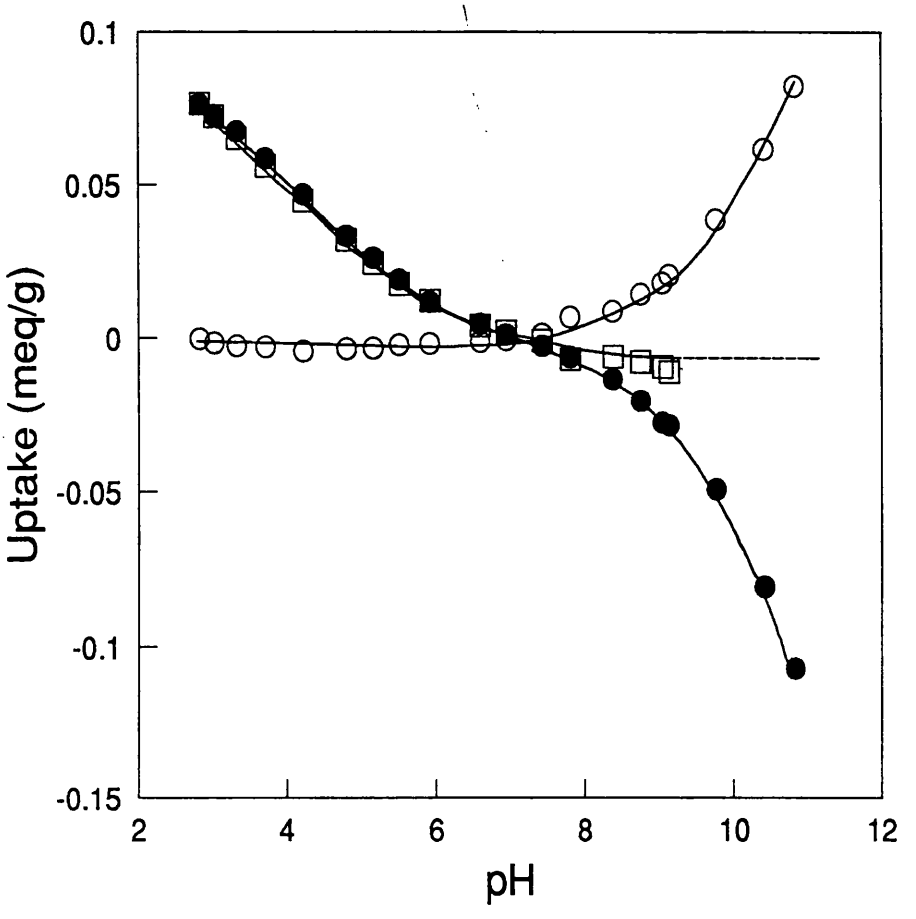

Figure 4.6 : Uptakes of H^+ (●), K^+ (○), Cl^- (□), as calculated by mass balance from ISE data of the titration shown in Figure 4.4, after correction for the suspension potential.

Titration File: ZIR5

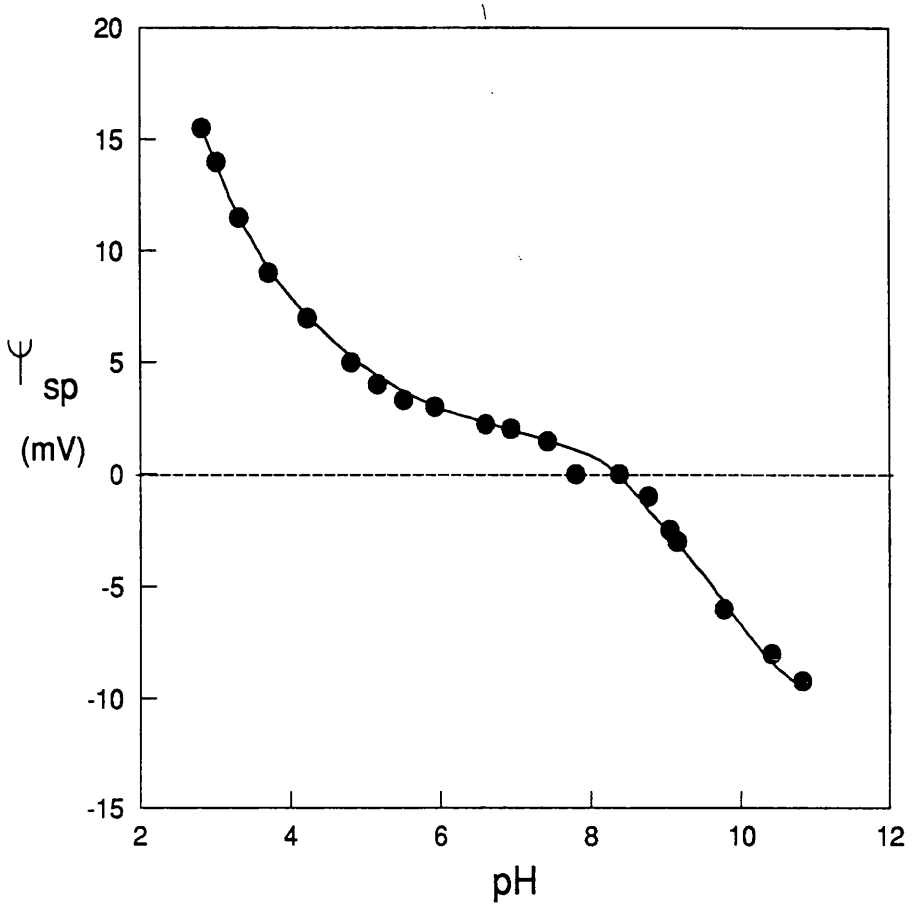

Figure 4.7 : Calculated Ψ_{sp} from the titration of zirconia shown in Figure 4.4.

Titration File: ZIR5

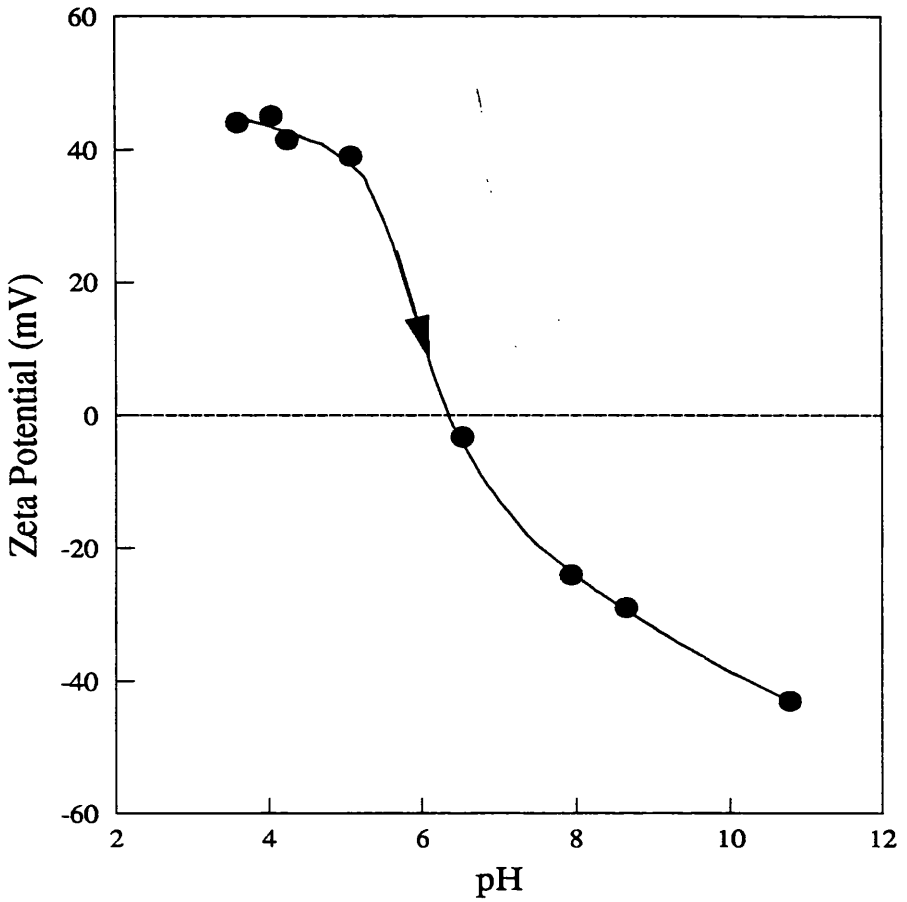

Figure 4.8 : Zeta potential measurements for particles of non-calcined zirconia. Results were obtained by sampling from a dispersion of non-calcined zirconia in distilled water (initially 0.0203g in 50ml), titrated with NaOH after initial addition of HCl. Activities of all ions were monitored by ISE. The ionic strength of the solution phase increased from an initial value of 3.7×10^{-4} at pH 3.6 to a final value of 1.33×10^{-3} at pH 10.8 in the course of the titration.

Electrophoretic File : EZRNACL

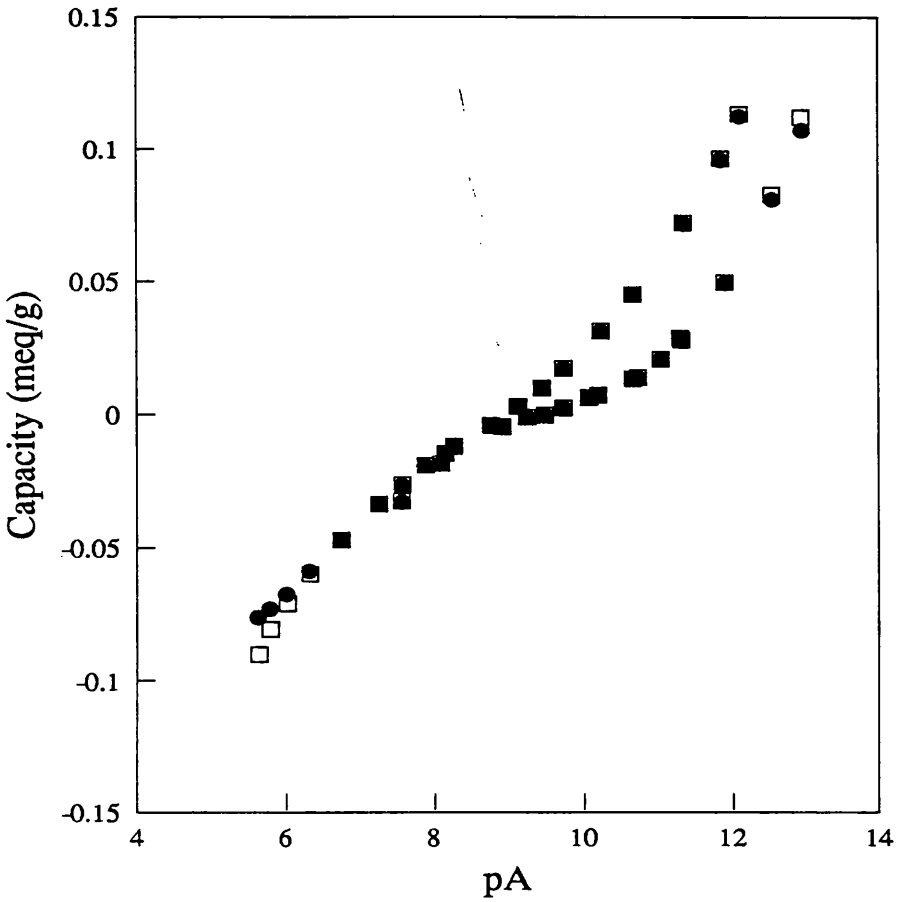

Figure 4.9 : Ion exchange capacities of calcined monoclinic zirconia on titration with HCl, KOH and KCl, plotted as a function of pA. Results are shown before correction (□) and after correction (●) for Ψ_{sp}.

Titration File: ZIR5

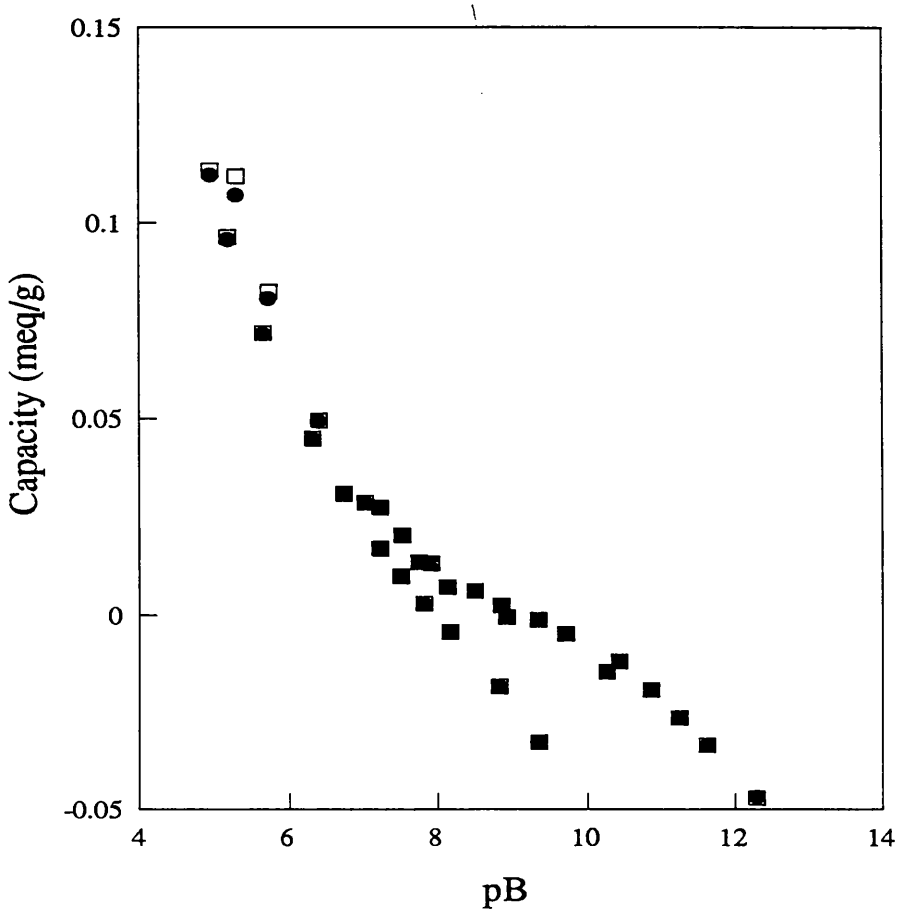

Figure 4.10 : Ion exchange capacities of calcined monoclinic zirconia on titration with HCl, KOH and KCl, plotted as a function of pB. Results are shown before correction (□) and after correction (●) for Ψ_{sp}.

Titration File: ZIR5

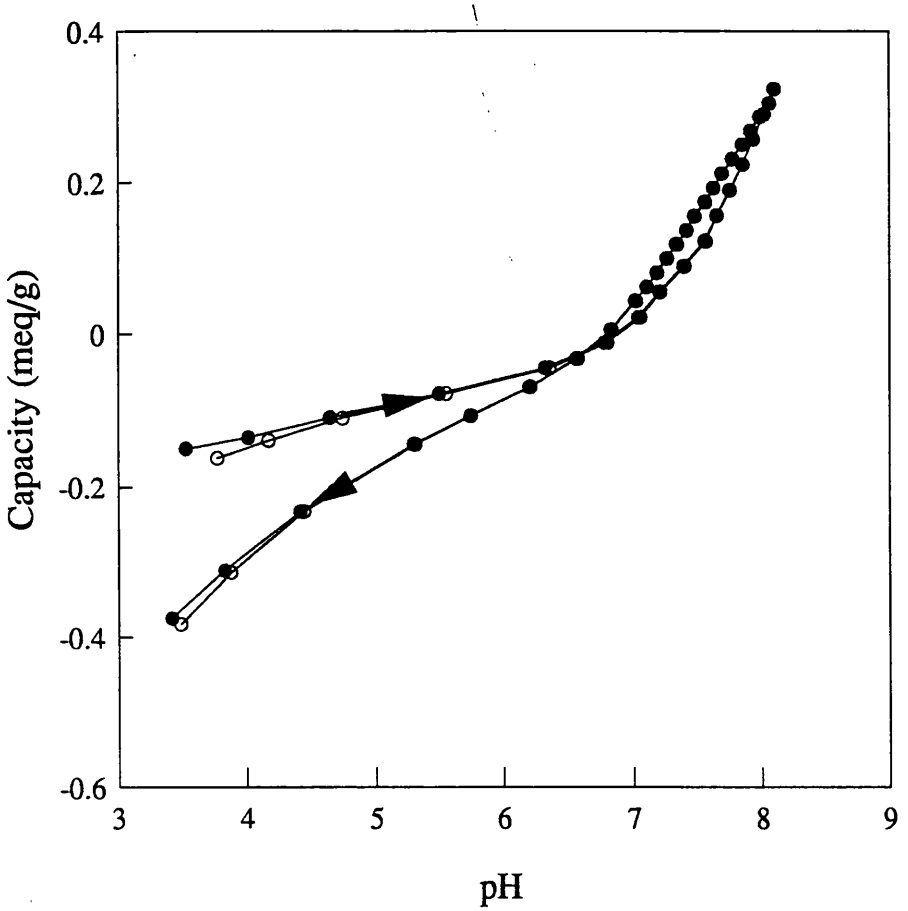

Figure 4.11 : Titration with 0.018M $Ca(OH)_2$ and 0.1M HCl of a dispersion of 0.263g non-calcined monoclinic zirconia in 25ml distilled water. Ion exchange capacities were calculated from ISE measurements. Results are shown before correction (○) and after correction (●) for Ψ_{sp}.

Titration File: NZR5

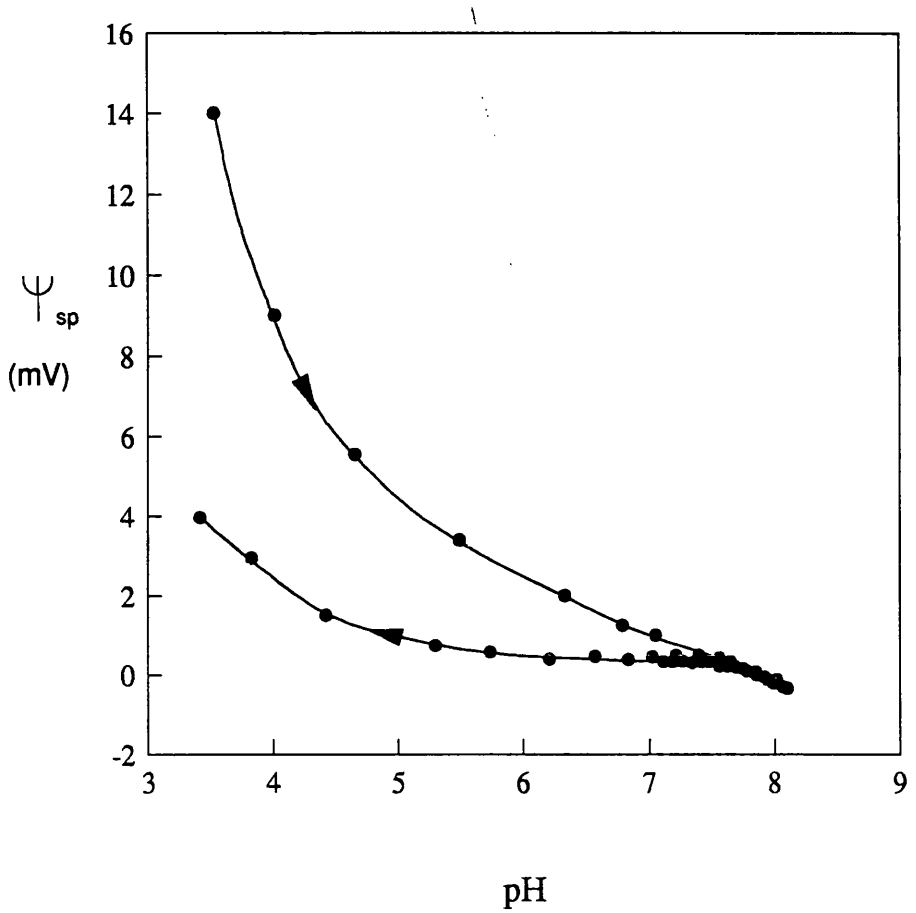

Figure 4.12 : Calculated Ψ_{sp} from titration of zirconia with HCl and $Ca(OH)_2$ shown in Figure 4.10.

Titration File: NZR5

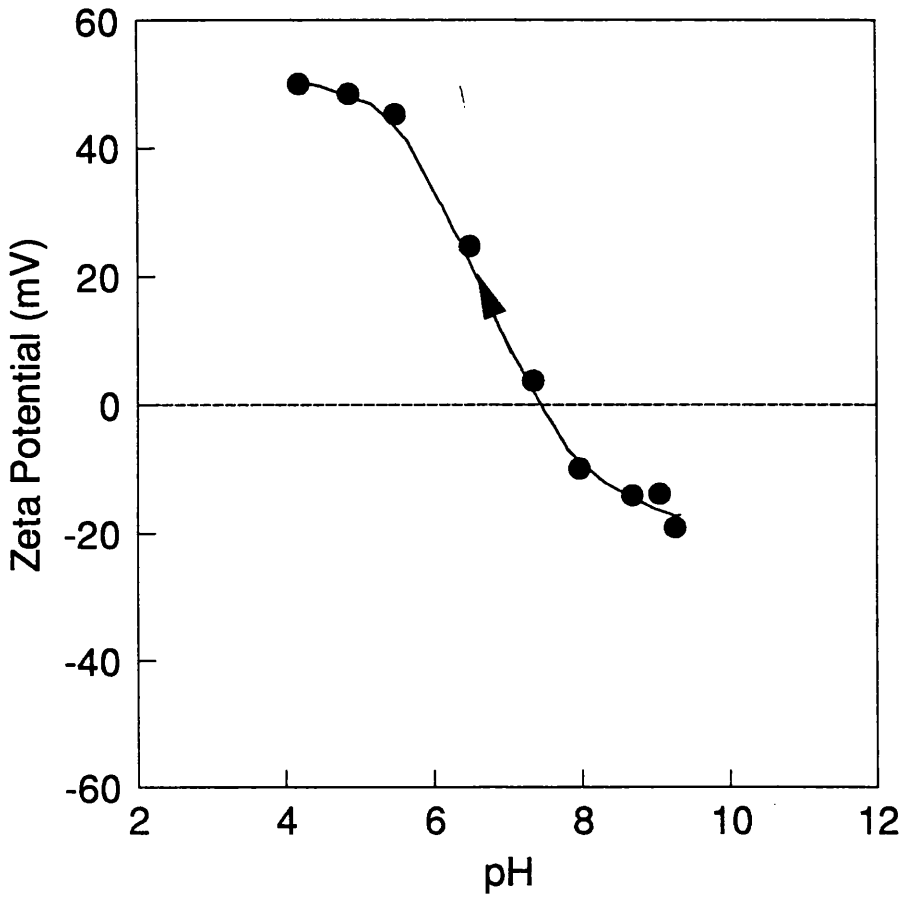

Figure 4.13 : Zeta potential measurements for particles of non-calcined zirconia dispersed in distilled water (initially 0.0206g in 50ml) and titrated with HCl after an initial addition of $Ca(OH)_2$. Activities of all ions were monitored by ISE. The ionic strength of the solution phase increased from an initial value of 1.84×10^{-4} at pH 9.26 to a final value of 6.01×10^{-4} at pH 4.20, with calcium ion concentration varying between $8.75 \times 10^{-5} M$ and $1.54 \times 10^{-4} M$.

Electrophoretic File : EZRCACL

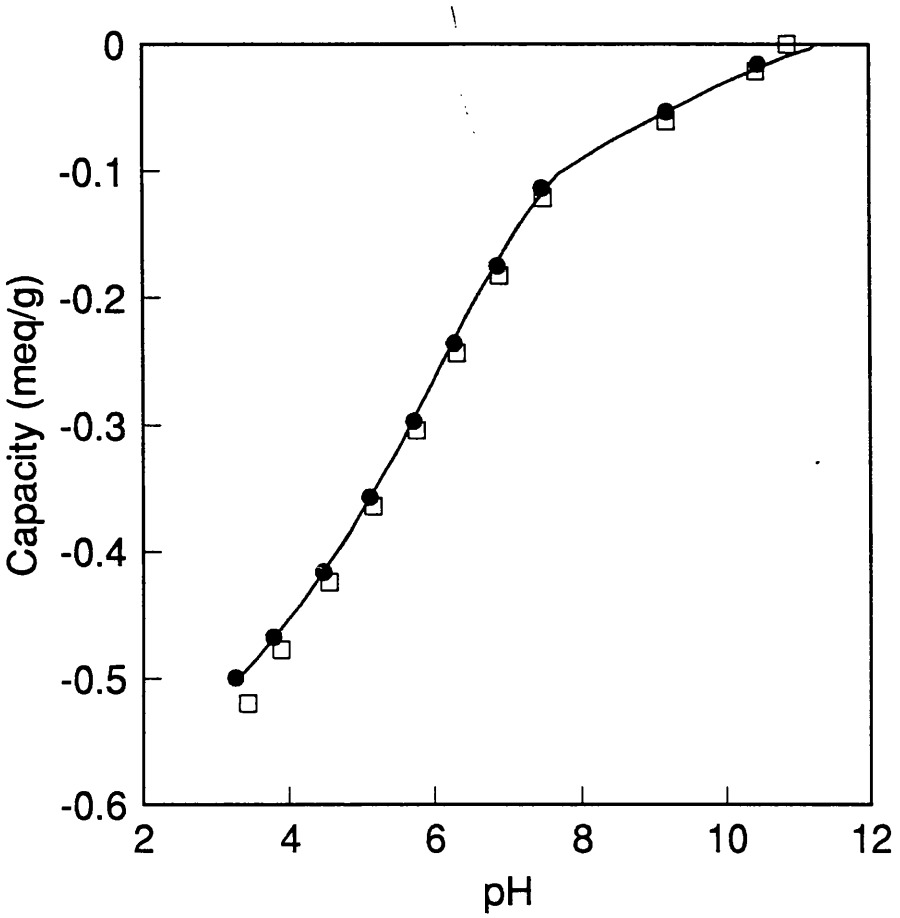

Figure 4.14 : Titration with 0.1M NaOH of a dispersion of 0.376g β FeOOH. Ion exchange capacities were calculated from ISE measurements. Results are shown before correction (□) and after correction (●) for suspension potential.

Titration File: FE1

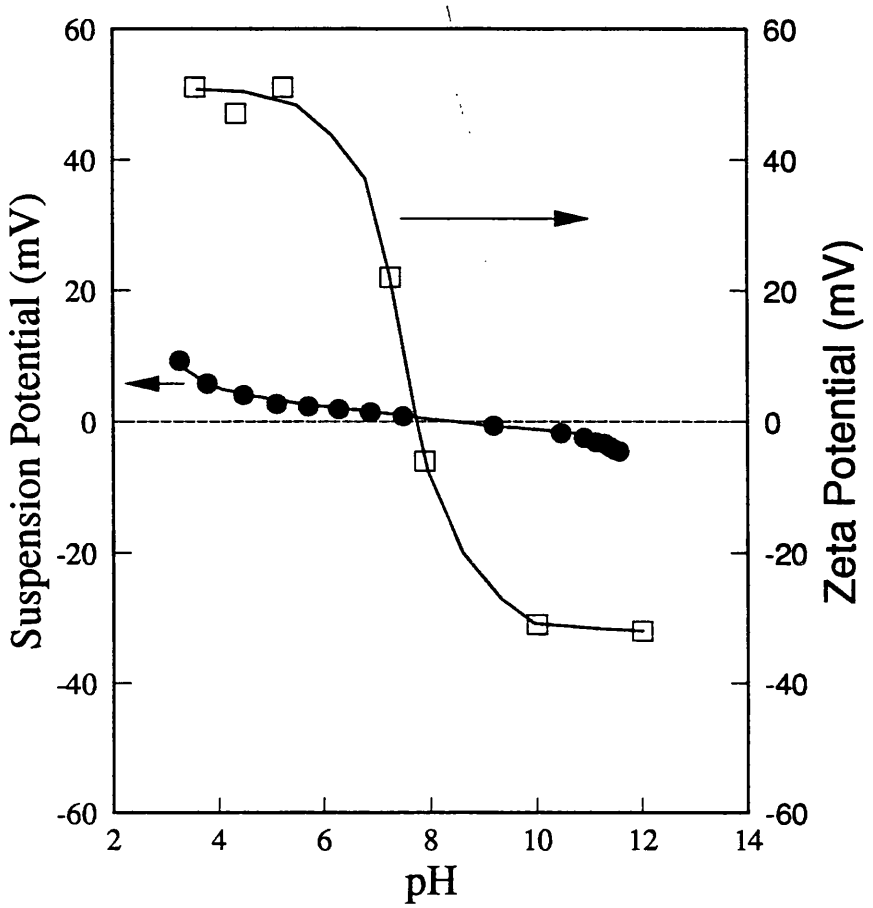

Figure 4.15 : Ψ_{sp} and zeta potential measurements on BFeOOH. Suspension potentials were obtained from the titration shown in Figure 4.12. Zeta potentials were obtained from electrophoretic mobility measurements on particles of βFeOOH dispersed in distilled water. Dispersion pH was adjusted by additions of 0.1M NaOH. For the electrophoretic studies the ionic strength of the dispersion varied between 3.57×10^{-4} (at pH 3.55) and 0.012 (at pH 12).

Titration File: FE1
Electrophoretic File: EPBFE1

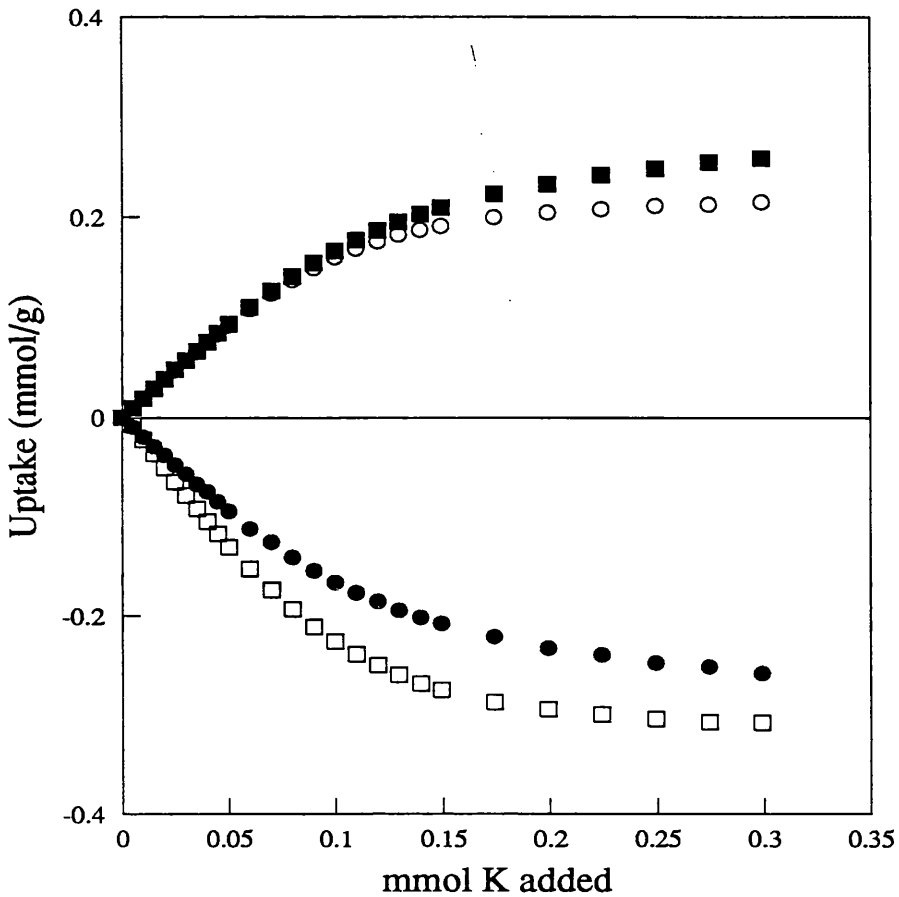

Figure 4.16 : Titration with 0.1M KCl of a dispersion of 0.511g Fithian Illite (Na^+ form) in 25ml distilled water. Equilibrium solution activities of K^+ and Na^+ were monitored by ISE. Ion uptakes before correction (K^+ ○, Na^+ □) and after correction for the suspension potential (K^+ ●, Na^+ ■) are plotted as a function of millimoles of potassium ion added to the dispersion.

Filename: MILLR#2

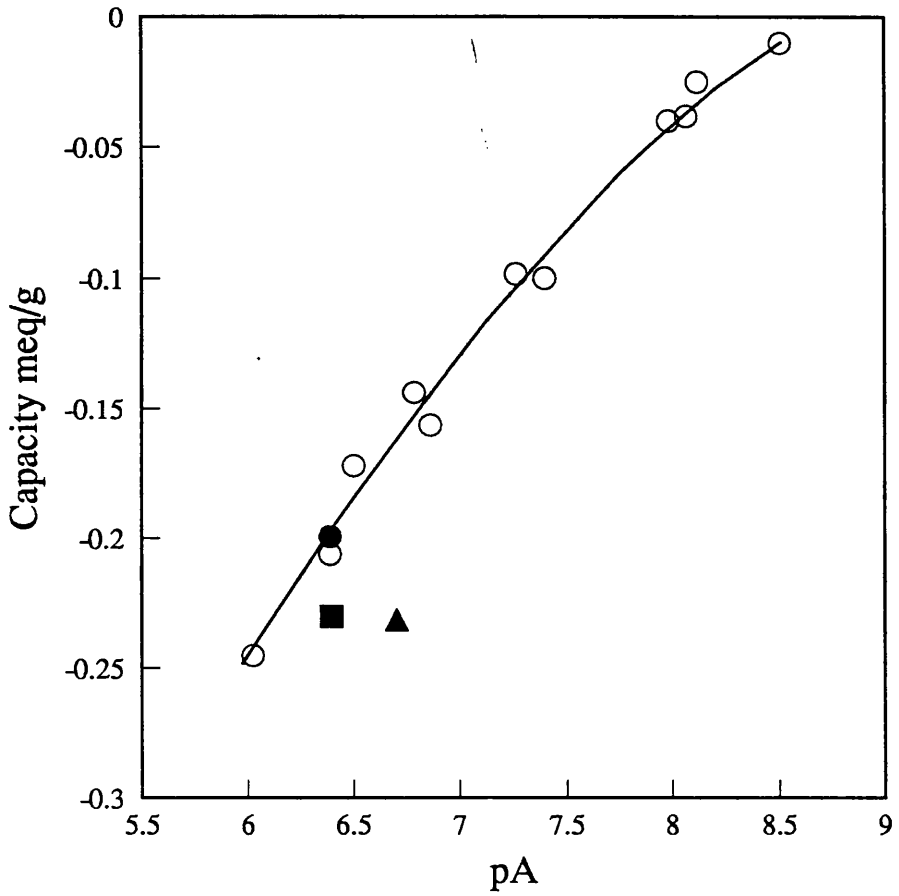

Figure 4.17 : Demonstration of the effect of the suspension potential. 0.16g of non-calcined zirconia was dispersed in 25ml water and titrated with 0.1M HCl and 0.1M NaOH. The true capacity/pA curve is shown, with experimental data (○). The initial titration point was obtained after addition of 0.5ml 0.1M HCl. Results for the initial titration point are shown for:

(a)single pH electrode titration, with the assumption that pCl = pH = 3.35 (▲).

(b)titration with pH electrode and chloride ISE, giving the correct value of pA (pH = 3.35, pCl = 3.05, pA = 6.4)(■).

(c)correction to remove the suspension effect (●).

Filename: OLDZIR

CHAPTER 5

ION EXCHANGE PROPERTIES OF ALUMINOSILICATE MATERIALS

Introduction

The ion exchange characteristics of a wide range of ion exchangers of the aluminosilicate type were studied using the potentiometric titration methods described in Chapter 3. As stated in Chapter 1, the research presented in this Chapter was performed in the course of a European Community Post-Chernobyl Action on the Improvement of Practical Countermeasures Against Nuclear Contamination in the Urban Environment (Contract No. B16-0270.UK(H)). Early studies on Chernobyl deposition showed that many urban surfaces had considerable potential for intercepting and retaining radiocaesium [1,2]. The aim of this research was to identify the urban surfaces which selectively adsorb radiocaesium and to determine the mechanisms of sorption, the total caesium binding capacity and its ease of displacement on these surfaces. To perform these studies, an electrode sensitive to caesium ion was developed, tested and used in the course of this work. Additionally, ion exchange processes involving common cations such as Na^+ and K^+ were also investigated.

To achieve a detailed assessment of the sorption of radiocaesium on urban surfaces, it was necessary to study the sorption of caesium on the constituent clay minerals, in addition to the urban surfaces themselves. While a considerable amount of work has already been done in this area, this new work provided detailed information of the ion exchange processes by the direct monitoring of all ions involved. The titration method also had the advantage of being considerably more rapid than traditional batch equilibration methods.

5.1 Aluminosilicates as Ion exchangers

Clay minerals are layer-lattice silicates, formed from the weathering of igneous rock. They consist of the stacking of sheets of tetrahedral ZO_4 (Z = Si or Al) with sheets of octahedral YO_4 (Y = Al, Mg, Fe, ...) into either 1:1 or 2:1 layer structures. The layers may be separated by interlayer materials such as cations, hydrated cations and metal hydroxides.

Most clay minerals demonstrate some ion exchange properties. Exchange capacities may be attributed to three principal causes :

a. Around the edges of the layers, broken bonds give rise to unsatisfied charges which may be balanced by adsorbed cations.
b. The hydrogens of exposed hydroxyl groups may be replaced by exchangeable cations. Anion exchange may also be occur on these sites.
c. Isomorphic substitution of cations of higher charge by cations of lower charge within the crystal lattice, which results in the clay mineral bearing an overall, fixed, negative charge. This charge is balanced by exchangeable or non-exchangeable cations.

Of these, by far the most significant contributory factor to ion exchange capacity is isomorphic substitution. This phenomenon occurs with many clay minerals with the double-layer structure. Consequently, many clay minerals of this type have considerable cation exchange capacities, whereas those minerals with single layer structures, where isomorphic substitution is rare, generally have low exchange capacities.

The mineralogy and chemical composition of urban surfaces are extremely varied. A distribution can be made between two broad classes of materials. The first class includes the various types of rock, including sedimentary, metamorphic and igneous rock, which

may be used, as such, as building materials or as crushed aggregates in mortar and concrete. The second class includes inorganic and organic man-made materials. The inorganic materials are mostly silica-based - including bricks, clay tiles, cement, mortar and concrete. The organic man-made materials include paints and bituminous or asphaltic materials.

The mineralogy of rocks is diverse, including materials which are relatively inert such as quartz and feldspars, a broad range of micas, clay minerals and zeolites, chemical minerals (carbonates, sulphates, sulphides) and some oxides (of iron, titanium, aluminium). For fired clay products, the mineralogy is varied, depending on the composition of the raw materials and the temperatures and duration of firing. The main constituents are a broad range of aluminosilicates, including feldspars, quartz and oxides of aluminium, iron, magnesium, calcium and titanium. The main mineral component of set cement is tricalcium disilicate hydrate, known as tobermorite. In addition, rock aggregates represent an important element in mortar and concrete.

Examination of the overall composition of these various materials revealed that most were characterised by the presence of components which are known to exhibit ion exchange properties. Accordingly, it might be expected that many of these materials would be selective towards caesium ion. Of particular importance was the nearly universal presence of micaceous materials, well-known for their fixation of caesium.

When discussing the sorption of caesium ions on clay minerals and urban surfaces, it is important to make distinctions with regard to the loading of caesium. There is considerable evidence for the existence of a small number (<1% of the total cation exchange capacity) of exchange sites which demonstrate extremely high selectivity for caesium ions - approximately 2000 times more selective for Cs^+ than the other sites (the macrosites) [3,4,5]. These highly selective microsites are thought to be located at frayed edges of the

layers of the minerals. Due to the exceptionally low exchange capacities of these sites, the only suitable technique for their study involves the use of ^{137}Cs radiotracer and a masking technique (using complexes such as silver thiourea, AgTU) to block out the effect of the much greater number of macrosites. Such experiments were performed in parallel research at the University of Leuven in parallel research as part of the Post-Chernobyl Improved Countermeasures Against Urban Contamination [6]. The significance of those results in relation to the research presented here will be discussed at the end of this Chapter. The research in this Chapter is concerned with the ion exchange behaviour of the macrosites of clay minerals and urban surfaces.

5.2 Caesium Ion Selective Electrode

The development of an accurate and reliable caesium selective electrode was central to this work, allowing caesium sorption onto building materials to be monitored and their caesium binding potentials assessed.

One of the most successful of modern ion selective electrodes (ISE) is the potassium valinomycin electrode [7,8]. Valinomycin itself is a natural antibiotic which complexes potassium specifically, rendering it soluble in the lipid layers of biological membranes [9]. The effective selectivity of valinomycin for potassium over sodium exceeds 10000:1. Potassium ion is selected partly on the basis of its size and partly due to its somewhat "hydrophobic" character, which makes it prefer a less polar medium than water. In these respects, caesium ion is similar to potassium and biologists report that valinomycin also has a high selectivity for caesium and rubidium ions. It was decided, therefore, to examine the characteristics of a valinomycin based electrode which, when used in conjunction with potassium extraction techniques, could be used to probe caesium concentration in solution.

Valinomycin based potassium ion selective electrodes are commercially available. The caesium ion electrode was prepared by immersing the valinomycin based Orion™ potassium selective electrode (model 93-19) in 0.25M caesium chloride for twelve hours, then transferring into a fresh 0.001M caesium chloride solution in which it was subsequently stored, when not in use. The electrode was ready for use as a caesium electrode after four hours. The internal electrolyte in these commercial electrodes is potassium chloride, but extensive leaching tests showed that there was no potassium leakage from the interior compartment of the electrode into test solutions. No further modification of the commercial electrode was necessary. The reference electrode used in all studies was the Orion model 90-02 double junction reference electrode, with the outer chamber filled with 0.12M NaCl saturated with AgCl, since in this application there must be no contamination of test solution with potassium salts.

The electrode response to added aliquots of caesium ion was monitored by measuring the e.m.f. over a range of concentrations of CsCl at 25°C. The results of a typical titration of CsCl into water are shown in Figure 5.1. A linear relationship between voltage and the negative logarithm of the concentration of caesium ions was observed within the concentration range 10^{-1} to 10^{-5}M CsCl. Analysis of the titration showed that the electrode had Nernstian behaviour (a slope of 59.16 mV ± 5% per -log [Cs] unit). The electrode response time was short, with stable readings obtained within 10 seconds after addition of CsCl solution to the stirred solution, Figure 5.2. This electrode was unaffected by changes in ionic strength up to 1M in NaCl media and so can be used directly to determine concentrations, without the need for activity corrections.

All measurements using ion selective electrodes are subject to interferences caused by the presence of other cations, if present at high enough levels. The interference produced by a particular cation was determined by monitoring the caesium electrode response in

solutions of known caesium concentration, with varying background levels of interfering ion. A caesium ion selective electrode, calibrated as described previously, was immersed in a standard solutions of 10^{-3}M CsCl at 25°C. Increasing amounts of interfering cation were added to the standard solution using a microsyringe and the change in potential determined. The new concentration of caesium was calculated after each addition, taking into account changes in volume. Electrode selectivity coefficients for caesium ion over the interfering ion were then calculated [10].

The selectivity coefficients were evaluated for the following interfering cations,- Na^+, NH_4^+, K^+, H^+, Ca^{2+}. Results are presented in Table 5.1, along with the corresponding selectivity coefficients of other caesium ion selective electrodes. In all respects other than selectivity over potassium, only the bis crown ether based electrode [11] matches the overall performance of the valinomycin electrode. Furthermore, for the current application of the caesium selective electrode, none of these electrodes would be suitable for use on unextracted samples due to interferences from potassium ions released by the material. A procedure for extraction of potassium would be necessary in all cases.

No evidence of anion interference (Cl^-, OH^-) on the electrode response was observed. pH effects were monitored by calibrating the electrode in solutions of varying pH. No interference was observed in alkaline solution, while in solutions of increasing acidity there was increasing interference, due to the increase in hydrogen ion concentration (Figure 5.3).

The results demonstrate that the valinomycin based electrode is a first class, readily available caesium ion sensor, with near ideal response in the range 10^{-1} to 10^{-5}M in aqueous caesium ion. The electrode showed good selectivity for caesium over other cations (with the exception of potassium) and was unaffected by pH in neutral and alkaline solutions. It displayed similar characteristics to the original potassium-valinomycin electrode, one

of the best electrodes commercially available. The only major restriction to the use of the caesium-valinomycin electrode was that is could not be used in the presence of potassium ion. Accordingly this electrode was used for the titration of mineral samples from which potassium ion had previously been extracted.

5.3 Sample Preparation

All samples of building materials and clay minerals were wet ground in a M^{c}Crone™ micronising mill for thirty minutes and analyzed in a particle size analyzer (Malvern Mastersizer™) to determine particle size and size distribution. A mean particle size of 2-3μm was obtained in all cases, independent of the material being ground.

Samples were extracted, using a modified version of the technique of Scott and Reid [17], which replaced all exchangeable potassium ions with sodium ions. The ground sample was dispersed for four days in a solution 0.05M in sodium tetraphenylboron and 1M in NaCl. The volume of solution was chosen such that there was approximately a five times excess of tetraphenylboron over the expected exchangeable potassium content in the sample. A precipitate of potassium tetraphenylboron was formed. An equivalent amount of acetone was added to the dispersion to dissolve the potassium tetraphenylboron precipitate. The mixture was then centrifuged, followed by successive washing and centrifuging with acetone/0.1M NaCl, 0.1M NaCl and finally, distilled water. Washings were retained for analysis by flame photometry.

5.4 Procedure for the Study of the Ion Exchange Properties of Aluminosilicate Materials by Potentiometric Titration

A known weight of exchanger, prepared as described previously, was dispersed for twenty-four hours in 25ml distilled water or supporting electrolyte of known concentration. The weight of exchanger used was chosen in order to optimise the precision of uptake measurements. This necessitated several initial experiments for each sample in order to gain an indication of the magnitude of exchange capacity. For samples with low capacity, larger weights were used. The range of sample weight used varied between 0.25g and 2g.

Typically, the dispersions were titrated with standardised solutions of caesium chloride or potassium chloride, using the automated titration system described in Chapter 3. Solution activities of caesium and sodium ions were monitored throughout the titration by the respective ion selective electrodes. Where appropriate, the activities of hydrogen, calcium or chloride ions were additionally monitored by ISE.

5.5 Results and Discussion

5.5.1 Ion Exchange Characteristics of Clay Minerals

The ion exchange characteristics of a number of clay minerals, particularly those which were known or were suspected to have particular affinity for caesium ion, were determined using the potentiometric titration method.

The clay minerals used in this research were supplied by Ward's Natural Science Establishment Inc., Rochester, New York.

The hydrous mica, illite, is a widely distributed clay mineral commonly found in sedimentary rock. It has a non-expanding layer structure, with the interlayer charge balanced by alkali ions co-ordinated between the 2:1 layers. In this research illite no.35 from Fithian, Illinois was used.

Montmorillonite is a member of the smectite group, with charged 2:1 layers and interlayer cations. Beidellite montmorillonite no.23 from Arizona was used.

Vermiculite is a 2:1 layer silicate clay mineral belonging to the mica group.

Kaolinite, a member of the kaolin group, is a silicate mineral with uncharged 1:1 layers. Kaolinite no.4 from Georgia was used in this work.

Fithian Illite

Samples of Fithian illite were ground and extracted, as described. About 0.5g of sample was accurately weighed and dispersed in 25ml distilled water for 24 hours prior to titration. Since the extraction process replaced all exchangeable cations with sodium ions, the concentration of sodium and caesium ions in solution were monitored by ISE throughout all titrations with CsCl. On addition of CsCl, the amount of caesium ion measured in the equilibrium solution was negligible in the early stages of the titration (Figure 5.4), indicating uptake of caesium ion. At later stages of the titration, significant amounts of caesium ion were measured in solution and a point was reached at which all subsequent additions of caesium ion resulted in equivalent increases in the amount of caesium ion observed in equilibrium solution, indicating no further uptake. Using the principles of mass balance, this result was expressed as an uptake (in meq/g) of caesium ion by the exchanger. Uptake of caesium increased until the cation exchange capacity of 0.29 meq/g was reached, beyond which there was no further uptake. Readings obtained from the sodium ISE showed that throughout the titration there was a stoichiometrically equivalent release of sodium ion for uptake of caesium ion. The symmetry of the exchange curves for each ion, shown in Figure 5.5, demonstrated that the sorption of caesium on illite occurs by a stoichiometric ion exchange process:

$$\overline{Na^+} + Cs^+ \rightleftharpoons \overline{Cs^+} + Na^+ \qquad \textbf{(5.1)}$$

The stoichiometry of the observed uptake of caesium ion and release of sodium ion confirmed that electroneutrality was maintained within the clay mineral. Furthermore, since no ions other than Na^+ and Cs^+ were involved in the exchange process,

confirmation was obtained that the sample pretreatment method had efficiently converted the illite sample to the sodium form, with all available exchange sites being occupied by sodium ion after the pretreatment process.

Cation exchange capacities of Fithian illite, measured by various methodologies, are given in Table 5.2 [18-24]. There is some variation in the illite CEC values quoted due to differences in illite source, index cation used, measurement methods and other experimental variables. However, the cation exchange capacity obtained by the current method is in good agreement with these results.

Similar titrations of dispersions of Fithian illite were performed with potassium chloride replacing caesium chloride as titrant and using potassium and sodium ISEs. Simultaneous uptake of potassium ion and release of sodium ion was observed, again demonstrating the occurrence of sorption by ion exchange. The two titrations, with caesium and potassium as sorbing ions respectively, are compared in Figure 5.6. To enable direct comparison, uptakes are plotted against the cationic fraction in solution of the respective sorbing ion, $[Cs^+] / ([Cs^+] + [Na^+])$ or $[K^+] / ([K^+] + [Na^+])$. The greater selectivity shown by illite for caesium is evident from the higher uptakes for caesium at equivalent cationic fractions.

In Chapter 2 the expression for the selectivity coefficient of an ion exchange process was given as

$$K_A^B = \frac{\overline{C_B}^{|z_A|} \; C_A^{|z_B|}}{\overline{C_A}^{|z_B|} \; C_B^{|z_A|}} \qquad \textbf{(2.11)}$$

Selectivity coefficients were calculated from titration data. It was convenient to use an equivalent fraction scale for the solid phase terms in eqn. 2.11. Since only monovalent

exchange processes were studied in this research, the choice of concentration scale did not affect the value of the calculated selectivity coefficient, since molar and rational selectivity coefficients are equivalent in these cases.

Equilibrium solution concentrations of the two cations involved in the exchange process (sodium and either caesium or potassium) were measured at each titration point by ISE. For the ion exchange process between Cs^+ and Na^+ with the exchanger initially in the Na^+ form, the equivalent fraction of sorbing cation (for example caesium, $\overline{X}_{Cs}$) in the exchanger was given by

$$\overline{X}_{Cs} = \frac{Cs_{uptake}}{C.E.C.} \tag{5.2}$$

where $C.E.C.$ is the cation exchange capacity (meq/g) of the exchanger.

The equivalent fraction of sodium ion in the exchanger was calculated from

$$\overline{X}_{Na} = \frac{C.E.C. + Na_{uptake}}{C.E.C.} \tag{5.3}$$

Since Na^+ is being released from the exchanger, Na_{uptake} is negative.

The selectivity coefficient K_{Na}^{Cs} was then calculated from

$$K_{Na}^{Cs} = \frac{\overline{X}_{Cs}\ [Na]}{\overline{X}_{Na}\ [Cs]} \tag{5.4}$$

Analogous calculations were used to obtain K_{Na}^{K}, the selectivity coefficient for the K^+ for Na^+ exchange process. These procedures were applicable within the fractional

loading range 0.2 to 0.8, since at either extreme of the loading range relatively small measurement inaccuracies would produce large effects on the calculated selectivity coefficient.

An estimate of the selectivity coefficient K_K^{Cs} for the exchange reaction Cs^+ for K^+ at 50% conversion was obtained from the ratios of K_{Na}^{Cs} and K_{Na}^{K} as measured at 50% conversion.

In Figure 5.7 the measured selectivity coefficients for the exchange reactions Cs^+ for Na^+ and K^+ for Na^+ are shown as a function of $\overline{X}_{Na}$. At 50% conversion to the Cs^+ form, K_{Na}^{Cs} was 70.6, whilst at 50% conversion to the K^+ form, K_{Na}^{K} equalled 16.6. The value of K_K^{Cs} at 50% conversion was estimated to be 4.5. These results give a general order of selectivity $Cs^+ > K^+ > Na^+$, characteristic for ion exchange processes on clay minerals. The selectivity coefficients for illite obtained in this study agree well with published values over the same fractional loading range [18,25]. It should be noted that the selectivity coefficients calculated by the present method were obtained over the fractional loading range 0.2 - 0.8. The quoted literature data refers to a corresponding fractional loading range. At lower loadings, considerably different selectivities may be observed.

Distribution coefficients K_d (ml/g) were calculated by dividing the uptake of the sorbing cation by its concentration in solution. In Figure 5.8 K_d values obtained from each titration of illite are plotted against pCs (pK). The general trend of high K_d at low ion concentration, with a gradual decrease as the solution concentration of the sorbing ion increases, is again characteristic of ion exchange processes on clay minerals. The higher selectivity for Cs^+ is again apparent from these results. (It should be noted, however,

that in these titrations the concentration of the competing ion, Na^+, increases as the titration proceeds. The increase in competing ion concentration will cause K_d for Cs^+ to decrease.)

Montmorillonite and Vermiculite

Similar studies were performed on dispersions of the clay minerals montmorillonite and vermiculite. Dispersions of each were titrated with both caesium chloride and potassium chloride and ion activities and uptakes monitored by caesium (or potassium) and sodium ISEs. Uptake data for montmorillonite and vermiculite titrations with CsCl are shown in Figures 5.9 and 5.10. As with illite titrations, uptake of caesium ion was accompanied by a stoichiometric release of sodium ion. Cation exchange capacities were measured as 0.52 mmol/g for montmorillonite and 1.20 mmol/g for vermiculite, in good agreement with literature quoted capacities [19,26]. The larger exchange capacities are characteristic for clay minerals with a double layer, expanding lattice structure.

On titration with KCl, uptake of potassium and release of sodium was observed with both clay minerals, with the uptake of potassium being less than that of caesium at equivalent ionic fractions in the solution phase, Figures 5.11 and 5.12. This indicated the greater selectivity shown by both materials for caesium over potassium. Selectivity coefficients for the exchange processes of Cs^+ for Na^+ and K^+ for Na^+ were calculated from the titration data, Figures 5.13 and 5.14. Vermiculite demonstrated particularly high selectivity for caesium ion at lower loadings of Cs^+, with a marked lowering of selectivity at higher loadings. The selectivity coefficients for exchange processes on montmorillonite were similar to those measured with illite. Selectivity coefficients at 50% conversion for each exchange reaction, along with estimated selectivities for the

Cs^+ for K^+ exchange process, are given in Table 5.3. The order of selectivity $Cs^+ > K^+ > Na^+$ was observed in both cases. The high capacities and caesium ion selectivities are reflected in the distribution coefficient plots shown in Figures 5.15 and 5.16.

Kaolinite

Considerably lower cation exchange capacities were measured on titration of dispersions of Georgian kaolinite (Figure 5.17). With minerals of the single layer lattice structure, there is rarely any isomorphous substitution within the lattice, hence the exchange capacity is low. The measured capacity of 0.014 mmol/g is consistent with literature values for the exchange capacity of Kaolinite [3,18,22,27,28].

Titrations of kaolinite differed from those of the other clay minerals in that there was no detectable release of sodium ion from the exchanger, indicating that another (unidentified) cation was participating in the exchange process. Corrections for suspension potentials could not be made in this case. Additionally, it was not valid to perform the selectivity coefficient calculations as described previously.

5.5.2 Ion Exchange Characteristics of Urban Building Materials

To achieve a realistic assessment of the potential for radiocaesium contamination in an urban environment, it was necessary to have a statistical evaluation of the prevalence and distribution of surface types within urban environments of the European Community. Such an evaluation was carried out, using the United Kingdom as a case study [29]. Following this, an inventory of construction materials in the urban environment of the United Kingdom was compiled. A representative selection of materials and their constituents was made for the purpose of screening their caesium ion sorption characteristics. A number of materials from other parts of Europe were also examined, including a sample of clay tile from Gävle in Sweden. This tile was of particular interest as significant Chernobyl fallout has been recorded at Gävle [30]. The building materials examined are listed in Table 5.4, together with suppliers and source area.

All samples were ground to 2μm and pretreated with sodium tetraphenylboron to remove all exchangeable potassium ions, as previously described. Table 5.5 lists the ionic composition (in mmol/l) of aqueous extracts (0.5g of sample dispersed in 25 ml distilled water) of the building materials under investigation, prior to extraction.

In the extraction process, all exchangeable cations were replaced by sodium ions. On titration with CsCl, a stoichiometrically equivalent release of sodium ion (mmol/g of exchanger) for uptake of caesium ion was observed in all cases, with the exception of the titrations of some concrete tile dispersions, where calcium ions participated in the exchange process. Typical results are presented in Figure 5.19 to 5.21, illustrating the stoichiometry of the ion exchange process on titration of a dispersions of clay rooftiles from Gävle (Sweden), Leuven (Belgium) and a slate rooftile from Stirling (Scotland).

Caesium ion sorption on urban building materials was found to take place by an ion exchange mechanism, with caesium ion replacing sodium ion in the solid phase by the mechanism in eqn.5.1. With increasing concentration of caesium ion in solution, the caesium ion uptake increased to a maximum level (the cation exchange capacity, CEC), after which no further sorption took place. Parallel titrations of aqueous dispersions of urban building materials were performed with KCl as the titrant. The potassium ion exchange capacity was equal to that for caesium ion, within experimental error. Typical results are shown in Figure 5.22, for a clay tile from Leuven, Belgium. In both cases, the total exchange capacity was 0.038 mmol/g, showing that the same number of sites were available for sorption of caesium, potassium and sodium ions. Potassium ion uptake approached saturation less sharply due the lower selectivity of the exchange sites for K^+, in comparison to Cs^+.

Cation exchange capacities (CEC) of a range of building materials were determined using the titrimetric method as described previously, with caesium as the sorbing cation. All urban materials examined in this study were observed to sorb caesium ions from aqueous solution by ion exchange mechanisms. Figures 5.23 to 5.25 are examples of plots of caesium uptake on a variety of materials against caesium equilibrium concentration in solution. Uptake increased with increasing equilibrium concentration until the cation exchange capacity was reached. The range of cation exchange capacities are summarised in Table 5.6. There is considerable variation in exchange capacities, from a maximum of 0.075 mmol/g for a sample of road aggregate, to a minimum of 0.008 mmol/g for a clay tile from Glasgow. The capacities of bricks and clay tiles vary significantly from sample to sample and location to location, but in all cases are about an order of magnitude less than those of clay minerals such as illite.

As with the clay mineral studies, ion selectivity coefficients K_{Na}^{Cs} and K_{Na}^{K} for exchange processes occurring on the building materials were calculated directly from titration data. K_{K}^{Cs} was estimated from the ratios of K_{Na}^{Cs} and K_{Na}^{K}. The selectivity coefficients for these exchange reactions on the sample materials at 50% conversion are listed in Table 5.7. The general order of selectivity was $Cs^{+}>K^{+}>Na^{+}$. The relative magnitudes of K_{Na}^{Cs} varied considerably, with ranging from 5.4 for a concrete tile sample to 55 for a road aggregate material.

Caesium ion distribution coefficients were also obtained directly from titration data. Examples are given in Figures 5.26 to 5.28.

Reversibility studies on the sorption of caesium by the macrosites of urban surfaces were performed by redispersion of the caesium loaded samples in concentrated (1.7M) NaCl. Caesium ion concentration in the equilibrium solution was measured by ISE. In all cases, caesium was desorbed, the cation selectivity coefficient determining the degree of conversion back to the sodium form. Desorption of caesium generally achieved a maximum level within 15 minutes of redispersion in NaCl, with no further increase in caesium ion concentration observed over a period of one week. Results showing desorbed caesium as a percentage of total caesium initially sorbed are presented in Table 5.8. In all cases 90-100% of sorbed caesium could be desorbed.

Parallel research indicated the existence of a small number (<5% of total exchange sites) of highly active sites on many urban surfaces, similar to those observed on illite [6,18]. For these sites, different selectivity coefficients are applicable and appear to bind caesium irreversibly. Analysis of sorption on these sites was outwith the scope of

the titration technique, since the exchange capacities were extremely low. However, the titration results show that caesium sorption on the majority of exchange sites (macrosites) was reversible.

The relationship between sorptive capacity and surface area was examined by measuring caesium uptake on three different particle sizes of Leuven clay tile. The surface area of each sample was determined by nitrogen sorption (BET). For the coarsest fractions (< 250μm and < 200μm), the surface area measurements were at the sensitivity limit for the nitrogen BET method. The surface area of the 2μm sample was the most reliable. Caesium uptake on each particle size fraction is shown in Figure 5.29. Caesium ion exchange capacity was directly proportional to the surface area for these samples, within the credibility limits for surface area determination. Based on the surface area of the 2-3 μm sample (13.27 m^2/g), the caesium ion exchange capacity per unit area was 3 $\mu mol/m^2$. The surface area per anionic exchange site was 55.5 $Å^2$, equivalent to a site to site distance of 7.5Å. The direct proportionality between surface area and sorption enabled predictions to be made on the sorption potentials of whole tiled areas of roofs. The total exchange capacity for a 1 m^2 area of clay rooftile (nominally 1 cm thick) was calculated as 47 mmol. Therefore a very large reservoir of cation binding sites underlies the geometric surface. These results explain the widespread observation that Post-Chernobyl radiocaesium contamination was limited to the outer 2-3mm of such urban surfaces [1].

5.6 Conclusions

The ultimate aim of this research was to measure the caesium binding capacity of materials predominant in U.K. urban environments. The research was extended to other building materials obtained from various sites in Europe. The caesium binding capacities were rapidly characterised using automated titrimetric methodology developed in the course of the research. The mechanism of Cs^+ sorption was shown to be ion exchange with Na^+ (or with counterions present in the natural material, such as K^+ and Ca^{2+}). The relative selectivities of the exchange sites on building materials were generally $Cs^+ > K^+ > Na^+$, with the magnitude of selectivity varying according to the nature of the material. Cation exchange capacity on a typical clay tile was shown to be directly proportional to the total surface area of the tile, enabling the determination of the caesium binding capacity per unit of superficial tile surface. The total exchange capacity of a 1cm deep section of clay rooftile was calculated to be around 30 000 times greater than that of the geometric surface, due to the "hidden surfaces" within its porous structure. This titrimetric survey provided a basic cationic exchange capacity for a wide range of urban materials. Consequently, in decontamination or preventive strategies, it would now be possible to assess the quantity of nuclides which can be bound, or the number of sites which need to be blocked or occupied.

In addition to the exchange sites identified and quantified in this work, a much smaller number (<1%) of sites with high selectivity for caesium ion were identified on urban building materials in parallel research [6]. The existence of such highly selective sites in sediments and soils has been established since the 1960s [3,4,5] and are known to be associated with micaceous clay minerals [31]. These sites typically have selectivities for Cs^+ over K^+ of around 10000 [25]. Sorption of caesium ion on the highly active sites is effectively irreversible, most of the caesium remaining bound even after extensive

decontamination procedures. It is these sites that are the ultimate destination of adsorbed radiocaesium. However, it is most likely that the exchange sites identified in the current research play an important role in the mechanism by which radiocaesium in rainwater is intercepted on urban surfaces. In this mechanism, these poorly selective but abundant ion exchange sites act as intermediate binding sites, providing initial catchment for fallout caesium. The sorbed caesium can then slowly migrate by surface diffusion to the small number of highly selective sites, where it remains, irreversibly bound. This mechanism explains the otherwise unlikely fact that radiocaesium is efficiently scavenged by the small number of high selectivity sites present on an exposed surface. The possibility is raised of preventing or reducing caesium sorption on urban building materials by blocking sorption on the intermediate binding sites, thus making it statistically less likely that caesium ions will find the highly selective sites. This approach has been employed on a preliminary basis, using cationic surfactants as site-blocking agents [32]. Pretreatment of urban materials with dilute solutions of these surfactants rendered the surfaces hydrophilic, excluding water penetration by up to 99%. The large excess of ion exchange sites within the pores of these materials were consequently inaccessible to caesium ions in aqueous solution. Initial experiments were promising, with the uptake of ^{134}Cs on Gävle clay tile being reduced by 80% on a surfactant-treated tile.

References

[1] J. Roed, Radiation Protection Dosimetry, **21**, No.1-3, 59 (1987)

[2] F.J. Sandalls, Radiation Protection Dosimetry, **21**, No.1-3, 65 (1987)

[3] T. Tamura and D.C. Jacobs, Health Physics, **2**, 391 (1960)

[4] T. Tamura and D.C. Jacobs, Transactions of the 7th International Congress of Soil Science, Madison, WI, **2**, 206 (1960)

[5] B.L. Sawhney and C.R. Frink, Transactions of the 8th International Congress of Soil Science, Bucharest, **3**, 423 (1964)

[6] A. Cremers, Chapter 6 in Improvement of Practical Countermeasures against Nuclear Contamination in the Urban Environment, Commission of European Communities, EUR 12555 EN

[7] M.S. Frant and J.W. Ross, Science, **167**, 987 (1970)

[8] S. Lal and G.D. Christian, Anal. Lett., 3^1, 11 (1970)

[9] M.M. Shemyakin et al., J. Membrane Biol., **1**, 402 (1969)

[10] A.K. Covington, Chapter 1 in Ion-Selective Electrode Methodology Volume I, CRC Press Inc. Florida, ISBN 0-8493-5247-9 (1979)

[11] K. Kimura, H. Tamura and T. Shono, J. Electroanal. Chem. Interfacial Electrochem., 105^2, 335 (1979)

[12] A.S. Attiyat et al., Microchem J., **37**, 122 (1988)

[13] D. Wang and J.S. Shih, Analyst, **110**, 635 (1985)

[14] G. Johansson and L. Risinger, Anal. Chim. Acta, **119**, 25 (1980)

[15] A.K. Jain, R.P. Singh and J.C. Bala, Chem. Tech. Biotechnol., 34^A, 363 (1984)

[16] C.R. Martin and H. Freiser, Anal. Chem., **53**, 904 (1981)

[17] A.D. Scott and M.G. Reed, Soil Science of America Proceedings, **26**, 45 (1962)

[18] R. Paterson and A. Cremers, Improvement of practical countermeasures against nuclear contamination in the urban environment, Interim Report No.1, Aug 1 1987 - Feb 1 1988, Contract Nos. B16-0270.UK(H) & B16-0268-B(GDF)

[19] B.L. Sawhney, Clays and Clay Minerals, **18**, 47 (1970)

[20] J.S. Wahlberg et al., U.S. Geol. Surv. Bull. 1140-D (1964)

[21] T. Tamura, International Clay Conference Proceedings Stockholm, **1**, 229 (1963)

[22] A.K. Ganguly and S.K. Mukherjee, Journal of Physical and Colloid Chemistry, **55**, 1429 (1951)

[23] D.R. Lewis, Reference Clay Minerals: American Petroleum Institute Research Project 49, 92 (1949)

[24] W.A. Beetem et al., U.S. Geological Survey Bulletin 1140-B (1962)

[25] E. Brouwer, B. Baeyens, A. Maes and A. Cremers, J. Phys. Chem., **87**, 1213 (1983)

[26] A.S. Abdel-Gawad et al., Isotopenpraxis, **18**, 355 (1982)

[27] H. Nishita et al., Soil Science, **89**, 317 (1956)

[28] H. Nishita et al., Soil Science, **94**, 187 (1962)

[29] M.A. Melvin and R. Paterson, Chapter 3 in Improvement of Practical Countermeasures against Nuclear Contamination in the Urban Environment, Commission of European Communities, EUR 12555 EN

[30] J. Roed and F.J. Sandalls, Proc. XVth Regional Congress of IRPA, Visby, Gotland, Sweden, 10-14 Sept 1989

[31] B.L. Sawhney, Clays and Clay Minerals., **20**, 93 (1972)

[32] S. M°Fadzean and R. Paterson, Chapter 8 in Improvement of Practical Countermeasures against Nuclear Contamination in the Urban Environment, Commission of European Communities, EUR 12555 EN

Table 5.1 : Comparison of selectivity coefficients K_2^{Cs} for the valinomycin based caesium electrode with other caesium ion selective electrodes.

Electrode Type	K_{Na}^{Cs}	K_{NH4}^{Cs}	K_K^{Cs}	K_H^{Cs}	K_{Ca}^{Cs}
Valinomycin	1000	25	0.5	400	1000
Bis (crown ether) **[11]**	1100	100	12	-	-
TMC-crown formazane **[12]**	300	-	20	300	300
15-crown-5-PW ppt. **[13]**	3	-	2	-	1500
Zeolite molec. Sieve **[14]**	15	-	2	-	2000
Copper Hexacyanoferrate **[15]**	31	-	2	-	12
Ionic polymer **[16]**	2	-	1.2	1.4	6

Table 5.2 : Comparison of the cation exchange capacity of illite as measured in the current research with literature values.

Ref No.	CEC (mmol/g)	Illite type
[18]	0.23	Morris illite
[19]	0.28	Fithian illite
[20]	0.28	illite 35
[21]	0.29	illite 35
[22]	0.24	-
[23]	0.25	illite 35
[24]	0.20	illite 35
Current study	0.29	illite 35

Table 5.3 : Selectivity coefficients for the Cs^+ for Na^+, K^+ for Na^+ and Cs^+ for K^+ exchange reactions on clay minerals. Results were measured at 50% conversion.

Material	K_{Na}^{Cs}	K_{Na}^{K}	K_{K}^{Cs}
Illite	70.6	16.6	4.25
Vermiculite	390.0	25.4	15.3
Montmorillonite	77.3	16.4	4.7

Table 5.4 : Building materials selected for examination in this study.

Material	Source Area	Supplier	Status	Source Material
Aggregate (road)		Tilcon	Ex works	Greywacke
Facing Brick	Glasgow	Butterley	Ex works	Carb. shale
Facing Brick	London	Butterley	Ex works	Weald clay
Fletton Brick	London	L.B.C.	Ex works	Oxford clay
Brick	Gävle		Field	Clay
Facing Brick	Scotland	S.B.C.	Ex works	Carb. clay
Pigment (concrete)		Redland	Ex works	iron oxide
Pigment (mortar)		Tilcon	Ex works	
Tile	Bavaria		Field	Clay
Tile	Leuven		Field	Clay
Tile	Glasgow		Field	Clay
Tile	Gävle		Field	Clay
Tile	Bavaria		Field	Concrete
Tile	Mendip	Marley	Ex works	Concrete
Tile	Stirling	Redland	Ex works	Concrete
Tile	Stirling		Field	Slate
Sandstone	Stirling		Field	Sandstone

Table 5.5 : Ionic composition (in mmol/l) of aqueous extracts of building materials.

Material	Source Area	**Liquid / Solid Ratio**	**pH**	**Na mmol/l**	**K mmol/l**	**Ca mmol/l**	**Cl mmol/l**
Facing Brick	Glasgow	50	7.55	0.22	0.10	0.20	0.05
Facing Brick	London	50	7.92	0.005	0.09	1.04	0.16
Fletton Brick	London	50	8.37	0.005	0.06	6.47	0.18
Brick	Gävle	50	7.98	0.64	0.37	8.88	0.04
Facing Brick	Scotland	50	8.62	0.17	0.12	1.45	0.04
Pigment		50	8.67	0.43	0.02	0.12	0.11
Clay Tile	Bavaria	50	7.80	0.20	0.12	1.11	0.06
Clay Tile	Leuven	50	6.74	0.04	0.06	0.01	-
Clay Tile	Glasgow	50	8.34	0.01	0.02	0.28	0.06
Clay Tile	Gävle	50	8.06	0.78	0.21	0.07	0.10
Concrete Tile	Bavaria	50	11.10	0.39	0.76	5.14	0.12
Concrete Tile	Mendip	50	11.55	0.02	0.05	7.60	0.06
Concrete Tile	Stirling	50	11.16	0.04	0.20	6.20	0.40
Slate Tile	Stirling	50	7.19	0.04	0.14	0.01	-

Table 5.6 : Cation exchange capacities of a range of urban building materials- 0.2μm particle size in all cases.

Material	Source Area	C.E.C. (mmol/g)
Aggregate (road)	Ex-works	0.075
Facing Brick	Glasgow	0.010
Facing Brick	London	0.010
Fletton Brick	London	0.014
Brick	Gävle	0.023
Facing Brick	Scotland	0.011
Pigment (concrete)	Ex-works	0.006
Pigment (mortar)	Ex-works	0.006
Clay Tile	Bavaria	0.021
Clay Tile	Leuven	0.038
Clay Tile	Glasgow	0.008
Clay Tile	Gävle	0.018
Concrete Tile	Bavaria	0.025
Concrete Tile	Mendip	0.042
Concrete Tile	Stirling	0.066
Slate Tile	Stirling	0.035
Sandstone	Stirling	0.025

Table 5.7 : Cation selectivity coefficients for a range of urban building materials. Measurements were taken at 50% loading in each case.

Material	**Source Area**	K_{Na}^{Cs}	K_{Na}^{K}	K_{K}^{Cs}
Aggregate (road)	Ex-works	55	20	2.75
Fletton Brick	London	8	8	1
Brick	Gävle	22	18	1.2
Clay Tile	Bavaria	22	12	1.8
Clay Tile	Leuven	37	27	1.4
Clay Tile	Gävle	33	25	1.3
Concrete Tile	Bavaria	5.4	0.9	6
Slate Tile	Stirling	30	30	1

Table 5.8 : Caesium desorption from materials in caesium form, on dispersion in 1.7M NaCl.

Material	Source	Supplier	%Cs desorbed
Clay Tile	Gävle		>95
Clay Tile	Leuven		>95
Clay Tile	Glasgow	Rosemary	>95
Concrete Tile	Glasgow	Marley	>95
Concrete Tile	Stirling	Redland	>95
Slate Tile	Stirling		90
Fletton Brick	London	LBC	>95

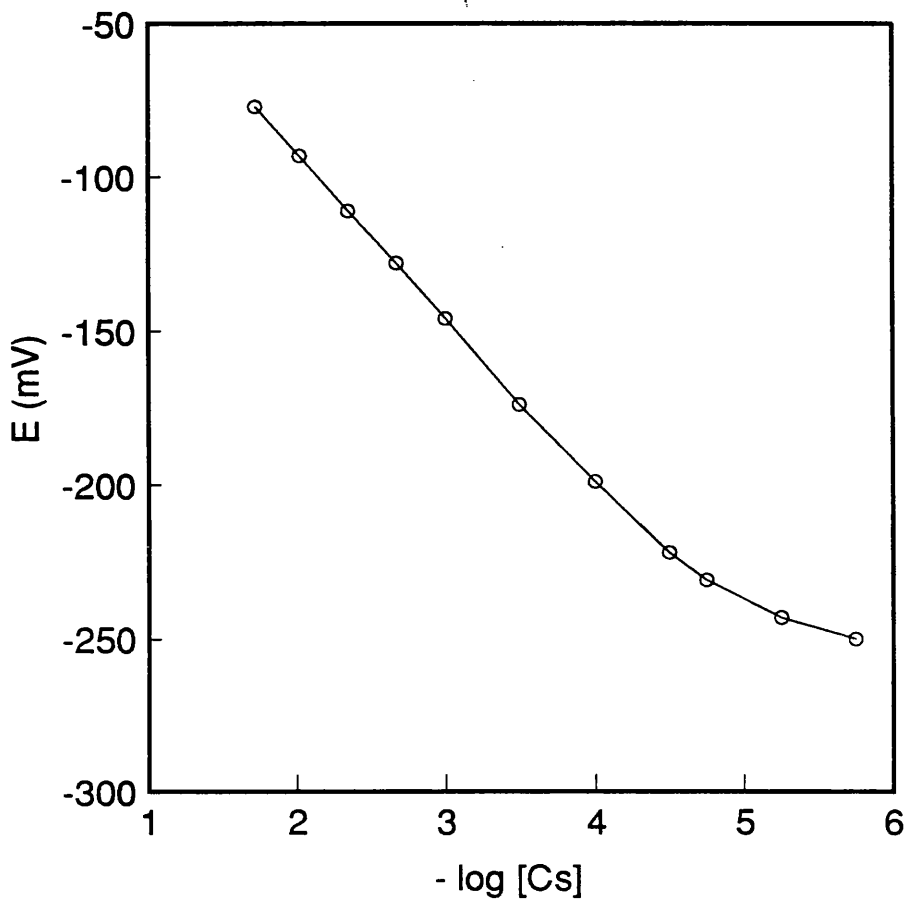

Figure 5.1 : Electrode potential of the caesium ion selective electrode / reference electrode cell, against -log [Cs] for a typical calibration experiment. Successive additions of 0.1M CsCl were made to an initial 25ml distilled water at 25°C. The electrode potential was recorded after each addition.

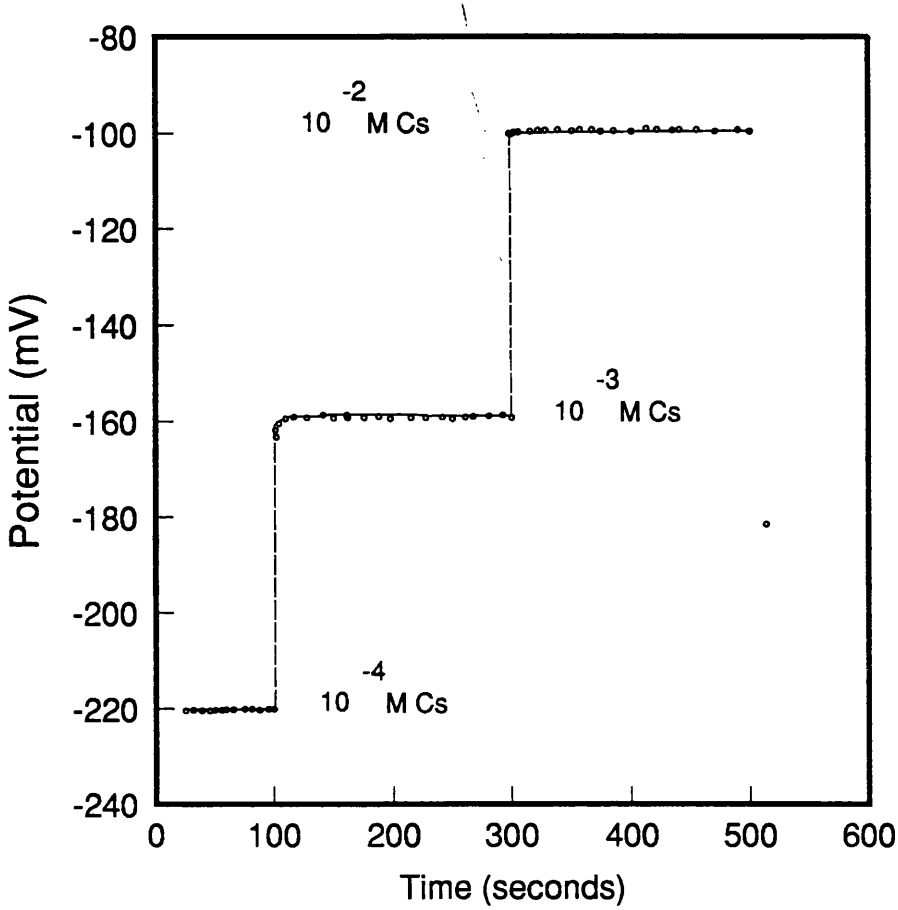

Figure 5.2 : Response time of the caesium ion selective electrode. The electrode potential was continuously monitored over a period of time. The caesium ion concentration was increased from the initial condition of 0.0001M to 0.001M at 100s and to 0.01M at 300s by addition of 0.1M CsCl to the solution.

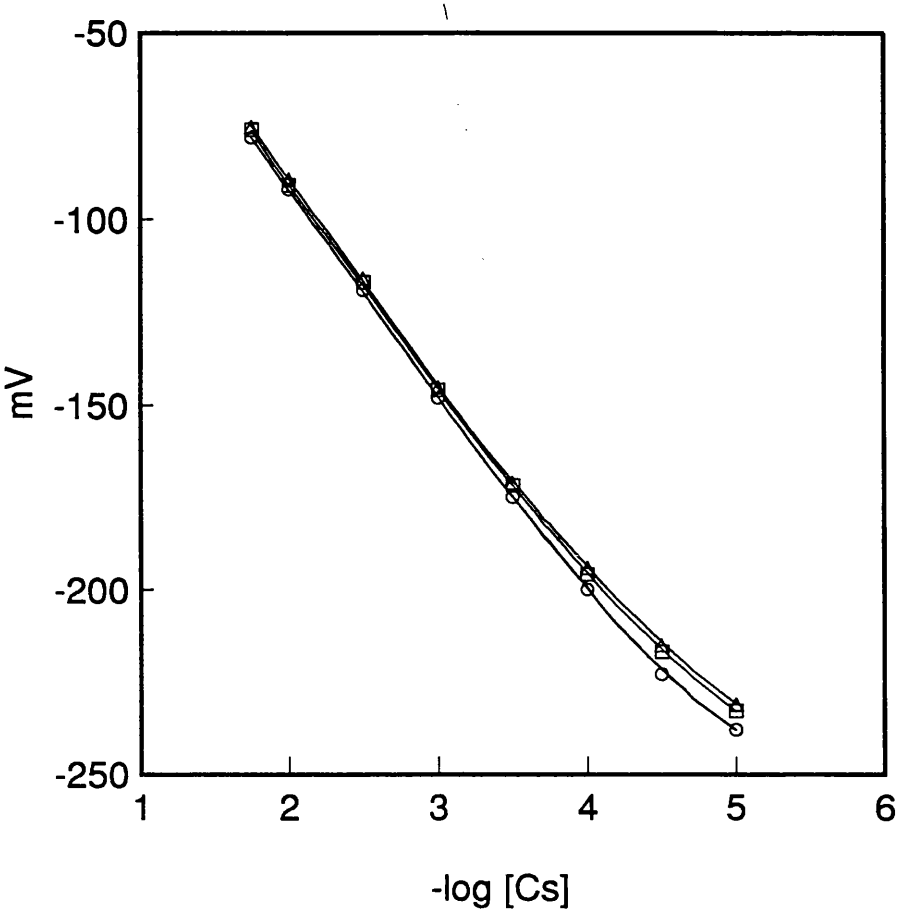

Figure 5.3 : Effect on pH on Cs ISE calibration curve. The electrode was calibrated by making additions of 0.1M CsCl to solutions with initial pH 3 (○), pH 7 (□) and pH 9 (△).

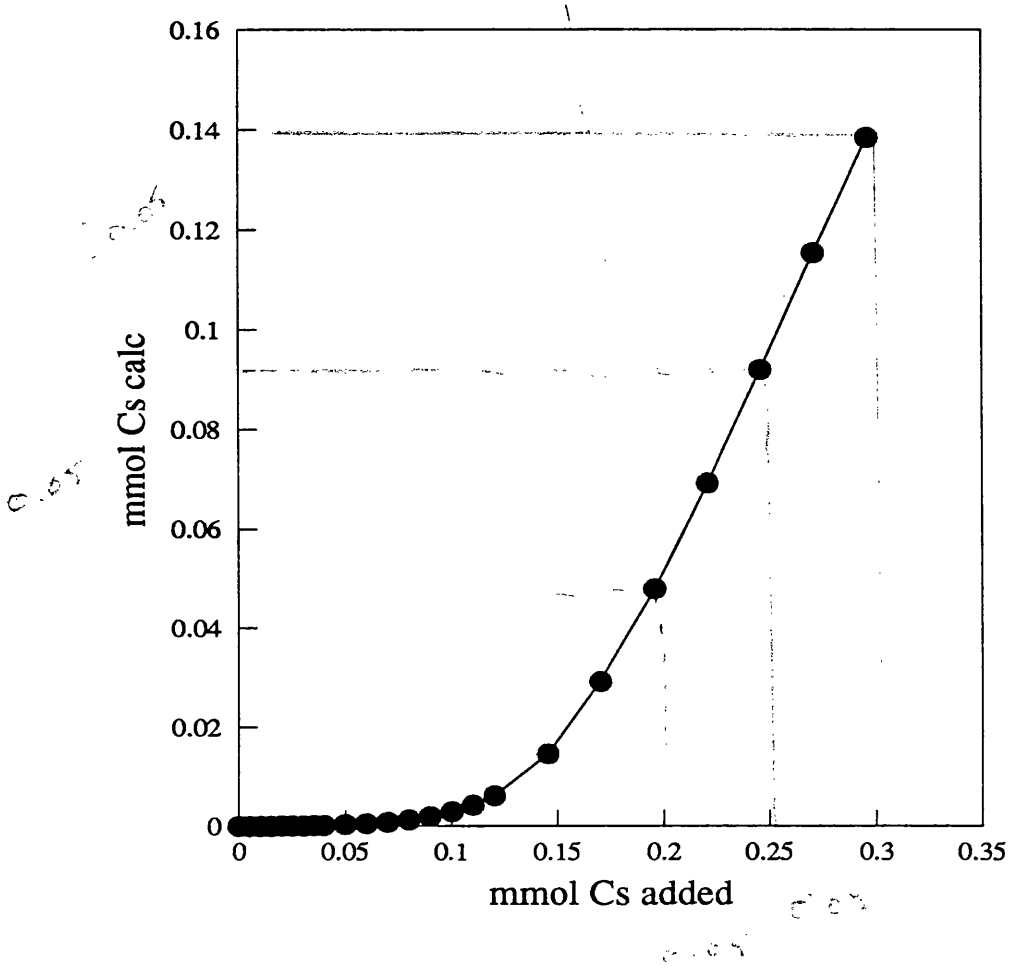

Figure 5.4 : Titration with 0.1M CsCl of a dispersion of 0.541g illite in 25ml distilled water. Concentration of caesium ion in equilibrium solution was monitored by caesium ion selective electrode.

Titration File: MILLR#1

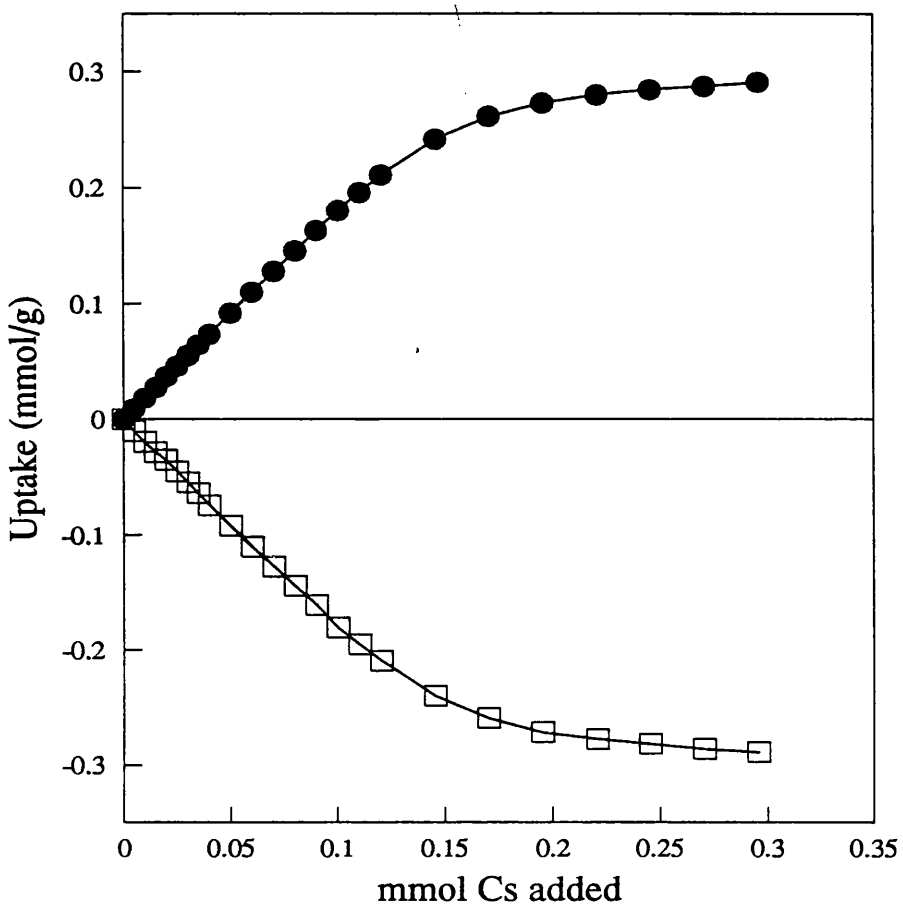

Figure 5.5 : Ion uptakes from the titration with CsCl of an illite dispersion, as described in Figure 5.4. Uptake of caesium ion (●) and release of sodium ion (□) were determined from ISE measurements.

Titration File: MILLR#1

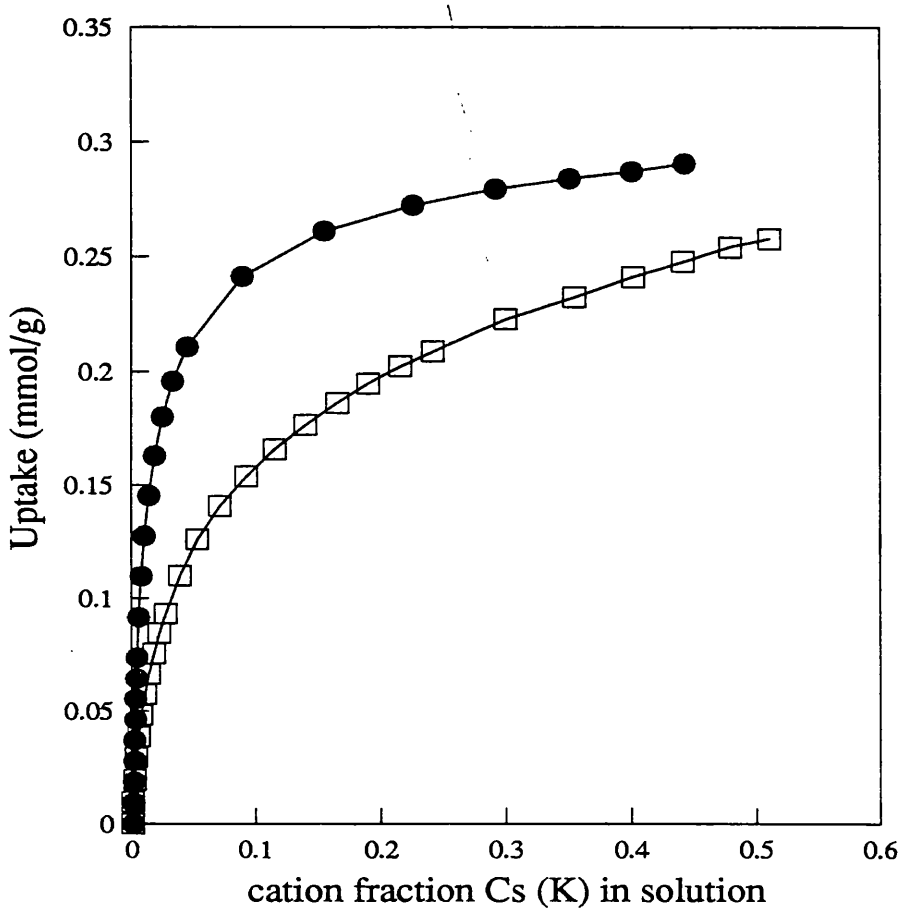

Figure 5.6 : Comparison of uptakes of caesium (●) and potassium (□) ions on titration of illite with CsCl and KCl respectively. Caesium ion uptake was determined from the titration described in Figure 5.4, whilst potassium uptake was determined in a separate titration with 0.1M KCl of a dispersion of 0.512g illite in 25ml distilled water. Uptakes are plotted as a function of the cationic fraction of the loading ion (Cs^+ or K^+) in solution.

Titration Files: MILLR#1, MILLR#2

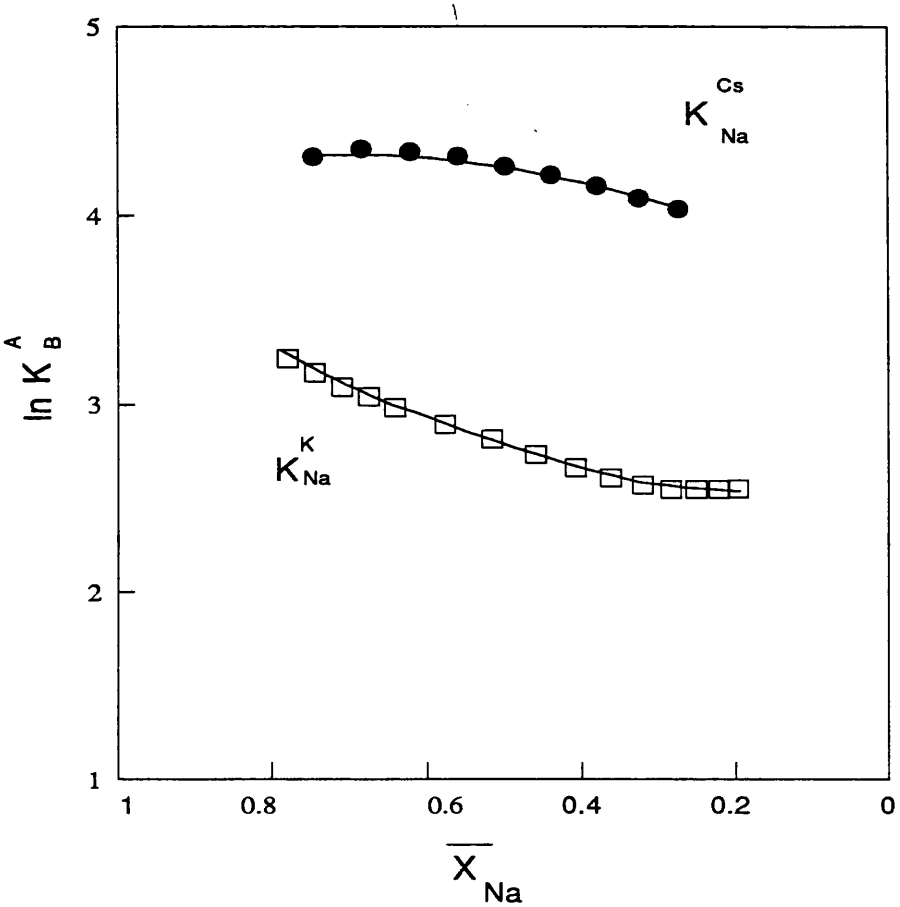

Figure 5.7 : Selectivity coefficients for ion exchange processes on illite plotted as a function of $\overline{X}_{Na}$, the equivalent fraction of Na^+ in the solid phase. K_{Na}^{Cs} refers to the exchange of Cs^+ for Na^+ and K_{Na}^{K} to the exchange of K^+ for Na^+.

Titration Files: MILLR#1, MILLR#2

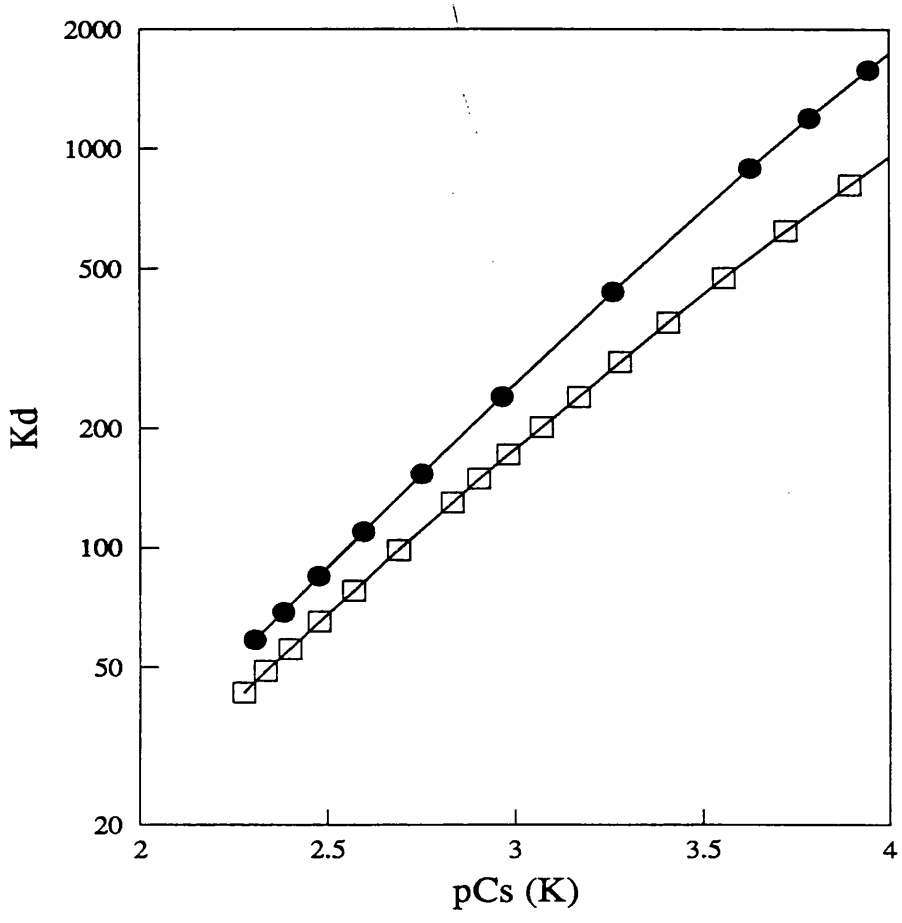

Figure 5.8 : Caesium ion (●) and potassium ion (□) distribution coefficients on illite (initial sodium ion concentration 0.001M).

Titration Files: MILLR#1, MILLR#2

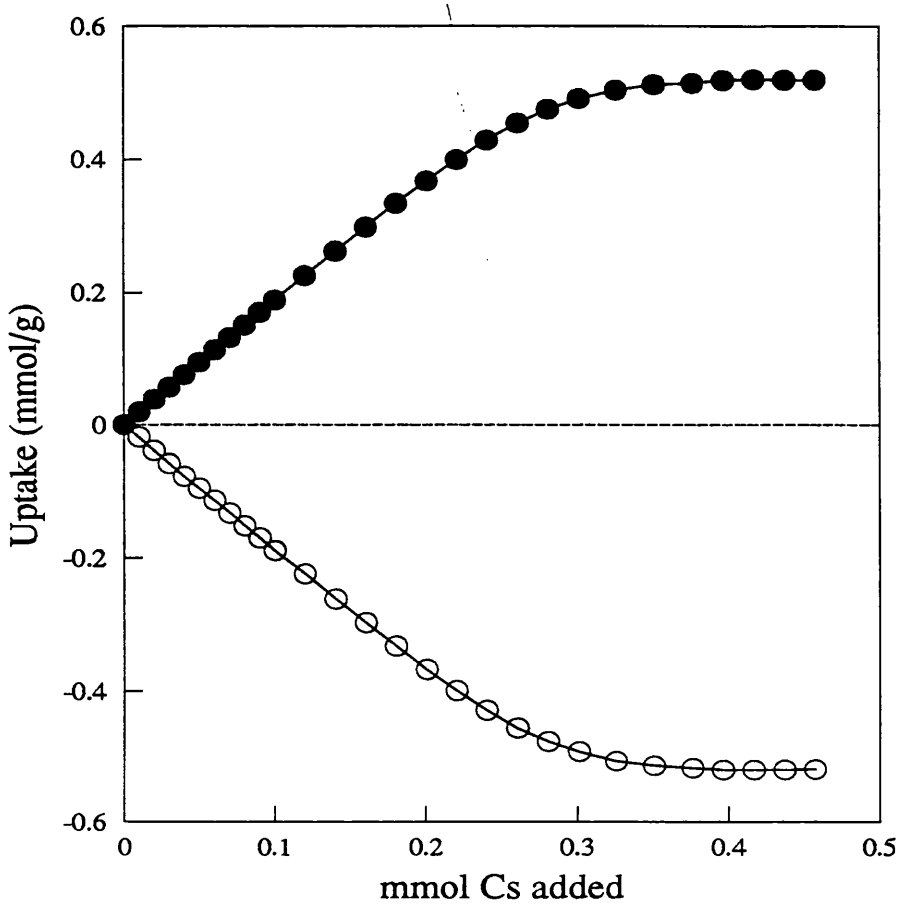

Figure 5.9 : Titration with 0.1M CsCl of a dispersion of 0.528g montmorillonite in 25ml distilled water. Uptake of caesium ion (●) and release of sodium ion (○) were determined from ISE measurements.

Titration File: MMON1#1

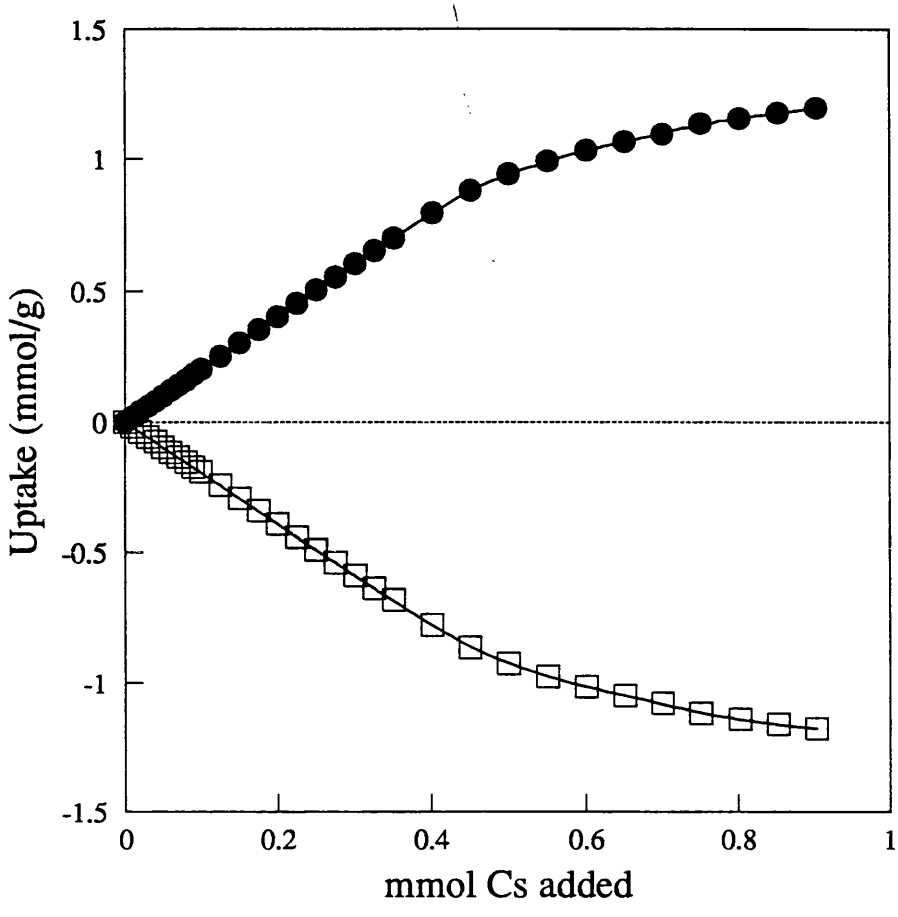

Figure 5.10 : Titration with 0.1M CsCl of a dispersion of 0.498g vermiculite in 25ml distilled water. Uptake of caesium ion (●) and release of sodium ion (□) were determined from ISE measurements.

Titration File: MVER2#1

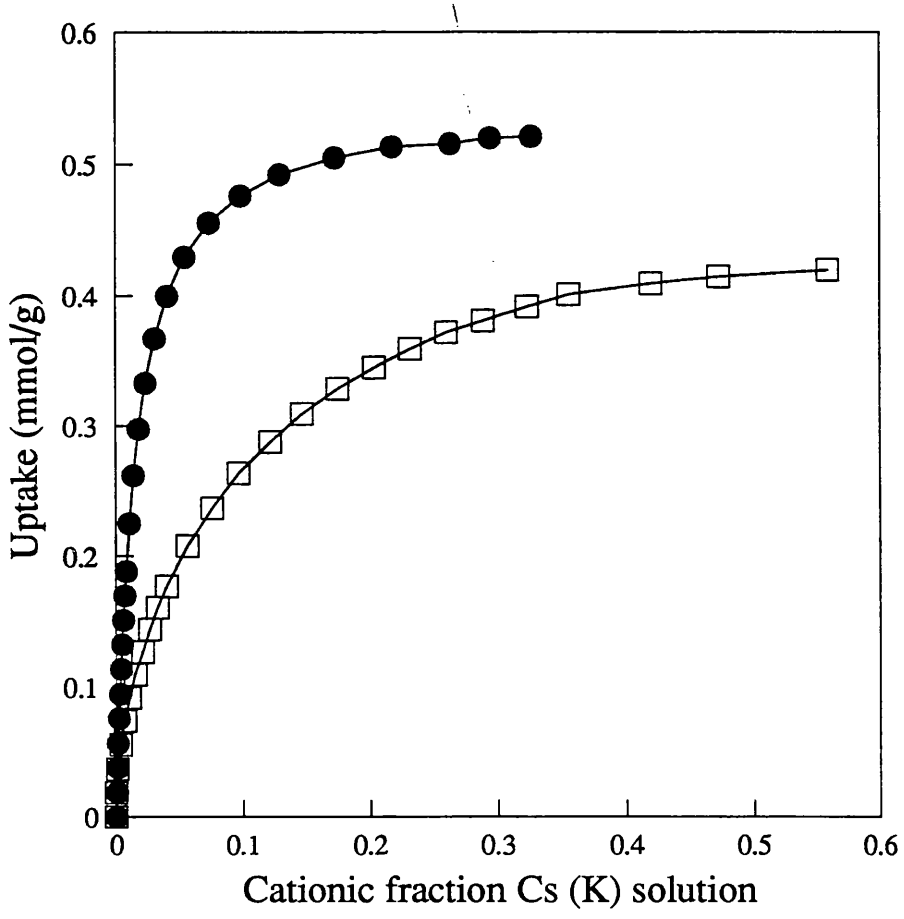

Figure 5.11 : Comparison of uptakes of caesium (●) and potassium (□) ions on titration of montmorillonite with CsCl and KCl respectively. Caesium ion uptake was determined from the titration described in Figure 5.9, whilst potassium uptake was determined in a separate titration with 0.1M KCl of a dispersion of 0.534g montmorillonite in 25ml distilled water. Uptakes are plotted as a function of the cationic fraction of the loading ion (Cs^+ or K^+) in solution.

Titration Files: MMON#1, MMON1#2

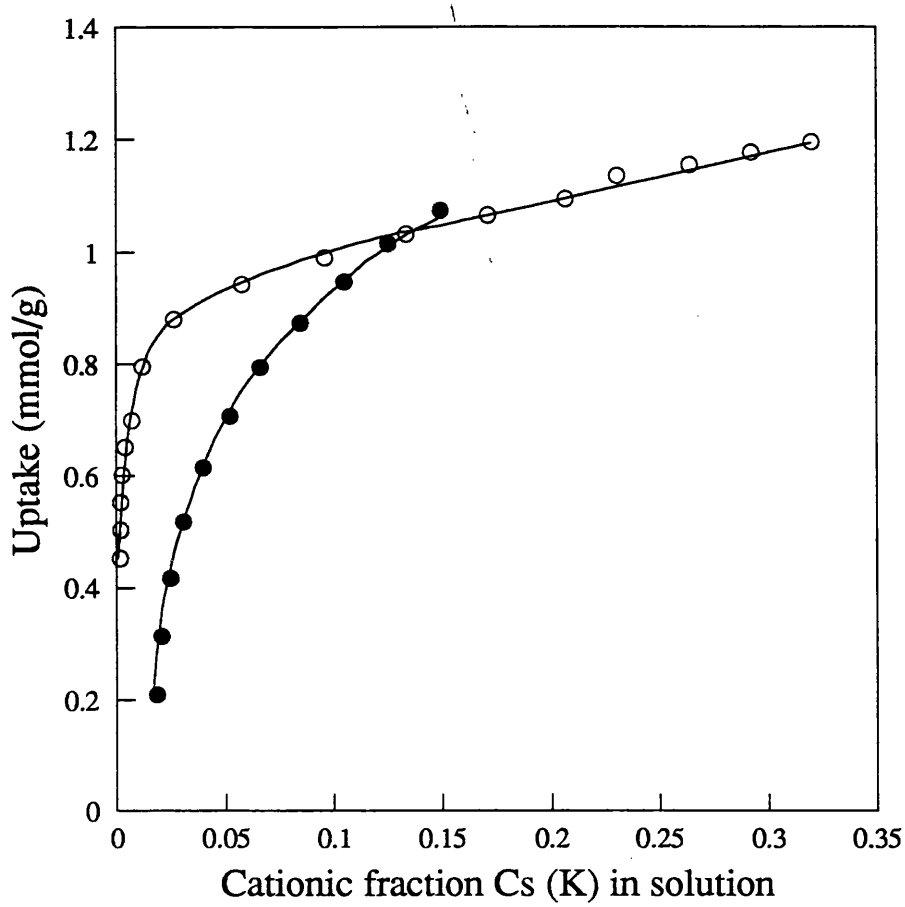

Figure 5.12 : Comparison of uptakes of caesium (○) and potassium (●) ions on titration of vermiculite with CsCl and KCl respectively. Caesium ion uptake was determined from the titration described in Figure 5.10, whilst potassium uptake was determined in a separate titration with 0.1M KCl of a dispersion of 0.461g vermiculite in 25ml distilled water. Uptakes are plotted as a function of the cationic fraction of the loading ion (Cs^+ or K^+) in solution.

Titration Files: MVER2#1, MVER2#2

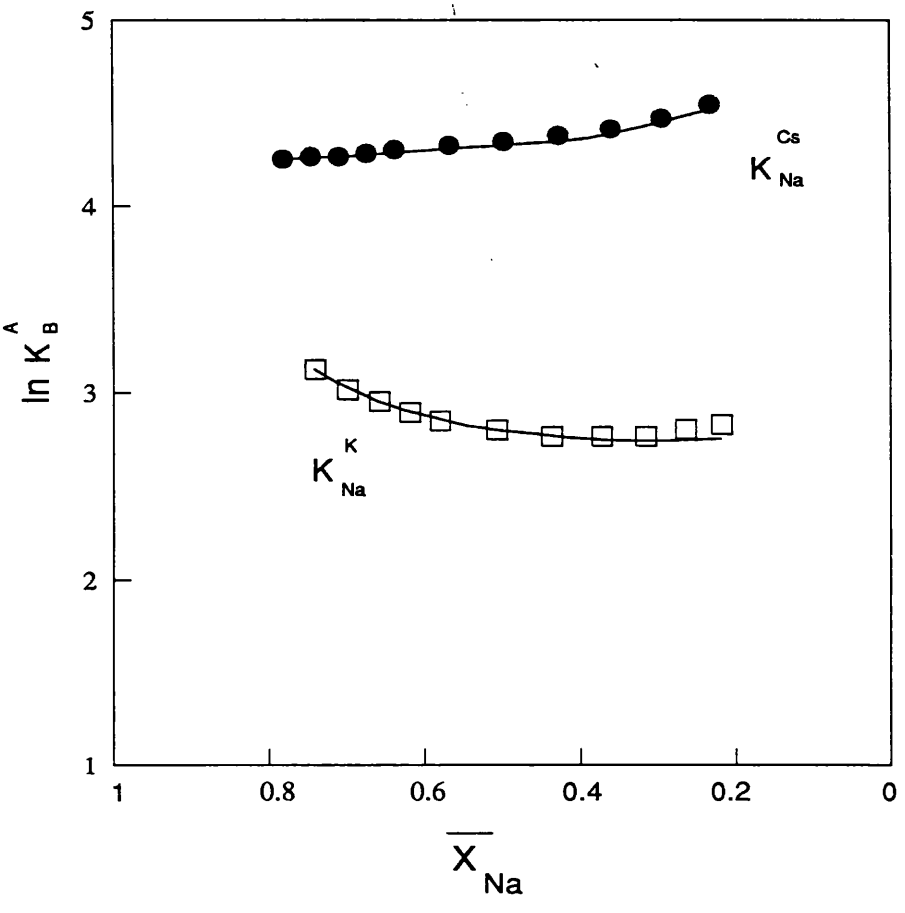

Figure 5.13 : Selectivity coefficients for ion exchange processes on montmorillonite plotted as a function of $\overline{X}_{Na}$, the equivalent fraction of Na^+ in the solid phase. K_{Na}^{Cs} refers to the exchange of Cs^+ for Na^+ and K_{Na}^{K} to the exchange of K^+ for Na^+.

Titration Files: MMON#1, MMON1#2

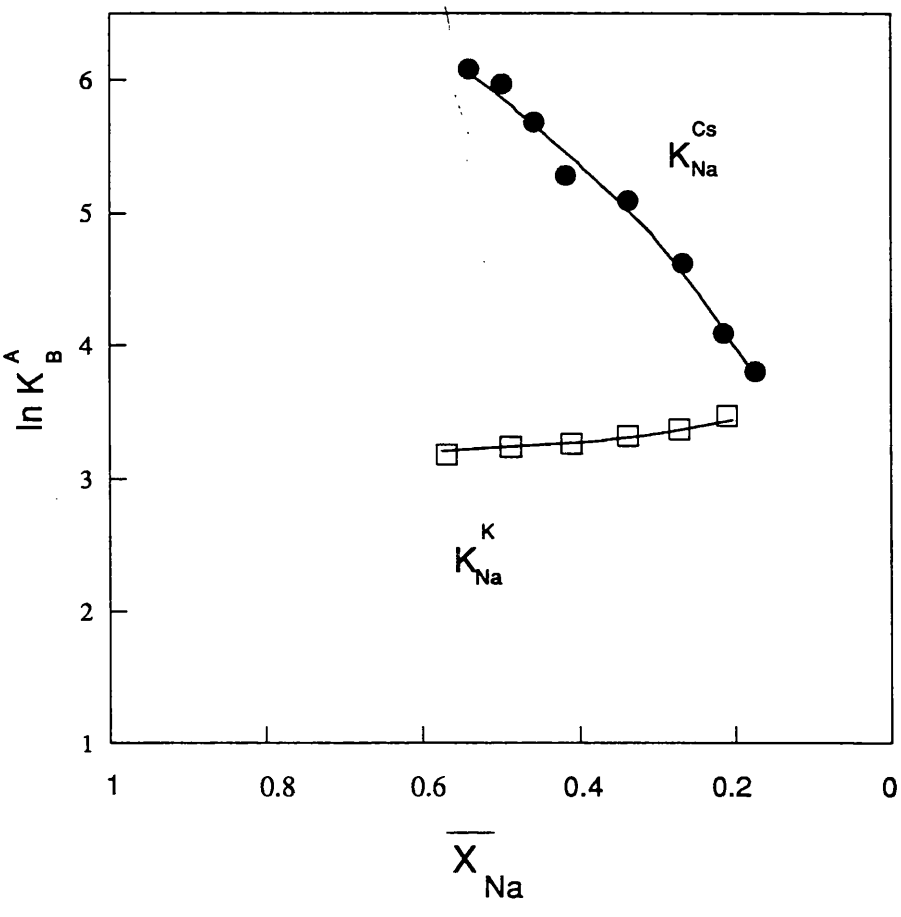

Figure 5.14 : Selectivity coefficients for ion exchange processes on vermiculite plotted as a function of $\overline{X}_{Na}$, the equivalent fraction of Na^+ in the solid phase. K_{Na}^{Cs} refers to the exchange of Cs^+ for Na^+ and K_{Na}^{K} to the exchange of K^+ for Na^+.

Titration File: MVER2#1, MVER2#2

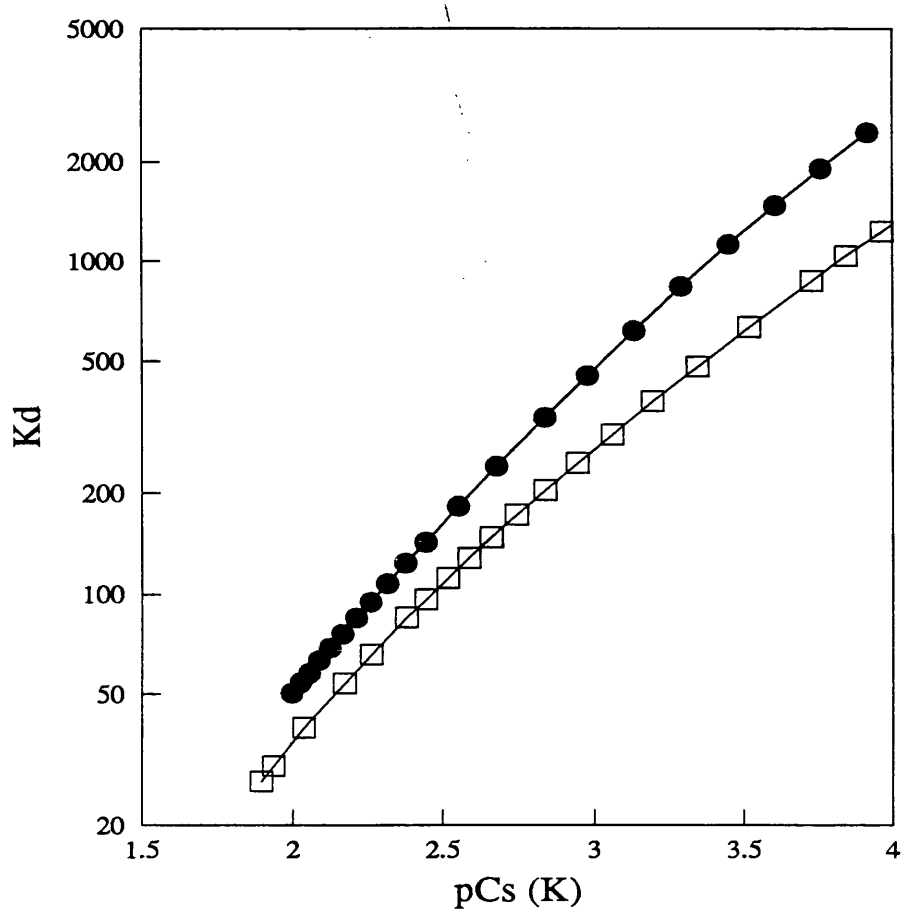

Figure 5.15 : Caesium ion (●) and potassium ion (□) distribution coefficients on montmorillonite (initial sodium ion concentration 0.001M)

Titration Files: MMON#1, MMON1#2

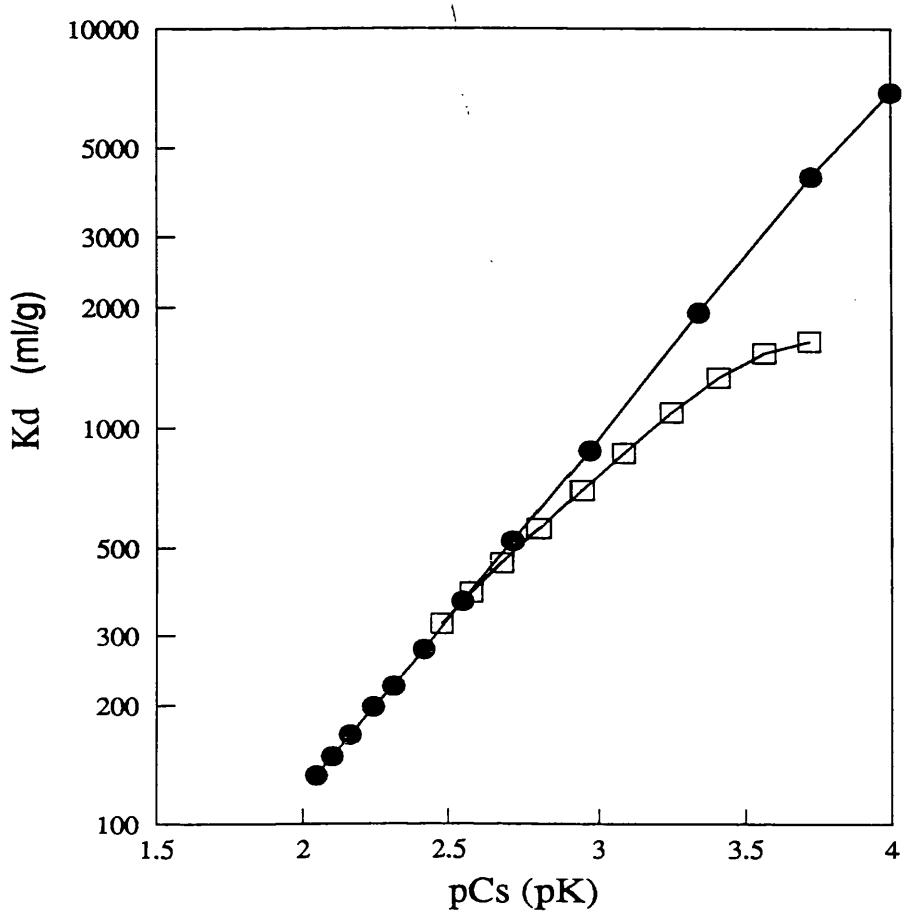

Figure 5.16 : Caesium ion (●) and potassium ion (□) distribution coefficients on vermiculite (initial sodium ion concentration 0.001M)

Titration File: MVER2#1, MVER2#2

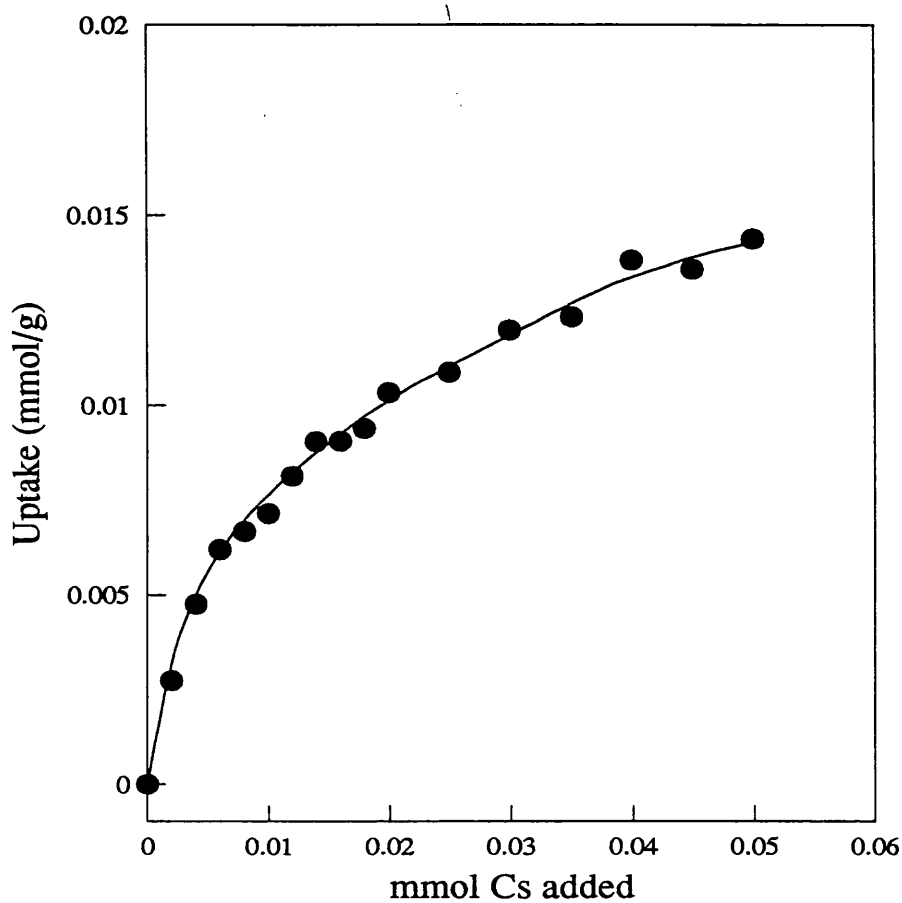

Figure 5.17 : Titration with 0.1M CsCl of a dispersion of 0.512g kaolinite in 25ml distilled water. Caesium ion uptake was determined from ISE measurements.

Titration File: MKAO#1

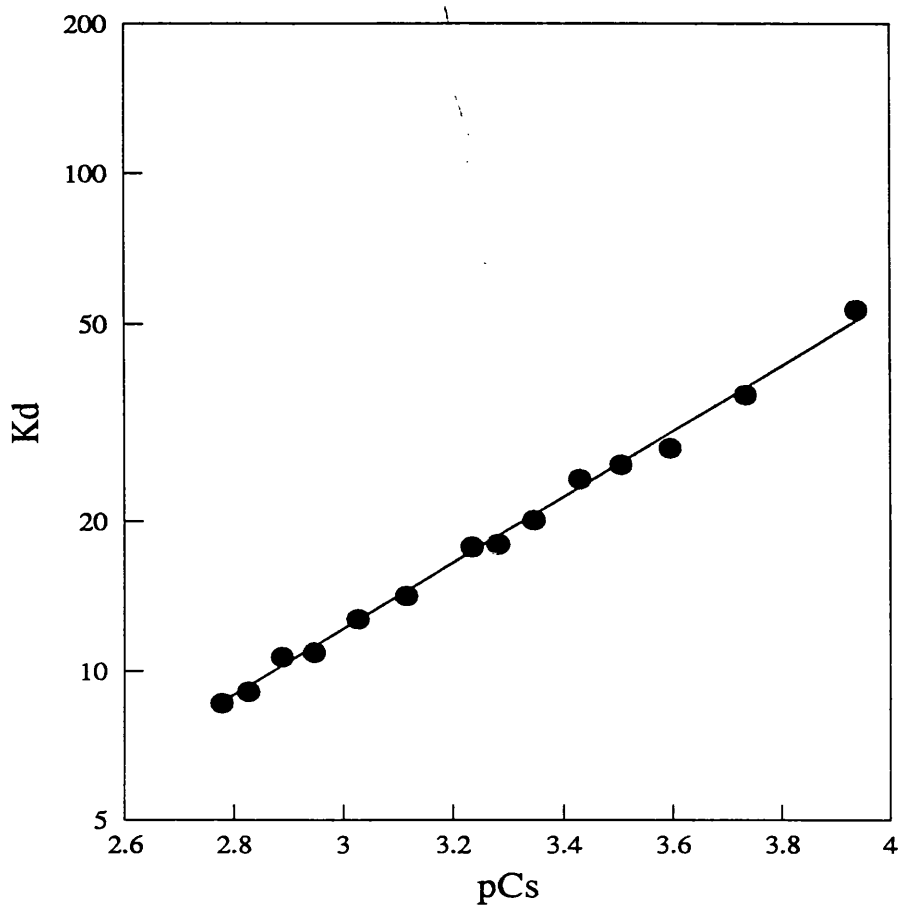

Figure 5.18 : Caesium ion distribution coefficients on kaolinite (initial sodium ion concentration 0.001M).

Titration File: MKAO#1

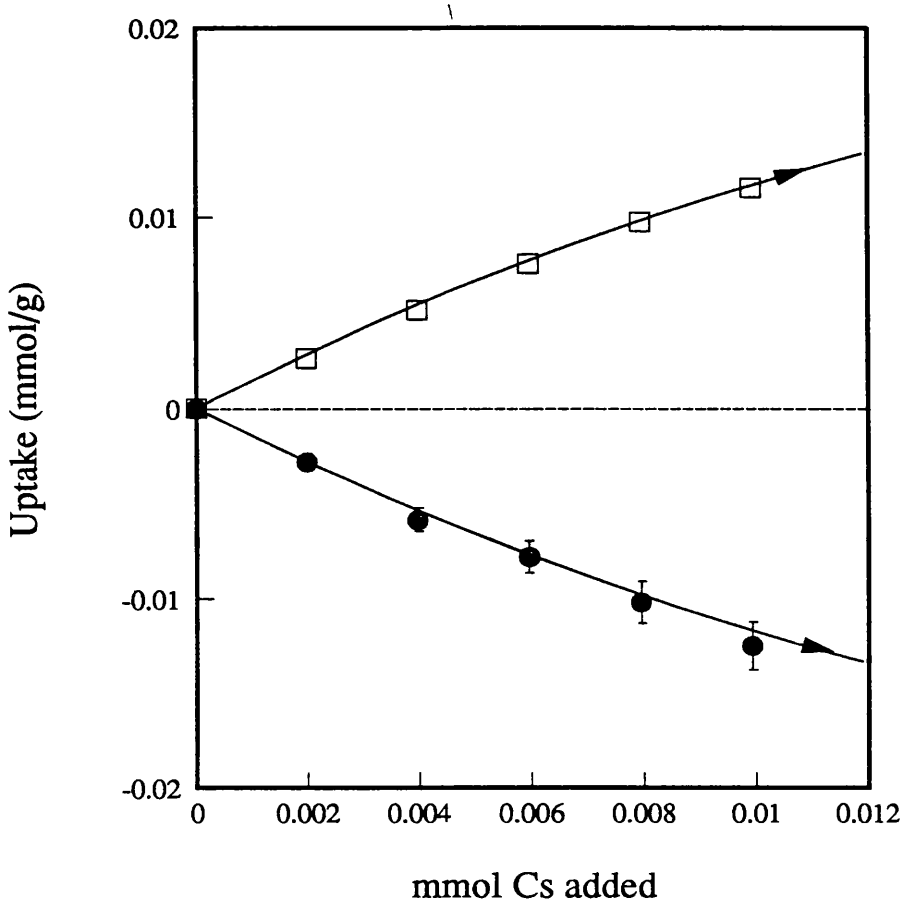

Figure 5.19 : Titration with 0.1M CsCl of a dispersion of clay rooftile (sodium form) from Gävle, Sweden, in 25ml distilled water. Uptake of caesium ion (□) and release of sodium ion (●) were determined from ISE measurements.

Titration File: TClRi1#7

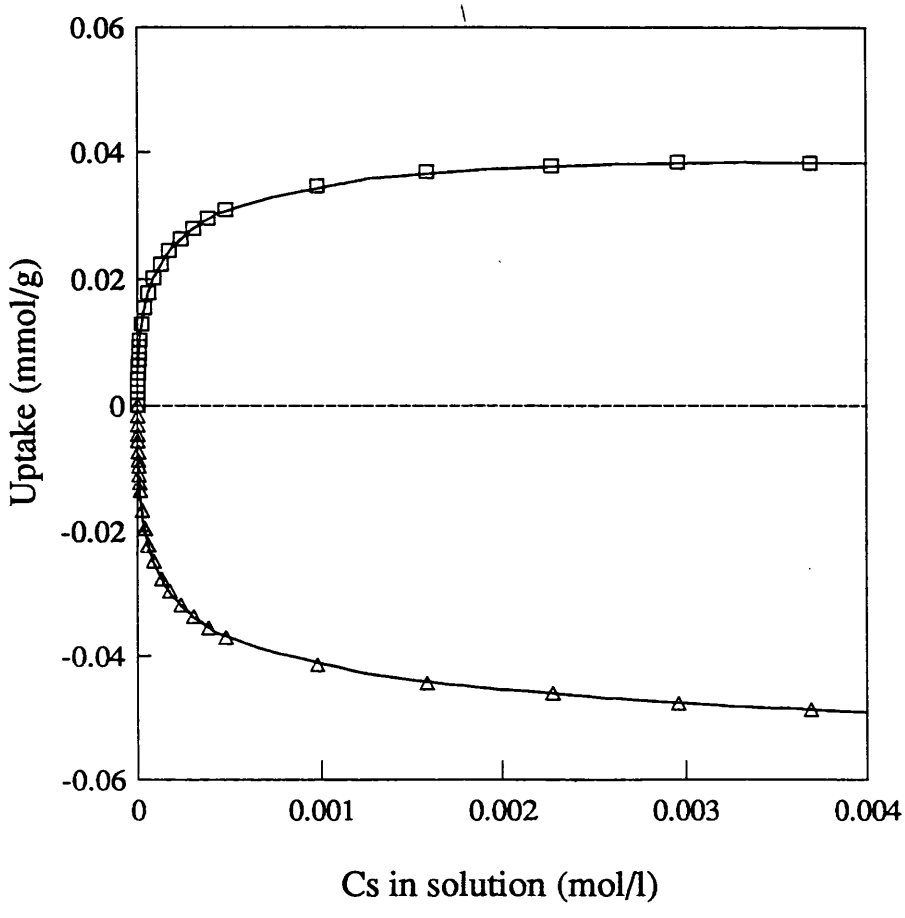

Figure 5.20 : Titration with 0.1M CsCl of a dispersion of 1.861g clay rooftile (sodium form) from Leuven, Belgium, in 25ml distilled water. Uptake of caesium ion (□) and release of sodium ion (△) were determined from ISE measurements.

Titration File: TClL1#6

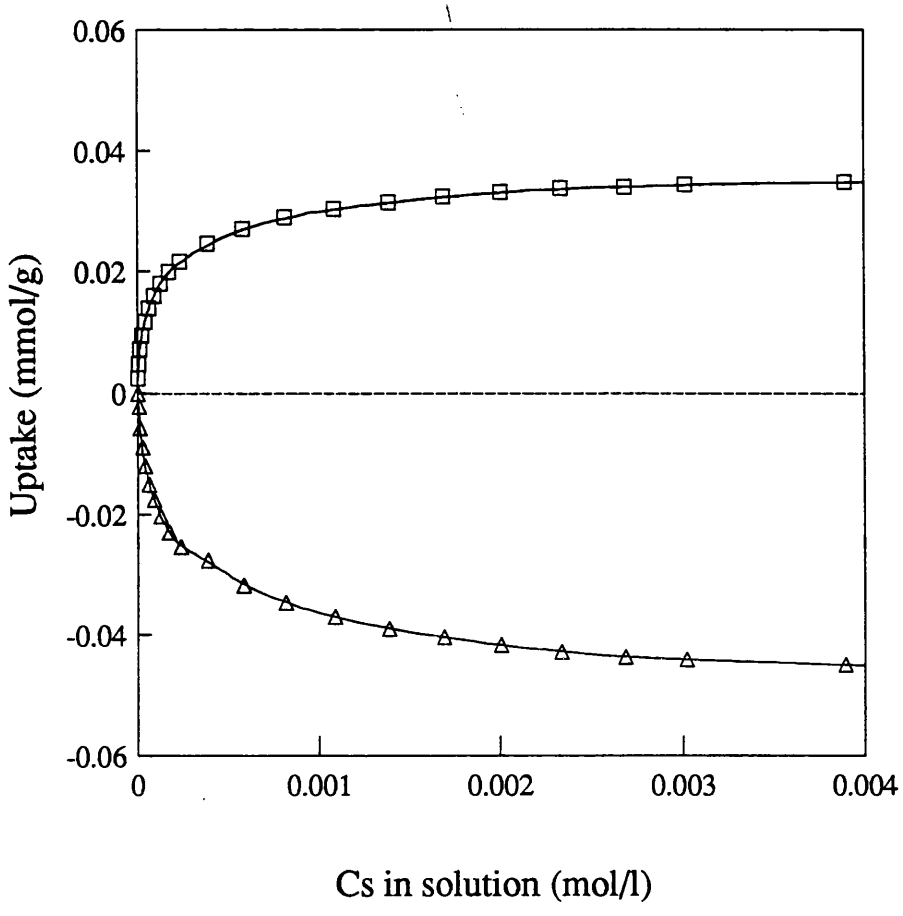

Figure 5.21 : Titration with 0.1M CsCl of a dispersion of 2.045g slate rooftile (sodium form) from Stirling, Scotland, in 25ml distilled water. Uptake of caesium ion (□) and release of sodium ion (△) were determined from ISE measurements.

Titration File: TS1#3

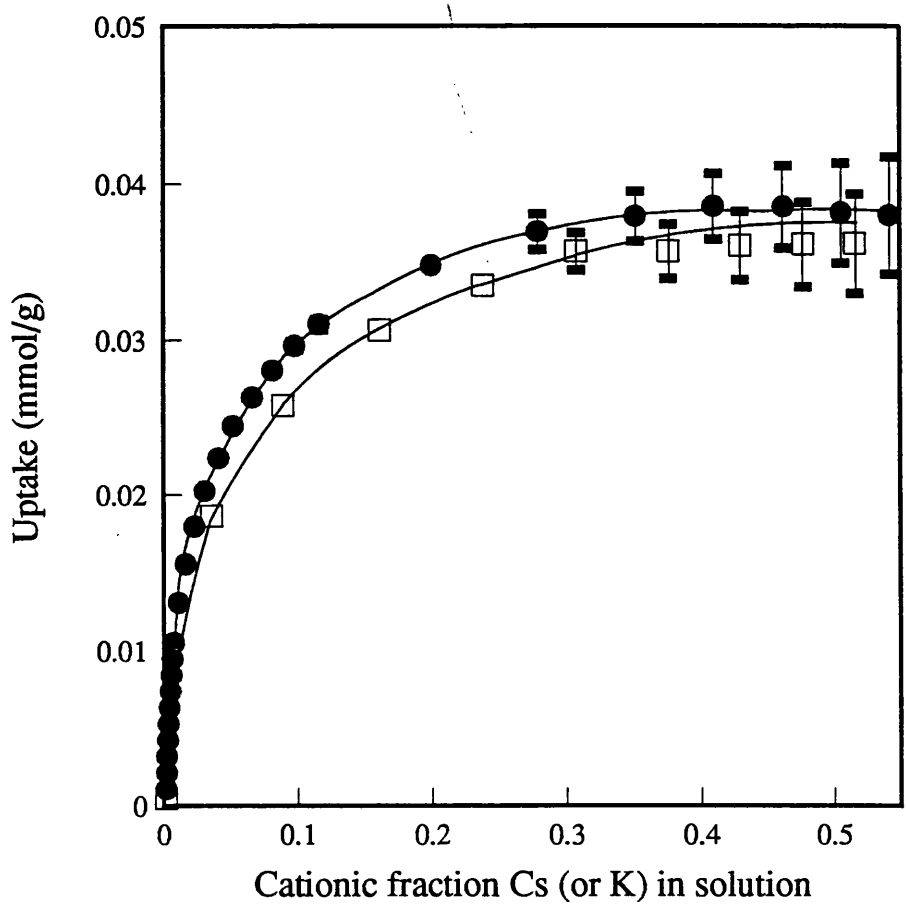

Figure 5.22 : Comparison of uptake of caesium ion (●) and potassium ion (□) (with error bars shown) on Leuven clay rooftile, plotted against the cationic fraction of the sorbing ion (Cs^+ or K^+) in solution. Caesium ion uptake was determined from the titration described in Figure 5.20, whilst potassium ion uptake was determined in a separate titration with 0.1M KCl of a dispersion of 0.502g Leuven clay tile in 25ml distilled water.

Titration Files: TClL1#4, TClL1#6

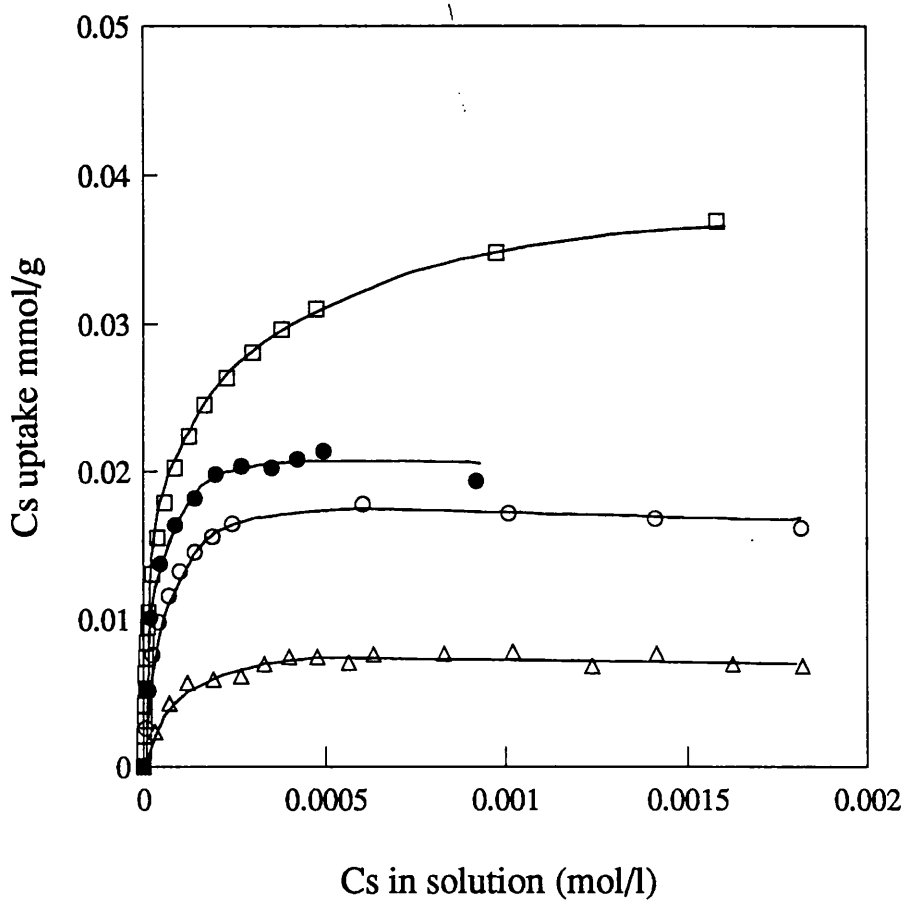

Figure 5.23 : Caesium ion uptake on titration with 0.1M CsCl of dispersions of clay rooftiles from Leuven, Belgium (□), Gävle, Sweden (○), Glasgow, Scotland (△) and Bavaria, Germany (●). Caesium ion uptakes on the clay tiles from Gävle and Leuven were determined from the titrations described in Figures 5.19 and 5.20. A dispersion of 0.507g clay tile from Glasgow was titrated with 0.1M CsCl. A dispersion of 0.356g Bavarian tile was titrated with 0.1M CsCl. In each case, caesium ion uptake was determined from ISE measurements.

Titration Files: TClL1#6, TClRi1#7, TClR1#1, TClB1#2

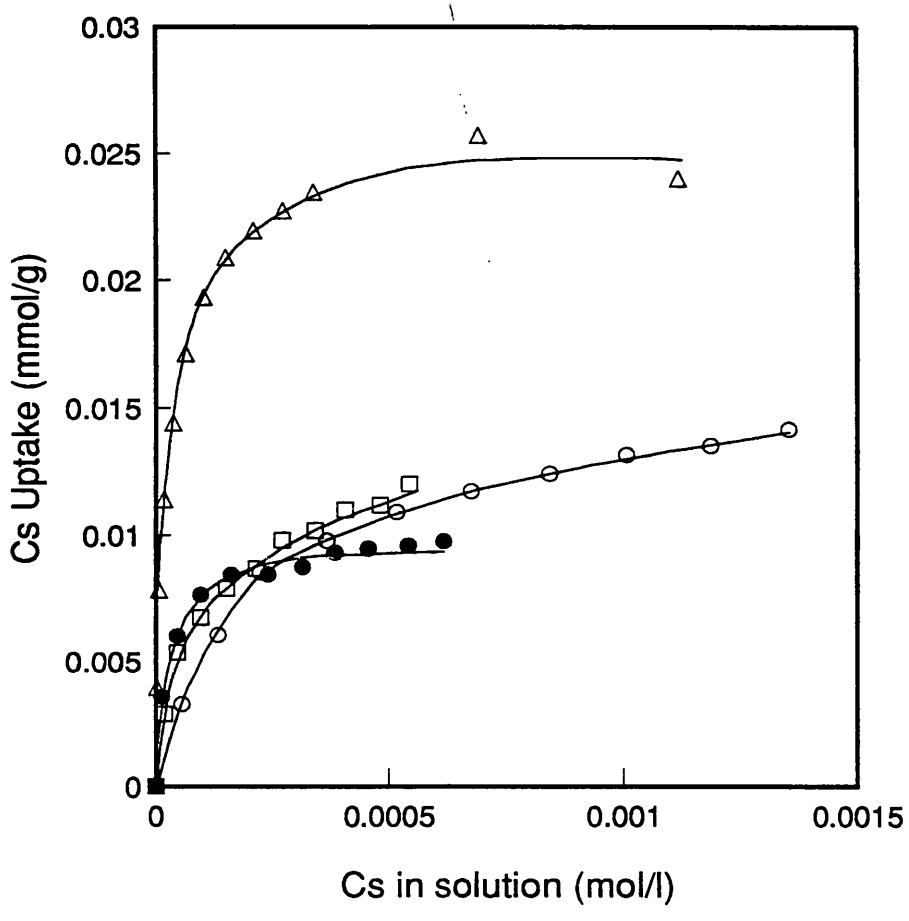

Figure 5.24 : Caesium ion uptake on titration with 0.1M CsCl of dispersions of brick samples (ex-works) supplied by Butterley Brick Limited, (●), Scottish Brick Corporation Limited, (□), London Brick Company Limited (○) and field sample from Gävle, Sweden (△). In each case the brick sample was dispersed in 25ml distilled water. The following weights of brick sample were used - Butterley Brick 0.473g, Scottish Brick 0.532g, London Brick 1.097g and Gävle brick 0.492g. For each titration caesium ion uptake was determined from ISE measurements.

Titration Files: BBB1#2, BSB1#2, BLB#3, BRi#2

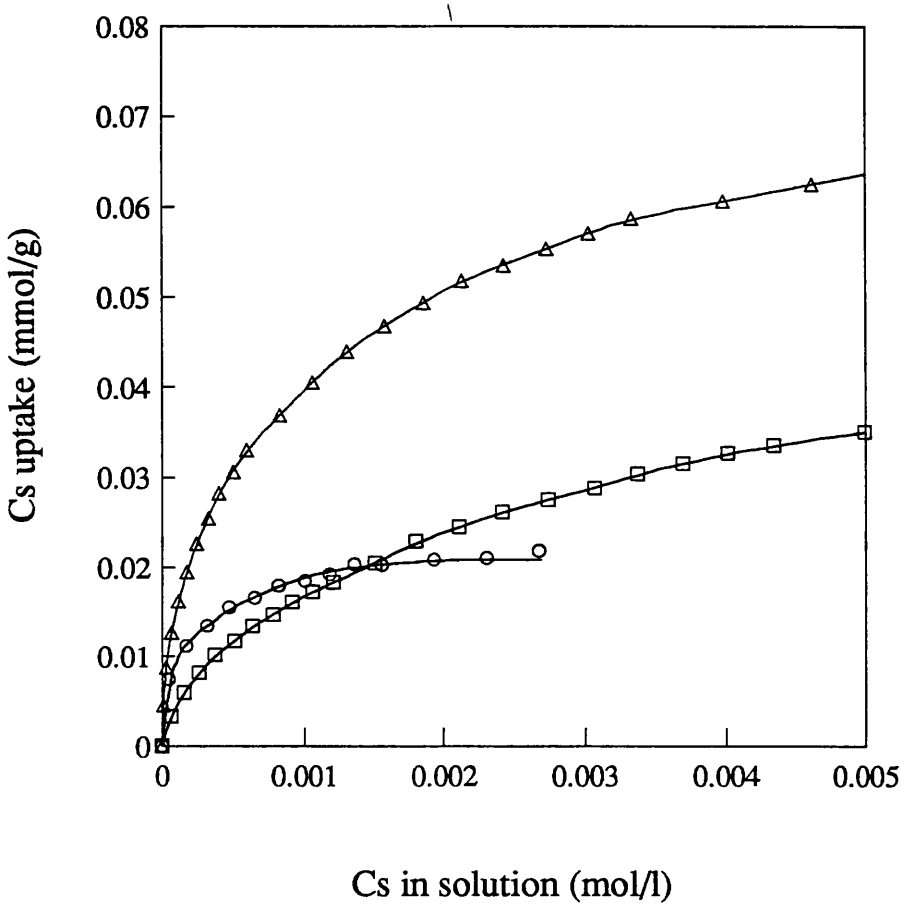

Figure 5.25 : Caesium uptake on titration with 0.1M CsCl of dispersions of concrete rooftile samples supplied by Marley Roof Tile Company Limited (□), Redland Roof Tiles Limited (△) (both ex-works) and field sample from Bavaria, Germany (○). In each case the concrete tile sample was dispersed in 25ml distilled water. The following weights of concrete tile sample were used - Marley tile 1.052g, Redland tile 0.494g and Bavarian tile 0.356g. For each titration caesium ion uptake was determined from ISE measurements.

Titration Files: TCoM1#5, TCoR1#4, TCoB#2

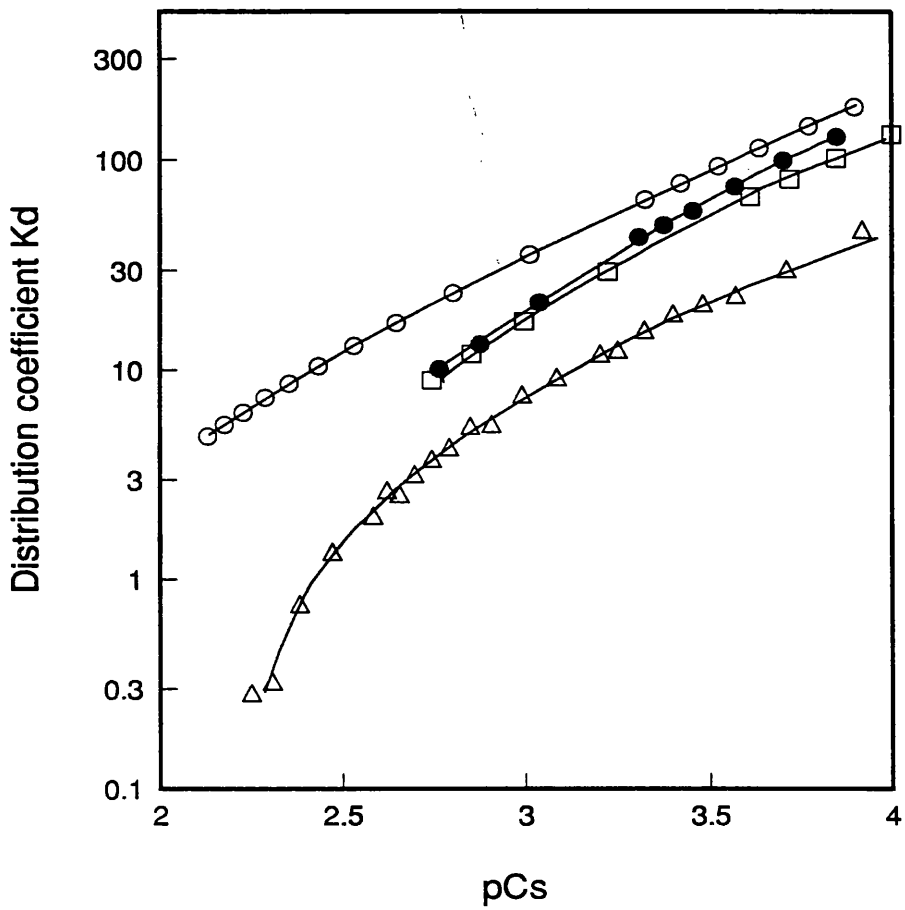

Figure 5.26 : Caesium ion distribution coefficients on clay rooftiles from Bavaria, Germany (●), Leuven, Belgium (○), Gävle, Sweden (□) and Glasgow, Scotland (△).

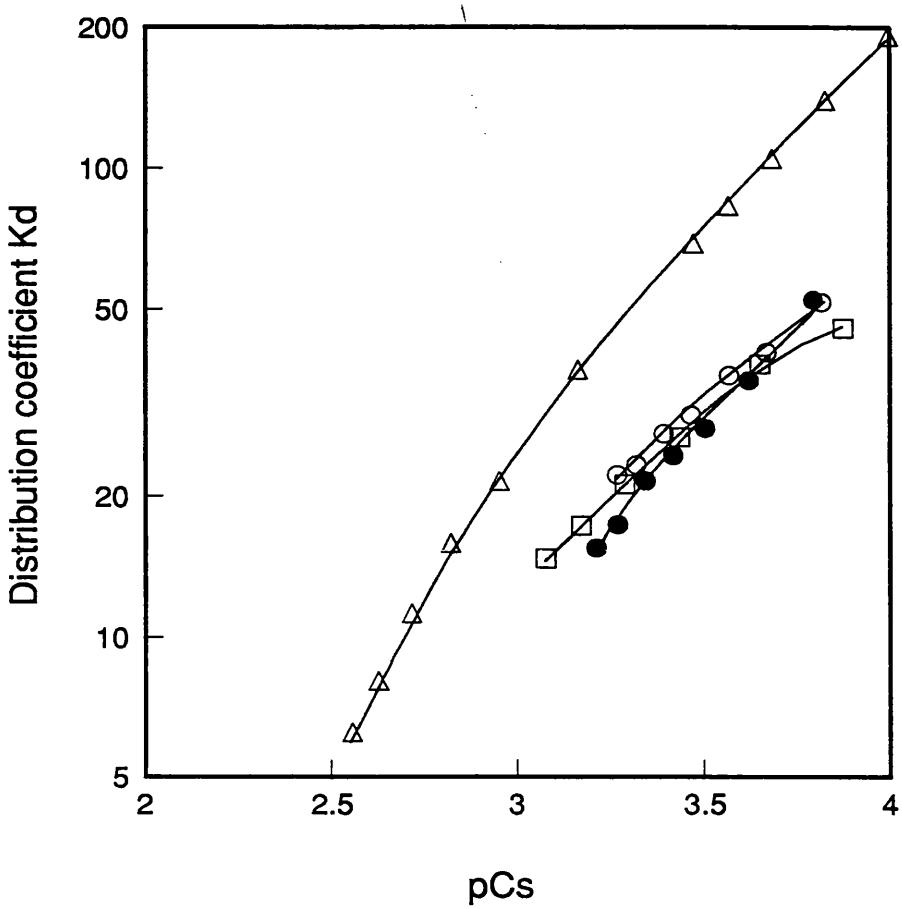

Figure 5.27 : Caesium ion distribution coefficients on brick samples supplied by Butterley Brick Limited (●), Scottish Brick Corporation Limited (○), London Brick Company Limited (□) (all ex-works) and field sample from Gävle, Sweden (△).

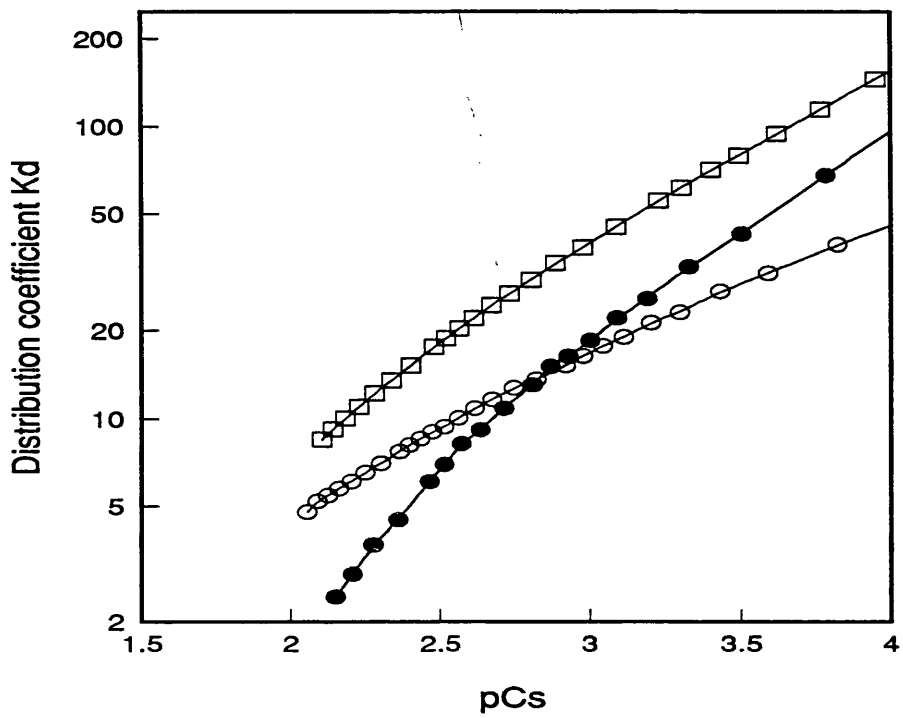

Figure 5.28 : Caesium ion distribution coefficients on concrete rooftiles supplied by Marley Roof Tile Company Limited (○), Redland Roof Tiles Limited (□) (both ex-works) and field sample from Bavaria, Germany (●).

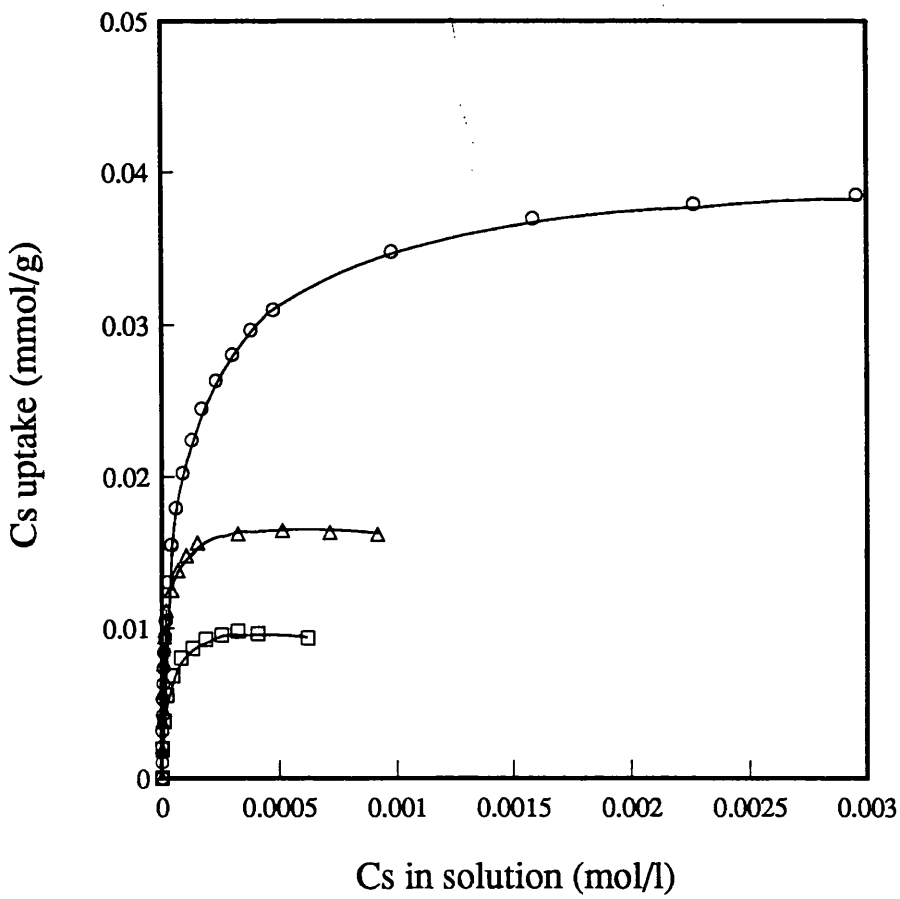

Figure 5.29 : Caesium ion uptake on titration with 0.1M CsCl of dispersions of samples of clay tile from Leuven, Belgium, mill ground to different particle sizes. Results are shown for samples ground to particle sizes of < 250 μm (□), < 200 μm (△) and 2-3 μm (○). In each case the samples were dispersed in 25ml distilled water. The following sample weights were used: < 250 μm fraction - 1.030g; < 200 μm fraction - 1.000g; 2-3 μm fraction - 1.861g.

Titration Files: TClL1B#1, TClL1C#1, TClL1#6

CHAPTER 6

ION EXCHANGE CHARACTERISTICS OF INORGANIC OXIDES

(I) INDIFFERENT ELECTROLYTE SORPTION

Introduction

Since the 1950s there has been a great deal of interest in the ion exchange properties of trivalent and tetravalent insoluble hydrous oxides (such as the hydrous oxides of Fe^{III}, Al^{III}, Zr^{IV}, Sn^{IV}, Ti^{IV}, Th^{IV}, Si^{IV}), primarily in relation to their possible use as ion exchangers in radiochemical separations of fission products [1,2]. In that role they had many advantages over conventional organic resin exchangers, such as resistance to high temperatures and high radiation doses. These advantages (along with those of chemical stability, resistance to compaction under high pressure and insensitivity to bacterial action) have led to a recent resurgence in interest of the ion exchanger behaviour of inorganic oxides, with respect to their use as the active layer components of ceramic membranes.

In the field of membrane technology, considerable attention has been paid to the development of inorganic membranes due to their inherent advantageous properties described above. These inorganic membranes have particular application in the fields of microfiltration, ultrafiltration and reverse osmosis. By far the greatest amount of research and development has been on inorganic membranes based on ceramic (fired) materials. These membranes typically consist of an active layer of oxide particles (generally between 3 and 10 μm thick in a commercial membrane) on a macroporous support (for example, $\alpha\ Al_2O_3$). In the manufacture of ceramic membranes, the sol-gel process provides the only generally applicable technique for producing thin ceramic active layers of controlled porosity on a wide range of macroporous substrates [3,4]. By this technique the active layer of inorganic oxide is deposited as a gel on the support.

Although the oxides which form the active layers of these membranes have been calcined, they still (as shown by the research presented in this Chapter) retain some of their original ion exchange properties. These properties have major implications in the efficient use of

ceramic membranes. The surface charge and ion sorption properties of the oxide active layer are major contributory factors to fouling by polar or ionic substrates, since surface sorption is often the first step in fouling leading to pore blocking within the membrane structure. By altering the surface charge density and changing its polarity, the opportunity exists for minimising fouling and optimising separation processes. Consequently a fundamental understanding of the surface charge and sorptive properties within the pores of the active layers of ceramic membranes is essential to their efficient use. This is particularly true for reverse osmosis membranes, in which surface charge plays a dominant role in determining the degree of salt rejection through the Donnan potential.

The major practical aim of this research was to perform fundamental studies on the factors influencing the ion exchange and ion sorption properties of the inorganic oxides which constitute the active layers of ceramic membranes. This research expands and develops from previous research on the ion exchange properties of the oxide precursors of ceramic membranes [5-10]. The advancements in techniques and theory described in Chapters 3 and 4 enabled the study of a wide variety of materials with capacities an order of magnitude less than those of the materials studied in the earlier work. This Chapter concentrates on the ion exchange properties of inorganic oxides in the presence of indifferent (non-specifically adsorbed) electrolyte. Some studies on the non-calcined oxide precursors are also included.

In addition to the research on the ion exchange properties of inorganic oxide "active layer" materials, studies were made on the exchange characteristics of the three-dimensional cation exchanger NASICON (Na^+ Super Ionic Conductor). Since this material has also been postulated as a likely active layer material, these results are included in this Chapter in the interests of thematic unity.

6.1 Mechanisms of Ion Exchange on Inorganic Oxides

The surface structure of a solid inorganic oxide in contact with water differs from the bulk crystal structure due to surface hydration, resulting in surface coverage by a layer of hydroxyl groups. The establishment of surface charge (including pore charges) arises from the protonation or dehydroxylation of these groups at the water-oxide interface. To maintain electroneutrality, the surface charge requires to be balanced by an equivalent amount of diffusable counterions of the opposite sign. The ion exchange properties are therefore a consequence of the surface charge arising from these reactions.

Many inorganic oxides have ion exchange properties when in contact with aqueous solution. Some have been shown to have amphoteric properties, exchanging anions in acidic solution and cations in basic solution, with no exchange capacity at a particular point on the pH scale (the zero point charge, zpc). Detailed research has been made on the ion exchange mechanisms of one such oxide - monoclinic zirconia [8]. In this case, positively charged surface sites are created in acid media by protonation of surface hydroxyl groups. Electroneutrality is preserved by the inclusion of the anions of the acid within the pores or on the external surface of the oxide particles. The mechanism for this reaction (with HCl as the acid) is given in eqn. 6.1. The oxide particles are therefore anion exchangers (positively charged surface) under these conditions.

$$\overline{M-OH} + H^+_{aq} + Cl^-_{aq} \rightleftharpoons \overline{M-OH_2^+ \quad Cl^-} \tag{6.1}$$

In basic media, oxides acquire a negative charge by the mechanism in eqn. 6.2. In this case (shown with NaOH as base), electroneutrality is preserved by the uptake of cations.

$$\overline{M-OH} \;+\; OH^-_{aq} \;+\; Na^+_{aq} \rightleftharpoons \overline{M-O^- \quad Na^+} \;+\; H_2O \tag{6.2}$$

The magnitude and sign of the surface charge is therefore sensitive to both pH and the activity of the counterion in solution (here, chloride in acid, sodium in alkaline solution). The mechanisms of equations 6.1 and 6.2 were validated by the observations that anion capacity is a single valued function of the negative logarithm of the total acid activity, pA (= pH + pCl) and cation capacity is a single valued function of the negative logarithm of the total base activity, pB (= pNa + pOH), below and above the zero point charge respectively [8].

It is evident from these mechanisms that the surface charge (and hence the ion exchange capacity) of zirconia varies according to the pH of the contacting solution. As will be shown, these mechanisms apply equally to a variety of inorganic oxides. These materials are therefore variable charge ion exchangers, with many exhibiting amphoteric (cationic or anionic) exchange behaviour. Since hydrogen ions (and hydroxide ions) exert a fundamental control on the surface charge and the surface potential of inorganic oxides, they are termed the potential determining ions (p.d.i.).

6.2 Preparation of Oxides

Since a major aim of this research project was to determine the ion exchange and sorptive characteristics of the calcined inorganic oxide materials which formulate the active layers of ceramic membranes, it was necessary that the oxides powders studied corresponded exactly to the materials actually used in ceramic membranes. This was achieved by obtaining oxide powders directly from the sol-gel process.

The sol-gel process for the preparation of ceramic membranes involved the preparation of a sol by peptization of an oxide precursor (metallic salt or hydrous oxide) followed by destabilisation of the sol and subsequent deposition of a gel layer on a support material. After heat treatment a thin layer of inorganic oxide with controllable porosity is formed.

The process is shown schematically in Figure 6.1. Ceramic membranes with active layers with active layers of γ Al_2O_3, SiO_2, TiO_2, ZrO_2 and NASICON were prepared by this method, from the precursors given in Table 6.1.

Powder samples of these inorganic oxides were obtained from the gel layers of the above process. After calcining in the same manner as used in the sol-gel process, oxide samples corresponding exactly to the active layer materials were obtained. Physical properties of these oxides are given in Table 6.2.

In addition to the calcined oxide materials, a sample of non-calcined zirconia was prepared by the method of Clearfield [11], for the purpose of comparing with the ion exchange behaviour of the calcined sample of zirconia.

6.3 Results and Discussion

6.3.1 Zirconia

Initial dispersions of zirconia indicated the presence of some HCl and salt remaining from the synthesis, giving a solution of pH 3-4. This was removed by adjusting to pH 7 with base and washing exhaustively with distilled water. After drying at 40°C, the pH of subsequent zirconia dispersions was between 6 and 7, with no salt background.

1.501g of calcined monoclinic zirconia was dispersed in 25ml distilled water and left stirring overnight to ensure complete hydroxylation of the oxide surface. Using the automated titration system, the dispersion was titrated with standardised solutions acid (0.1M HCl), base (0.12M NaOH) and salt (0.1M NaCl). An initial addition of 1.5ml acid was made to reduce the pH to 3.15, then the dispersion was titrated forward with base to pH 11.08. At this point an addition of 2ml of 0.1M NaCl was made, followed

by back-titration with acid. Throughout the titration, pH, pNa and pCl were monitored directly by the respective ion selective electrodes. In this way the uptake and/or release of all ions present in the dispersion could be determined. (note - since the Na ISE is inoperable in acid conditions due to the high interference of H^+, uptake data obtained from this electrode in acid conditions were rejected. Similarly rejected were the uptake data obtained from the Na and Cl ISEs after the salt addition, since the uptake measurement errors were relatively large at high salt concentrations. Hydrogen uptake data remained reliable under these conditions).

The titration curves for both sections of this titration (before and after the addition of salt) are shown in Figure 6.2. Two distinct curves were observed, which cross each other between pH 7 and 8. No distinct end-point was observed.

Uptakes for hydrogen, sodium and chloride ions, as measured by ISE (after correction for the suspension potential), during the initial stages of the titration, are presented in Figure 6.3. Addition of acid resulted in an uptake of hydrogen ions, with a concurrent uptake of chloride counterions. This capacity for chloride decreased as sodium hydroxide was added, eventually becoming zero between pH 7 and 8. There was no capacity for sodium ion in acid solution, due to Donnan exclusion (although this could not be reliably determined from the Na ISE readings in solution with pH below 5). Above pH 8, stoichiometric uptake of sodium and release of hydrogen was observed, with no chloride uptake. The exchanger therefore had cation capacity in basic solution.

Ion exchange capacities for the titration before and after the addition of salt are presented in Figure 6.4 (as stated in Chapter 3, anion capacity is expressed as negative capacity and cation capacity as positive). The increase in salt concentration results in a higher cation exchange capacity at equivalent points above pH 8 and a higher anion exchange

capacity at equivalent points below pH 7. An alternative, though equivalent, viewpoint is that the addition of salt at any point on the first curve would cause a transition to the second curve, resulting in a decrease in pH in basic solution and an increase in pH in acidic solution. There was one point in the pH range where the change in salt concentration had no effect on the exchange capacity - this occurred between pH 7 and 8, where the exchanger had no exchange capacity (the zero point charge). That the salt (NaCl) concentration has no effect on the location of the zpc is characteristic of indifferent (non-specific sorption).

The results showed that neither cation nor anion capacities are single valued functions of pH. Since anion exchange was considered to occur by protonation of surface sites accompanied by equivalent uptake of chloride counterions, the anion capacity would be expected to be a single valued function of the activity of the total acid (HCl) in solution. This was conveniently expressed in logarithmic form as pH + pCl (pA). Exchange capacity is plotted against pA in Figure 6.5. The plot shows that below the zpc (that is, where zirconia is an anion exchanger and the mechanism in eqn. 6.1 applies), capacity is a single valued function of pA. In basic solution, the anion exchange mechanism no longer applies, so there is no pA relationship and the curves are divergent. This result demonstrates that eqn. 6.1 fully describes the anion exchange behaviour of zirconia in this titration.

Similar principles were applied in order to validate the proposed mechanism of cation exchange. From eqn. 6.2 the cation capacity was expected to be a single valued function of the activity of total base (NaOH) in solution. Exchange capacity is plotted against pNa + pOH (pB) in Figure 6.6. In this case, cation exchange capacity (above pH 8) was a single valued function of pB, with the curves diverging in acid solution.

The results obtained from this titration of calcined zirconia were qualitatively similar to those found with non-calcined zirconia [8], with exchange capacities considerably reduced. Dual effects of pH and salt concentration on the exchange capacity, with zpc between pH 7 and 8, were observed. The monofunctional relationships between pA and anionic capacity and between pB and cationic capacity branches respectively, as predicted by the exchange mechanisms (eqns. 6.1 and 6.2) previously established for the oxide precursors of ceramic membranes, apply equally to calcined oxides. The enhanced precision of the automated titration method is readily apparent, with capacities of around 0.1 meq/g being resolved with confidence, an order of magnitude smaller than previously achieved.

To investigate the effect of having potassium (rather than sodium) as the sorbing cation on the exchange capacities of calcined monoclinic zirconia, a titration similar to that previously described was performed, with KOH replacing NaOH as the base and making a salt addition of KCl rather than NaCl. Uptakes of all ions were monitored using H, K and Cl ion selective electrodes (since the hydrogen ion interference on K ISE was less than on Na ISE, potassium ion uptake data in acid media were more reliable in this case). Otherwise, the titration proceeded exactly as before.

The amphoteric properties of zirconia were again demonstrated, with anion exchange in acid and cation exchange in base, Figure 6.7. In acid solution there was a stoichiometric uptake of hydrogen and chloride, while in base a stoichiometric uptake of potassium and release of hydrogen was observed (Figure 6.8), with no cationic exchange in acid nor anionic exchange in base. pA and pB relationships were observed as before, (Figures 6.9 and 6.10), indicating that the mechanisms of eqns. 6.1 and 6.2 applied. The only difference between the two titrations was that in the case of the titration with sodium as the sorbing cation, the cation exchange capacities were somewhat higher

than with potassium as the sorbing cation, at equivalent pB (as seen by comparison of Figures 6.6 and 6.10. This would seem to indicate a slightly higher selectivity for sodium over potassium. Apart from this, the exchange characteristics of calcined zirconia remain largely unaffected when the supporting electrolyte is changed from NaCl to KCl. The same ion exchange mechanisms apply, exchange capacities are similar and neither electrolyte causes a shift in the zpc, indicating the absence of specific sorption.

The ion exchange capacities measured on the calcined sample of monoclinic zirconia were considerably lower than those reported elsewhere for non-calcined zirconia [8]. Kraus et. al. [1] have shown that an increase in the drying temperature of zirconia causes a decrease in capacity. To verify this, a sample of non-calcined zirconia, prepared by the method of Clearfield [11], was titrated with HCl, NaOH and NaCl in the same manner as with calcined zirconia, with solution activities and uptakes for all ions monitored by ion selective electrode. The difference in the ion exchange capacities of each sample are illustrated in Figures 6.11 and 6.12. In the pH range anion capacity applied, greater anion capacities were measured on the non-calcined sample at any given value of pA. The same effects were observed with cation exchange at given values of pB.

Surface areas for each sample of zirconia were determined by BET, giving measurements of $66m^2/g$ for the calcined sample and $197.7m^2/g$ for the non-calcined sample. The determination of this parameter enabled the expression of ion exchange capacities per unit of area. When the ion exchange capacity data from Figures 6.11 and 6.12 were expressed in units of $\mu mol/m^2$, remarkably good agreement between the samples was obtained (Figures 6.13 and 6.14). This result strongly suggests that the loss of capacity on calcination was due to a loss of total surface area and that the remaining exchange sites were equivalent (although less in number) to those on the non-calcined sample.

6.3.2 Silica

Calcined silica, as produced by the method described earlier, was found to contain some sodium ions. It was necessary to remove these ions prior to titration by pre-equilibrating the silica at around pH 2.5 and washing with distilled water.

Dispersions of silica were titrated with acids, bases and salt solutions, with ion concentrations monitored by ISE, in a similar manner to the titrations of zirconia dispersions. With titrations of silica dispersions, it was necessary to terminate the titration below pH 10 to ensure that no significant dissolution of the solid occurred.

A dispersion of silica was titrated with HCl, NaOH and NaCl. After an initial addition of acid, the dispersion was titrated forward with base to above pH 9. An addition of NaCl solution was made, followed by back-titration with acid. pH, pNa and pCl were monitored directly by the respective ion selective electrodes.

Uptake data for hydrogen, chloride and sodium ions are shown in Figure 6.15. In contrast to the zirconia titrations, there was no uptake of hydrogen and chloride ions in acid solution. Only cation exchange behaviour was observed, with a stoichiometric uptake of sodium and release of hydrogen. No uptake of chloride was observed at any point in the titration. The effect of salt on the exchange capacity was clearly observed (Figure 6.16), with the addition of salt resulting in a shift in the pH to lower values. No common (crossover) point for the two curves was seen within the titrated pH range, indicating that the cation exchange branch covered the entire titrated range, with the zero point charge consequently being below pH 3.

The two capacity curves overlapped when plotted as a function of pB, showing that cation exchange was a single valued function of the activity in solution of total base (Figure 6.17). The exchange mechanism of eqn. 6.2 therefore applies in this case.

When a similar titration was performed with potassium instead of sodium as the sorbing cation (KOH and KCl titrants replacing NaOH and NaCl), similar results were obtained. Purely cationic exchange was observed throughout the titration range, with capacity a single valued function of pB. As with zirconia, a slightly higher selectivity for sodium over potassium ion was observed.

6.3.3 γ Alumina

To investigate the ion exchange characteristics of calcined γ alumina, titrations were made on dispersions of this material in distilled water, with HCl and NaOH (or KOH), with salt additions. In order to avoid dissolution of γAl_2O_3, the pH range for these titrations was between 4.5 and 10.

Titrations of γAl_2O_3 by HCl 0.1M and NaOH 0.13M (Figure 6.18) demonstrated the amphoteric nature of this oxide. Simultaneous uptake of H^+ and Cl^- was observed in the anion exchange branch, below a zpc around 8. Cation exchange behaviour of γAl_2O_3 was less obvious in these titrations, as the "upper limit" of pH 10 meant that it was only possible to titrate over a small range of the cation exchange branch. The pA dependence of hydrogen uptake below pH 8 is shown in Figure 6.19 where the results from Figure 6.18 are plotted against pA. The anion exchange mechanism in eqn. 6.1 was therefore shown to apply in this case. There were insufficient data obtained to illustrate a pB relationship for cation exchange, although it would be expected to also apply.

Almost exactly the same observations were made when KOH replaced NaOH as the titrating base, Figure 6.20. Again, the titration by HCl 0.1M and KOH 0.1M below pH8 showed Cl^- uptake for forward titration and Cl^- release for back titration confirming the reversibility of the process. A pA relationship for anion exchange was again observed, Figure 6.21.

6.3.4 Titania

Titrations of dispersions of calcined titania showed that this oxide was amphoteric, behaving as an anion exchanger below and cation exchanger above a z.p.c. of around 7. Figure 6.22 shows capacity data for titrations with and without added NaCl, the crossover occurring at the zpc of 7. Ion exchange capacities were fairly small - around one third of those observed at equivalent conditions with calcined zirconia. The pA and pB relationships are apparent (Figures 6.23 and 6.24), though not as convincingly so as with the other oxides, probably as a consequence of the very low capacities for this oxide.

6.3.5 α Alumina

To complete this study of the ion exchange properties of ceramic membrane oxide materials, samples of the membrane support material, α alumina, were titrated. The exchange capacities were extremely low - at the sensitivity limit of the current methodology- and meaningful data were not readily obtained. The main conclusion from the titrations of the support material was that the ion exchange capacities are very low relative to the capacities of the active layer oxides.

6.3.6 NASICON

The NASICON abbreviation stands for Na^+ Super Ionic Conductor. This material is an inorganic network formed by a three-dimensional association of tetrahedral SiO_4, PO_4, or both $(Si,P)O_4$ and octahedral ZrO_6. This backbone is negatively charged, with the charge compensated for by cations, for example Na^+. These cations are free to move within the network along three-dimensional pathways and may be exchanged for other

cations in aqueous solution. The ion exchange properties of NASICON were examined titrimetrically. Titrations were performed with acid, base and salt titrants as required and ion activities in solution were monitored by ion selective electrodes.

A complicating factor in the performance of these titrations was due to the leaching of phosphate into the solution phase on dispersion of NASICON. Colorimetric analysis of phosphate ion concentration in solution, performed using acidified sodium molybdate solution, showed that a dispersion of 0.4g NASICON in 25ml water for 24 hours produced a solution approximately 10^{-3}M in phosphate. Therefore, before titration, it was necessary to remove leachable phosphate, by dialysis or by repeated washing of NASICON. These treatments efficiently reduced the phosphate concentrations in dispersions to around 10^{-5}M.

Dispersion of 0.1g NASICON in 25 ml distilled water produced a pH within the range 9.5-10.5, initially thought to be due to further release of phosphate. Analysis of the supernatant showed this not to be the case. The creation of a background concentration of sodium on dispersion suggested that hydrolysis of water occurs with sodium exchanging for hydrogen (eqn. 6.3). This was confirmed by titration of the NASICON suspension with NaOH and the observation of proton release and sodium uptake (Figure 6.25). Data are plotted against pH - pNa because, as shown below, uptake is a single valued function of this parameter. Since NASICON is a purely cationic exchanger, uptake of cation is balanced by equivalent release of cation. On dispersion there is an uptake of protons of around 0.12 meq/g ($\overline{X}_H = 0.03$).

$$\overline{Na^+} + H_2O \rightleftharpoons \overline{H^+} + Na^+ + OH^- \qquad \textbf{(6.3)}$$

A dispersion of 0.15 g NASICON in 25 ml distilled water was titrated with 0.1M HCl. Solution activities of H^+ and Na^+ were measured by ISE and the uptakes of these ions determined from the measurements. The cationic exchange behaviour of NASICON was observed with H^+ uptake and Na^+ release increasing with the addition of acid, Figure 6.26. Stoichiometric exchange was observed. The exchange capacity of NASICON was approximately 3.7 milliequivalents per gram, representing the exchange with H^+ of around 60% of the theoretical number of sodium ions present in NASICON. The exchange process was reversible by back titration with NaOH (Figure 6.27) although hysteresis was observed, most likely as a consequence of the slow kinetics of the exchange process, as discussed below.

In a separate titration, a dispersion was made of NASICON which had been converted to the H^+ form by titration with HCl. The dispersion was titrated with NaOH to pH 7.2, where an addition of 3ml 0.1M NaCl was made. The salt addition caused a reduction in the solution pH to 6.1. The dispersion was then further titrated with NaOH. The measured uptake of H^+ in this titration is shown as a function of pH in Figure 6.28. When the same data were plotted against pH - pNa, a smooth curve was obtained, demonstrating that ion uptake is a single valued function of pH - pNa, Figure 6.29.

The potassium ion exchange properties were investigated by titration with KOH of a dispersion of NASICON in the H^+ form. A lower exchange capacity (around 1 meq/g) for potassium was observed, suggesting the inaccessibility of a proportion of the exchange sites to the larger potassium ion (under the conditions employed for the titrations). Again, this process was reversible.

By monitoring chloride ion activities with ISE, it was shown that there was no observable anion exchange on NASICON under these experimental conditions.

In the course of NASICON titrations, the same electrode stability criteria were used as for the inorganic oxide titrations - these criteria had been found to be more than adequate for all exchangers previously examined in this particle size range. However, with NASICON titration, the pH electrode response changed very slowly over a considerably longer period of time than any other exchanger examined. Figure 6.30 shows a decrease in pH electrode response of 60 mV (1 pH unit between pH 3 and 4) over a period of 14 hours, corresponding to a slow removal of H^+ from the solution. When the exchange process was reversed, the pH electrode showed a continued rise in mV (drop in pH) demonstrating the slow release of H^+ ions from the exchanger. The exchange diffusion of Na^+/H^+ through NASICON is therefore extremely slow, probably as a consequence of exchange taking place within the three-dimensional network structure of this material.

The implications of slow kinetics with respect to the titration results are as follows : (a) within the pH range 4-10, the uptake values (calculated by mass balance) at each titration point are accurate but the solution pH is not the equilibrium pH. For forward titrations, the equilibrium pH is higher than the measured value; for back titrations, the equilibrium pH is lower; (b) when pH<4 and pH>11, the inaccuracy of the uptake values becomes increasingly large and titration data of little value.

The selectivity coefficient K_{Na}^{H} for the exchange reaction between H^+ and Na^+ was calculated by

$$K_{Na}^{H} = \frac{\overline{X}_{H^+} \cdot [Na^+]}{\overline{X}_{Na^+} \cdot [H^+]} \qquad (6.5)$$

where $\overline{X}_{H^+}$ and $\overline{X}_{Na^+}$ are the ionic fractions in the exchanger of H^+ and Na^+ respectively.

Since titration data were obtained before final equilibrium was reached, the measured pH was less than the equilibrium pH, so the true (equilibrium) value of K_{Na}^{H} was greater than the measured value. In the case of reverse titrations (H^+ to Na^+ form), measured pH is greater than equilibrium pH - consequently, the true value of K_{Na}^{H} was less than the measured value. In Figure 6.31, the logarithm of the measured selectivity coefficients K_{Na}^{H} are plotted as a function of the ionic composition of the exchanger. It is most likely that the true (equilibrium) value of log K_{Na}^{H} lies between the measured values obtained in the forward and back titrations.

6.3.7 Prediction of Surface Charge of Active Layer Oxides

The results of the research presented in this Chapter show clearly that the sorptive properties of these oxides can be radically and predictively altered by adjusting the pH and/or the salt concentration in the solutions to which they are exposed. Since the ion exchange properties are single valued functions of pA or pB, it is possible to estimate the exchange characteristics of any of these materials at a particular pH and salt concentrations.

The effect of changing pH and salt concentration on the sorption of sodium and chloride ion on calcined zirconia are shown in Figures 6.32 and 6.33. Distribution coefficients (in ml/g) for the sorbing ions on each oxide were also obtained. In the case of sodium sorption on zirconia, the ratio of adsorbed sodium ion to sodium ion in solution increases when the solution pH is raised, Figure 6.34. Similarly, the ratio of adsorbed chloride ion to chloride ion in solution increases with decreasing pH. These results are

characteristic of all amphoteric oxides studied in this research. It is therefore possible to predict the surface charge and sorptive properties of these oxides from the ionic composition of the solution. Further examples are given in Figures 6.35 to 6.40.

6.4 Conclusions

The ion exchange and sorptive properties of the active layers of ceramic membranes have been characterised. The factors influencing these properties have been isolated and their influence explained in mechanistic terms. These mechanisms for ion exchange were shown to be the same as for those previously determined on non-calcined microcrystalline oxides, but ion exchange capacities are an order of magnitude smaller than observed previously for their non-calcined analogues. These were determined precisely using improved computer controlled titration methods.

The main factors affecting the membrane active layer sorptive properties are solution pH, the activity of the sorbing ion and the sorbing ion species. By changing these parameters, it has been demonstrated that it is possible to alter the membrane surface charge density and reverse the polarity in a predictable way. The ion exchange and sorption characteristics of the membrane are correspondingly altered.

By appropriate selection of the membrane active layer material and manipulation of the operational parameters, it should be possible to optimise conditions for separation processes across UF/RO membranes. Similarly, optimisation of operating conditions and membrane surface modifications raise the possibility of reducing membrane fouling by charged substrates such as proteins, thus improving efficiency and increasing the membrane lifetime.

Preliminary fouling studies were made on the sorption of amino acids on calcined oxides [12]. Amino acids were chosen as the fouling substrates in order to gain elementary

information on the mechanisms and factors affecting fouling by proteins. The effects of pH and salt concentration on amino acid sorption were assessed. No sorption was observed at pH where the sign of the oxide surface charge and the amino acid charge was the same. Sorption was observed when the sign of the amino acid charge and the sign of the oxide surface charge were opposite. By increasing the salt concentration, higher uptake of amino acid occurred, as a consequence of the pA/pB dependency of surface charge. These studies demonstrate that by manipulation of the operating conditions (pH and salt concentration), the degree of sorption of a charged substrate may be controlled.

Filtration studies were performed on supported ultrafiltration zirconia membranes with solutions of known pH and ion concentration [12]. The highest fluxes were observed when the pH of the solution was close to the zpc of zirconia (pH 7), corresponding to a minimal surface charge. Fluxes were shown to decrease when the oxide surface charge increased (pA decrease in acid range, or pB decrease in alkaline range, at fixed ionic strength) as a consequence of the increasingly interfacial interactions between the solution and the charged oxide. Higher fluxes were observed when the surface charge was kept constant and the ionic strength of the solution was increased. This was due to the collapsing of the double layer inside the pores, leading to lesser interfacial interaction.

In the following Chapter the potentiometric titration techniques are applied to systems where specific ion sorption processes are occurring.

References

[1] K.A. Kraus, H.O. Phillips, T.A. Carlson and J.S. Johnson, Proc. 2nd International Conference on Peaceful Uses of Atomic Energy, **28**, 3 (1958)

[2] C.B. Amphlett, Inorganic Ion Exchangers, Elsevier, Amsterdam, (1964)

[3] L. Cot, Proc. 1st International Conference on Inorganic Membranes, Montpellier, 17 (1989)

[4] A. Larbot, A. Julbe, J. Randon, C. Guizard, L. Cot, Proc. 1st International Conference on Inorganic Membranes, Montpellier, 31 (1989)

[5] R. Paterson, H. Rahman, J. Coll. Int. Sci., **94**, 60 (1983)

[6] R. Paterson, H. Rahman, J. Coll. Int. Sci., **97**, 423 (1984)

[7] R. Paterson, H. Rahman, J. Coll. Int. Sci., **98**, 494 (1985)

[8] R. Paterson, H. Rahman, J. Coll. Int. Sci., **103**, 106 (1985)

[9] R. Paterson, A. Smith, J. Coll. Int. Sci., **124**, 581, (1988)

[10] R. Paterson, Proc. 1st International Conference on Inorganic Membranes, Montpellier, 127 (1989)

[11] A. Clearfield, Inorg. Chem., **3** 146 (1964)

[12] R. Paterson, L. Cot et al., Chapter 8 in Final Report for C.E.C. Contract No. SC1 0178-C(EDB) between E.N.S.C.Montpellier, Univ. of Glasgow and U.S.T.Languedoc (1991)

Table 6.1 : Chemical precursors of active layer materials.

Oxide	Precursors
ZrO_2	Hydrous metal oxide
TiO_2	Hydrous metal oxide
SiO_2	colloidal SiO_2
γAl_2O_3	Boehmite
NASICON	$Zr(OC_3H_7)_4$, $NaNO_3$, SiO_2, $NH_4H_2PO_4$

Table 6.2 : Physical characteristics of oxides of the active layers of ceramic membranes.

Oxide	Structure	Calcining Temp. (°C)	Specific Area (m^2/g)	Density (g/cm^3)	Average Particle Diameter (Å)	% H_2O
ZrO_2	Monoclinic	750	66	5.6	160	7.5
TiO_2	Tetragonal	480	25	3.9	600	1.5
SiO_2	Amorphous	600	135	2.2	200	4
γAl_2O_3	Cubic	540	250	3.2	80	12.5

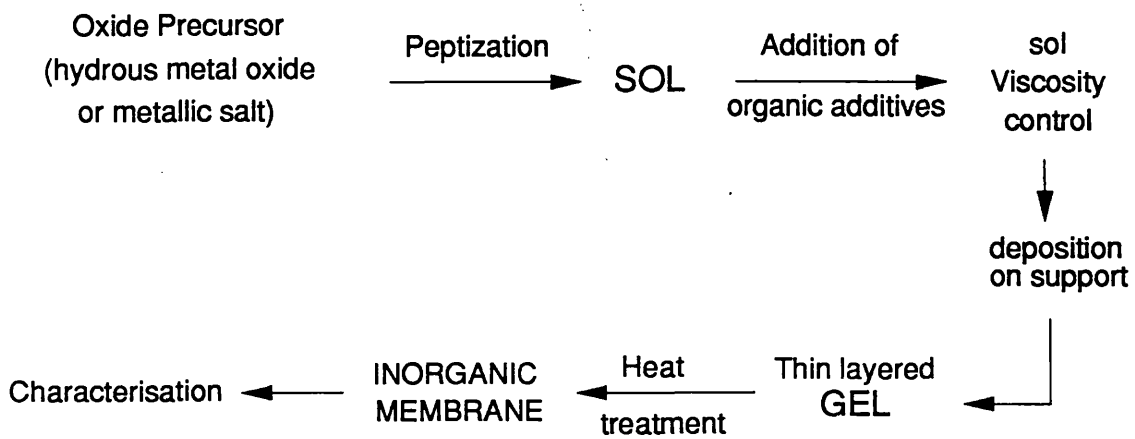

Figure 6.1 : General preparation scheme for inorganic membranes by the sol-gel process.

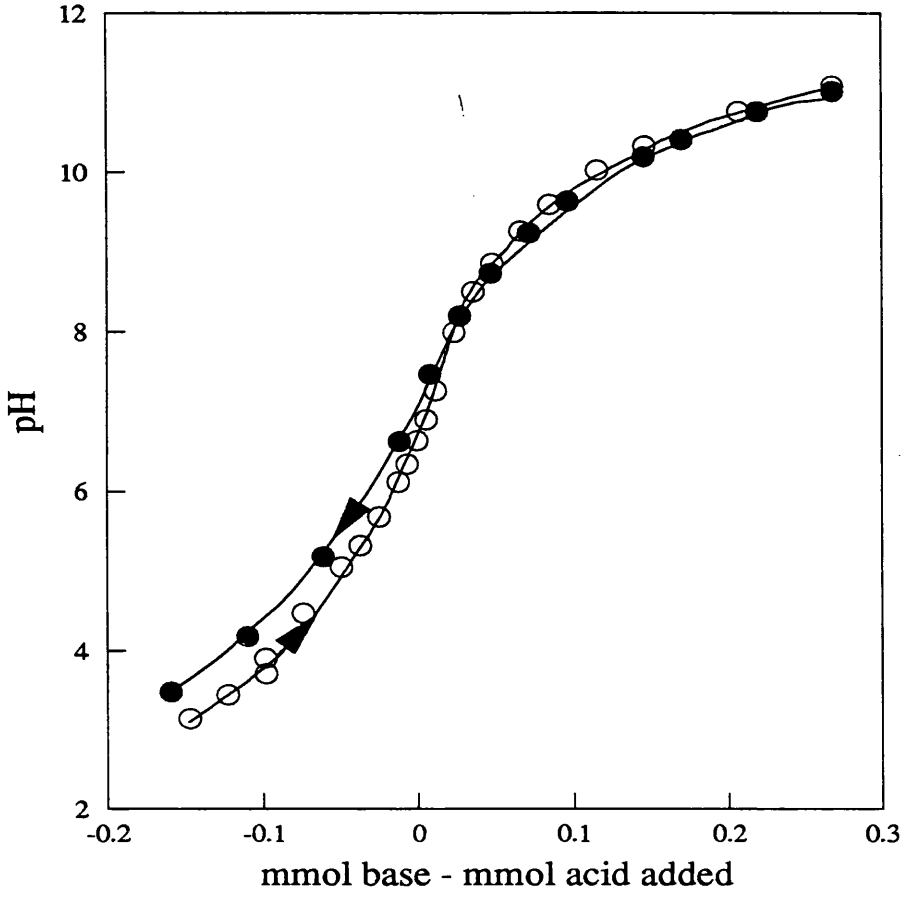

Figure 6.2 : pH titration of a dispersion of 1.5g calcined monoclinic zirconia in 25ml distilled water. After an initial addition of 1.5ml 0.1M HCl, the dispersion was titrated with 0.12M NaOH (○). At pH 11.08 an addition of 2ml 0.1M NaCl was made and the dispersion back-titrated with 0.1M HCl (●).

Titration File: ZIR4

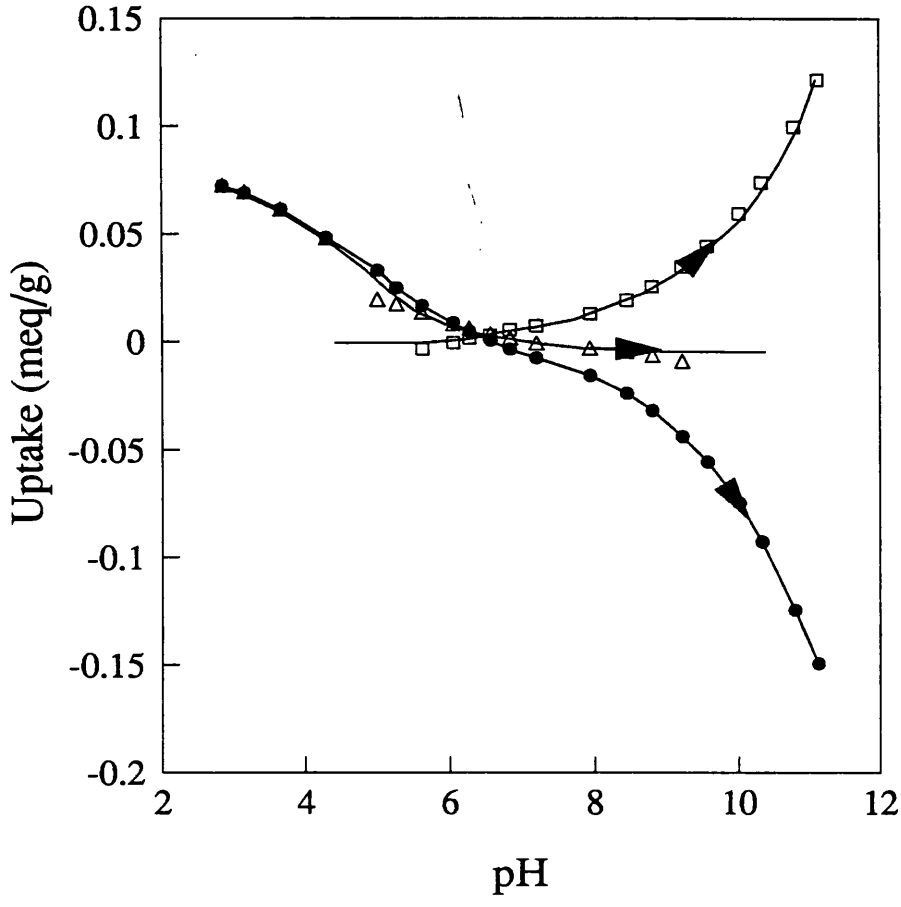

Figure 6.3 : Ion uptakes, as determined from ion selective electrode readings from the titration described in Figure 6.2. Results are shown for the section of the titration before the salt addition. Uptakes for H^+ (●), Na^+ (□) and Cl^-(△) are presented.

Titration File: ZIR4

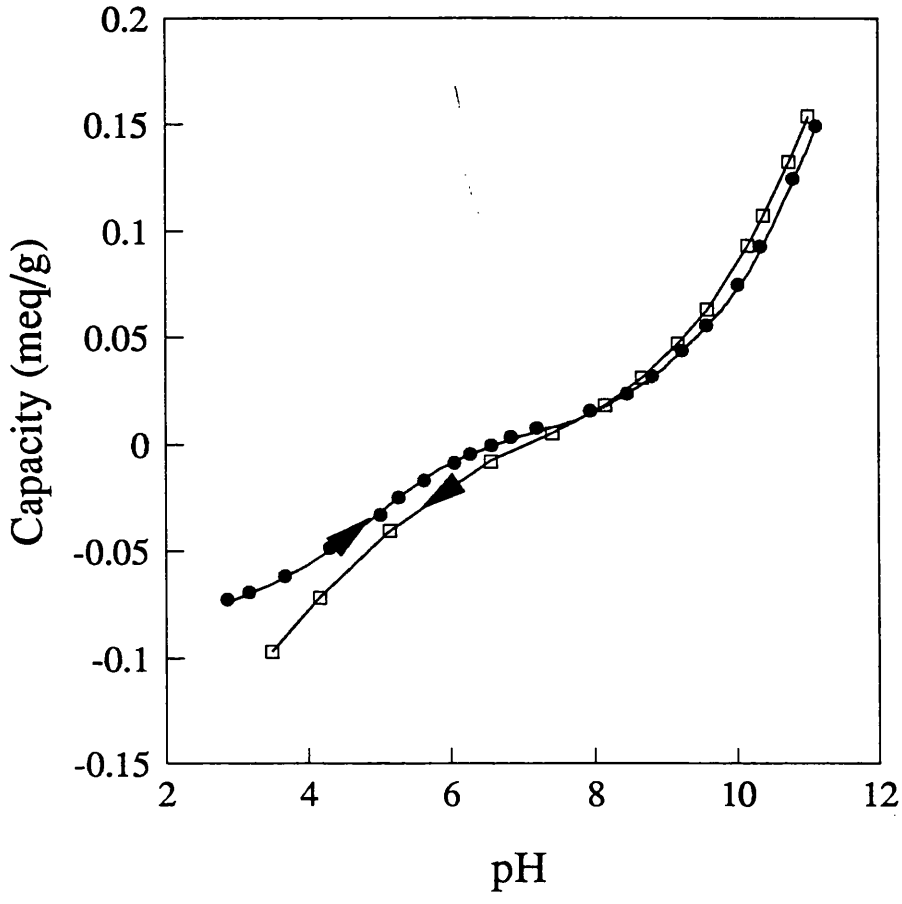

Figure 6.4 : Ion exchange capacity of monoclinic zirconia as a function of pH, as measured from the titration described in Figure 6.2. Results are shown before addition of NaCl (●) and after the salt addition (□).

Titration File: ZIR4

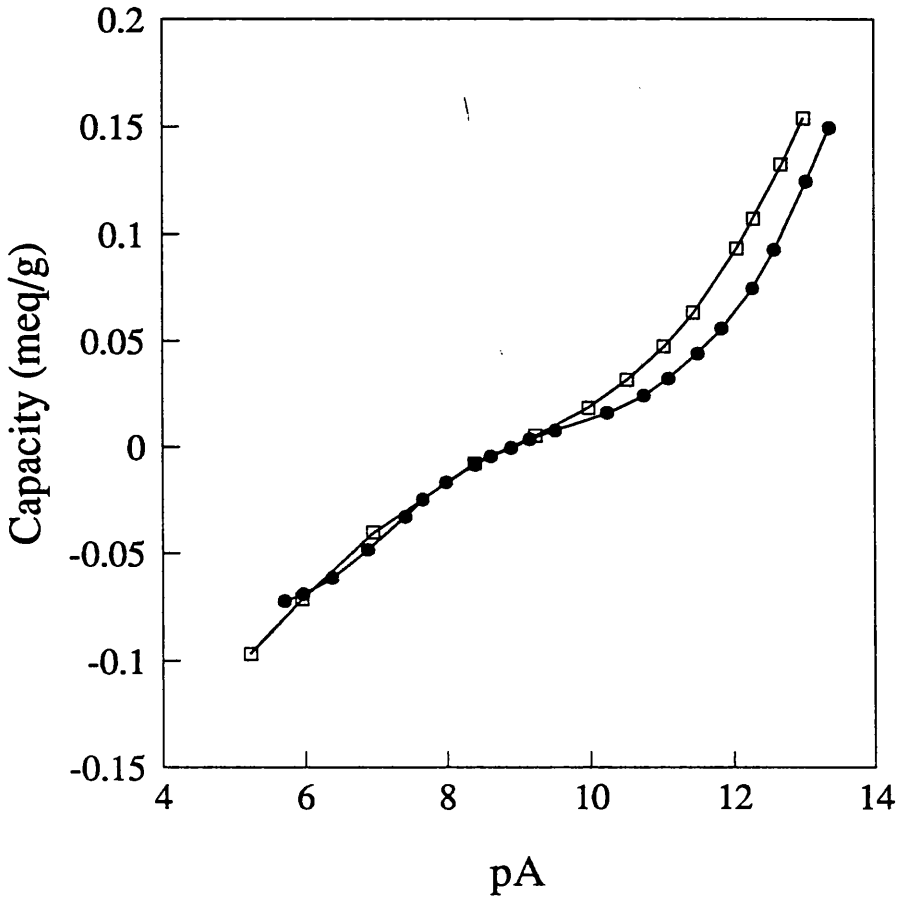

Figure 6.5 : Exchange capacity data from Figure 6.4 as a function of pA (= pH + pCl).

Titration File: ZIR4

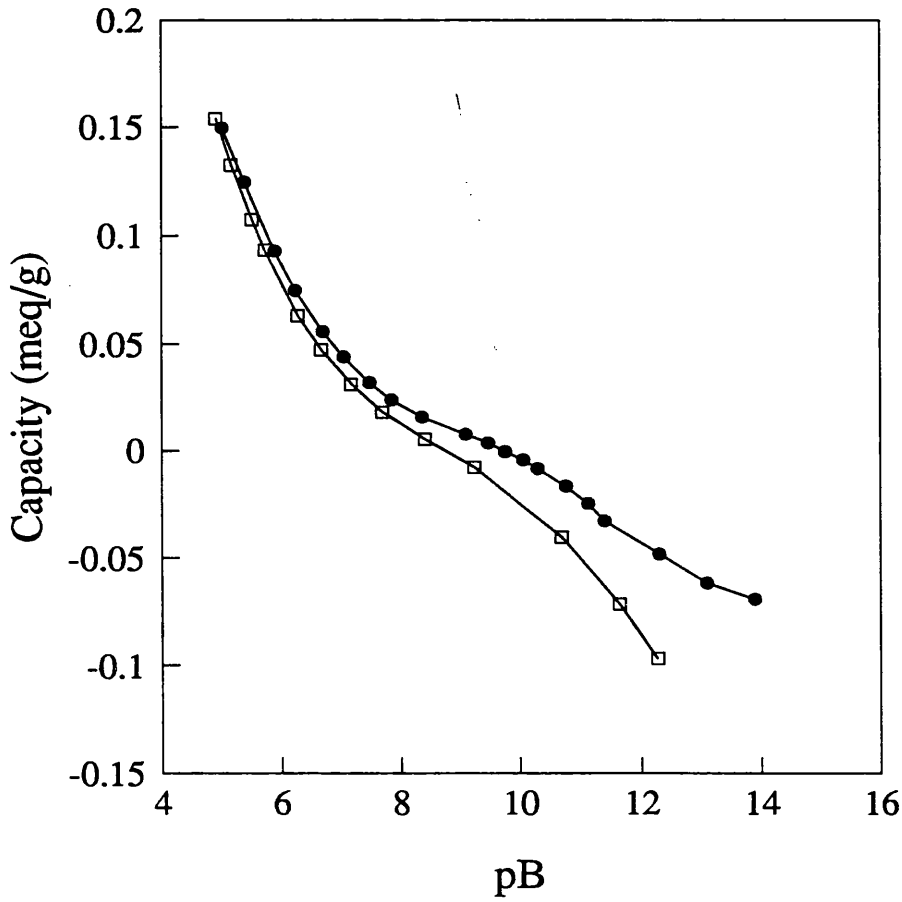

Figure 6.6 : Exchange capacity data from Figure 6.4 as a funcion of pB (= pNa + pOH).

Titration File: ZIR4

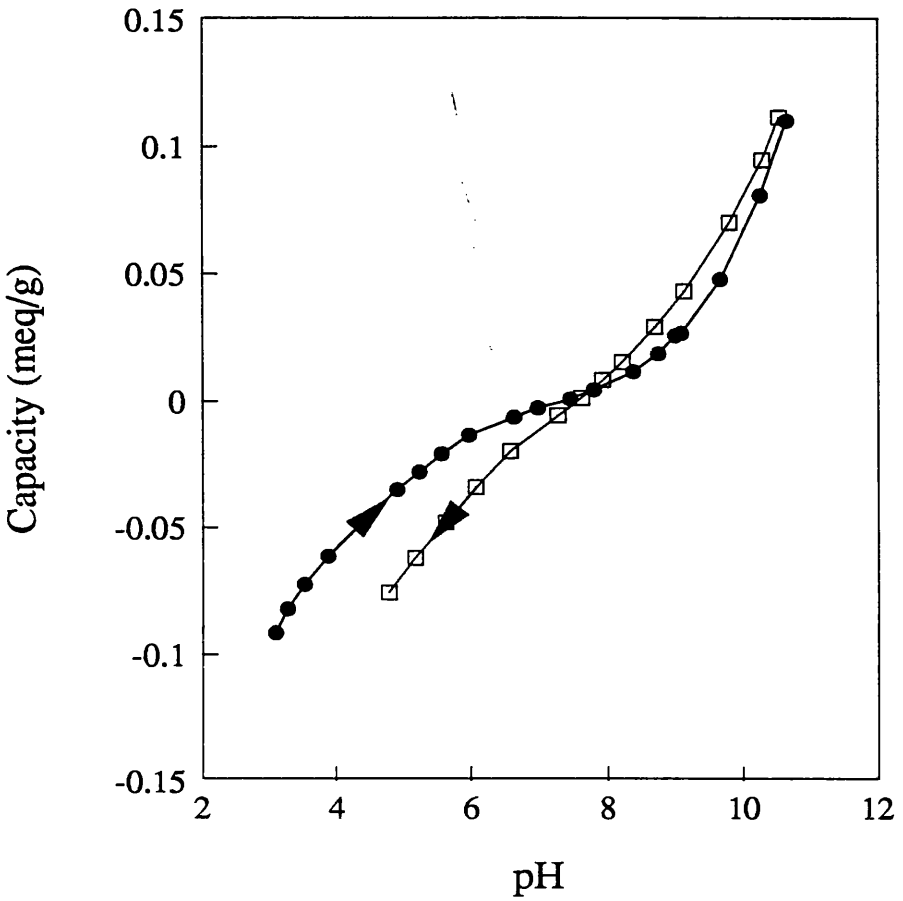

Figure 6.7 : Exchange properties of calcined monoclinic zirconia. A dispersion of 1.4g calcined monoclinic zirconia in 25ml water was titrated with 0.1M KOH after an initial addition 1.5ml 0.1M HCl. At pH 10.65, 2ml 0.5M KCl was added and the dispersion back-titrated with 0.1M HCl. Capacities before the addition of KCl (●) and after the salt addition (□) are shown.

Titration File: ZIR5

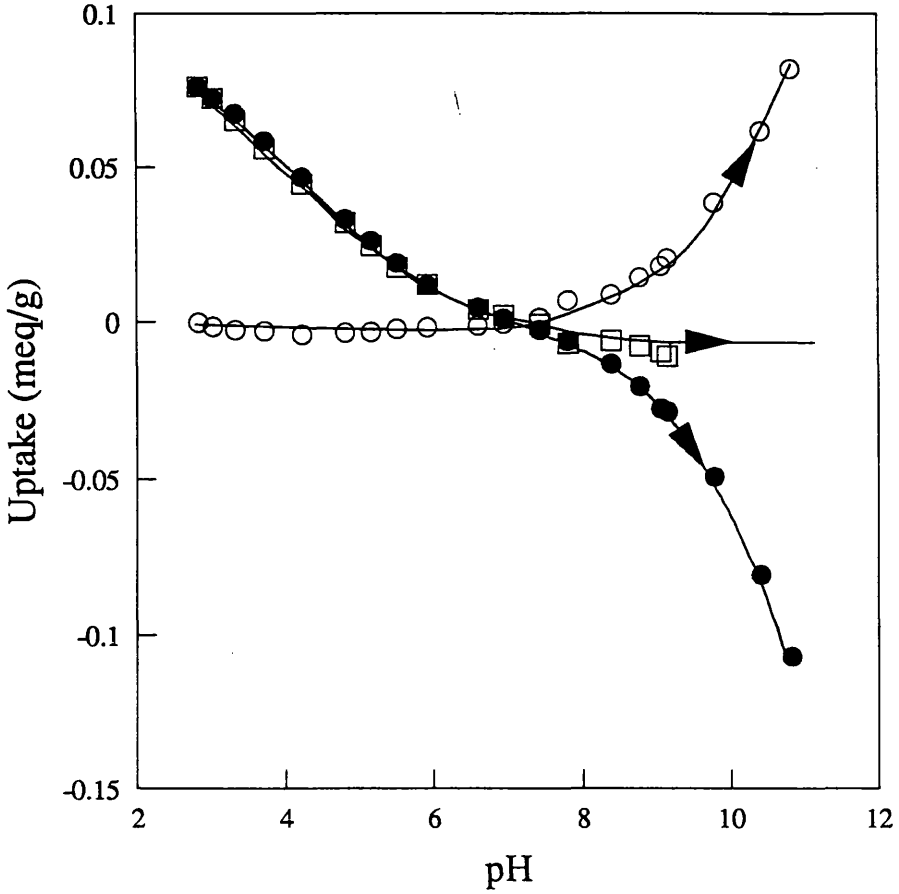

Figure 6.8 : Ion uptakes (as measured by ISE) from the titration described in Figure 6.7. Results are presented for the section of the titration before the salt addition and have been corrected for the suspension potential. Uptakes for H^+ (●), K^+ (△) and Cl^- (□) are presented.

Titration File: ZIR5

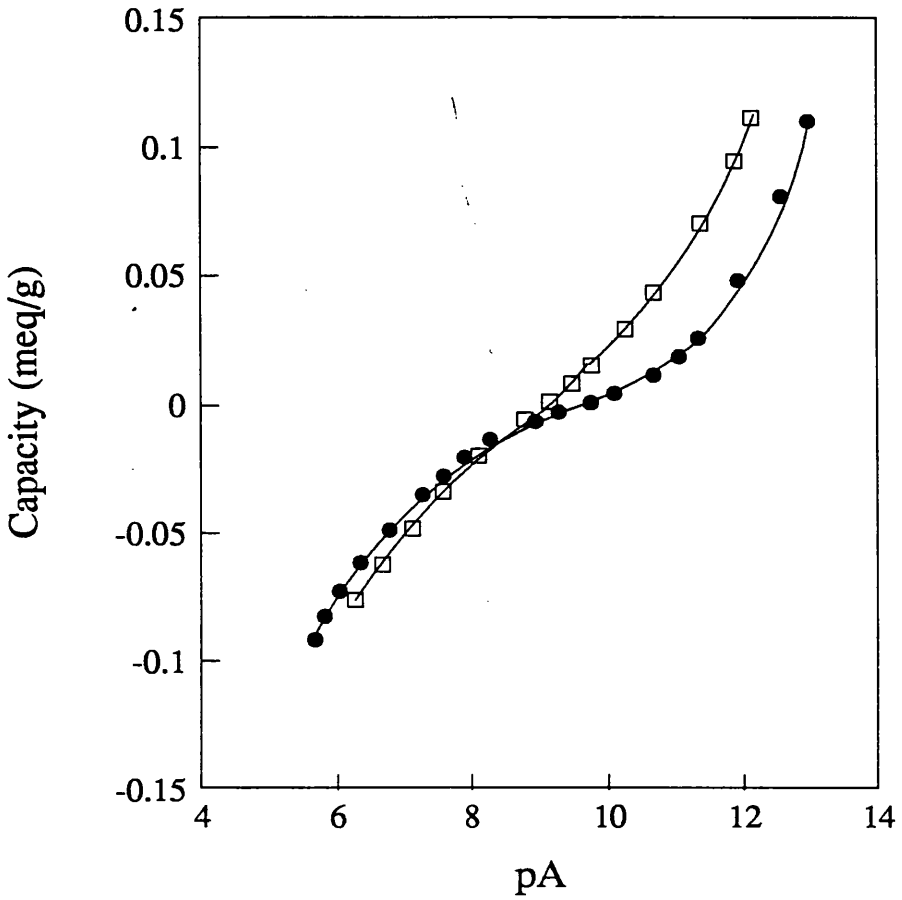

Figure 6.9 : Exchange capacity data from Figure 6.7 shown as a function of pA (= pH + pCl)

Titration File: ZIR5

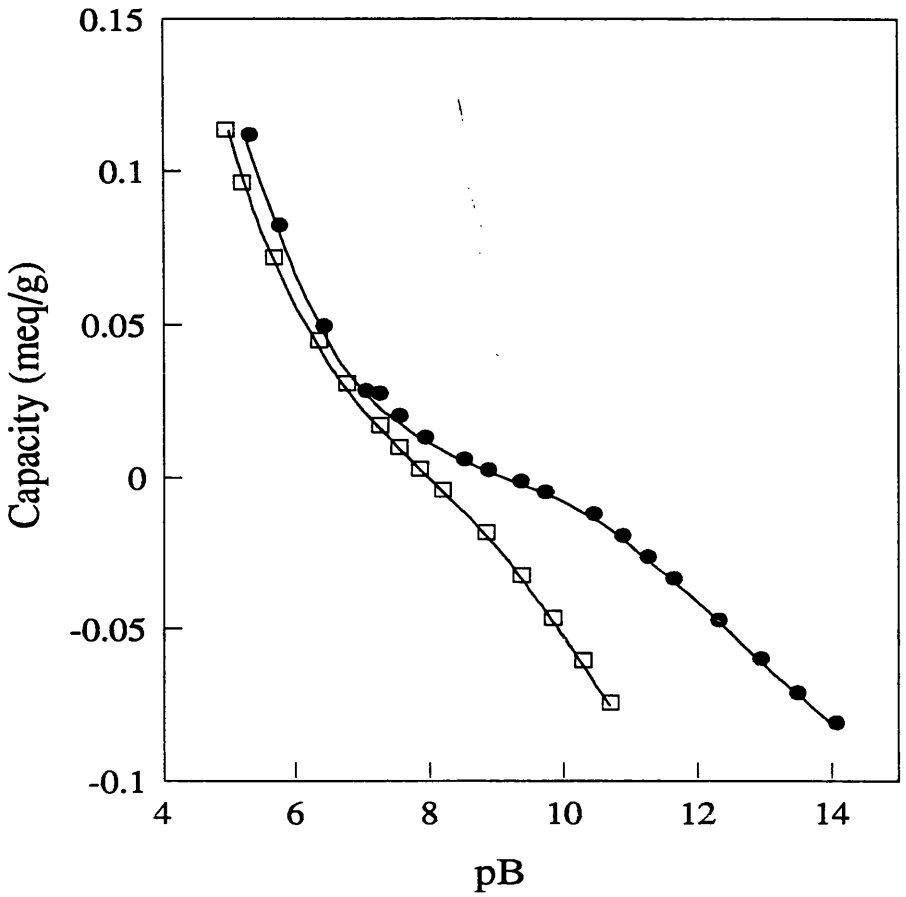

Figures 6.10 : Exchange capacity data from Figure 6.7 shown as a function of pB (= pK + pOH)

Titration File: ZIR5

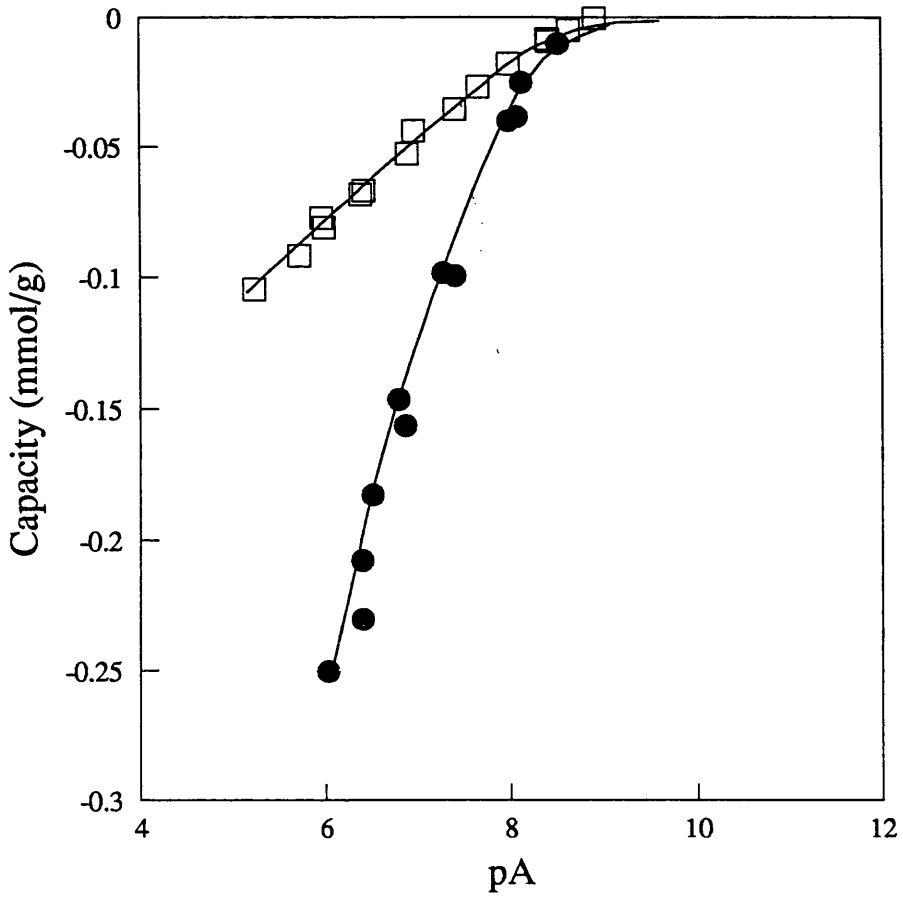

Figure 6.11 : Anion exchange capacities of non-calcined zirconia (●) and calcined zirconia (□). A dispersion of 1.5g calcined monoclinic zirconia in 25ml distilled water was titrated with 0.1M HCl and 0.12M NaOH. In a separate titration, 0.1922g non-calcined monoclinic zirconia in 25ml distilled water was titrated with 0.1M HCl and 0.1M NaOH. Exchange capacities were determined from ISE measurements and are shown as a function of pA (= pH +pCl).

Titration Files: OLDZIR, ZIR4

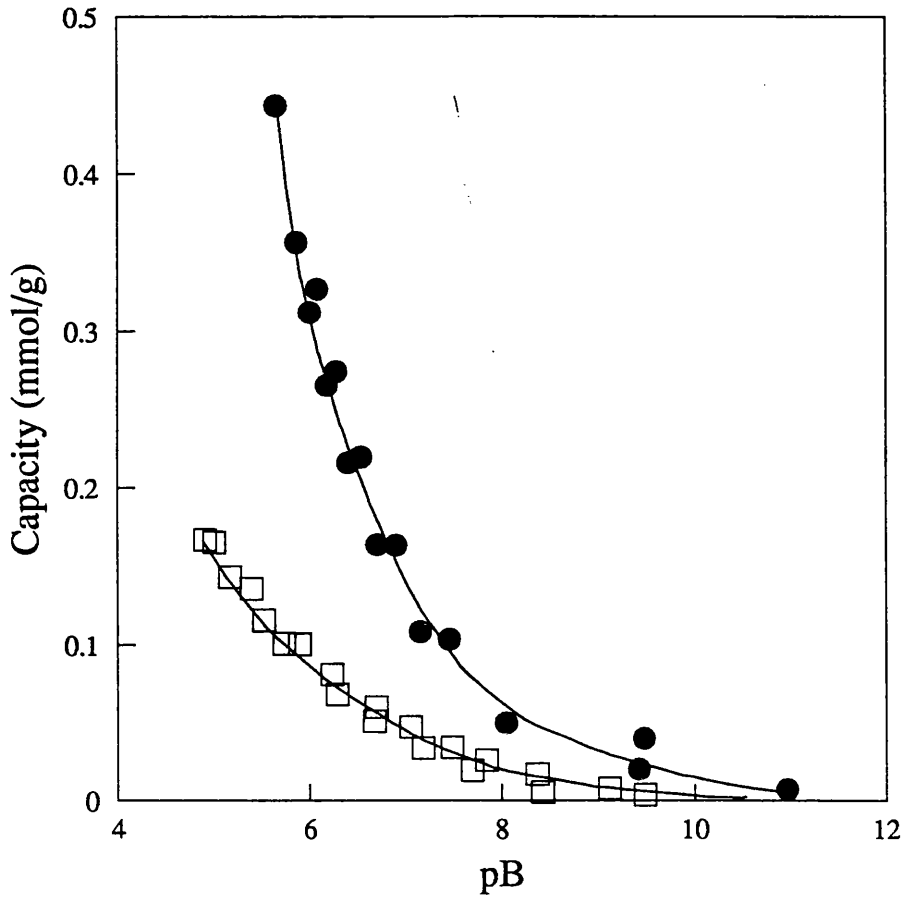

Figure 6.12 : Cation exchange capacities of non-calcined zirconia (●) and calcined zirconia (□). Dispersions of each sample were titrated as described in Figure 6.11. Exchange capacities are shown as a function of pB (= pNa +pOH).

Titration Files: OLDZIR, ZIR4

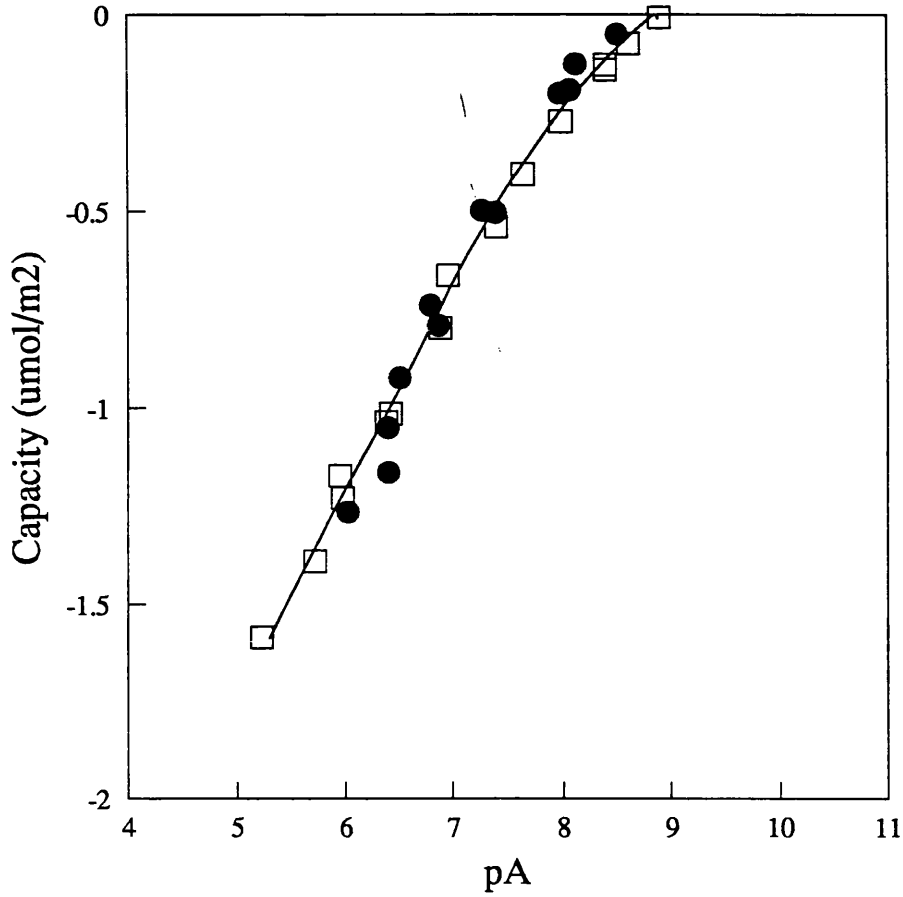

Figure 6.13 : Anion exchange capacity data from Figure 6.11 expressed as capacity per unit area ($\mu mol/m^2$).

Titration Files: OLDZIR, ZIR4

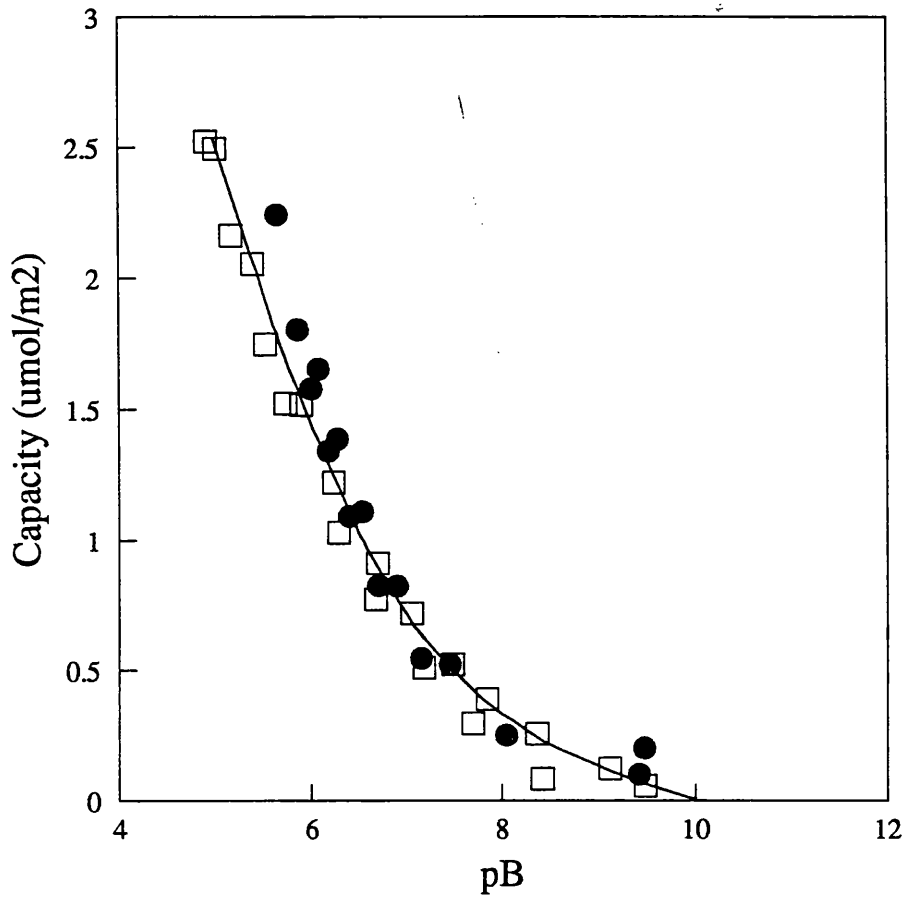

Figure 6.14 : Cation exchange capacity data from Figure 6.12 expressed as capacity per unit area (μmol/m^2).

Titration Files: OLDZIR, ZIR4

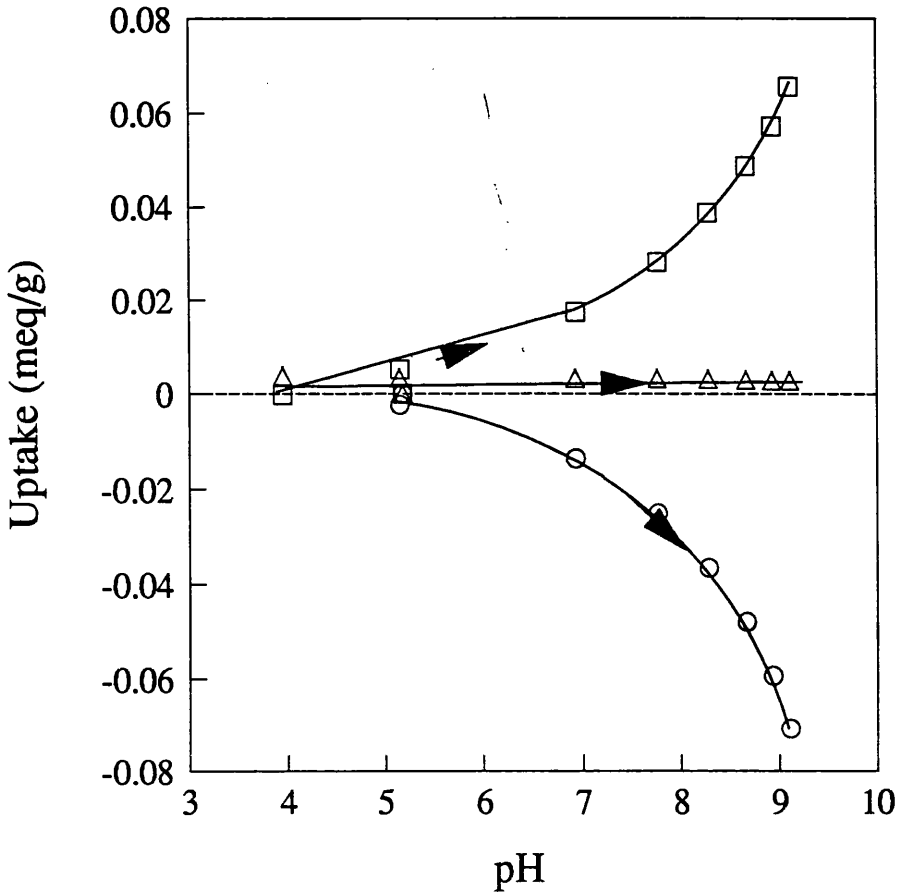

Figures 6.15 : Titration of a dispersion of 1.061g calcined silica in 25ml distilled water. After an initial addition of 0.1ml 0.1M HCl the dispersion was titrated with 0.12M NaOH. Uptake data for H^+ (○), Na^+ (□) and Cl^- (△) were obtained from ion selective electrode measurements.

Titration File: JSI2

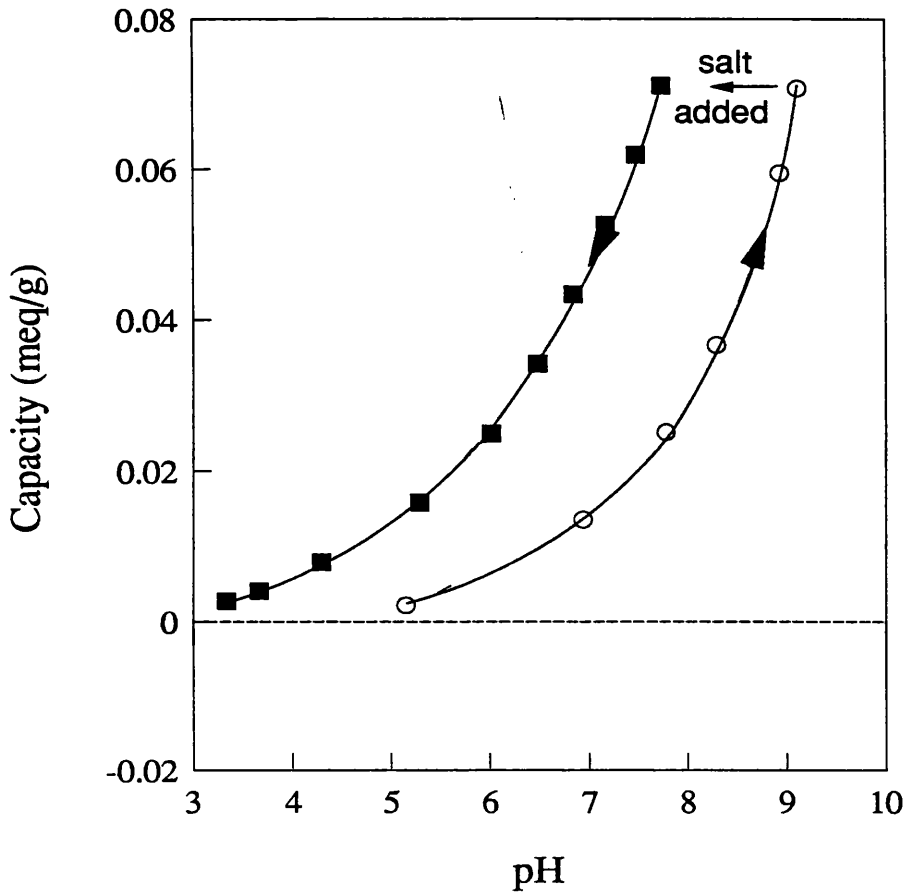

Figures 6.16 : Ion exchange capacities of calcined silica. A dispersion of 1.061g silica in 25ml distilled water was titrated with 0.12M NaOH, after an initial addition of 0.1ml 0.1M HCl (○). At pH 9, 1ml 1M NaCl was added and the dispersion back-titrated with 0.1M HCl (■).

Titration File: JSI2

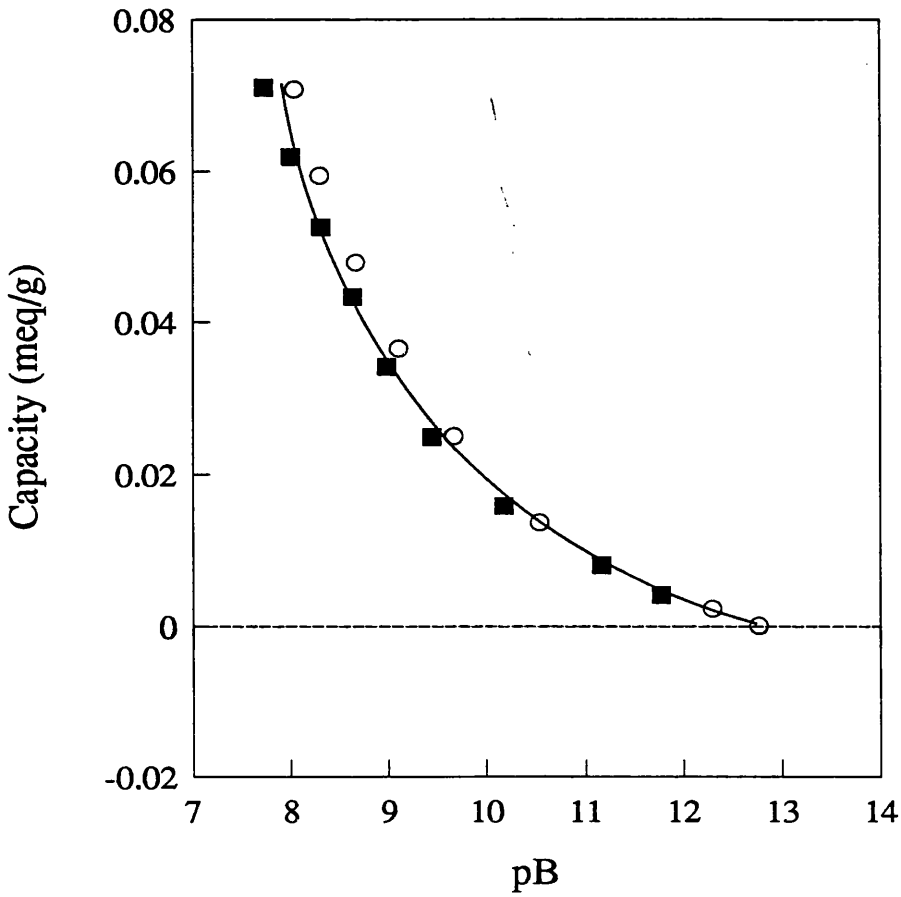

Figures 6.17 : Ion exchange capacity data from Figure 6.16 shown as a function of pB (= pNa + pOH).

Titration File: JSI2

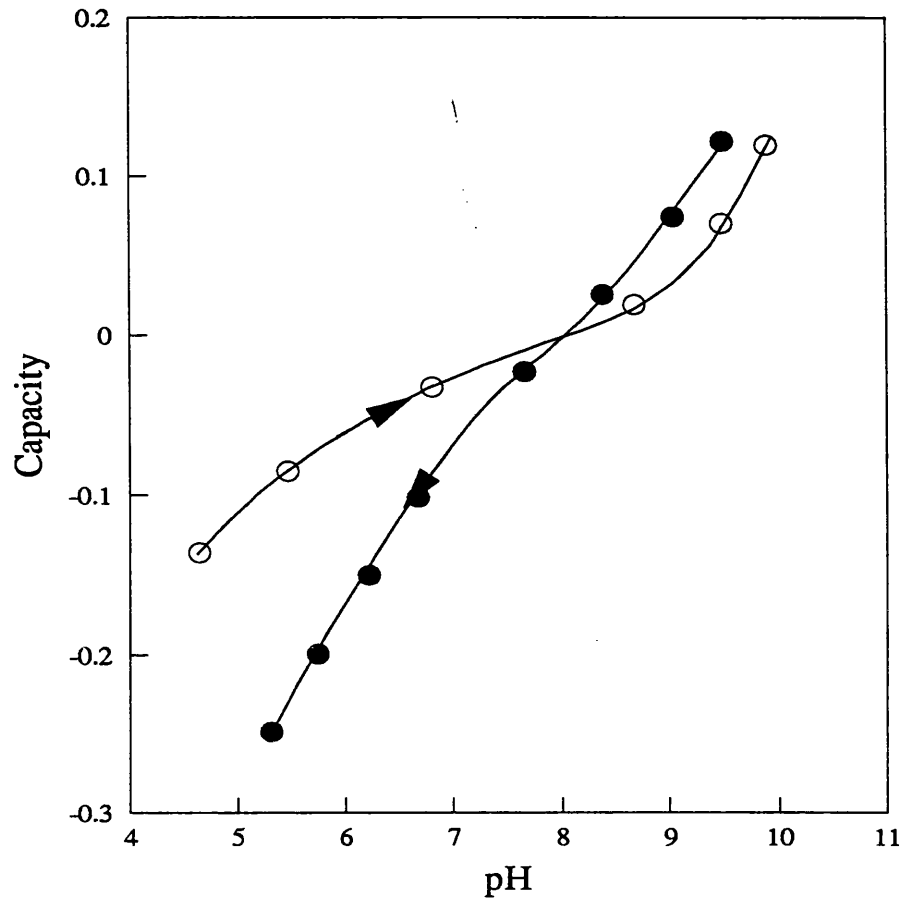

Figure 6.18 : Ion exchange capacities from titration of a dispersion of 0.501g γ alumina in 25ml distilled water. An addition of 0.7ml 0.1M HCl was made, followed by titration with 0.13M NaOH (○). At pH 9.8, 1.5ml 1M NaCl was added and the suspension back-titrated with 0.1M HCl (●).

Titration File: GAL1

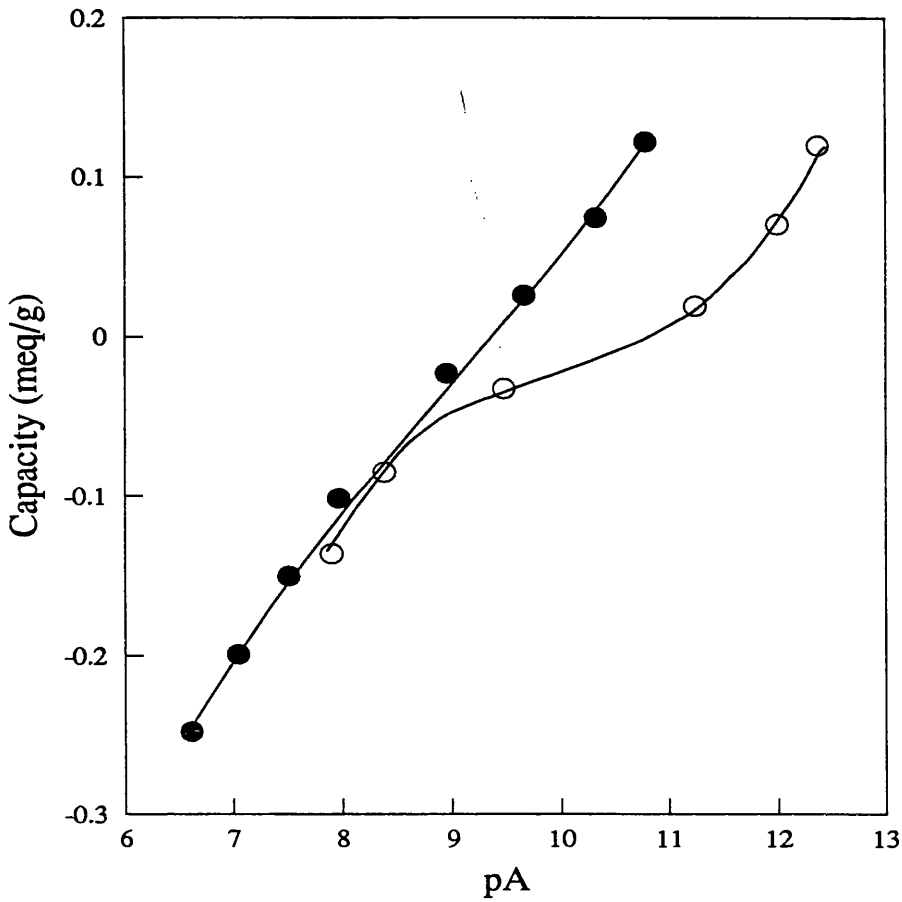

Figure 6.19 : Ion exchange capacity data from Figure 6.18 plotted against pA (= pH + pCl).

Titration File: GAL1

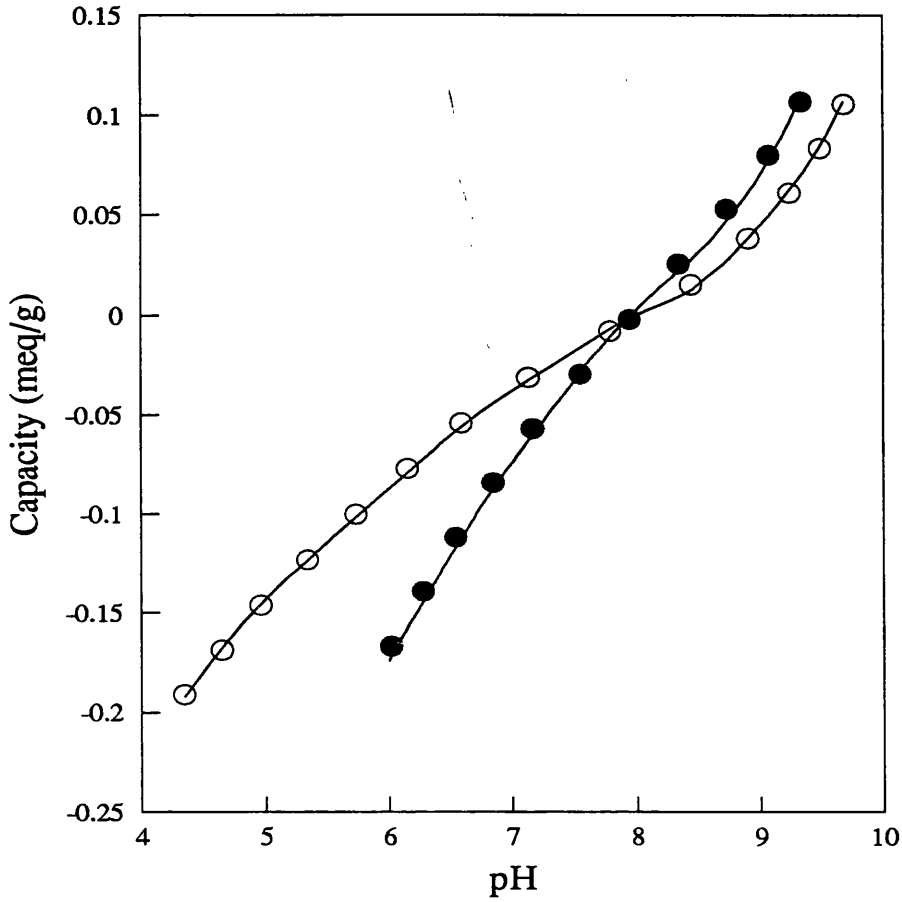

Figure 6.20 : Ion exchange capacities from titration of a dispersion of 0.607g γ alumina in 25ml distilled water. An addition of 1.18ml 0.1M HCl was made, followed by titration with 0.1M KOH (○). At pH 9.5, 2ml 0.5M NaCl was added and the suspension back-titrated with 0.1M HCl (●).

Titration File: JGAL2

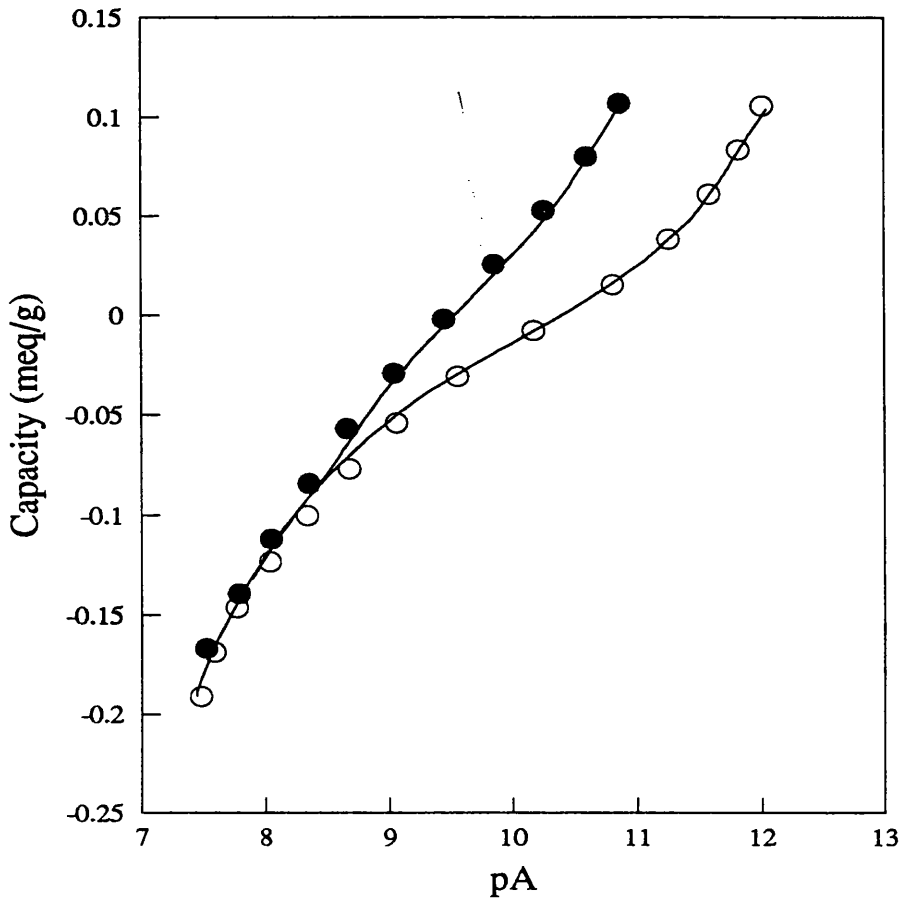

Figure 6.21 : Ion exchange capacity data from Figure 6.20 plotted against pA (= pH + pCl).

Titration File: JGAL2

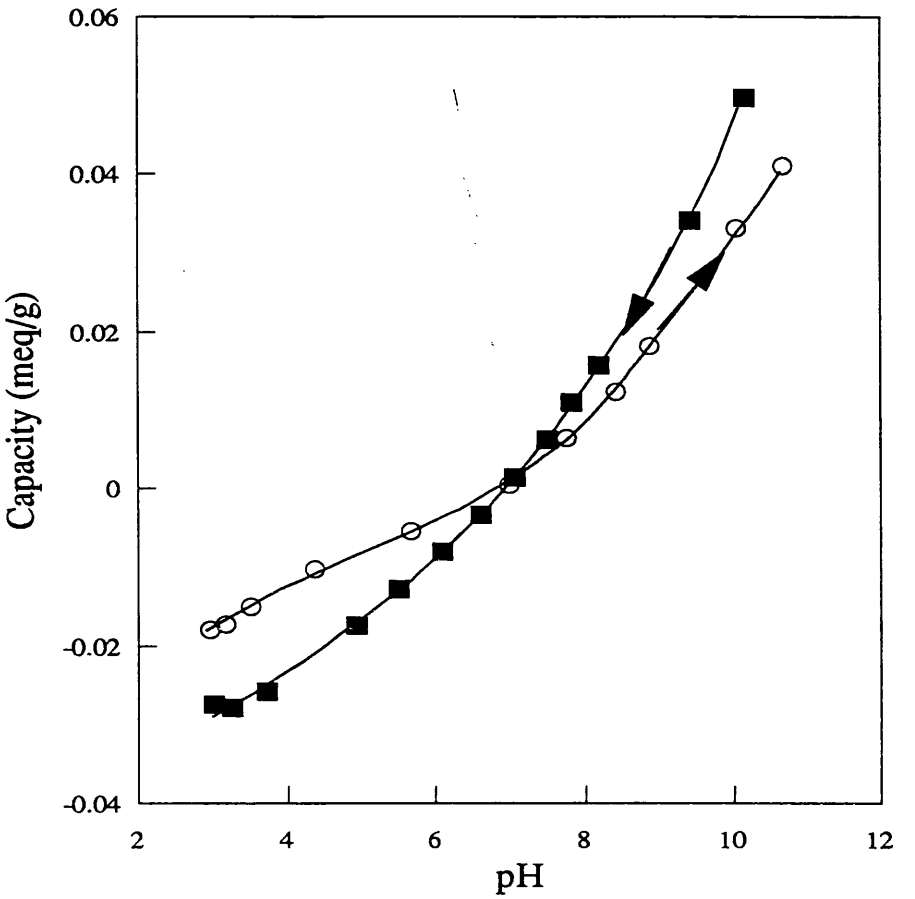

Figure 6.22 : Titration of a dispersion of titania (1g of exchanger in 25ml of water). 0.9 mls 0.1M HCl was added then the dispersion was titrated with 0.12M NaOH (○). At pH 10.5, 1ml 1M NaCl was added and the dispersion back-titrated with 0.1M HCl (■).

Titration File: TI#2

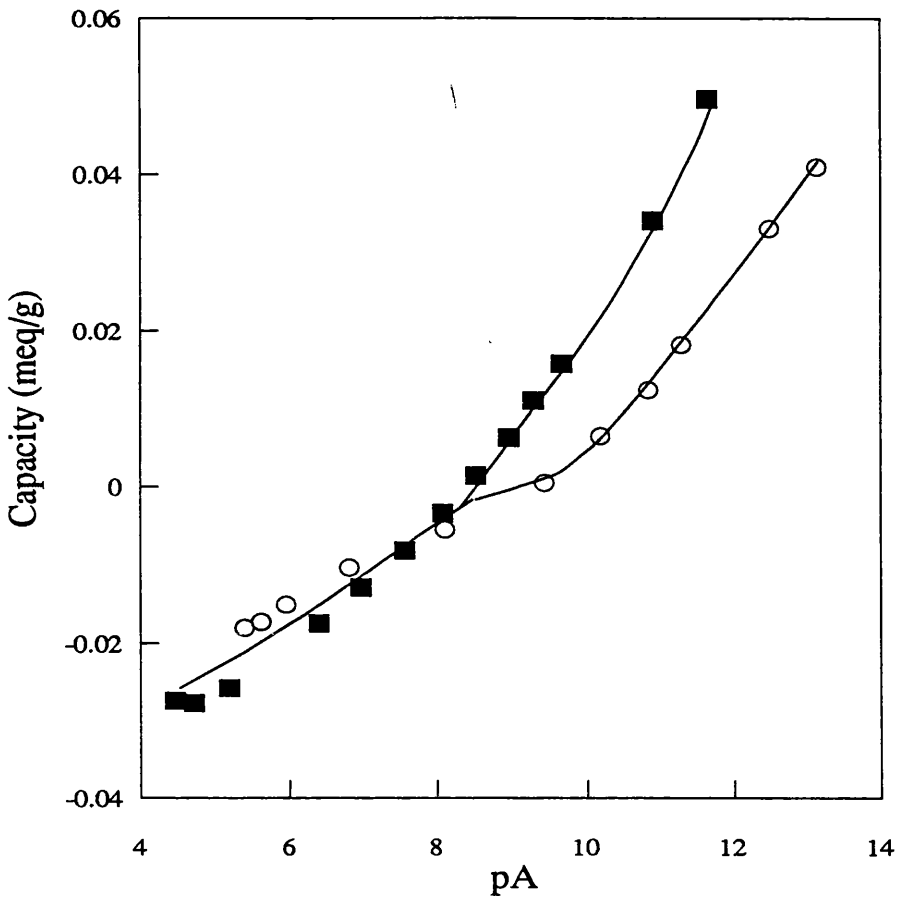

Figure 6.23 : Ion exchange capacity data from Figure 6.22 plotted against pA (= pH + pCl).

Titration File: TI#2

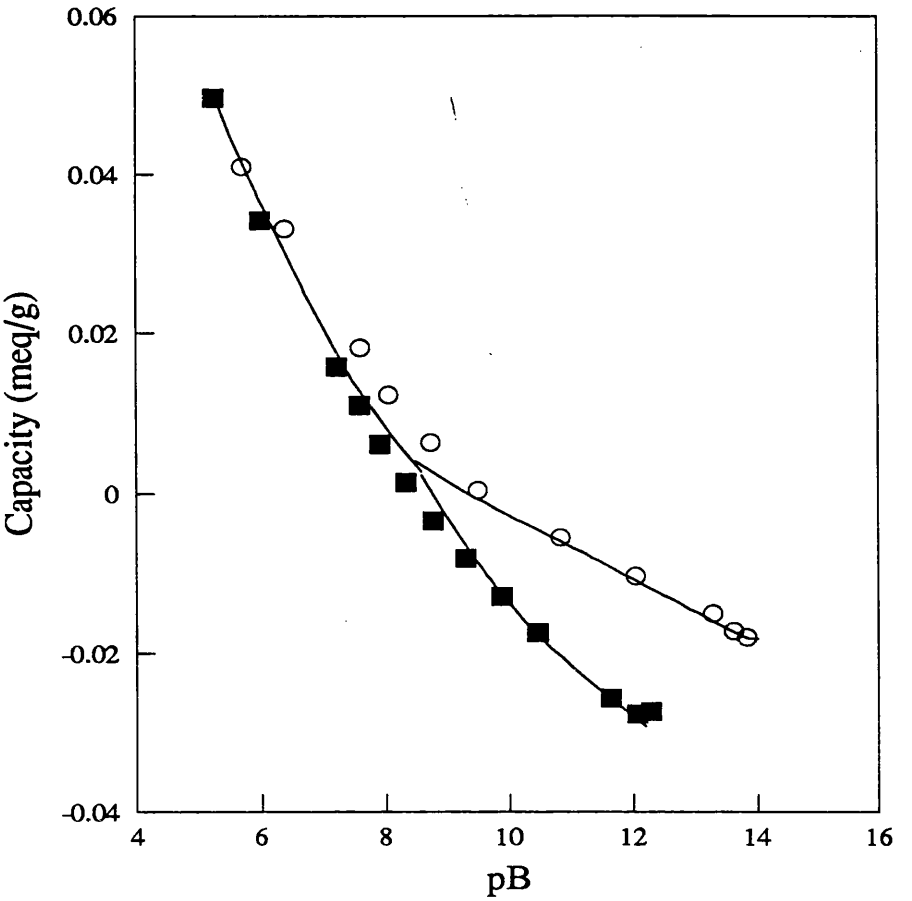

Figure 6.24 Ion exchange capacity data from Figure 6.22 plotted against pB (= pNa + pOH).

Titration File: TI#2

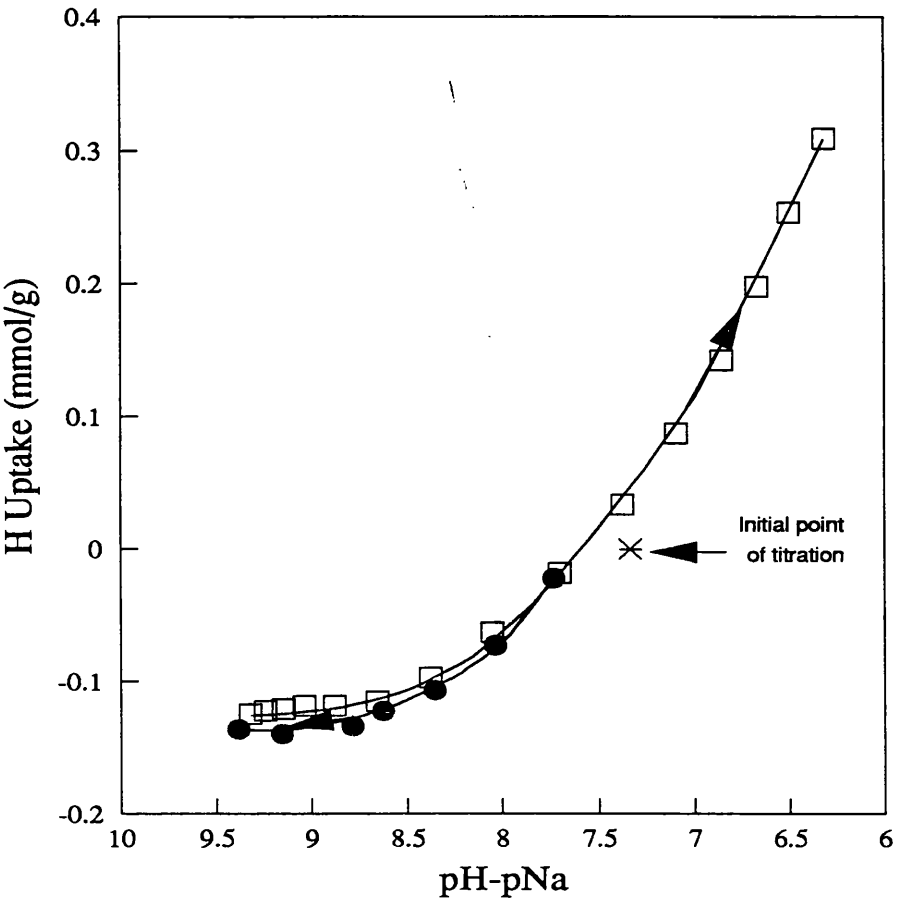

Figure 6.25 : H^+ uptake on titration of a dispersion of 0.175g NASICON in 25ml distilled water, with an initial pH of 10.4. The dispersion was titrated with 0.1223M NaOH to pH 11.3 (●), followed by titration with 0.1M HCl (○). H^+ uptakes were determined from ISE measurements and are shown as a function of pH - pNa.

Titration File: JNAS7

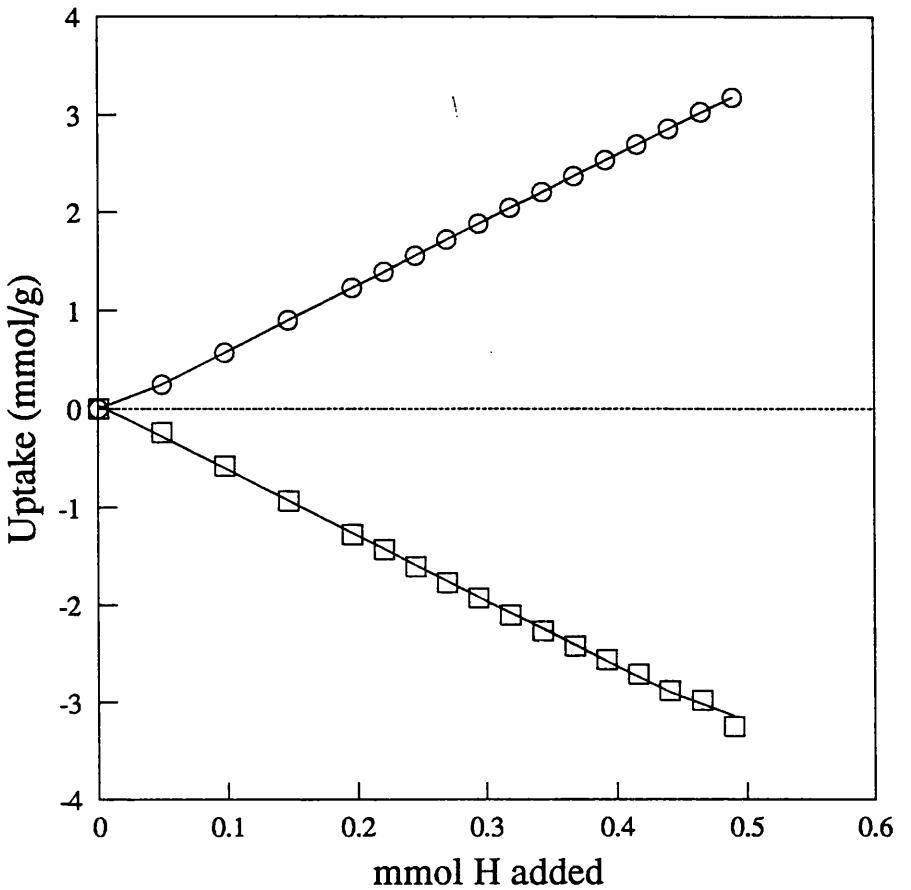

Figure 6.26 : Stoichiometric uptake of H^+ (○) and release of Na^+ (□), determined from ISE measurements, on titration with 0.1M HCl of a dispersion of 0.149g NASICON in 25ml distilled water.

Titration File: JNAS2

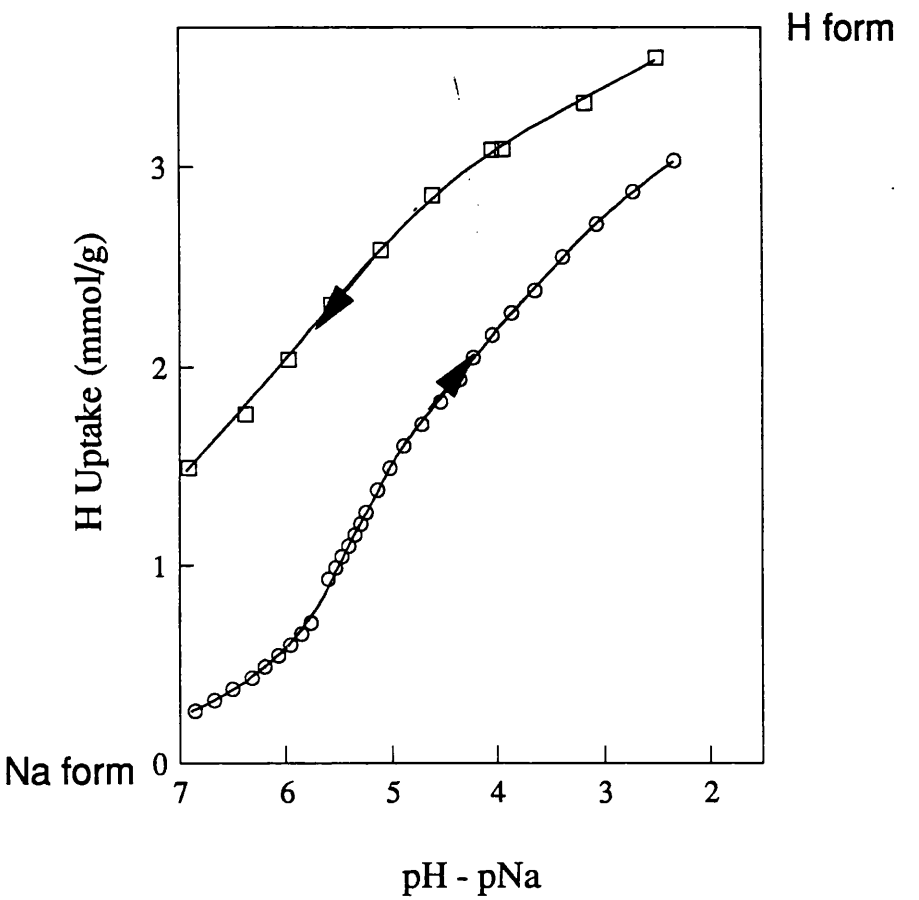

Figure 6.27 : Comparison of measured H^+ uptakes on titration of dispersions of H^+-form NASICON and Na^+-form NASICON. 0.1336g H^+ form NASICON was dispersed in 25ml distilled water and titrated with 0.1223M NaOH (□). In a separate titration 0.175g Na^+ form NASICON was dispersed in 25ml distilled water and titrated with 0.1M HCl (○). Uptakes are presented as a function of pH - pNa.

Titration Files: JNAS3B, JNAS7

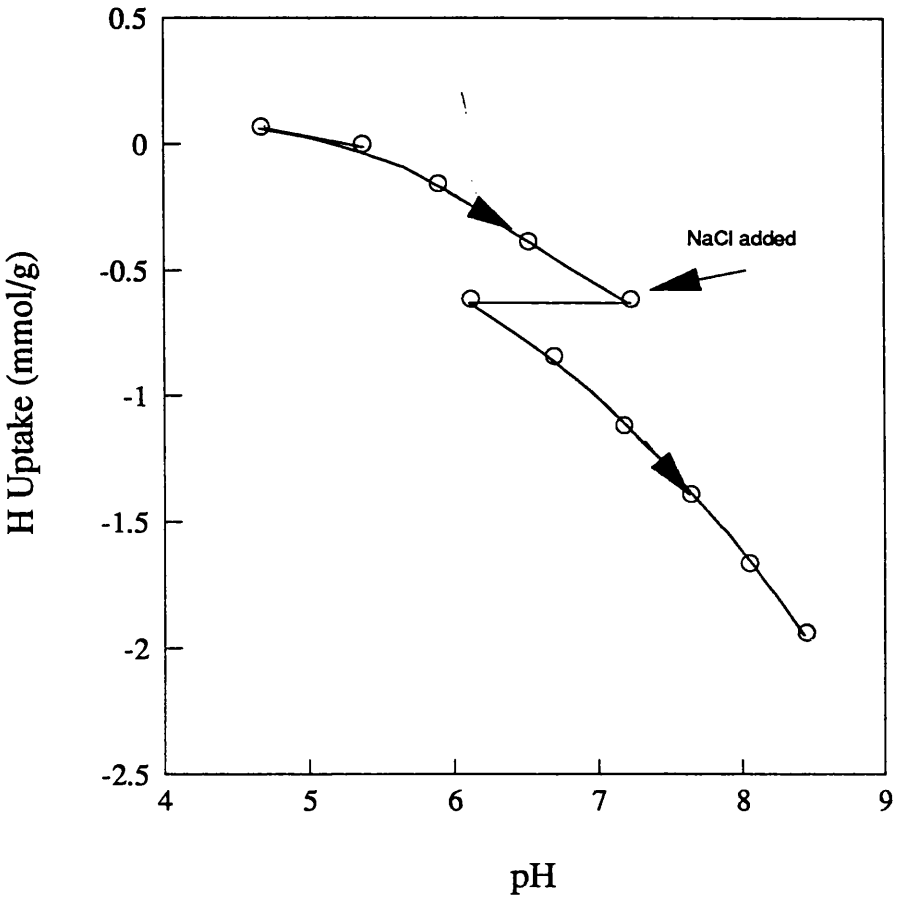

Figure 6.28 : Release of hydrogen ion on titration with 0.1223M NaOH of a dispersion of 0.1336g NASICON (H^+ form) in 25ml distilled water. At pH 7.2 an addition of 3ml 0.1M NaCl was made, followed by further additions of NaOH.

Titration File: JNAS3B

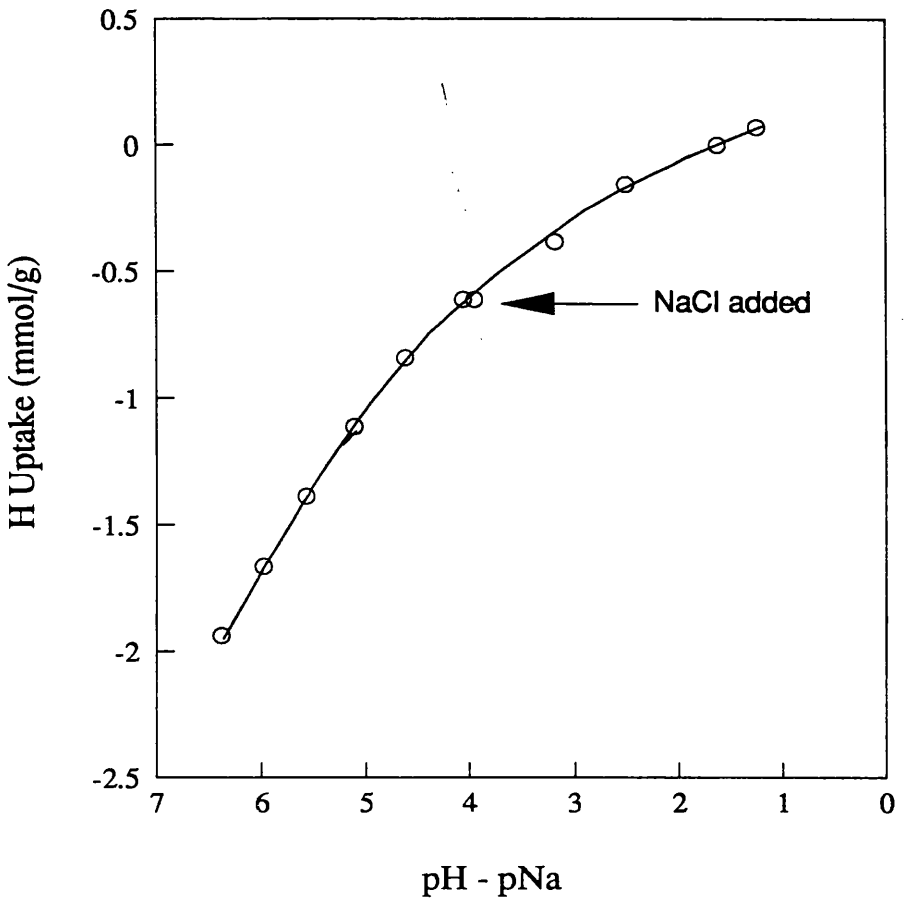

Figures 6.29 : Uptake data from Figure 6.27 plotted as a function of pH - pNa.

Titration File: JNAS3B

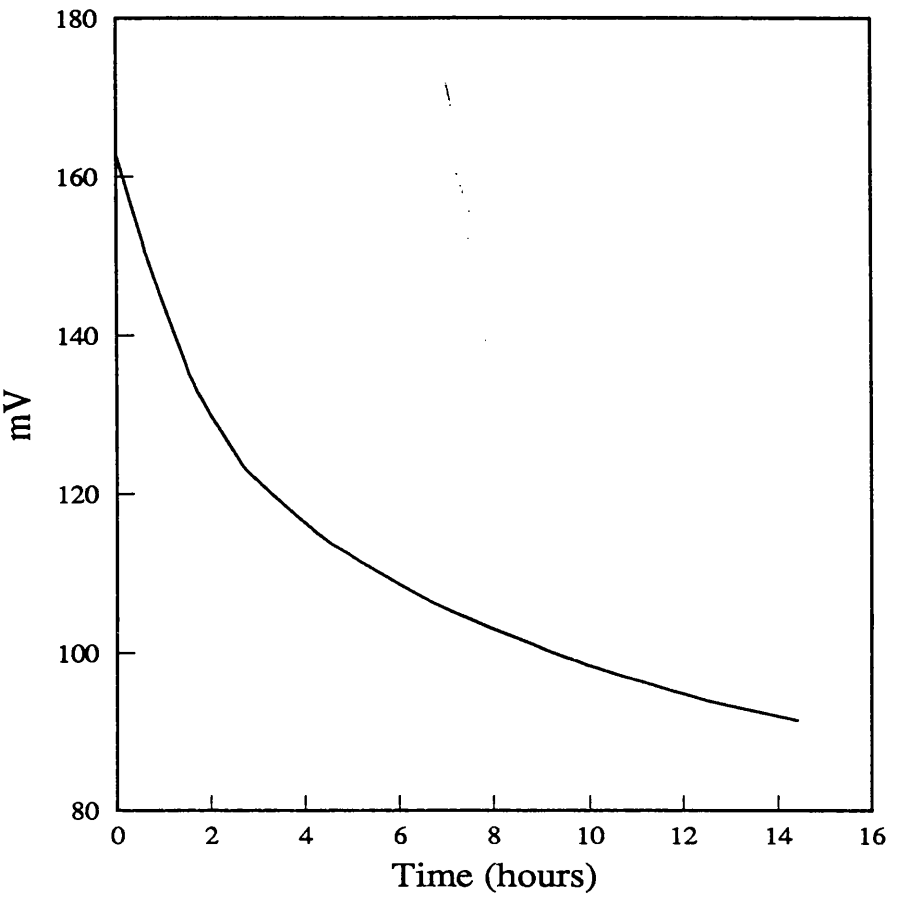

Figure 6.30 : Change of pH electrode response with time for a NASICON dispersion in HCl (initial pH approx. 4.3).

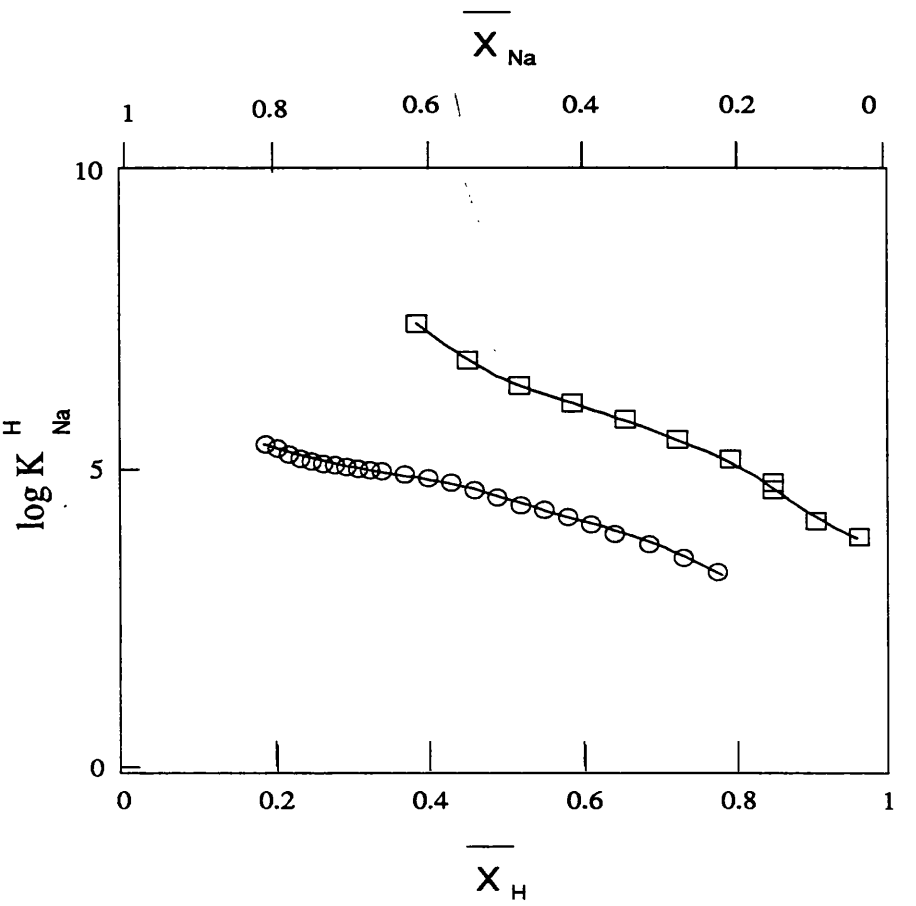

Figure 6.31 : Logarithms of selectivity coefficients K^{H}_{Na} as obtained by titration of the Na^{+} form of NASICON with HCl (○) and titration of the H^{+} form of NASICON with NaOH (□). Results are plotted as a function of the ionic composition of the exchanger.

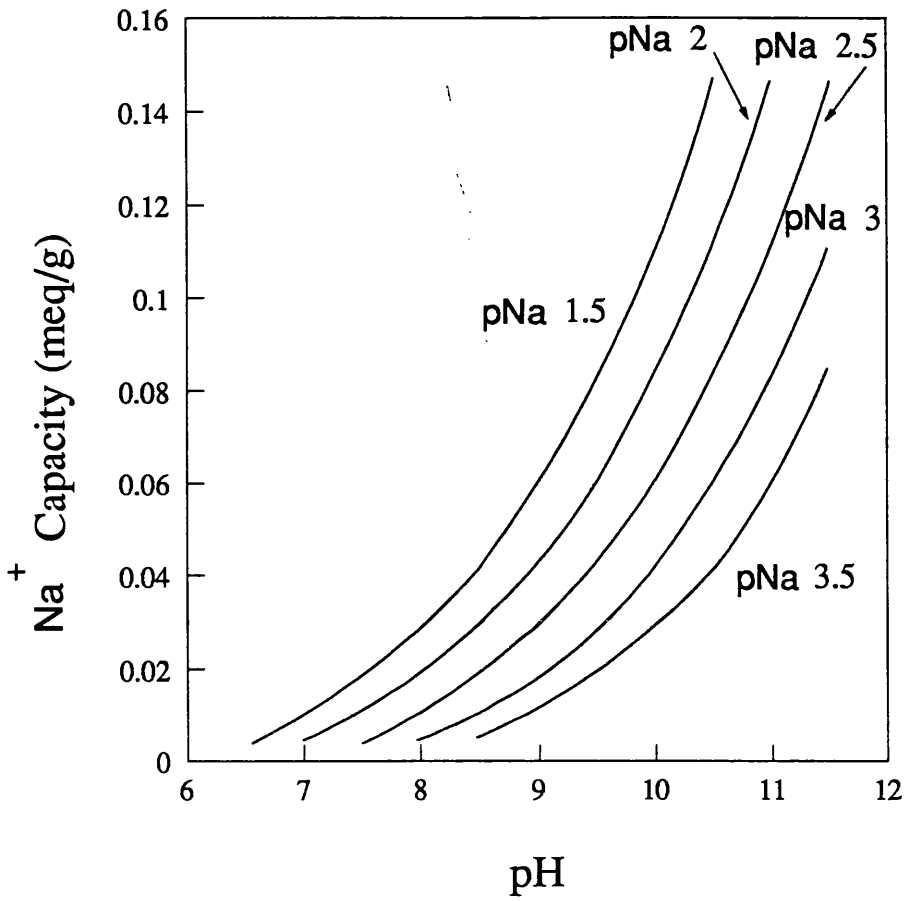

Figure 6.32 : Variation of sodium capacities on zirconia as a function of pH, at fixed sodium ion activities.

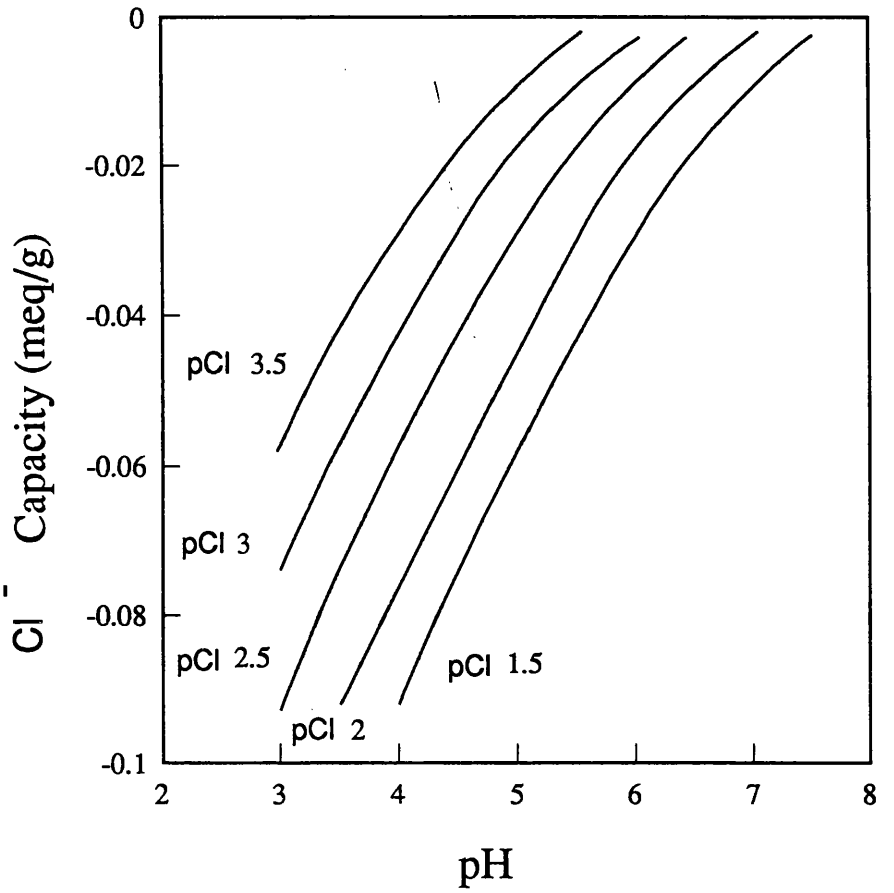

Figure 6.33 : Variation of chloride capacities on zirconia as a function of pH, at fixed chloride ion activities.

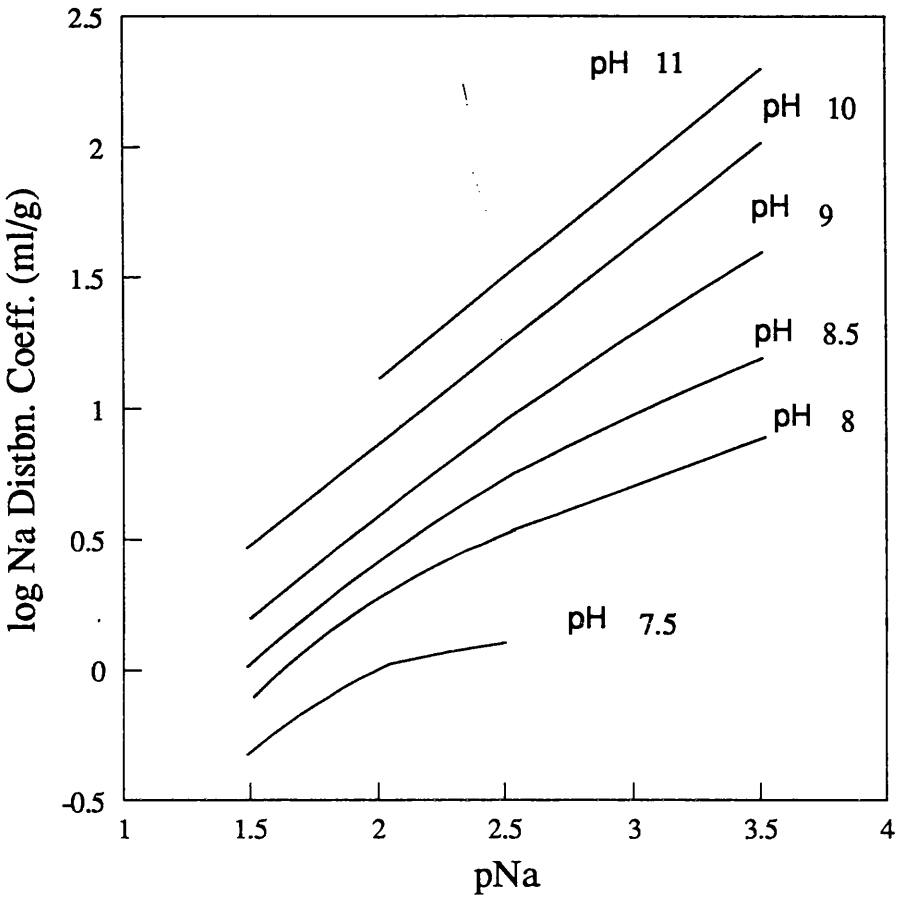

Figure 6.34 : Distribution coefficients (in ml/g) for sodium ion on zirconia as a function of pNa at fixed pH.

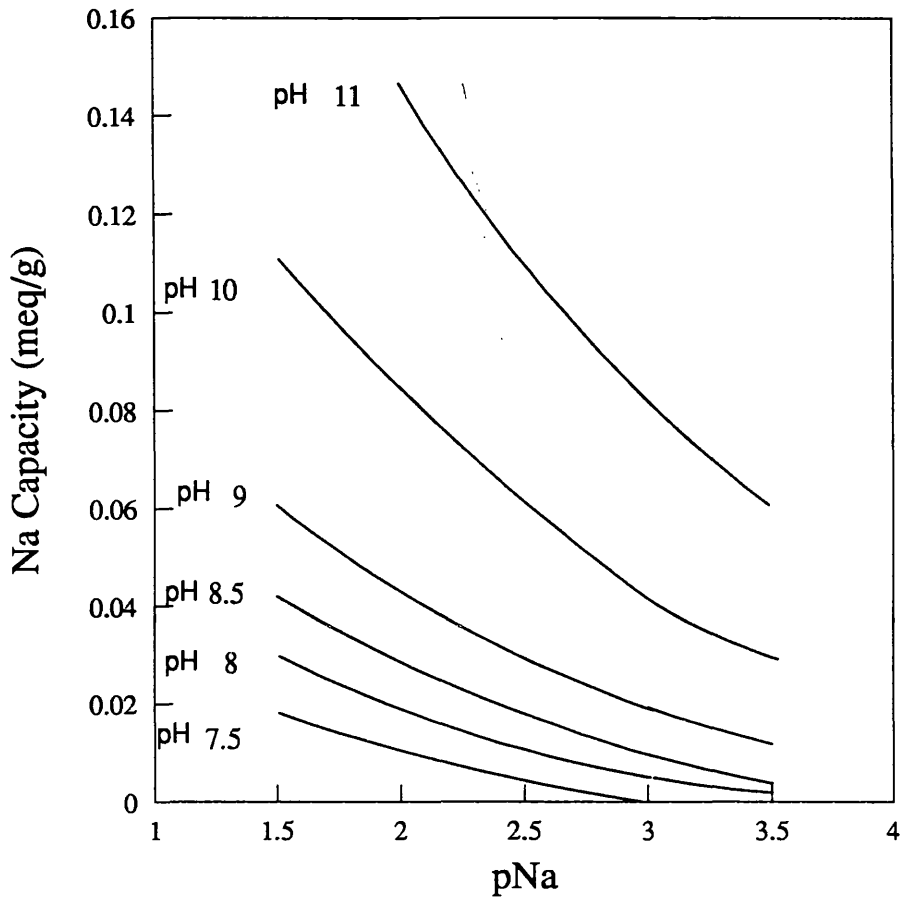

Figure 6.35 : Variation of sodium capacities on zirconia as a function of pNa, at fixed pH.

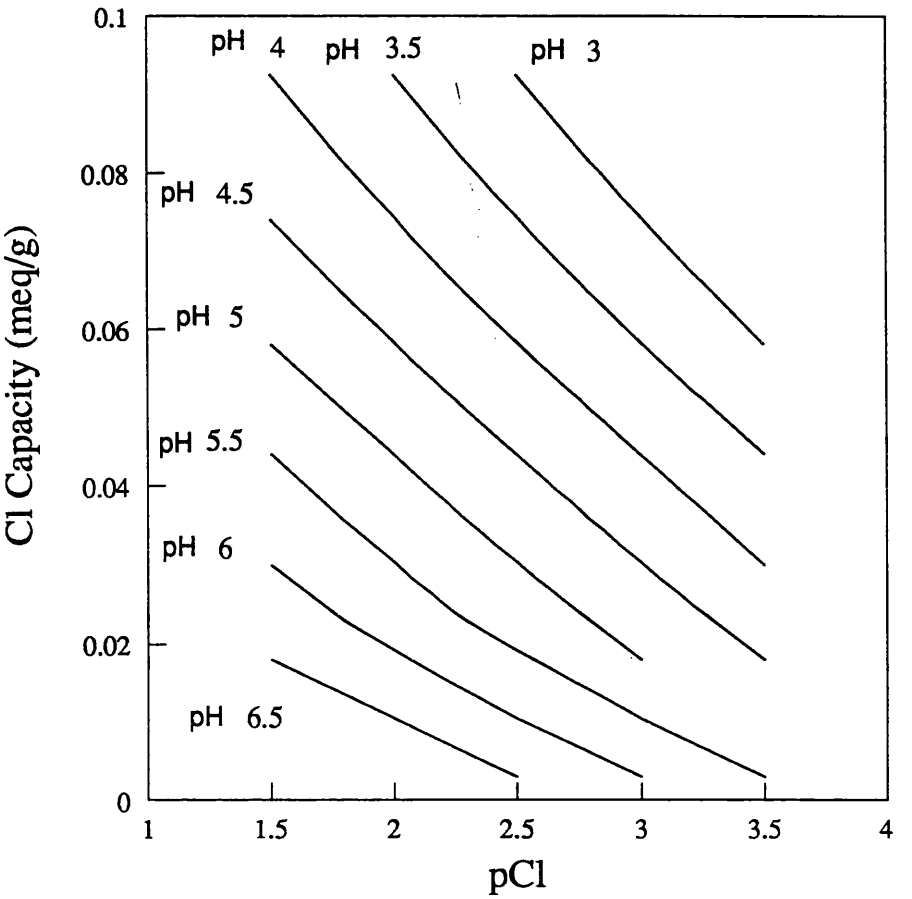

Figure 6.36 : Variation of chloride capacities on zirconia as a function of pCl, at fixed pH.

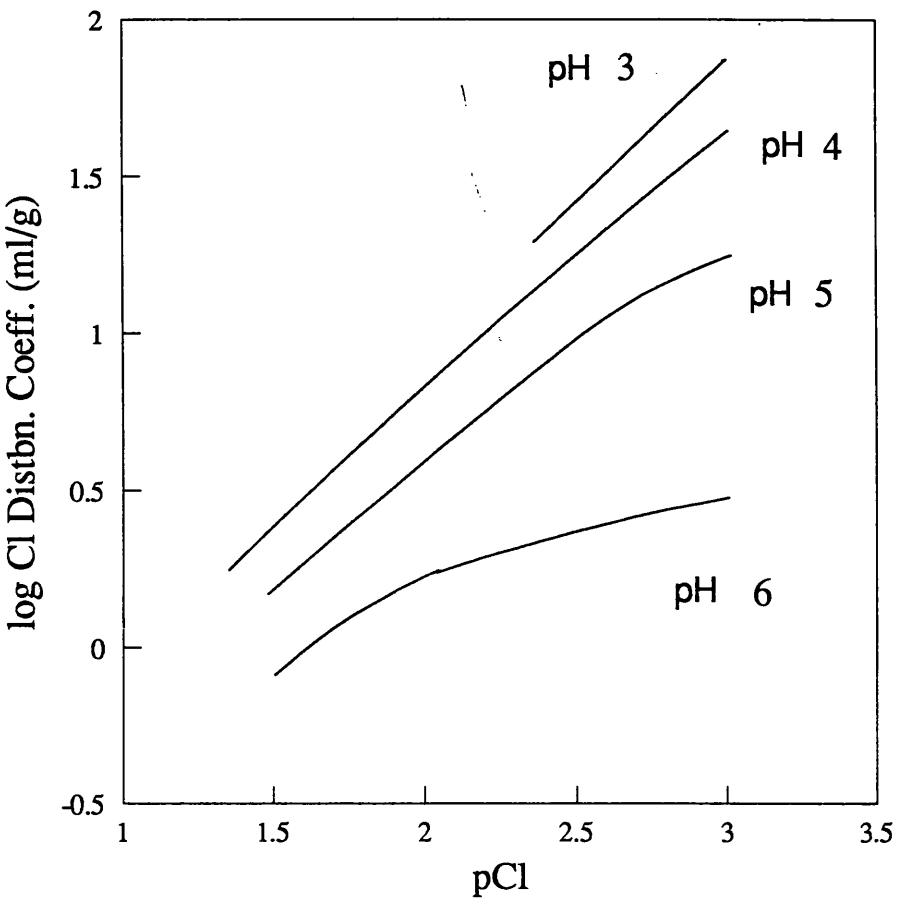

Figure 6.37 : Distribution coefficients (in ml/g) for chloride ion on zirconia as a function of pCl at fixed pH.

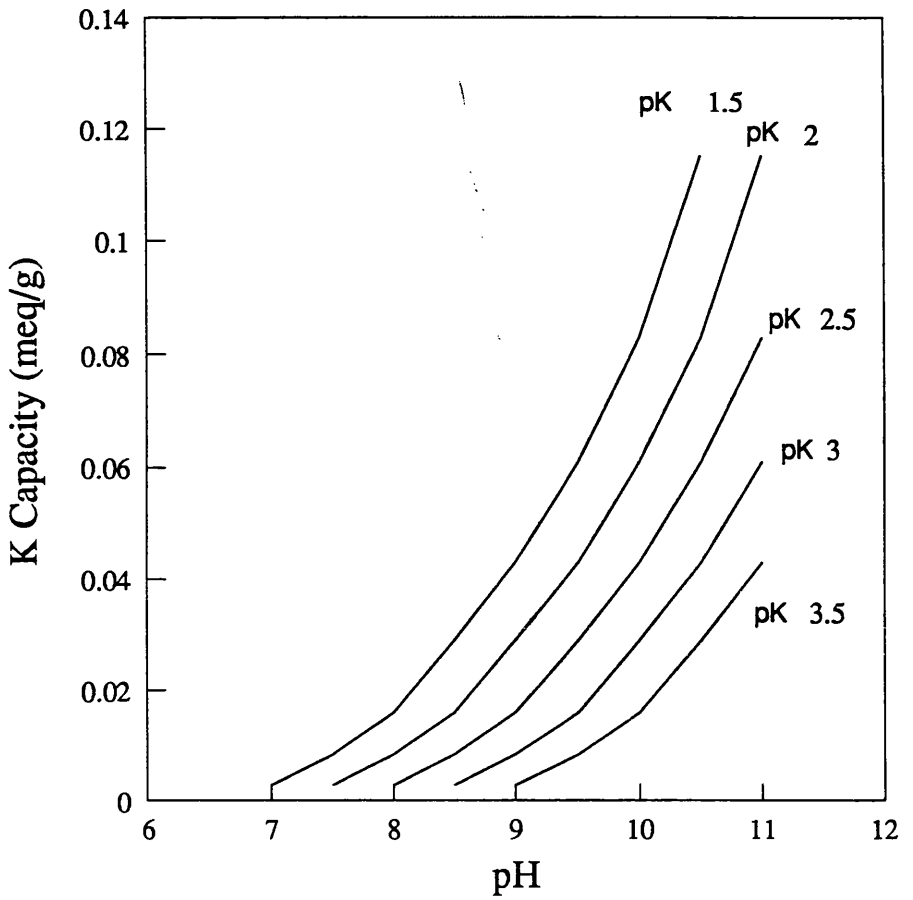

Figure 6.38 : Variation of potassium capacities on zirconia as a function of pH, at fixed potassium ion activities.

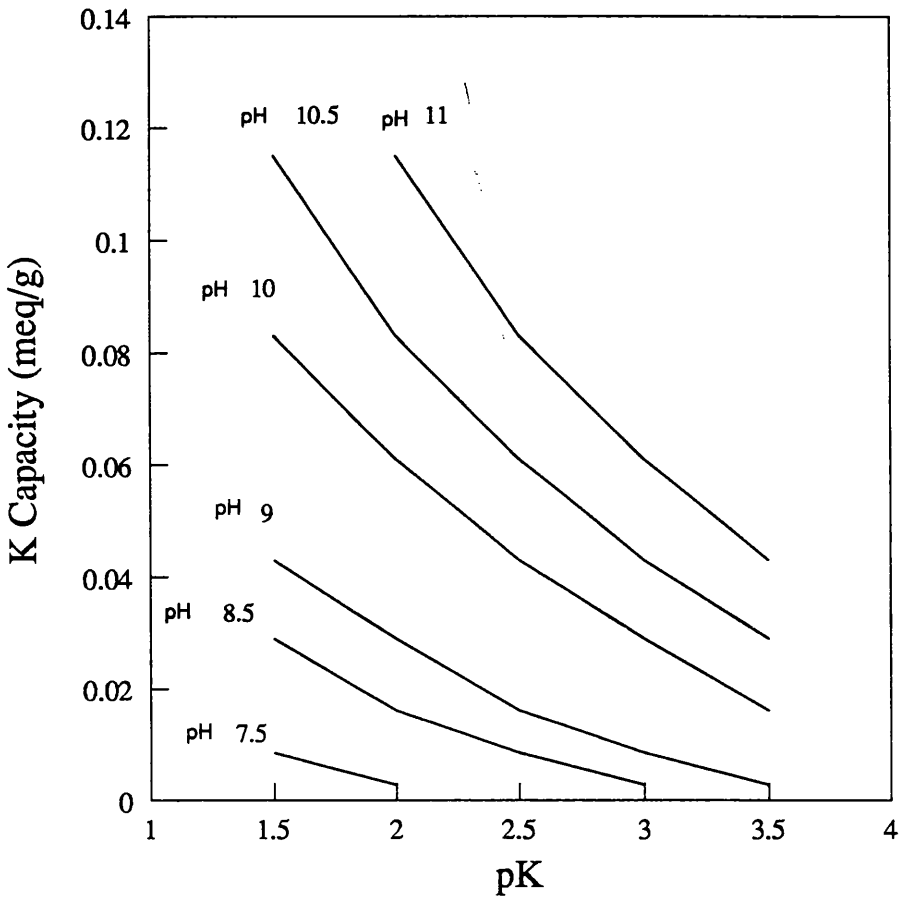

Figure 6.39 : Variation of potassium capacities on zirconia as a function of pK, at fixed pH.

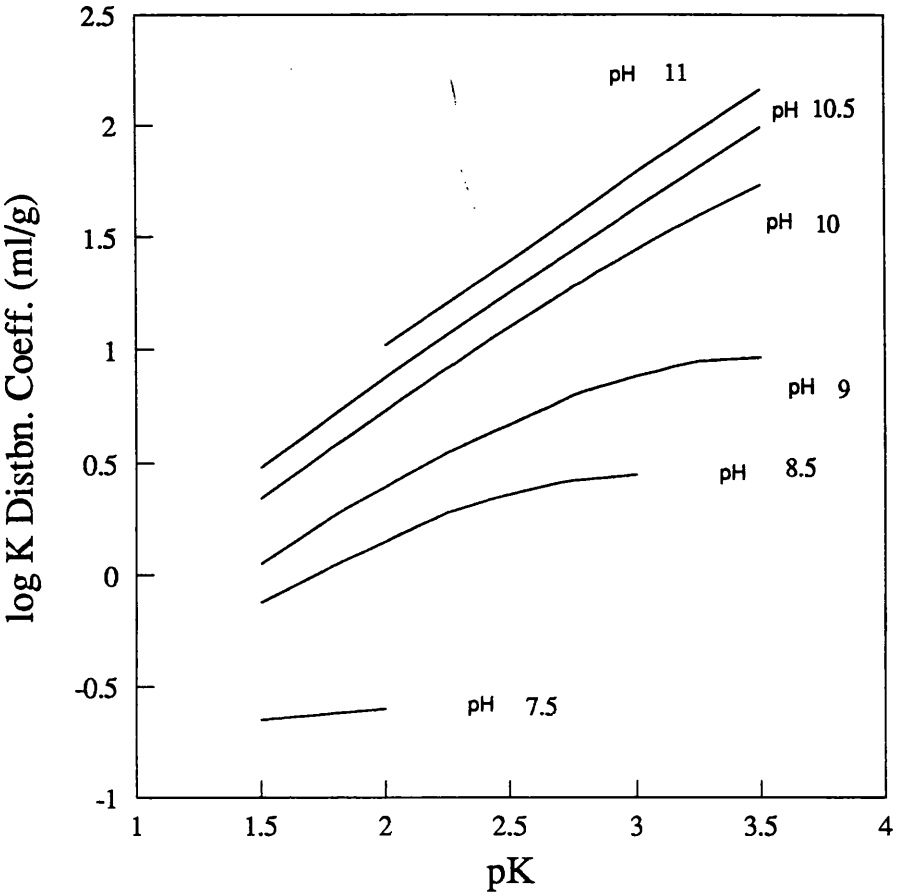

Figure 6.40 : Distribution coefficients (in ml/g) for potassium ion on zirconia as a function of pK at fixed pH.

CHAPTER 7

ION EXCHANGE CHARACTERISTICS OF INORGANIC OXIDES

(II) SPECIFIC SORPTION

Introduction

It was shown in Chapter 6 that for ion exchange experiments involving univalent ions, such as chloride in acid and sodium or potassium in base, the exchange processes are reversible. With some other ions, particularly multivalent ions, specific sorption and a degree of irreversibility is observed. Kraus [1] noted a degree of irreversibility in the sorption of sulphate on zirconia and a virtually irreversible sorption of multivalent ions such as phosphate, tungstate and chromate.

Titrimetric studies of ion exchange and sorption on the calcined oxide active layer materials were extended to include ions which may be specifically adsorbed, particularly calcium and sulphate ions. The methods used were essentially the same as those for indifferent ion sorption, with the necessary modifications to uptake calculations being employed, as described in Chapter 3.

7.1 Specifically Sorbed Ions

The sorption of an ion at a solid surface by the influence of forces other than the electrical potential at the surface may be regarded as being specifically sorbed. The additional forces may have a chemical nature, with some degree of covalent bonding between the sorbed ion and the surface atoms. Alternatively, they may be more physical in nature, such as van der Waals forces between the ion and the surface.

In the previous Chapter the effects of electrolyte concentration on the oxide surface charge was discussed. It was shown while an increase in electrolyte concentration increased the surface charge (and therefore the ion exchange capacity), the condition whereby the oxide

had no surface charge (the zero point charge, zpc) was determined entirely by the concentration of potential determining ions (H^+ and OH^-) and was independent of electrolyte concentration.

In contrast, when specific sorption occurs, the zpc is affected by the concentration of specifically adsorbed ions. An increase in the concentration of specifically adsorbed anions results in a shift in the zpc to lower concentrations of positive potential determining ions, that is, to higher pH. Analogously, specific sorption on cations would cause a shift in the zpc to lower pH.

7.2 Modifications to Uptake Calculations

The principles for the determination of ion uptake, as described in Chapter 3, were extended to include the determination of ion uptake under conditions where one ion species is not monitored by ISE (necessary in cases where there no reliable selective electrode for a given ion) and when one ion species is not fully dissociated in solution.

All ion species fully dissociated in solution, one species not monitored by ISE

For titrations in which one, and only one, ion species was not monitored by ISE (but all ions were fully dissociated in solution), the uptake of the unmonitored species was calculated by consideration of electroneutrality in the solution phase. A first estimate of the solution concentration of the unmonitored species was obtained. The ionic strengths and activity coefficients were then calculated, giving new solution concentrations and ion uptakes. The process was repeated until the calculated concentrations were constant.

In order to perform these calculations, it was necessary that all ion selective electrodes were accurate and free from error caused by interfering ions. This requirement limits the conditions under which the calculations may be made with confidence. However, if from

prior research an ion was known to be excluded from an ion exchanger under given conditions (for example by Donnan exclusion), the concentration of that ion was assumed to be equivalent to the amount added as titrant, with the uptake equal to zero. The assumed ion concentration was then used in the estimation of the concentration of the unmonitored ion by electroneutrality considerations.

Using this method for the determination of ion uptake of an unmonitored ion species, it was not possible to make corrections for the suspension potential since, as shown in Chapter 4, its calculation requires the monitoring by ISE of all ion species participating in the exchange process.

All ion species monitored by ISE, one species not fully dissociated

In some titrations the activities of all fully dissociated ion species are measured but the experimental conditions result in the presence of undissociated species in significant quantities. An example of this situation occurred in titrations with $Ca(OH)_2$, HCl and $CaCl_2$, with ion activities and uptakes monitored by ISEs for H^+, Cl^- and Ca^{2+}. Below pH 10 the only ion species present are those monitored by ISE. Above pH 10 the ion species $CaOH^+$ and $Ca(OH)_2$ occur in increasingly significant amounts with increasing pH due to dissociation (pK_{b1} = 1.4 and pK_{b2} = 2.43 at 25°C). The formation of these ion species result in an apparent (as recorded by ISE) uptake of OH^- (or release of H^+) and an apparent uptake of calcium ion, since the Ca^{2+} ISE responds only to the activity of the fully dissociated species. The contribution of the undissociated species on the apparent uptake of H and Ca^{2+} can be corrected for. From the concentrations of H^+, OH^- and Ca^{2+} as measured by ISE and the dissociation constants pK_{b1} and pK_{b2}, the concentrations of $CaOH^+$ and $Ca(OH)_2$ were determined. A new value for the ionic strength was then calculated, followed by recalculation of activity coefficients. The entire process was repeated until constant

calculated concentrations were obtained. The apparent uptakes of calcium and hydroxyl ion due in reality to the formation of undissociated species were then subtracted from the measured uptakes, giving the ion uptake by the exchanger.

One ion species not fully dissociated and not monitored by ISE

This situation combines the two main difficulties encountered in the previous cases. The species (for example, phosphate, amino-acids) is neither fully dissociated over the full pH range investigated nor followed by ISE. However, by applying the same principles as previously, the sorption of an unmonitored, undissociated ion may be determined with confidence, provided that all other ions present are monitored and reliable dissociation constants are available. From the solution pH and the ion dissociation constants, the relative ratios of each ion species (for example, in the case of phosphate titrations, PO_4^{3-}, HPO_4^{2-}, $H_2PO_4^-$ and H_3PO_4) were calculated. From ISE measurements, the total charge imbalance due to the presence of these unmonitored ions in the solution phase was determined. A total concentration of the unmonitored species was then calculated which minimised the charge imbalance. Ionic strength and activity coefficients were then recalculated and the process repeated until calculated concentrations were consistent. Uptake of hydrogen ion was recalculated, taking into account the apparent uptake or release due to the dissociation processes. The uptake of the unknown species was also calculated by mass balance. It should be noted that this method of calculation does not give any indication as to which charge species of the unmonitored ion is adsorbed. Furthermore, the measured uptake of H^+ refers to the total uptake as calculated by mass balance, including the uptake of free hydrogen ions and the uptake of hydrogen ions associated with the unmonitored species. For example, no differentiation could be made between the uptake of 1 mmol of H^+ and 1 mmol of $H_2PO_4^-$ and the uptake of 2 mmol H^+ and 1 mmol of HPO_4^{2-}. In each case the total (mass balance) uptake of H^+ is 3 mmol. Since the charge on the adsorbed phosphate species

cannot be calculated from titration data alone, it was therefore found to be more convenient to express the uptake of total phosphate in terms of millimoles, rather than as charge equivalents.

7.3 Results and Discussion

7.3.1 Calcium Ion Sorption

The sorption of calcium ion and its influence on the ion exchange properties of inorganic oxides was determined by potentiometric titration of dispersions of zirconia with $Ca(OH)_2$ and HCl, with additions of $CaCl_2$ salt. Multi-electrode automatic titrations were performed as described previously. Since a reliable calcium ion selective electrode was available, it was possible to monitor the solution activities and uptakes of all ions present. The only restriction was that above pH 10, the species $CaOH^+$ and $Ca(OH)_2$ exist in increasingly significant proportions. Although corrections for the occurrence of these species was possible by the method described earlier, these were not required since the pH was generally kept below 10 in these titrations and the concentrations of the undissociated and monovalent species remained negligible.

A sample of 0.954g of calcined monoclinic zirconia, dispersed in 25ml of distilled water, was titrated with 0.018M $Ca(OH)_2$ to pH 10 and back-titrated with 0.1M HCl to below pH 4. Solution activities and ion uptakes of all ions were monitored with pH electrode, Ca and Cl ion selective electrodes. The uptakes of calcium, hydrogen and chloride ions during the forward and back legs of this titration are shown in Figure 7.1. Amphoteric exchange properties were observed. In basic solution there was an exact balance in milliequivalents (1 milliequivalent = 1 millimole H^+ = 1/2 millimole Ca^{2+}) between Ca^{2+} uptake and H^+ release, whilst in acid there was a stoichiometric uptake of Cl^- and H^+.

As was observed with titrations of zirconia in the presence of monovalent cations, the exchange capacity was not a function of pH alone. In the light of the previous work, it was proposed that exchange capacity be plotted against the activity of total base in solution. The activity of total base is given by $\{Ca\}.\{OH\}^2$ (in logarithmic terms, pCa + 2.pOH). In order to allow direct comparison with NaOH and KOH titrations, it was more convenient to express pB as 0.5.pCa + pOH. When the titration data from Figure 7.1 was plotted against this function, the cation exchange capacity curves for forward and back titration overlapped, indicating that the uptake of calcium ion is completely determined by the activities of OH^- and Ca^{2+} in solution, Figure 7.2.

The cation exchange capacity for calcium ion was considerably higher than for the monovalent cations at equivalent values of pB (Figure 7.3), indicating a greater selectivity shown by zirconia for calcium over sodium or potassium ions. The effects of changing pH and calcium concentration on the sorption of calcium ion on calcined zirconia are shown in Figures 7.4 and 7.5.

A second major difference was that sorption of calcium ion commenced in weakly acidic solution, whereas with sodium and potassium ions there was no cation exchange capacity below pH 7. To illustrate this feature more clearly, a titration with HCl and $Ca(OH)_2$ of a dispersion of non-calcined monoclinic zirconia (0.324g in 25ml distilled water) was performed. The larger capacities of this material allowed this effect to be determined more accurately. An addition of 0.6ml 0.1M HCl was made to the dispersion, followed by titration with 0.015M $Ca(OH)_2$. The uptakes of hydrogen, chloride and calcium ion, as determined by ISE, are shown in Figure 7.6. Uptake of calcium ion in weakly acidic solution was observed, as shown in Figure 7.7. Within this region both anion and cation exchange processes are occurring. From the definition of the zero point charge as the point at which there is an equivalent uptake of cations and anions (and consequently the

point at which H uptake is equal to zero), it is clear that the presence of calcium ion has caused a shift in the zpc to a lower pH (cf. titrations of zirconia with Na^+ and K^+ cations: cation uptake = anion uptake = 0 at the zero point charge).

The results obtained from these titration strongly suggested the occurrence of specific (but reversible) interactions between calcium ions and the zirconia surface. This could not be conclusively shown from titrimetric studies alone, since the uptake data do not enable differentiation between mechanisms of ion sorption. Supporting evidence for specific sorption of calcium ion on monoclinic zirconia was provided by parallel studies [2] performed at E.N.S.C. Montpellier on the electrophoretic properties of calcined zirconia particles in the presence of calcium ion which showed that by increasing the calcium ion concentration in basic solution, the sign of the measured zeta potential was reversed from negative to positive.

Qualitatively similar results were obtained for studies of calcium sorption on calcined γ alumina. On titration of a dispersion of γ alumina (0.3711g in 25ml distilled water) with 0.018M $Ca(OH)_2$ followed by back-titration with 0.1M HCl, an equivalent uptake of calcium ion and release of hydrogen ion was measured in basic solution, with anion exchange occurring (uptake of chloride and hydrogen ions) in acid solution, Figure 7.8. Between pH 5 and 8, both anion and cation exchange occurred, with exchange capacities being measured for Ca^{2+} and Cl^-. The zpc (the point of equivalent uptake of cation and anion) was observed at pH 7 whereas the zpc for γ alumina in the absence of specific sorption was approximately 8, as shown in Chapter 6.

The pB (= $\frac{1}{2}pCa + pOH$) dependence of the cation exchange process, previously not convincingly observed with γ alumina (Chapter 6), was now clearly demonstrated, as shown in Figure 7.9. Higher calcium capacities on γ alumina were observed than for sodium or potassium at equivalent pH values.

The shift in the zpc and the high selectivity shown by γ alumina for calcium ion again suggested strongly that, as with zirconia, specific interactions were occurring between calcium ions and the oxide surface

The effect of calcium ion on the ion exchange properties of silica were studied by titration of a silica dispersion (0.316g in 25ml distilled water) with 0.018M $Ca(OH)_2$ (after an initial addition of 0.4ml 0.1M HCl) to pH 8.5, at which point an addition of 2ml 0.075M $CaCl_2$ solution was made. The dispersion was then back-titrated with 0.1M HCl.

Calcium ion exchange capacity is plotted as a function of pH in Figure 7.10. In contrast to zirconia and γ alumina observations, cation exchange properties of silica were not dramatically affected when calcium was the sorbing cation. The exchange capacity for calcium ion was similar to those for sodium and potassium ion exchange on silica. Again, cation capacity was a single valued function of pB, as shown in Figure 7.11. There was no evidence to suggest the occurrence of any specific interaction between calcium ion and the silica surface.

7.3.2 Sulphate Ion Sorption

The investigation of sulphate sorption on zirconia was performed by titration of aqueous suspensions of calcined monoclinic zirconia with sulphuric acid, with additions of Na_2SO_4 salt. Forward titration of the dispersions was performed using either NaOH,

KOH or $Ca(OH)_2$. As there is no reliable electrode for sulphate ion, the uptake of sulphate by the exchanger was determined by the method described earlier for situations where one ion is not monitored by ISE. For titration points below pH4, corrections were made for the presence of undissociated species.

Figure 7.12 shows the results from a titration with KOH of a zirconia dispersion after an initial addition of 0.14 mmol of H_2SO_4. The sulphate uptake was calculated by the requirements of electroneutrality in both phases, hydrogen and potassium uptakes and solution activities being measured directly by ISE. The initial addition of sulphuric acid resulted in a large uptake of H^+ relative to that observed with HCl as the titrating acid. By the electroneutrality requirement this uptake of H^+ was accompanied by an equivalent uptake of sulphate ion, since sulphate was the only other ion species in the solution phase in significant quantities. On addition of base a slight K^+ sorption was observed in the pH range 6-7, which occurred although sulphate was still present in the solid phase. Titration of a dispersion of zirconia with 0.13M NaOH after an addition of H_2SO_4 (0.016 mmol) gave similar results, with some Na uptake in the acid branch, shown in Figure 7.13.

The comparison of the hydrogen uptake on calcined zirconia when HCl and H_2SO_4 were the titrating acids (Figure 7.14) shows a much larger uptake when H_2SO_4 was the added acid, because of the stronger sorption of counter ion sulphate.

Further titrations were performed with H_2SO_4 0.05M and $Ca(OH)_2$ 0.018M (Figure 7.15). In this titration, care was taken to ensure that the solubility product for calcium sulphate was never exceeded. Once again, the uptake of calcium commenced while sulphate was still present in the solid phase. The shift in the zpc was slightly less than in the titrations with sodium and sulphate. Uptake of calcium ion was not significantly affected by the presence of sulphate ion in the solid phase, as shown in Figure 7.16, demonstrating that

calcium ion uptake is a function of pB, regardless of the nature of the titrating acid.

For all titrations with sulphate ion of monoclinic zirconia dispersions, a degree of irreversibility was observed in the sorption of sulphate, with sulphate remaining bound to the exchanger above pH 9, characteristic of specific adsorption. The pH at which H^+ uptake equalled zero was shifted toward higher pH values (not exceeding 10) as a function of sulphate concentration, as shown in Figure 7.17, where the titrations of zirconia were performed with KOH or NaOH after various H_2SO_4 additions. In the presence of sulphate ion, the clear distinction between cationic and anionic exchange branches is lost, both overlapping in the basic pH range.

Further evidence for the specific sorption on sulphate on zirconia was provided by parallel studies [2] on the electrophoretic mobility of particles of calcined zirconia dispersed in solutions of Na_2SO_4 at varying pH. An increase in sulphate ion concentration in acidic solution resulted in a reversal of sign of the zeta potential from positive to negative. Additionally, F.T.I.R. measurements showed a lowering of the symmetry of adsorbed sulphate from T_d to C_{3V}, characteristic of sulphate as a monodentate ligand in inorganic complexes [3].

7.3.3 Phosphate Ion Sorption

A dispersion of non-calcined monoclinic zirconia (0.3087g in 25ml distilled water) was titrated with 0.088M H_3PO_4. pH was monitored by ISE. Since there is no reliable ion selective electrode for phosphate ion, uptakes of this ion were calculated from pH measurements and H_3PO_4 dissociation constants (pK_{a1} 2.23, pK_{a2} 7.21, pK_{a3} 12.32) as described previously in this Chapter. Hydrogen ion uptake was then recalculated to correct for self-protonation of phosphate ions in solution. This method of calculation gave the <u>total</u> uptake of H^+ by the exchanger. No direct information on the form of adsorbed H^+ was available from this titration (for example, sorption of H^+ as free proton

counterions or as part of a bound phosphate species). It was more convenient to express uptakes in moles rather than in the usual units of equivalents, since the actual charge on the bound phosphate species was unobtainable by this method.

In Figure 7.18 the total uptake of H^+ by the exchanger is shown, as calculated after the corrections described above. Also shown for comparison in this Figure are the measured H^+ uptake data before correction for association of protons with phosphate ions in solution. Comparison of the two sets of data shows that above pH 5, there was little difference between the corrected and uncorrected H^+ uptake. This was due to the near complete uptake of phosphate by the exchanger within this pH range - practically no phosphate remains in this solution phase at this stage of the titration, so the corrections were consequently small.

Uptake of phosphate ion was calculated by the method described above. The molar ratio of total hydrogen ion uptake to phosphate ion uptake was 3:1. Phosphate ion distribution coefficients indicate the high affinity shown by zirconia for phosphate, Figure 7.19.

Electrophoretic studies were performed on particles of non-calcined zirconia suspended in solutions containing phosphate ions using a Doppler Electrophoretic Light Scattering Analyzer (Coulter ™ DELSA 440). An increase in the solution concentration of phosphate ion in acidic solution (pH 3-4) resulted in a sign reversal of the zeta potential from positive to negative, Figure 7.20. Evidence that phosphate sorption on zirconia was at least partially irreversible (reported by Kraus [1] and Amphlett [4]) was provided by the observation that the zeta potential of phosphate-treated zirconia particles was negative in acid solution even after the particles had been thoroughly washed and dried, indicating that phosphate ions remained bound to the particles.

7.3.4 Fluoride Ion Sorption

The fluoride ion exchange capacities of non-calcined monclinic zirconia have been studied previously [5]. In this research similar titration experiments were performed on dispersions of calcined monoclinic zirconia. For comparison the original titrations on non-calcined zirconia were repeated. Activities of hydrogen ion and fluoride ion were determined by ISE and uptake of these ions on the exchanger calculated as before.

In each titration, the pH of the dispersion was adjusted to 5-6 by addition of HCl. At this point, an addition of NaF solution (0.2 meq NaF to the non-calcined zirconia dispersion, 0.1 meq NaF to the calcined zirconia dispersion) was added and the pH brought back to 5 by addition of HCl. These steps were repeated until the addition NaF no longer produced a significant pH shift. At all points after the first addition of NaF, the solution pH was kept above 5 in order to avoid the formation of the undissociated species HF in significant amounts.

The initial addition of 0.2 meq NaF to the dispersion of non-calcined zirconia gave a pH shift of 4 units (5.2 to 9.2). On readjustment of the solution pH to its original value by addition of HCl, there was a concurrent uptake of fluoride and hydrogen ion. Subsequent additions of 0.2mmol NaF gave progressively smaller pH shifts. As shown in Figure 7.21, the uptake of fluoride at the end of the titration was 3.6 meq/g, after a total addition of 1.15 mmol NaF. This capacity for fluoride was remarkably high compared to capacities observed for other anions such as chloride or sulphate. The ion exchange capacity at pH 5 increased as the fluoride ion activity in the dispersion was increased. When the ion exchange data from Figure 7.21 was plotted as a function of total acid pHF, a nearly smooth curve was obtained, Figure 7.22. Fluoride ion exchange capacity is therefore a function of the activity of both hydrogen ion and fluoride ion.

Similar fluoride uptake experiments were performed on samples of calcined zirconia prepared by the sol-gel method. When titrated in the presence of fluoride as above, the obtained results were qualitatively similar to those obtained with non-calcined zirconia, with the capacities being somewhat lower. Again, the capacity for fluoride on this sample of zirconia was considerably greater than the capacity for chloride or sulphate ion. In Figures 7.23 and 7.24 these data are presented as functions of pH and pHF respectively.

For both samples of zirconia, a linear relationship was observed between pF and the logarithm of the fluoride ion distribution coefficient (for titration points where the pH was between 5 and 6), Figures 7.25 and 7.26. The magnitudes of the fluoride ion distribution coefficients on the calcined sample were lower due to the reduced fluoride capacity of this sample.

To determine the reversibility of fluoride sorption, samples of non-calcined zirconia were loaded with fluoride as described above. The dispersions were filtered, washed with distilled water, dried at 40°C, reweighed and redispersed. The dispersion was then titrated through to pH 11 with NaOH. The release of fluoride from the loaded zirconia was monitored by fluoride ISE.

On titration through to pH 11, the first redispersion of fluoride loaded zirconia released a total of 2.75 meq/g of fluoride, Figure 7.27. Subsequent redispersions released progressively less fluoride, with negligible amounts (0.01 meq/g) being released on the fourth redispersion. The total amount of fluoride released from loaded zirconia was around 3 meq/g. Comparison with the fluoride uptake value of 3.6 meq/g shows that the sorption of fluoride is not entirely reversible, with an estimated 0.6 meq of irreversibly bound fluoride per gram of zirconia.

After removing all exchangeable fluoride, samples of zirconia were titrated with KOH and HCl. The exchange properties of "fluoride treated" zirconia were markedly different from those observed on zirconia which had not been exposed to fluoride. The effects of fluoride treatment are shown in Figure 7.28. There was an apparent shift in the zero point charge to around 6.5, a reduction of around 1 pH unit. Enhanced cation capacities for Na^+ were observed, with greater exchange capacities at a given pH above the zero point charge. The anion capacity of fluoride treated zirconia was considerably lower than on untreated zirconia.

7.4 Conclusions

The research presented in this Chapter shows that the presence of ions which can be specifically adsorbed can dramatically affect the ion exchange and sorptive properties of inorganic oxides. Of particular importance to the use of these oxides as active layers of ceramic membranes is the degree of irreversible sorption observed with several of the ions studied, which may change the membrane character totally and irreversibly. This raises the possibility of using specific chemical bonding to permanently alter ceramic membrane surfaces. Specific sorption therefore promises to be a useful tool in establishing minimum fouling conditions and optimising separation processes.

References

[1] K.A. Kraus, H.O. Phillips, T.A. Carlson and J.S. Johnson, Proc. 2nd International Conference on Peaceful Uses of Atomic Energy, **28**, 3 (1958)

[2] R. Paterson, L. Cot et al., Chapter 6 in Final Report for C.E.C. Contract No. SC1 0178-C(EDB) between E.N.S.C.Montpellier, Univ. of Glasgow and U.S.T.Languedoc (1991)

[3] R. Paterson, L. Cot et al., Chapter 5 in Final Report for C.E.C. Contract No. SC1 0178-C(EDB) between E.N.S.C.Montpellier, Univ. of Glasgow and U.S.T.Languedoc (1991)

[4] C.B. Amphlett, Chapter 5 in Inorganic Ion Exchangers, Elsevier, Amsterdam (1964)

[5] A.M. Smith, Ph.D. Thesis, Glasgow University (1988)

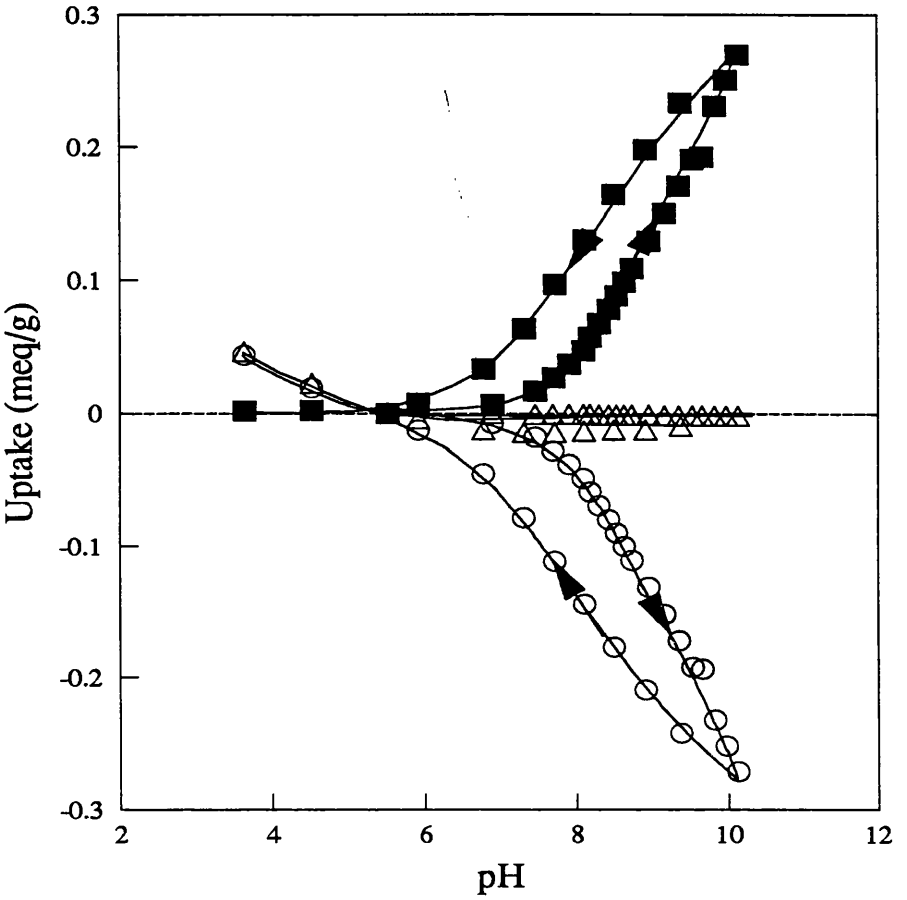

Figure 7.1 : Titration of a dispersion of 0.954g calcined monoclinic zirconia in 25ml distilled water with $Ca(OH)_2$ (0.018M) and back-titrated with HCl (0.1M). Uptakes of H^+ (○), Ca^{2+} (■) and Cl^- (△) were determined by ISE.

Titration File: JZR6A

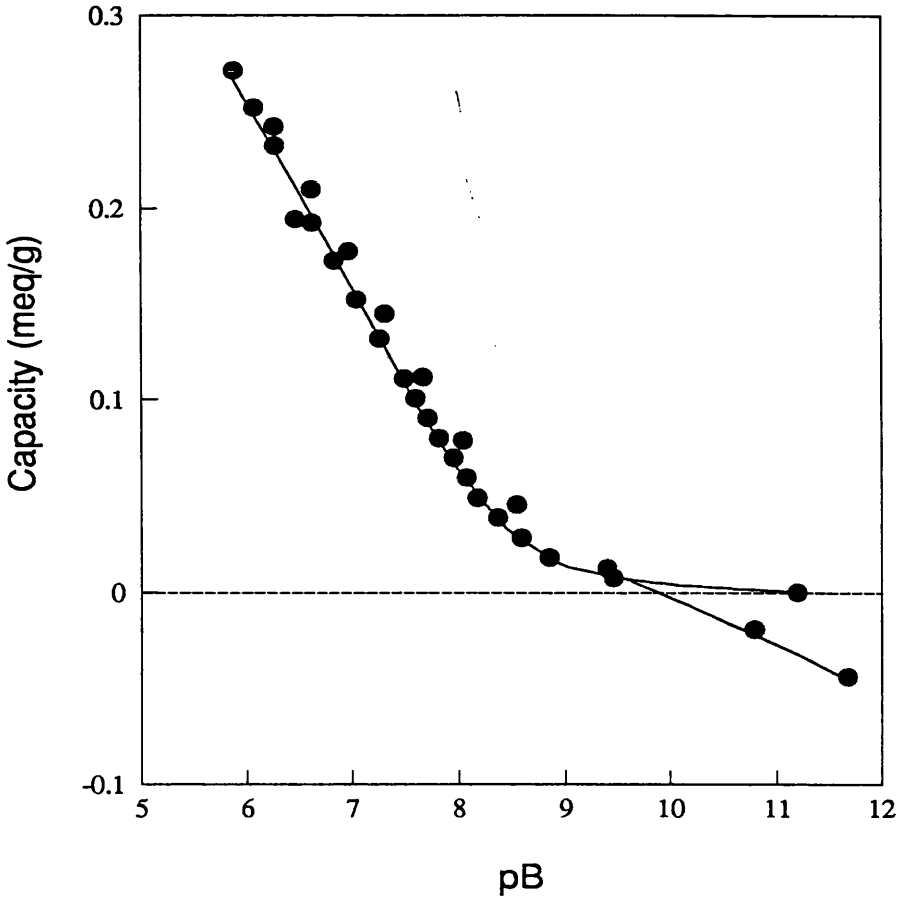

Figure 7.2 : Exchange capacities from the titration described in Figure 7.1, plotted as a function of pB ($=\frac{1}{2}$ pCa + pOH).

Titration File: JZR6A

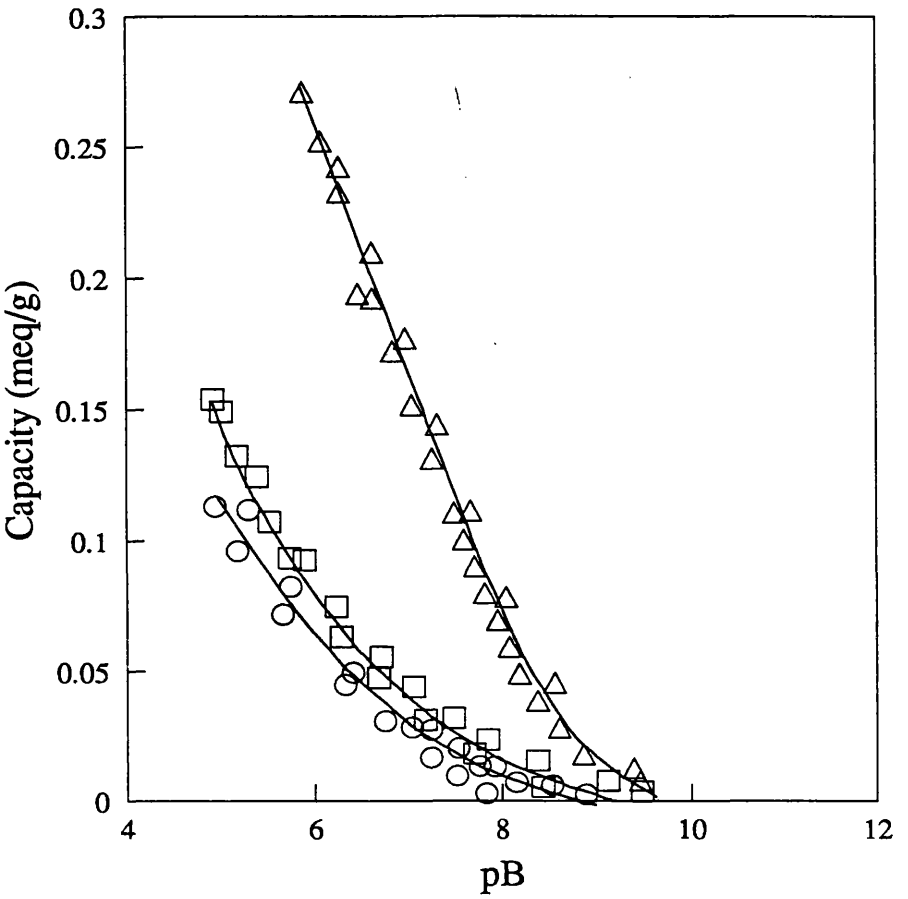

Figure 7.3 : Cation capacities of calcined monoclinic zirconia with Na^+ (□), K^+ (○) and Ca^{2+} (△) as the sorbing cations.

Titration Files: JZR6A, ZIR4, ZIR5

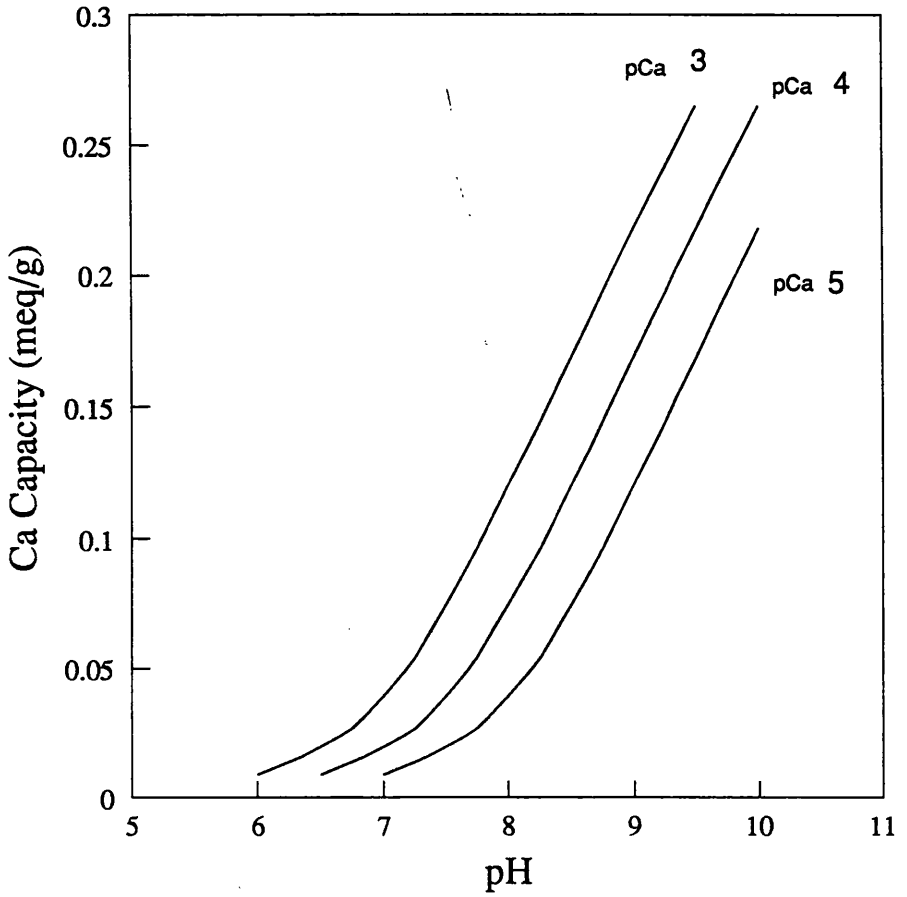

Figure 7.4 : Variation of calcium capacities of calcined monoclinic zirconia as a function of pH, at fixed calcium ion activities.

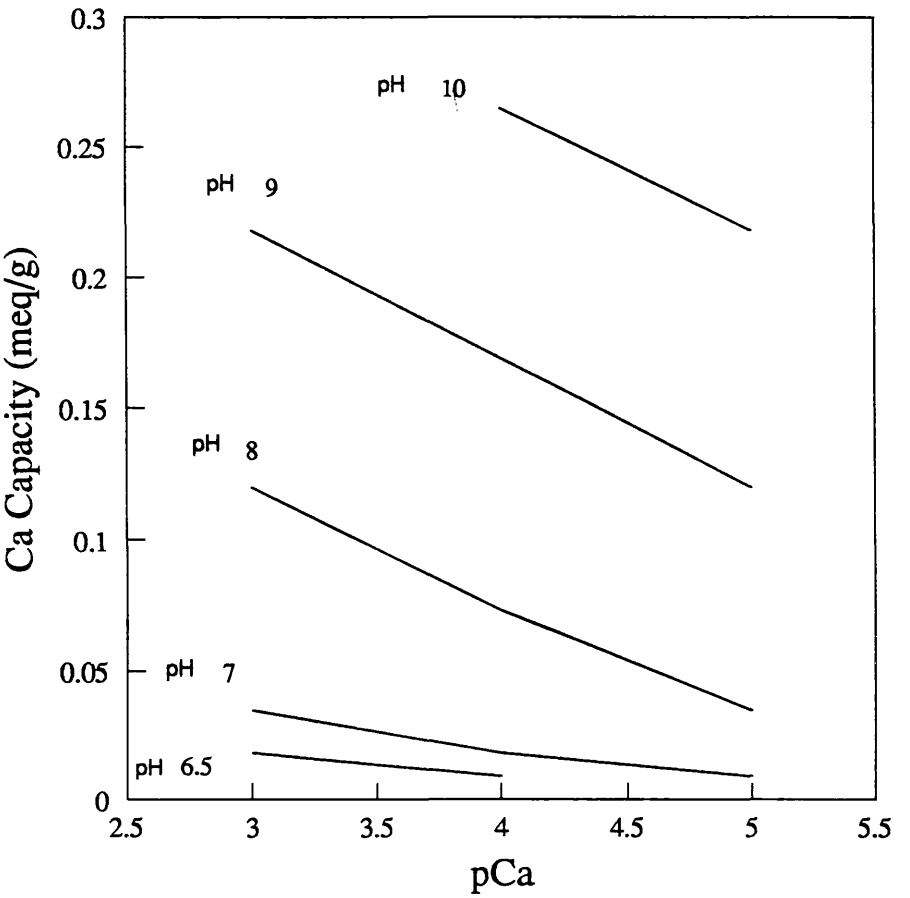

Figure 7.5 : Variation of calcium capacities of calcined monoclinic zirconia as a function of pCa, at fixed pH.

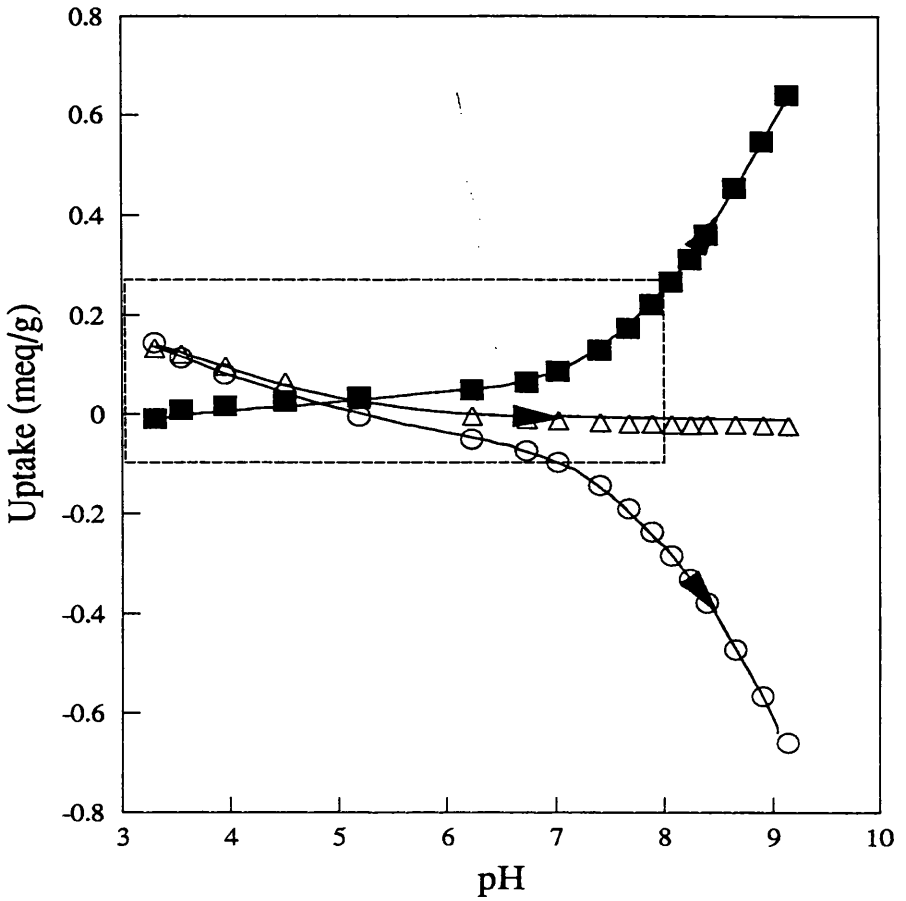

Figure 7.6 : Titration of a dispersion of 0.324g monoclinic zirconia (non-calcined) in 25ml distilled water. After an initial addition of .6ml 0.1M HCl, the dispersion was titrated with 0.015M $Ca(OH)_2$. Uptakes of H^+ (○), Ca^{2+} (■) and Cl^- (△) were determined by ISE.

Titration File: OLDZIR30

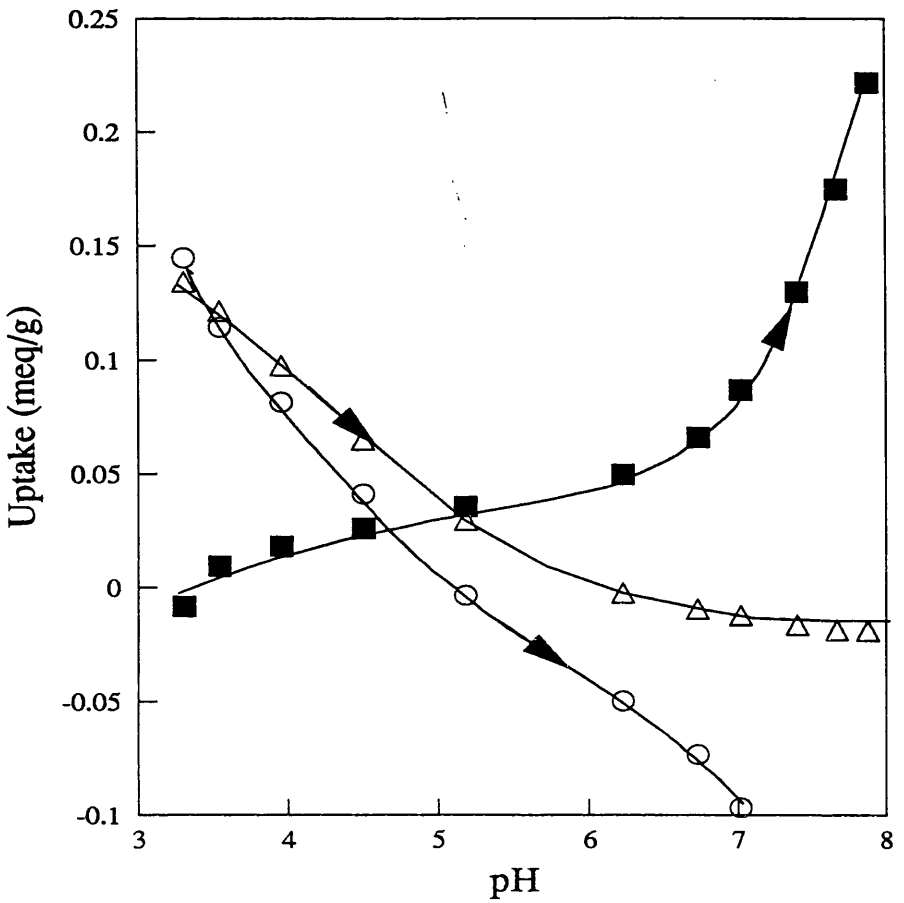

Figure 7.7 : Enlargement of data within the box drawn in Figure 7.6. Uptakes of H^+ (○), Ca^{2+} (■) and Cl^- (△) are shown.

Titration File: OLDZIR30

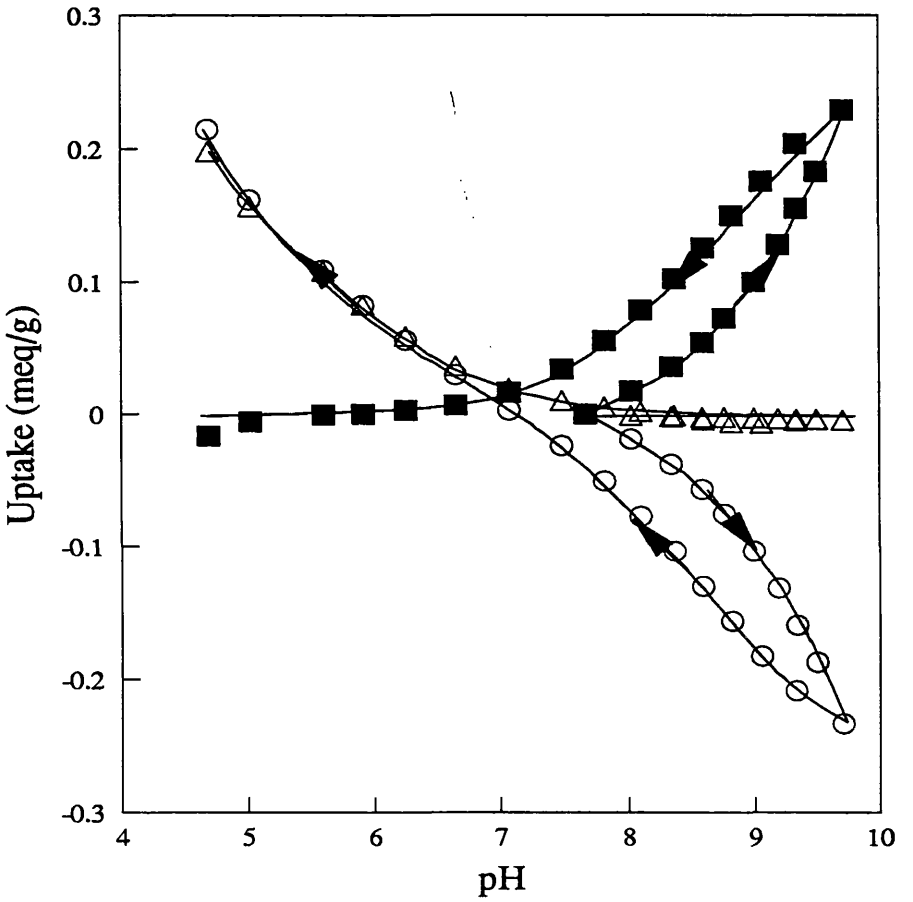

Figure 7.8 : Titration of a dispersion of 0.3711g γ Al_2O_3 in 25ml distilled water. The initial pH was 7.5. The dispersion was titrated with $Ca(OH)_2$ (0.018M) and back-titrated with HCl (0.1M). Uptakes of H^+ (○), Ca^{2+} (■) and Cl^- (△) were determined by ISE.

Titration File: GAL3

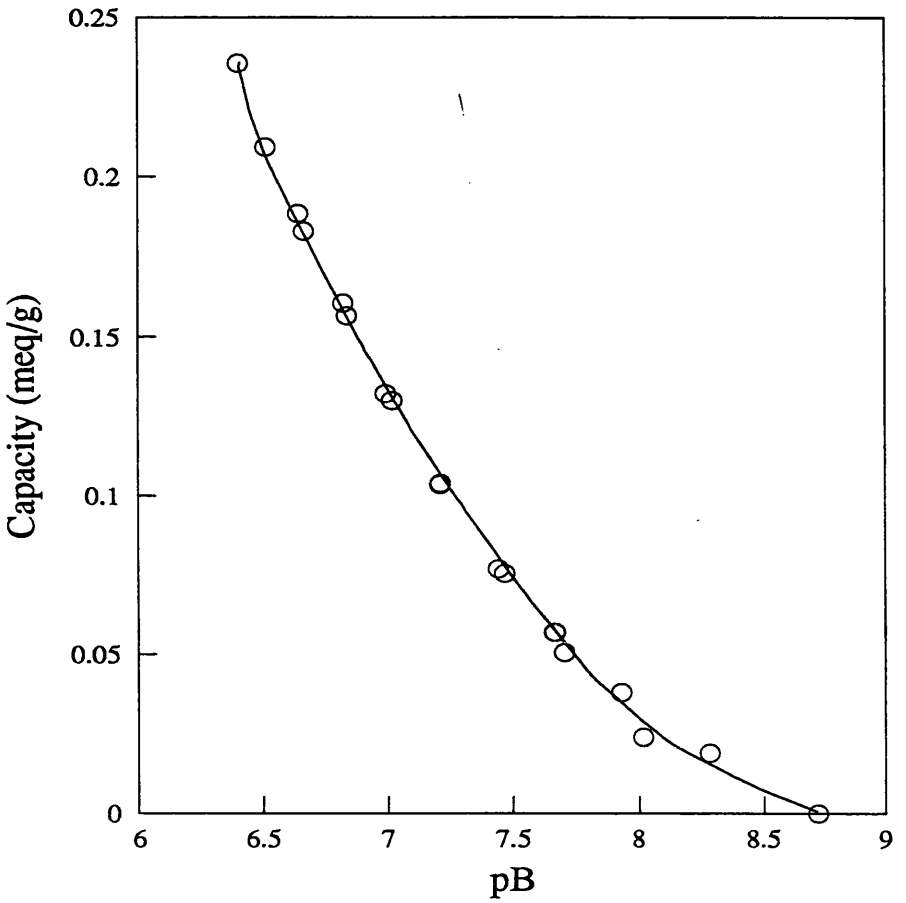

Figure 7.9 : Calcium capacities of γ Al_2O_3 from Figure 7.8 plotted as a function of pB ($=\frac{1}{2}$ pCa + pOH).

Titration File: GAL3

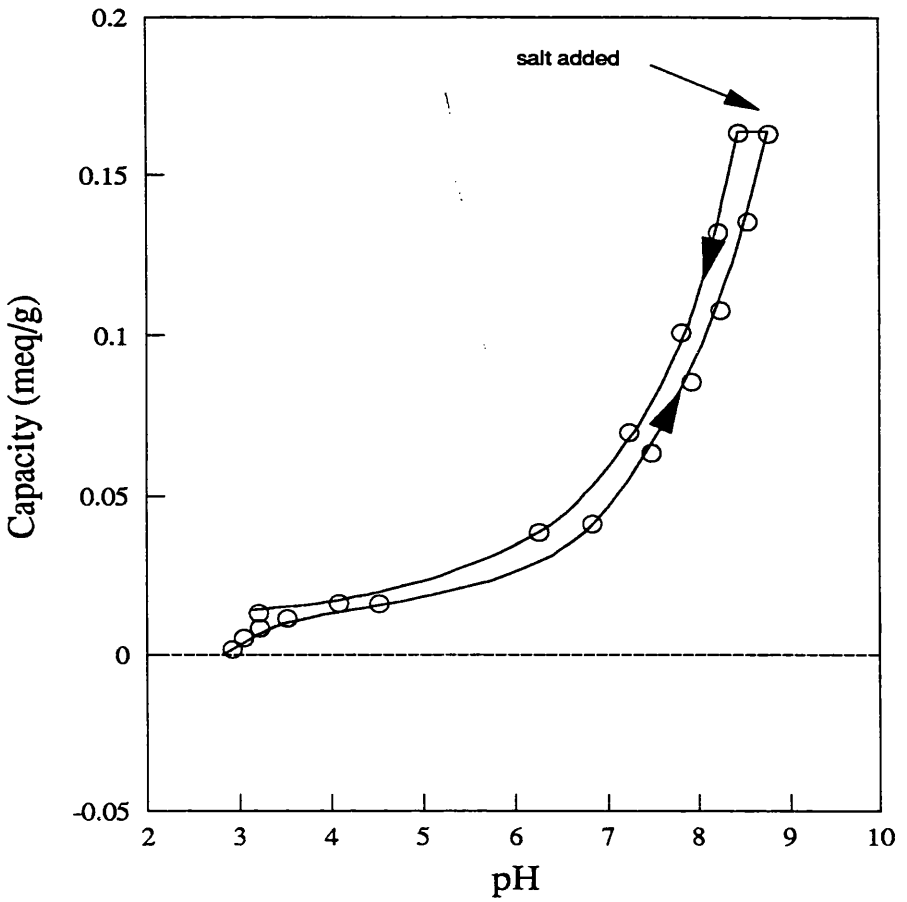

Figure 7.10 : Titration of a dispersion of 0.316g silica in 25 ml distilled water. 0.4mls 0.1M HCl was added to the dispersion, followed by titration with 0.018M $Ca(OH)_2$. 2mls 0.075M $CaCl_2$ was added at pH 8.8, followed by back-titration with 0.1M HCl.

Titration File: SSI1

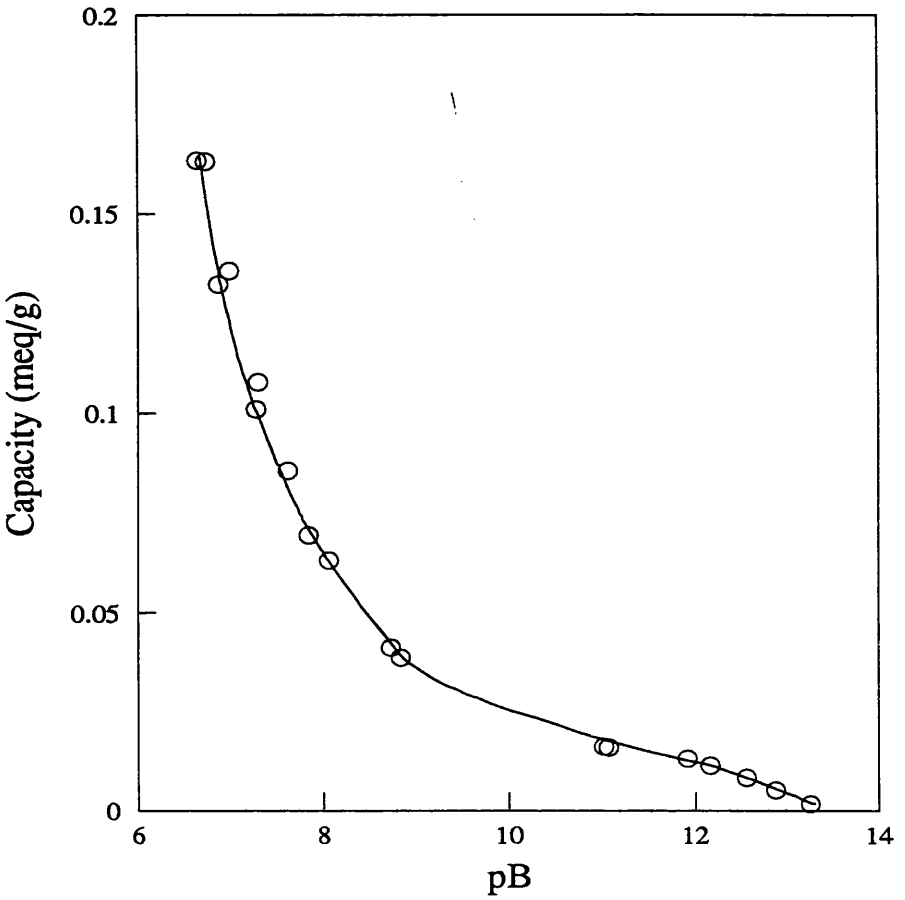

Figure 7.11 : Calcium capacities of silica from Figure 7.10 plotted against pB ($=\frac{1}{2}$ pCa + pOH).

Titration File: SSI1

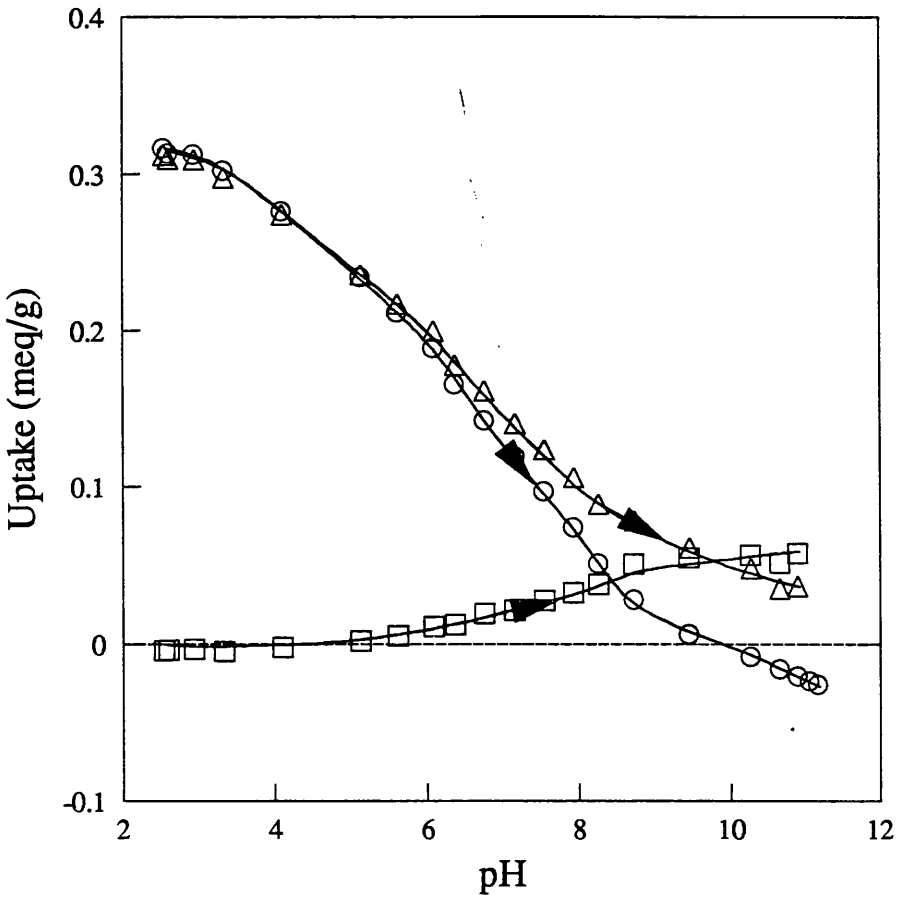

Figure 7.12 : Titration of a dispersion of 0.612g calcined monoclinic zirconia in 25ml distilled water with 0.1M KOH after addition of 2.9ml 0.049M H_2SO_4. Uptakes of hydrogen ion (○) and potassium ion (□) were determined by ISE. Sulphate uptake (△) was calculated from electroneutrality considerations.

Titration File: JZR8

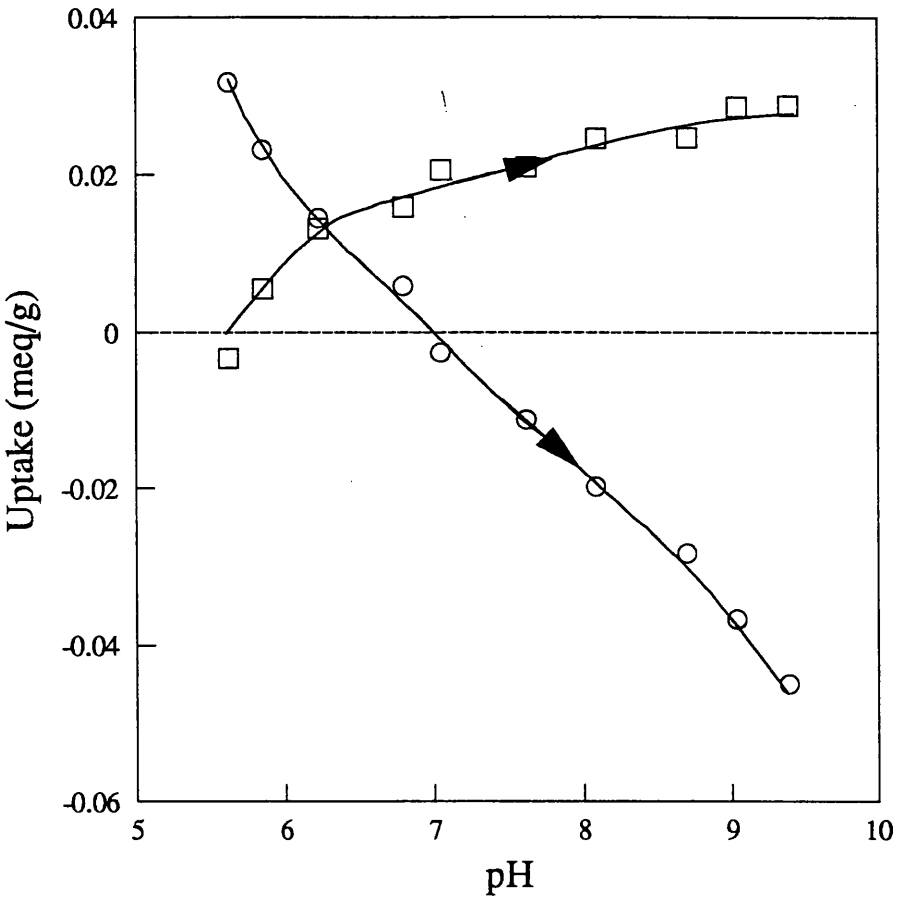

Figure 7.13 : Titration of a dispersion of 0.9912g calcined monoclinic zirconia in 25ml distilled water with 0.13M NaOH after addition of 0.32ml 0.049M H_2SO_4. Uptakes of hydrogen ion (○) and sodium ion (□) are shown.

Titration File: JZR4

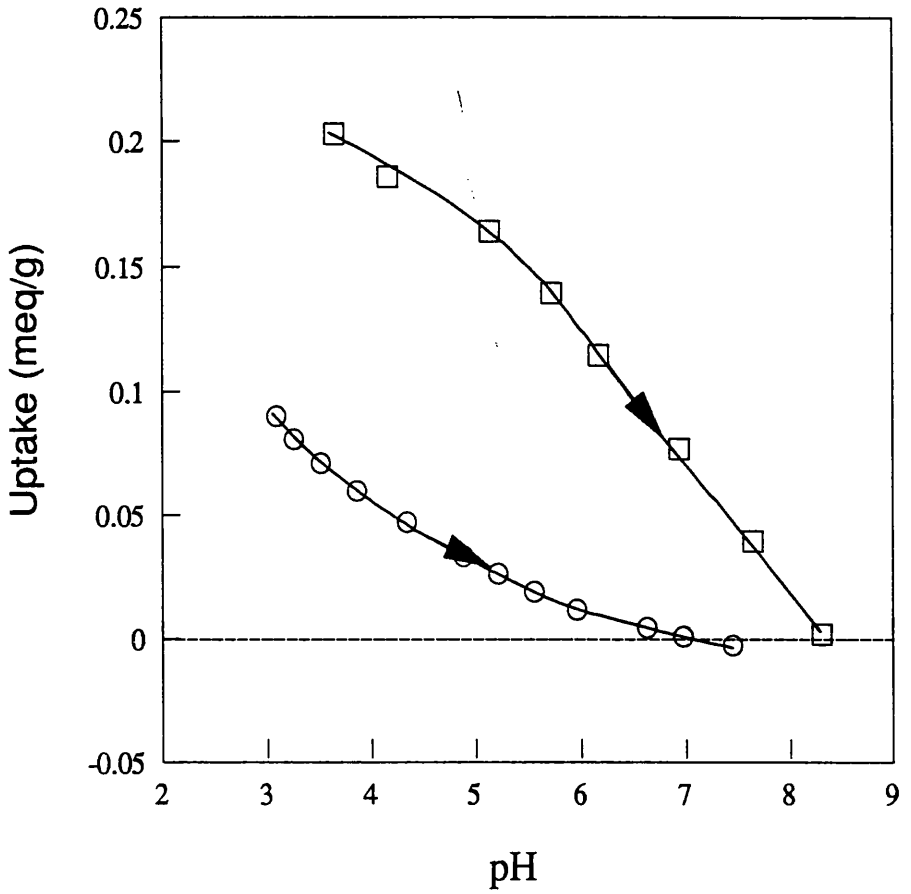

Figure 7.14 : Comparison of H^+ uptake on calcined monclinic zirconia with HCl and H_2SO_4 as the titrating acid. A dispersion of 1.39g calcined zirconia in 25ml distilled water was titrated with 0.1M KOH after an initial addition of 1.5ml 0.098M HCl (○). A second dispersion of calcined zirconia (0.564g in 25ml distilled water) was titrated with 0.1M KOH after addition of 1.36mls 0.0492M H_2SO_4 (□).

Titration Files: ZIR5, JZR9

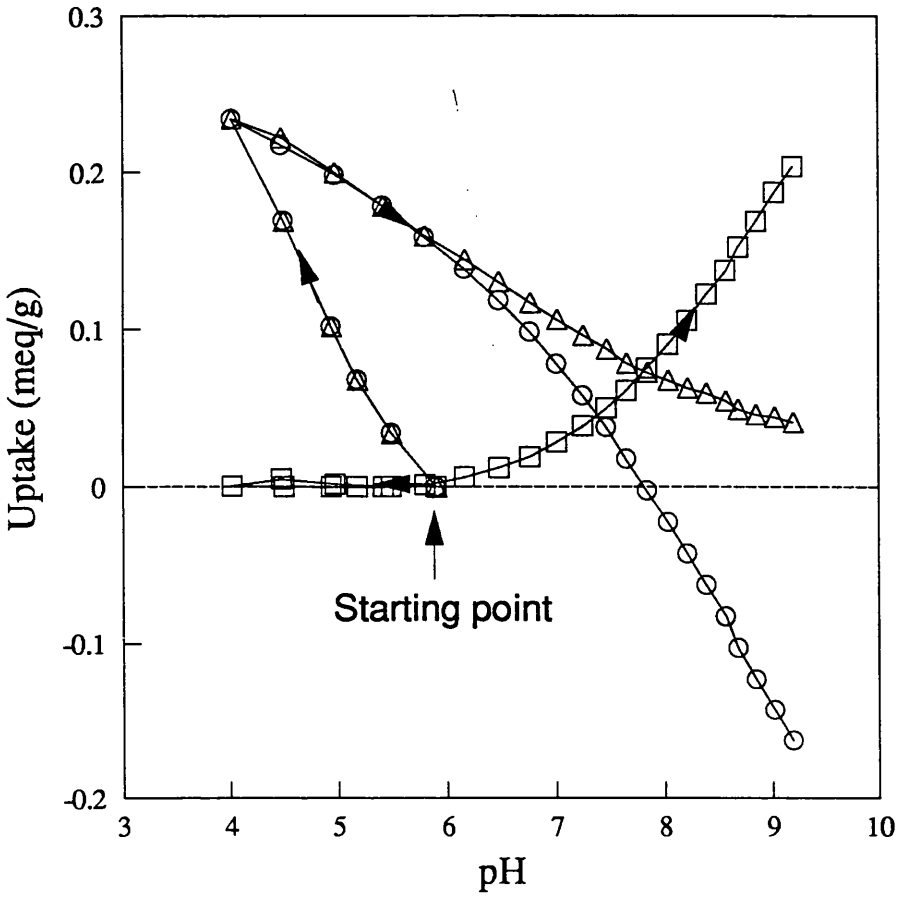

Figure 7.15 : Titration of a dispersion of 0.489g calcined monoclinic zirconia in 25ml distilled water with 0.018M $Ca(OH)_2$ after addition of 1.2ml 0.049M H_2SO_4. Uptakes of H^+ (○) and Ca^{2+} (□) were determined by ISE. Uptake of SO_4^{2-} (△) was calculated from electroneutrality requirements.

Titration File: JZR12

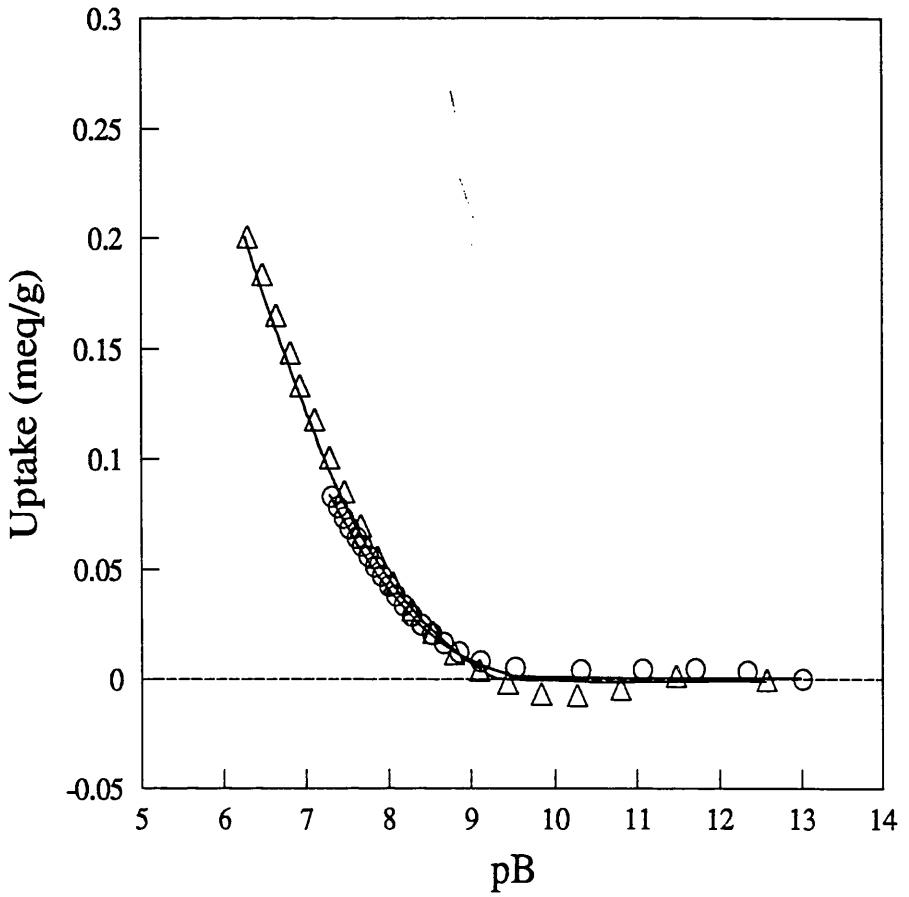

Figure 7.16 : Comparison of Ca^{2+} uptake on calcined monclinic zirconia with HCl and H_2SO_4 as the titrating acid. A dispersion of 0.994g calcined zirconia was dispersed in 25ml distilled water was titrated with 0.018M $Ca(OH)_2$ after an initial addition of 0.24ml 0.098M HCl (○). A second dispersion of calcined zirconia (0.489g in 25ml distilled water) was titrated with 0.018M $Ca(OH)_2$ after an initial addition of 1.2ml 0.049M H_2SO_4 (△). Calcium ion uptakes were determined by ISE. Results are presented as a function of pB ($= \frac{1}{2}$ pCa + pOH).

Titration Files: JZR12, JZR5

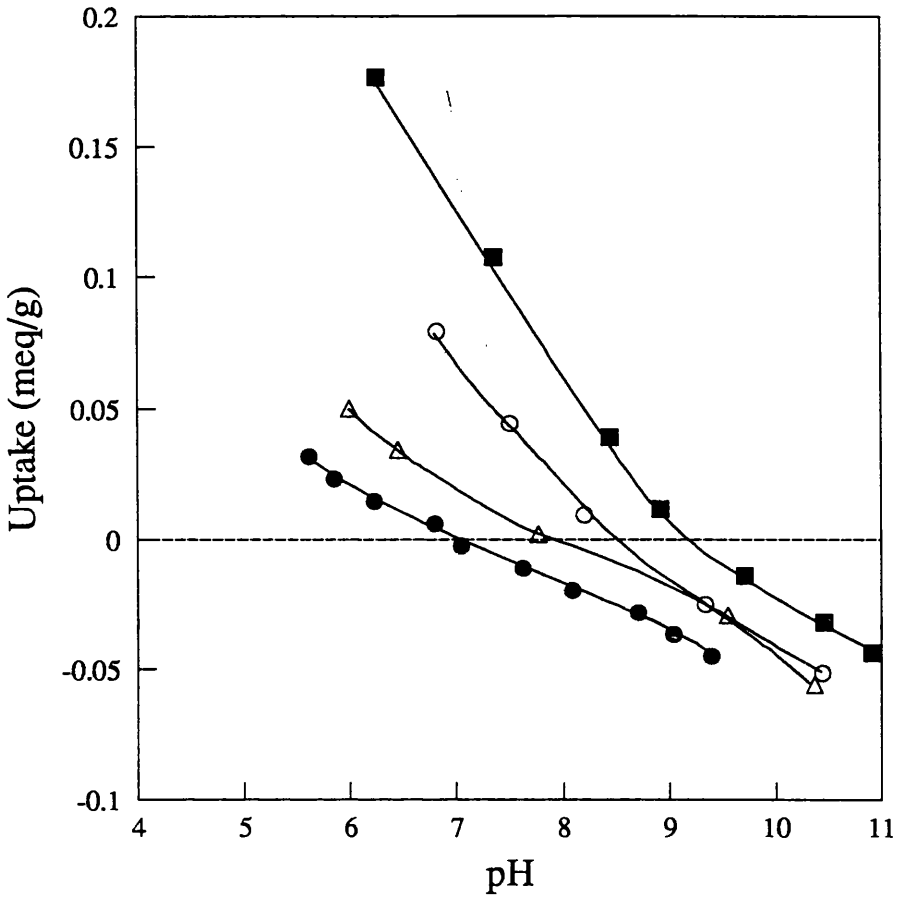

Figure 7.17 : Effect on the zpc of the amount of H_2SO_4 added to dispersions of calcined monoclinic zirconia. In each case an addition of H_2SO_4 (0.049M) was made to a dispersion of calcined zirconia in 25ml distilled water, followed by titration with 0.13M NaOH. H^+ uptake was calculated from ISE measurements. Results are shown for the following titrations:

0.32ml H_2SO_4 added to dispersion of .991g zirconia in 25ml water, titrate with NaOH (●)
1.51ml H_2SO_4 added to dispersion of 1.14g zirconia in 25ml water, titrate with NaOH (△)
1.95ml H_2SO_4 added to dispersion of .933g zirconia in 25ml water, titrate with NaOH (○)
5ml H_2SO_4 added to dispersion of .945g zirconia in 25ml water, titrate with NaOH (■)

Titration Files: ZIR10, ZIR9, JZR4, JZR7

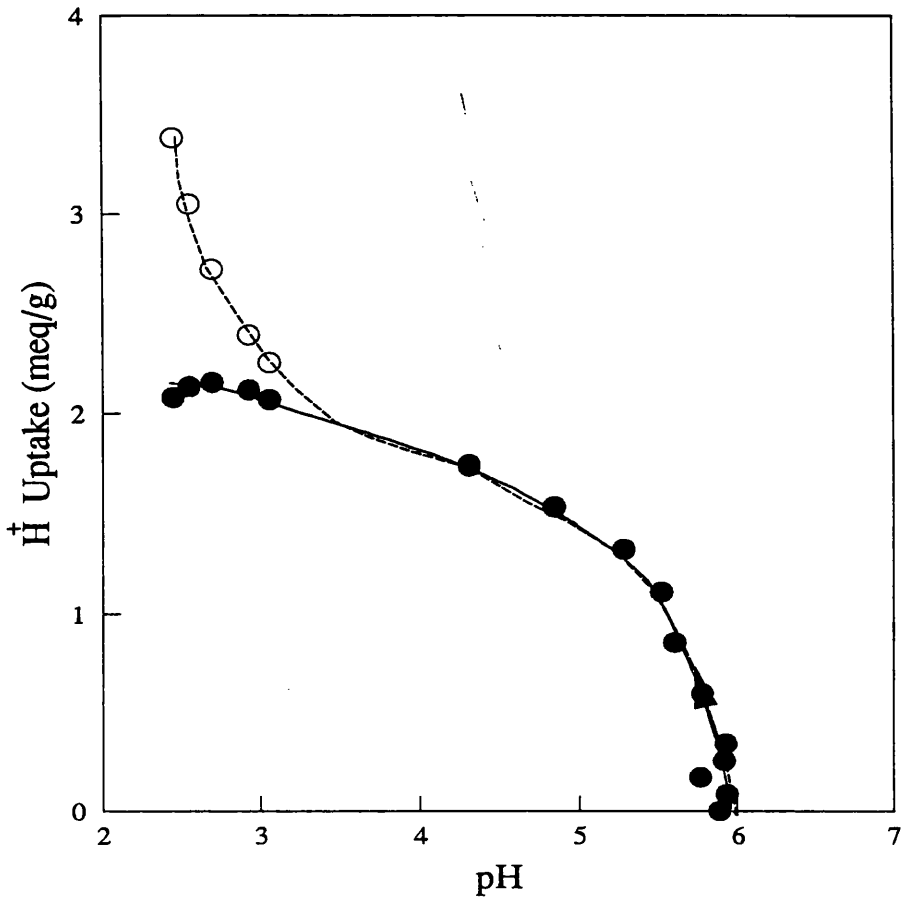

Figure 7.18 : Titration of a dispersion of non-calcined zirconia (0.3087g in 25ml distilled water) with 0.088M H_3PO_4. Hydrogen ion uptake, measured by ISE and corrected for self-protonation of phosphate ions in solution, is presented as a function of pH (●). Uncorrected H^+ uptake data are also shown (○).

Titration File: OLDZIR32

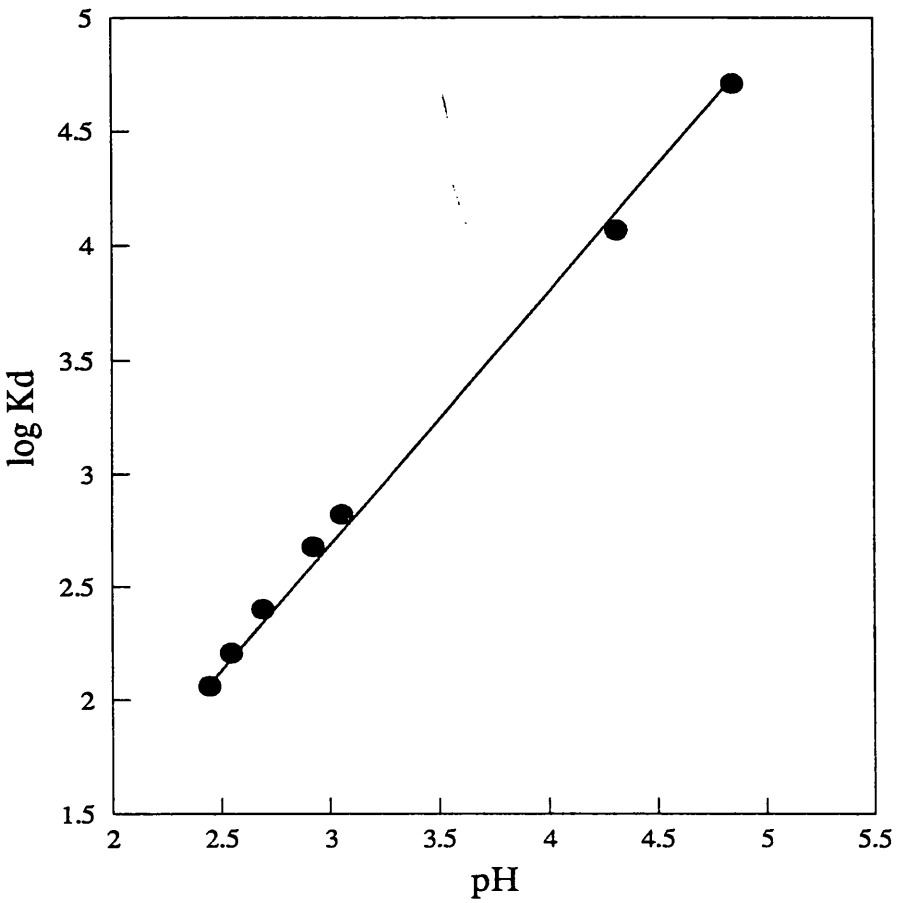

Figure 7.19 : Logarithm of phosphate ion distribution coefficients (ml/g) as a function of pH. Results refer to the titration in Figure 7.18.

Titration File: OLDZIR32

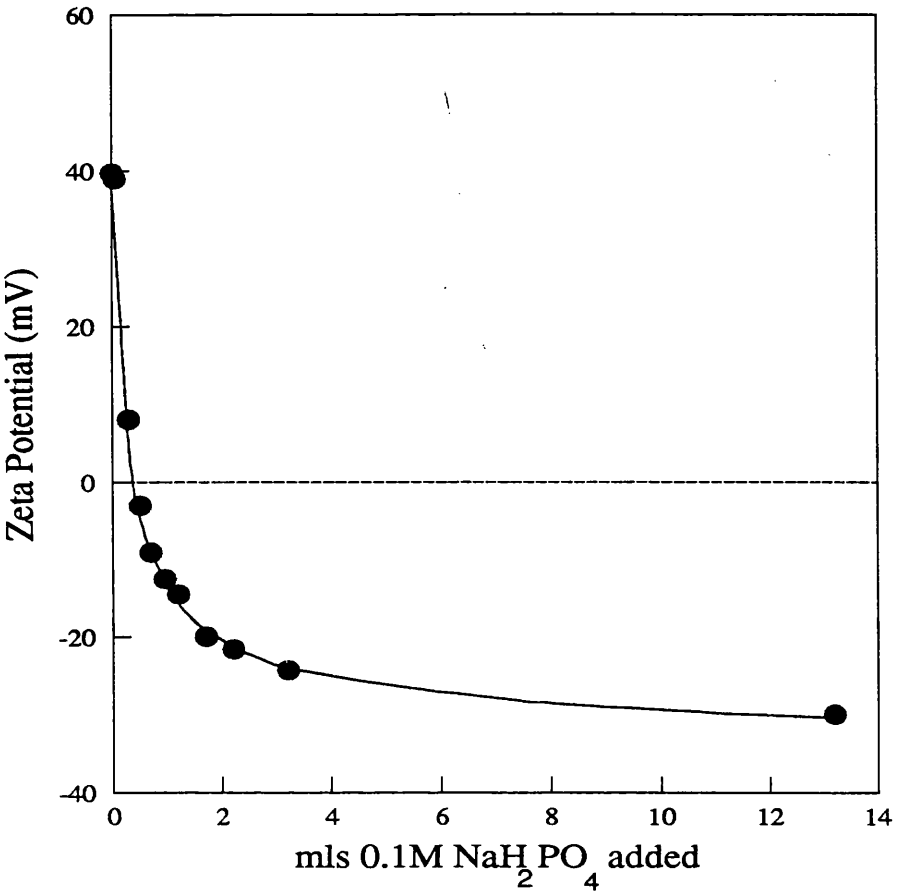

Figure 7.20 : Zeta potential measurements for particles of non-calcined zirconia dispersed in 0.1M NaCl (initially 0.0215g in 50ml) and titrated with 0.1M NaH_2PO_4 after an initial addition of 0.75mls 0.1M HCl. Throughout the titration the solution pH was between 3 and 4.

Electrophoretic File : POZR5

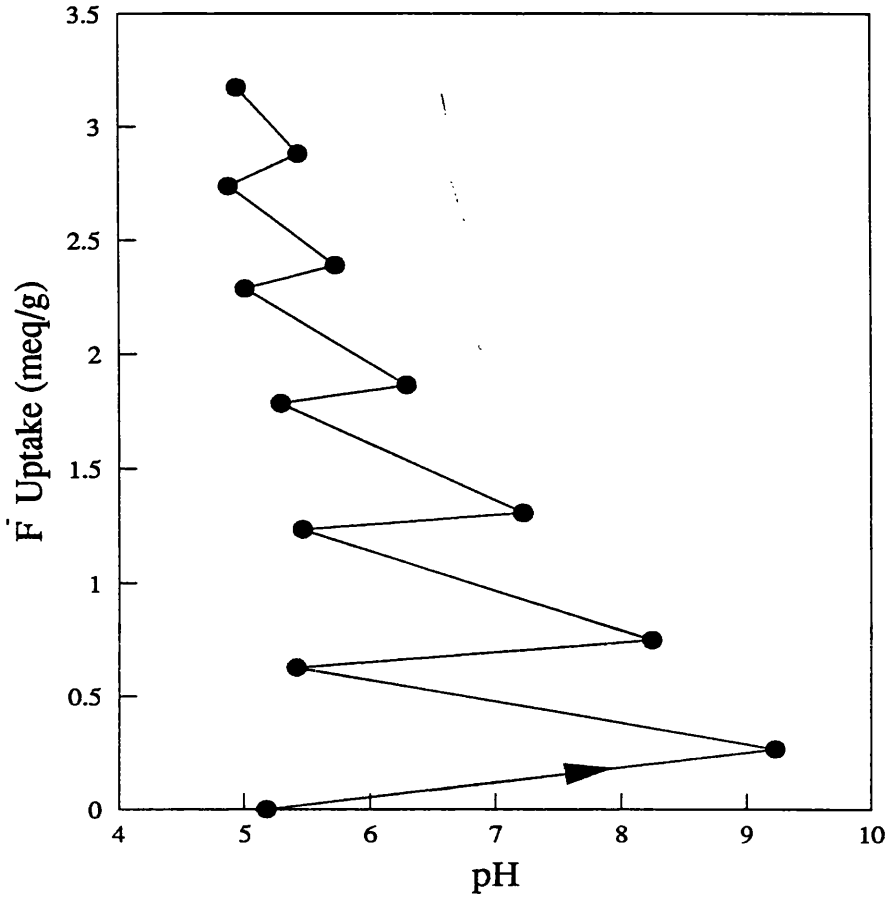

Figure 7.21 : Fluoride ion uptake on non-calcined monoclinic zirconia. 0.4ml 0.48M NaF was added to a dispersion of 0.305g zirconia in 25ml distilled water, initially at pH 5. The initial pH was restored by addition of 0.1M HCl to the dispersion. The procedure was repeated until a total of 2.4ml 0.48M NaF had been added. Fluoride ion uptakes were calculated from ISE measurements.

Titration File: EZR1

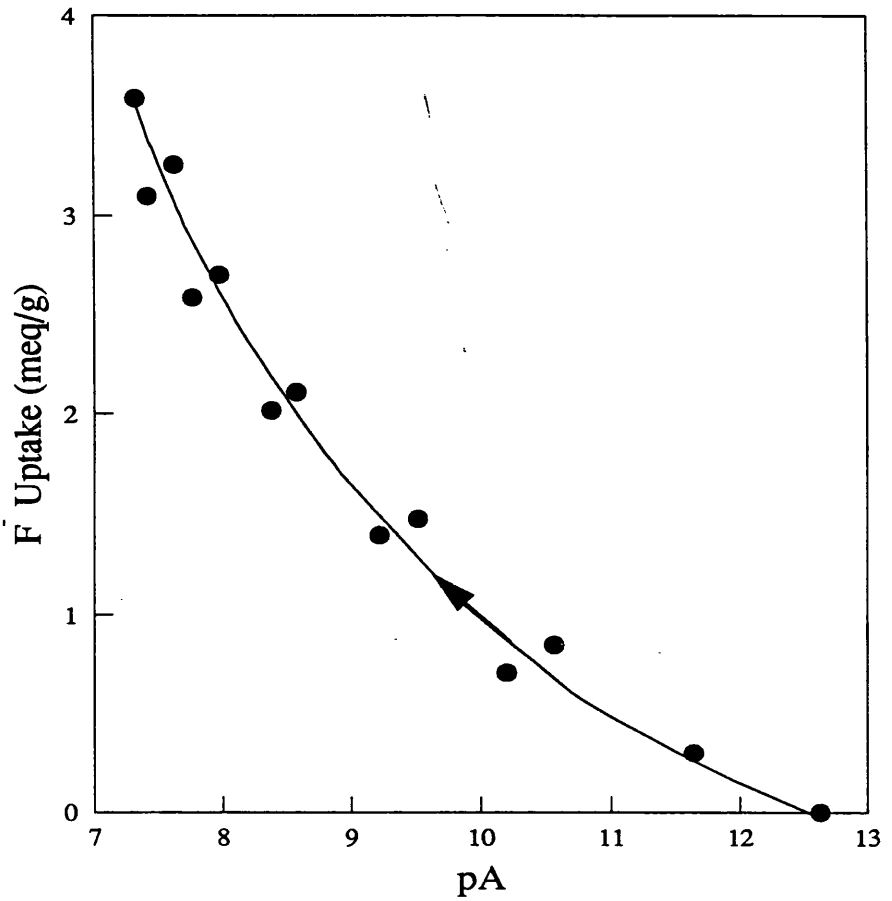

Figure 7.22 : Fluoride ion uptake data from Figure 7.21 presented as a function of pA = pH + pF.

Titration File: EZR1

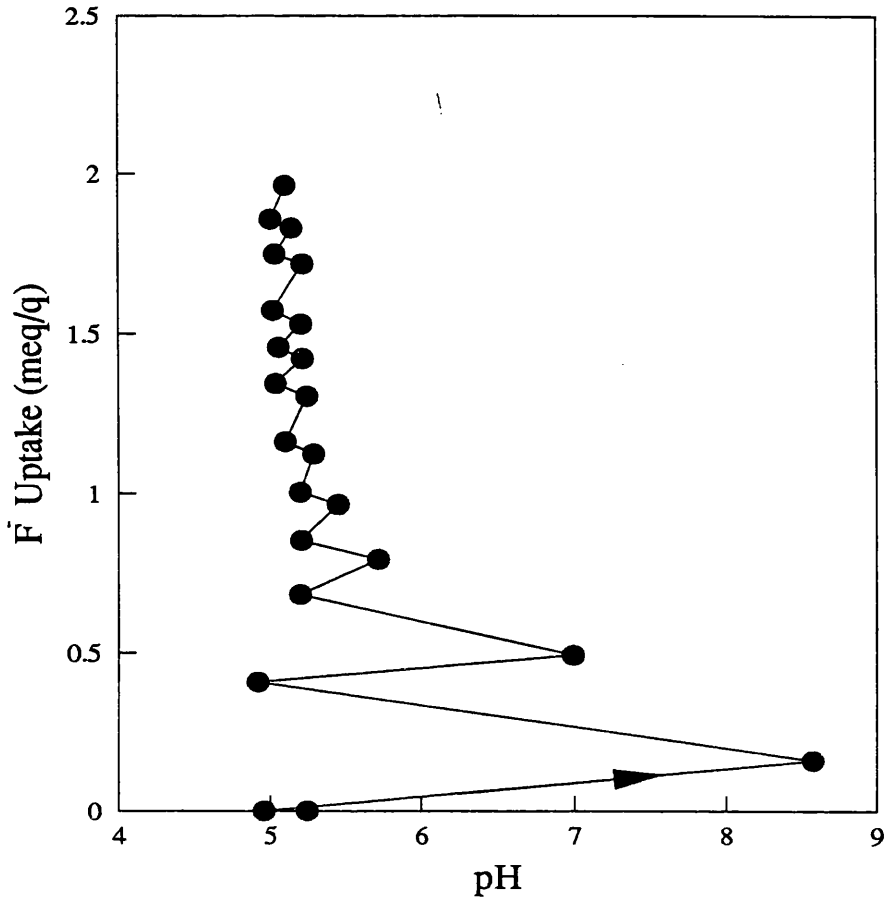

Figure 7.23 : Fluoride uptake on calcined monoclinic zirconia. 0.2ml 0.48M NaF was added to a dispersion of 0.251g zirconia in 25ml distilled water, initially at pH 5. The initial pH was restored by addition of 0.1M HCl. Further additions of NaF were made, followed by restoration of initial pH with HCl, until a total of 2.3ml 0.48M NaF had been added. Fluoride ion uptakes were calculated from ISE measurements.

Titration File: EZR(CAL)

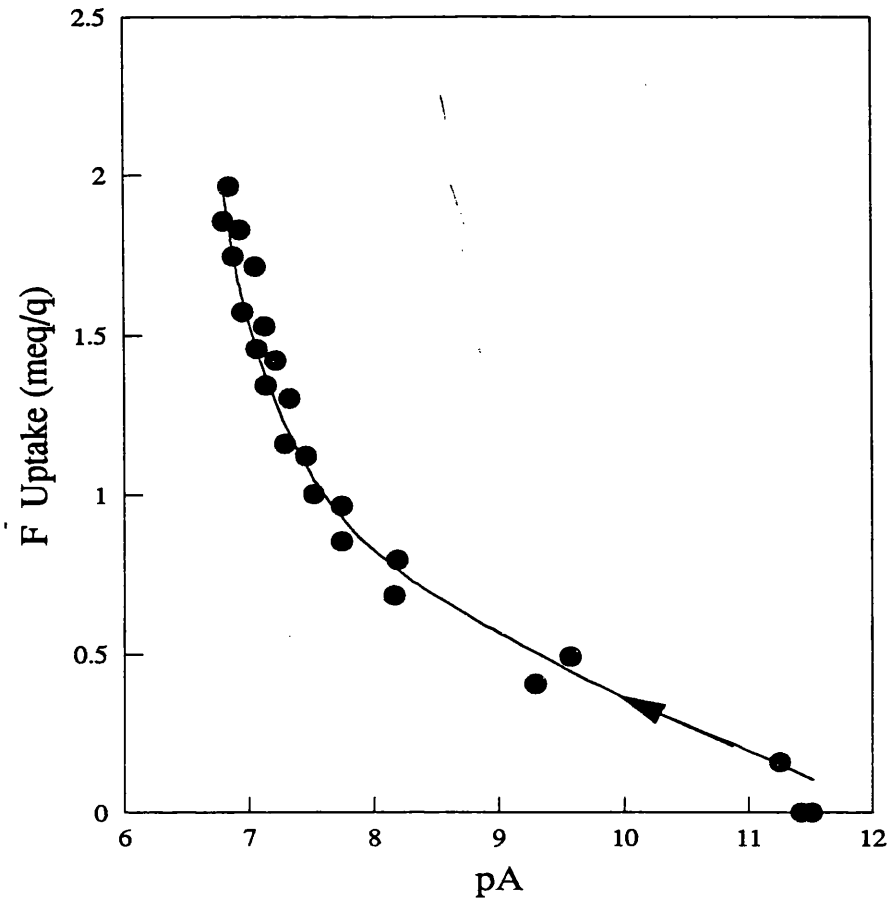

Figure 7.24 : Fluoride uptake data from Figure 7.23 presented as a function of pA = pH + pF.

Titration File: EZR(CAL)

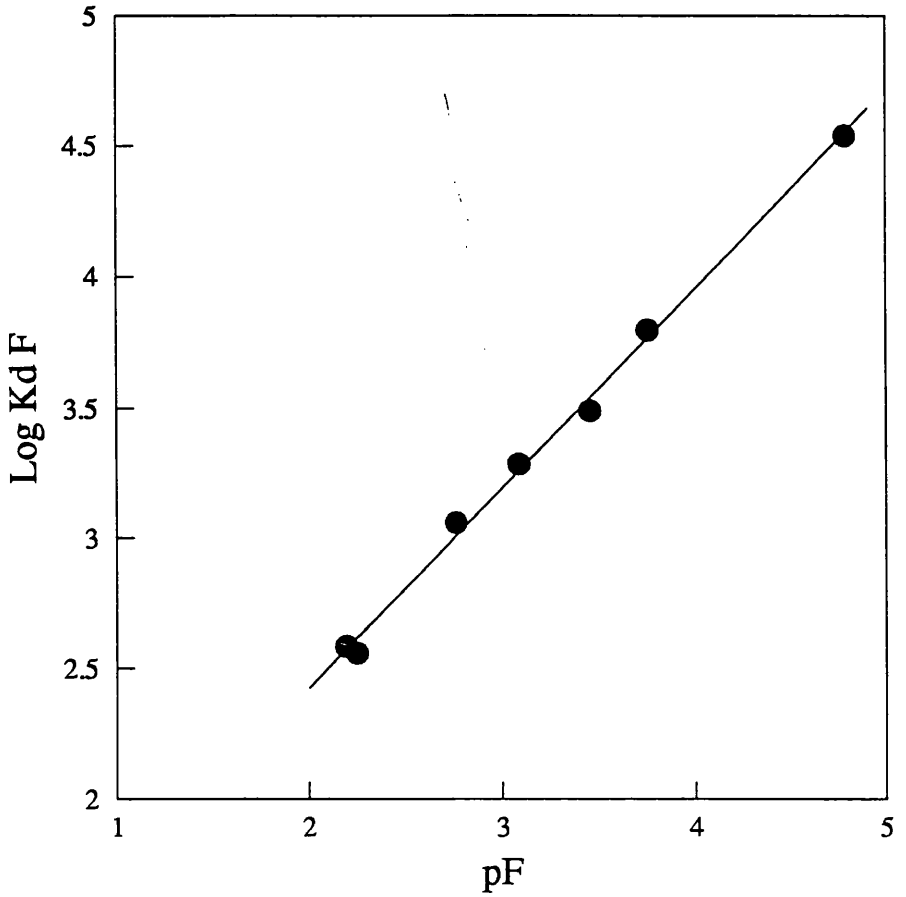

Figure 7.25 : Fluoride distribution coefficients on non-calcined monoclinic zirconia, at pH 5-6, against pF. Data are taken from Figure 7.21.

Titration File: EZR1

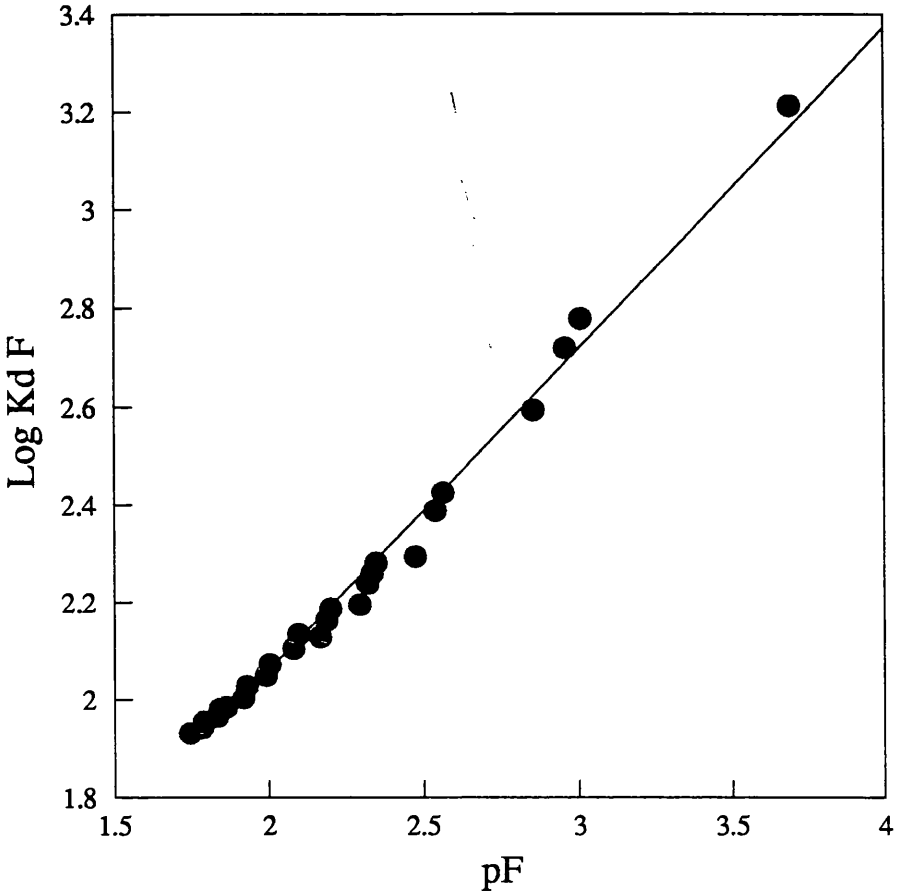

Figure 7.26 : Fluoride distribution coefficients on calcined monoclinic zirconia, at pH 5-6. Data are taken from Figure 7.23.

Titration File: EZR(CAL)

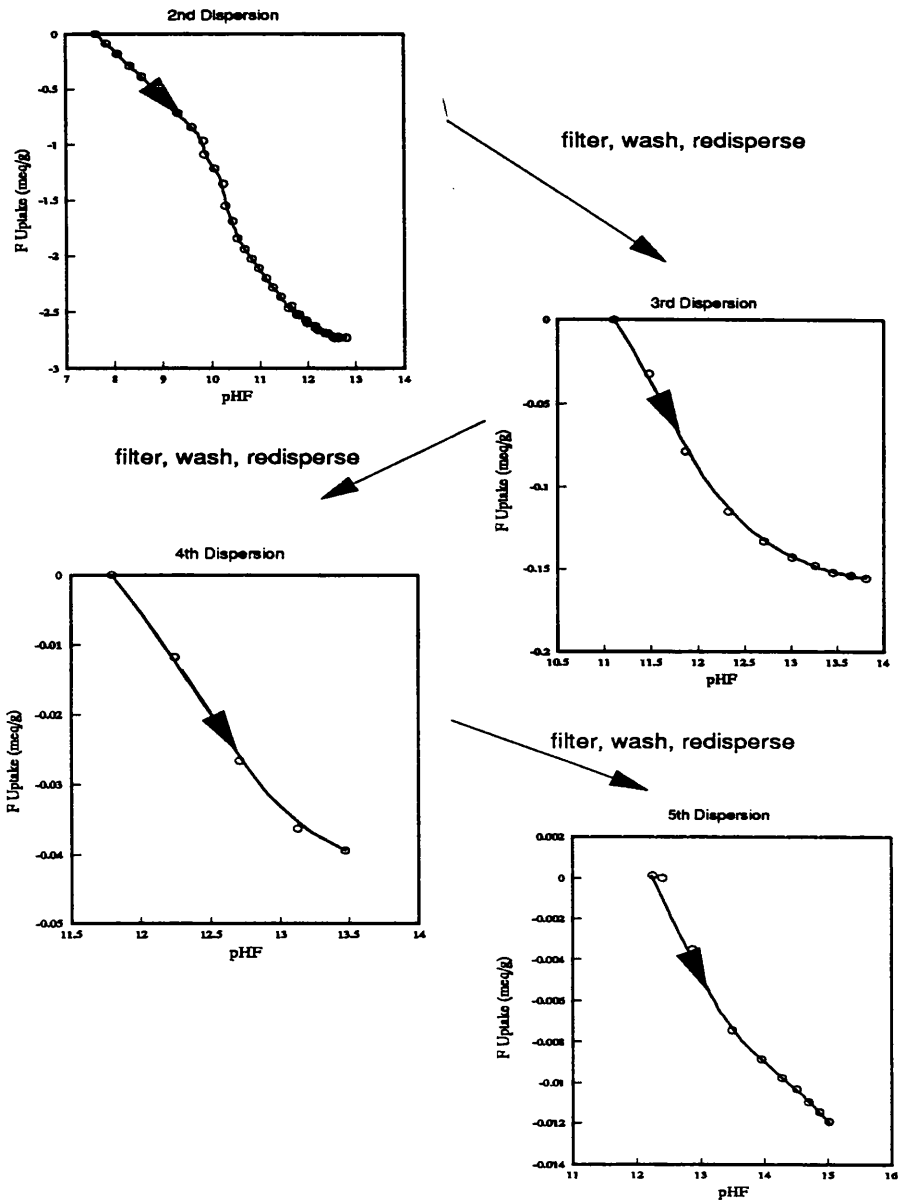

Figure 7.27 : Reversibility of fluoride uptake on non-calcined zirconia. Samples were loaded with fluoride and titrated with NaOH after filtering and redispersing. Progressively less fluoride was released on each subsequent dispersion. Total amount of fluoride released was around 3 meq/g.

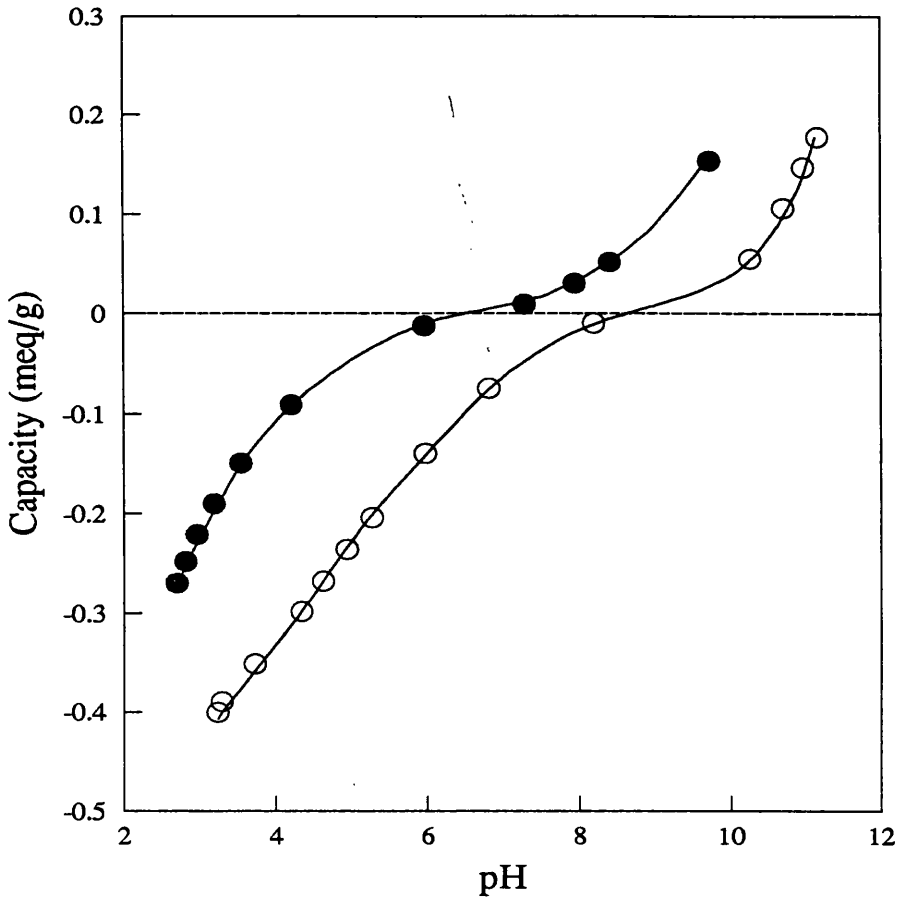

Figure 7.28 : Effect of irreversibly bound fluoride on the ion exchange capacity of non-calcined monoclinic zirconia. A sample of zirconia was treated with fluoride (Figure 7.21) and successively washed with NaOH (Figure 7.27). After drying at 40°C, 0.23g of this sample was dispersed in 25ml distilled water and titrated with 0.1M HCl and 0.1M KOH. Ion exchange capacities, determined from ISE measurements, are shown as a function of pH (●). For comparison, ion exchange capacities for non-calcined monoclinic zirconia which had not been treated with fluoride were determined by titration of a dispersion (0.3098g in 25ml distilled water) with 0.1M HCl and 0.1M KOH (○).

Titration Files : NZR6, EZR6

CHAPTER 8

GENERAL CONCLUSIONS

The research presented in this thesis was concerned with the investigation of the ion exchange and sorption processes which occur on the surfaces and within the pores of inorganic ion exchangers. Exchangers of the aluminosilicate type (clay minerals, fired clay products, urban building materials) and inorganic oxide ion exchangers were studied.

The main research technique, applicable to all studied systems, was multi-electrode potentiometric titration of colloidal dispersions of ion exchangers in aqueous media. The development of a computer controlled, automated titration system was central to this research. With this system, it was possible to monitor simultaneously the activities of up to four ions using ion selective electrodes. A maximum of six titrants could be used in a titration. After activity corrections, solution concentrations of the monitored ions were obtained and the uptake or release of these ions calculated by mass balance. These calculations were performed automatically. The criteria for electrode stability were predetermined by the user. This removed operator bias from the experiments and was particularly convenient in the titration of materials which were slow to reach equilibrium, such as NASICON. The enhanced precision of the automated titration method enabled capacities of less than 0.1 meq/g to be resolved with confidence, an order of magnitude smaller than previously achieved.

A traditional problem in the determination of pH or other p(ion) in colloidal solution, particularly in dilute solutions with highly charged colloidal particles, is the problem of the suspension effect, due to the potential of the electrical double layer surrounding charged particles. In the region of the double layer, the activity of counterions exceeds those of coions due to the influence of the electrical potential near the surface. It is not possible to detect a suspension effect in a single electrode titration. It was shown in this research that

if all ions which participate in exchange processes are monitored by ion selective electrode it is possible to determine and correct for suspension potentials. The ion exchange data in this research were corrected for the suspension potential by this method.

The ion exchange characteristics of a wide range of ion exchangers of the aluminosilicate type (clay minerals, urban building materials) were studied using the potentiometric titration methods. This research was performed as part of a European Community Post-Chernobyl Action on the Improvement of Practical Countermeasures Against Nuclear Contamination in the Urban Environment (Contract No. B16-0270.UK(H)). The aim of this work was to identify the urban surfaces which selectively adsorb radiocaesium and to determine the mechanisms of sorption, the total caesium binding capacity and its ease of displacement on these surfaces. To perform these studies, an electrode sensitive to caesium ion was developed and tested. The valinomycin based caesium ion selective electrode was shown to be a first class, readily available caesium ion sensor, with near ideal response in the range 10^{-1} to 10^{-5}M in aqueous caesium ion. The electrode showed good selectivity for caesium over other cations, the only major restriction being that is could not be used in the presence of potassium ion, due to high selectivity for this ion. Accordingly this electrode was used for the titration of samples from which potassium ion had previously been extracted. The caesium ion binding capacities of clay minerals and urban surfaces were rapidly characterised using the automated titration method. The mechanism of Cs^+ sorption was shown to be ion exchange with Na^+ (or with counterions present in the natural material, such as K^+ and Ca^{2+}). The relative selectivities of the exchange sites on clay minerals and building materials were generally $Cs^+ > K^+ > Na^+$, with the magnitude of selectivity varying according to the nature of the material. Cation exchange capacity on a typical clay rooftile was shown to be directly proportional to the total surface area of the tile, enabling the determination of the caesium binding capacity per unit of superficial tile surface. This

provided a basic cationic exchange capacity for a wide range of urban materials. Consequently, in decontamination or preventive strategies, assessments may now be made on the quantity of nuclides which can be bound to a particular surface, or the number of sites which need to be blocked or occupied to prevent contamination.

Studies on the ion exchange characteristics of inorganic oxides were performed as part of two research projects on the fundamentals of ceramic membrane design and performance - a European Community funded joint project (Jumelage) between Ecole Nationale Supérieure de Chimie de Montpellier, Université des Sciences et Techniques du Languedoc and University of Glasgow (Contract No. SC 1 0178-C(EDB)) and a S.E.R.C. funded research project on fouling of ceramic membranes by charged substrates, Contract No. GR/F 64296. The surface charge and ion sorptive properties of the oxides which form the active layers of ceramic membranes have extremely important implications in the design and the efficient use of ceramic membranes. These properties are major contributory factors to membrane fouling by polar or ionic substrates, since surface sorption is often the first step in fouling leading to pore blocking within the membrane structure. By altering the surface charge density and/or changing its polarity, the opportunity exists for minimising fouling and optimising separation processes.

The ion exchange and sorptive properties of the oxide active layer of ceramic membranes were determined using the automated titration method. The ceramic oxides studied were ZrO_2, TiO_2, SiO_2 and γAl_2O_3. Additionally, titrations of dispersions of the three-dimensional cation exchanger NASICON were performed. pH and salt concentration effects were evaluated. The mechanisms for ion exchange were consistent with those previously determined on non-calcined oxides, with anion exchange a function of the activity of total acid pA and cation exchange a function of the activity of total base pB. The ion exchange

capacity of calcined zirconia was considerably lower than that of its non-calcined analogue. Good agreement was observed when the capacities of each zirconia sample were expressed per unit area.

Ion exchange properties were determined in the presence of a range of ions to which the ceramic membrane may be routinely exposed. Specific sorption of multivalent ions calcium, sulphate and phosphate were observed in titrations of zirconia dispersions in the presence of these ions. Fluoride ions also were specifically adsorbed. A degree of irreversibility was observed in the sorption of sulphate, phosphate and fluoride.

These results showed that the sign of the oxide surface charge and the exchange capacities for each counterion may be altered in a predictive way, by changing the pH and the activity of the sorbing ion. Initial studies on the practical applications of this work were encouraging. The effects of pH and salt concentrations on fluxes and on membrane fouling by charged substrates were shown to be as predicted by the relationships determined in this research. By appropriate selection of the membrane active layer material and manipulation of the operational parameters, it should therefore be possible to optimise conditions for separation processes across UF/RO membranes. Similarly, optimisation of operating conditions and membrane surface modifications could lead to a reduction in membrane fouling by charged substrates such as proteins, thus improving efficiency and increasing the membrane lifetime. The degree of irreversibility in the sorption of multivalent ions raises the possibility of using specific chemical bonding to permanently alter ceramic membrane surfaces.

List of Symbols

Symbol	Name	Units
a_i	Activity of ion i	
A	milliequivalents (meq) of acid added to dispersion	meq
B	milliequivalents (meq) of base added to dispersion	meq
c_i	Concentration of ion i	mol l^{-1}
$C.E.C.$	Cation exchange capacity	meq g^{-1}
E	Electrode potential	V
E^o	Standard state electrode potential	V
E_{DON}	Donnan potential	V
$Err\%$	% error on electrode measurement of concentration	
F	Faraday constant	C mol^{-1}
G	Weight of ion exchanger	g
I	Ionic strength	
K_T	Thermodynamic equilibrium constant	
K_A^B	Selectivity coefficient for ion B over ion A	
K_d	Distribution coefficient	ml g^{-1}
pA	negative logarithm of total acid activity	
pB	negative logarithm of total base activity	
pK_a	negative logarithm of acid dissociation constant	
pK_b	negative logarithm of base dissociation constant	
pX	negative logarithm of the activity of ion X	
R	Gas Constant	J K^{-1} mol^{-1}

List of Symbols

Symbol	Name	Units
S	milliequivalents of salt added to dispersion	meq
$S.F.(\%)$	Significance factor for ion uptake measurements	
T	Temperature	K
V	Total volume of dispersion	ml
V_o	Initial volume of dispersion	ml
V_a	Volume of acid added to dispersion	ml
V_b	Volume of base added to dispersion	ml
V_s	Volume of salt added to dispersion	ml
X_{UPT}	Uptake of ion X	meq/g
$[X]_o$	Initial concentration of ion X in solution	mol l^{-1}
X_M	Equivalent fraction of ion M	
z_i	Valency, including sign, of ion i	
γ_i	Activity coefficient for ion i	
$\gamma_\pm$	Mean activity coefficient	
ζ	Zeta potential	V
$\tilde{\mu}_i$	Electrochemical potential of ion i	J mol^{-1}

List of Symbols

Symbol	Name	Units
μ_i^o	Chemical potential of ion i in the standard state	J mol^{-1}
Ψ	Electrical potential	V
Ψ_{sp}	Effective suspension potential experienced by ISE	V
	Barred terms (for example, $\bar{\mu}_i$) refer to the solid phase	
	subscript (x) refers to value of parameter at distance x from colloidal surface, for example $p\,I_{(x)}$	
	subscript (∞) refers to value of parameter at infinite separation from colloidal surface, for example $p\,I_{(\infty)}$	
	subscript m refers to value measured by ISE, for example pX_m	

PUBLISHED PAPERS

Commission of the European Communities

Report EUR 12555 EN

RADIATION PROTECTION

Improvement of practical countermeasures:
the urban environment

Post-Chernobyl action

CHAPTER 5

ION EXCHANGE AND CAESIUM SORPTION CAPACITIES ON URBAN BUILDING MATERIALS

Stephen Gallagher, Donald Young and Russell Paterson
University of Glasgow
Department of Chemistry

5.1 INTRODUCTION

During the course of this research, a caesium ion selective electrode was developed and tested [1]. With this electrode and titration methods developed earlier [2], a methodology was created by which the uptake of caesium and the corresponding release of any displaced counterion could be measured rapidly and precisely. This titration technique was fully computerised and automated so that samples of materials could be tested in a much shorter time than by conventional procedures using radioactive isotopes or other analytical methods. The urban materials, usually minerals, bricks, tiles, clays etc., were ground to a fine powder and titrated in dispersion in aqueous solutions. The release of naturally occurring ions on dispersion, particularly of potassium ion, proved a good indication that high caesium binding potentials were to be expected. This titrimetric survey provided a basic cationic exchange capacity for a wide range of urban materials, many collected from sites across Europe. In particular, experiments were conducted with Gävle rooftiles which were found to be contaminated by caesium due to Chernobyl fallout in the town of Gävle in Sweden. This material has been studied extensively and various aspects of that sorption have been recorded in other chapters of this book. It should be made clear at the outset that this method provides an accurate measure of the total caesium binding sites of the urban material sample, which will be shown in **Chapter 6** to be greatly in excess of the very small minority of high selectivity sites, discovered by the Leuven group. The large number of low selectivity sites observed provide initial catchment for fallout caesium, which can subsequently migrate to the very small number of highly active sites, where it may remain, perhaps permanently. In this work, in nearly all samples investigated, caesium is selected over potassium, is selected over sodium. In any decontamination strategy or preventive strategy, such as the pretreatment strategy in **Chapter 8**, all cationic sites will be occupied by the displacing ion, for example by ammonium ion. One qualification should be noted at this point- that the specific ion capacities refer to unit areas of the particles involved. A detailed study, given below, shows clearly that the binding potentials of these materials are proportional to the areas exposed. Smaller particles, having larger surface areas, have larger capacities. In consequence, the relative surface area of particles was determined, using BET methods and the number of available sites for binding caesium per unit area of exposed surface was determined. Consequently, in decontamination or preventive strategies, it will now be possible to assess the quantity of nuclides which can be bound, or the number of sites which need to be blocked or occupied.

5.2 Theoretical and Methodological Aspects

5.2.1 Ion Selective Electrodes

Ion Selective Electrodes (ISEs) are intrinsically thermodynamic devices, responding to activity changes in their selected ion. The electrode potential (E) of an ISE is given by the Nernst Equation, **eqn 5.1.**

$$E = E^{\circ} + \frac{RT}{z_i F} \ln a_i \tag{5.1}$$

where E° is the reference potential, a_i is the specific ion activity and z_i its ionic valency, including sign. Satisfactory corrections for activity coefficients may be obtained using the Davies equation, (an extended Debye Huckel equation) **eqn 5.2.** This equation is valid in media with ionic strengths less than 0.2M.

$$-\log\gamma = 0.5\left(\frac{\sqrt{I}}{(\sqrt{I}+1)} - 0.3I\right) \tag{5.2}$$

where I is the ionic strength.

Many ISEs obey the Nernst equation closely over a useful range of conditions but all are subject to errors caused by interfering ions or to specific limitations related to their functional chemistry. These limitations are well-documented and understood. A number of reliable electrodes are available and the commercial electrodes used in this research are for Ca^{2+}, Cl^{-}, K^{+}, Na^{+} (from Orion Research Inc., Boston, USA), the H^{+} glass electrode (from Russell Electrodes, Auchtermuchty, Scotland) and the Cs^{+} electrode which we ourselves have developed and tested, as described below. The lower operational ranges for these electrodes are typically at or close to 10^{-5}M for the selected ion. The exception is the H^{+} glass electrode which is viable in the pH range 1-12. For the newer ISE, the linearity of the Nernst response is good and the theoretical slope of 59.16 mV (59.16/2 mV for Ca^{2+}) is achieved to within 95%. At very low concentrations the slopes deviate increasingly and the electrode is subject to considerable error, which determines the lower limits of their use.

5.2.2 Caesium Ion Selective Electrode

The development of an accurate and reliable caesium selective electrode was central to this work, allowing caesium sorption onto building materials to be monitored and their caesium binding potentials assessed.

The use of a valinomycin-based ion selective electrode as a caesium ion sensing device was previously not considered worthwhile, due to its high selectivity for potassium ion [3].

However, if the sample solutions under investigation are free of potassium, it is be possible to use the valinomycin electrode as a caesium electrode. This caesium electrode was used to determine caesium binding sites on samples from which potassium had been removed by an extraction process, described in the next section.

Valinomycin based potassium ion selective electrodes are commercially available. The caesium ion electrode was prepared by immersing the valinomycin based Orion potassium selective electrode (model 93-19) in 0.25M caesium chloride for twelve hours, then transferring into a fresh 0.001M caesium chloride solution in which it was subsequently stored, when not in use. The electrode was ready for use as a caesium electrode after four hours. The internal electrolyte in these commercial electrodes is potassium chloride, but extensive leaching tests showed that there was no potassium leakage from the interior compartment of the electrode into test solutions. No further modification of the commercial electrode was therefore necessary. The reference electrode used in all studies was the Orion model 90-02 double junction reference electrode, with the outer chamber filled with 0.12M NaCl saturated with AgCl, since in this application there must be no contamination of test solution with potassium salts.

The electrode response to added aliquots of caesium ion was monitored by measuring the e.m.f. over a range of concentrations of CsCl at 25°C. The results of a typical titration of CsCl into water are shown in **Figure 5.1**. Linear response to the activity of caesium ions is observed within the concentration range 10^{-1} to 10^{-5}M CsCl. Analysis of the titration showed that the electrode had Nernstian behaviour (that is, a slope of 59.16 mV ± 5% per pCs unit). The electrode response time is short, with stable readings obtained within 10 seconds. This electrode was unaffected by changes in ionic strength up to IM in NaCl media and so can be used directly to determine concentrations, without the need for activity corrections.

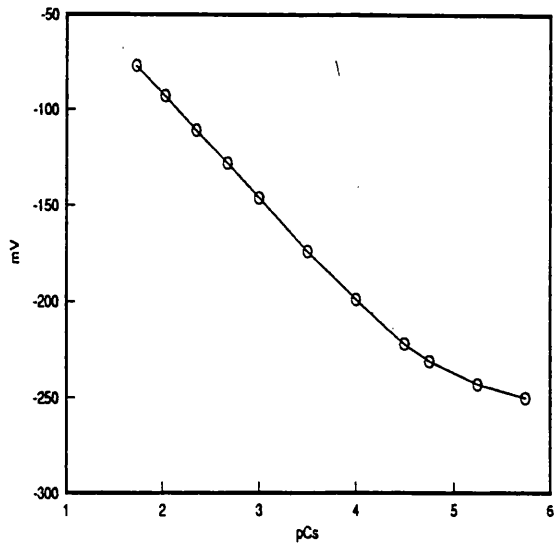

Figure 5.1 Electrode Potential of the Caesium Electrode / Reference Electrode Cell, against pCs for a Typical Calibration Experiment

All measurements using ion selective electrodes are subject to interferences caused by the presence of other cations, if present at high enough levels. The interference produced by a particular cation was determined by monitoring the caesium electrode response in solutions of known caesium concentration, with varying background levels of interfering ion. Interference was expressed in terms of a selectivity coefficient, K_M^{Cs}, indicating the selectivity the electrode shows for caesium over the interfering ion, M. The selectivity coefficients were evaluated for the following interfering cations,- Na^+, NH_4^+, K^+, H^+, Ca^{2+}. Results are presented in **Table 5.1**, along with the corresponding selectivity coefficients of other caesium ion selective electrodes. In all respects other than selectivity over potassium, only the bis crown ether based electrode [3] matches the overall performance of the valinomycin electrode. Furthermore, for the particular application to caesium sorption on urban materials, none of these electrodes would be suitable for use on unextracted samples due to interferences from potassium ions released by the material. A procedure for extraction of potassium would be necessary in all cases.

Table 5.1 Comparison of Selectivity Coefficients K_M^{Cs} for the Valinomycin based Caesium electrode with other Caesium Selective Electrodes

Electrode Type	K_{Na}^{Cs}	K_{NH4}^{Cs}	K_K^{Cs}	K_H^{Cs}	K_{Ca}^{Cs}
Valinomycin	1000	25	0.5	400	1000
Bis (crown ether) [3]	1100	100	12	-	-
TMC-crown formazane [4]	300	-	20	300	300
15-crown-5-PW ppt. [5]	3	-	2	-	1500
Zeolite molec. Sieve [6]	15	-	2	-	2000
Copper Hexacyanoferrate [7]	31	-	2	-	12
Ionic polymer [8]	2	-	1.2	1.4	6

No evidence of anion interference (Cl^-, OH^-) on the electrode response was observed. pH effects were monitored by calibrating the electrode in solutions of varying pH. No interference was observed in alkaline solution, while in solutions of increasing acidity there was increasing interference, due to the increase in hydrogen ion concentration.

The results demonstrate clearly that the valinomycin based caesium electrode is a first class, readily available caesium ion sensor, the only major restriction being that it cannot be used in the presence of potassium ion. Accordingly this electrode is used in the titration of samples from which potassium ion has been extracted. Thereafter, the sorption of caesium using the new caesium electrode or potassium using the original potassium electrode can be studied, employing automatic multi-electrode titration methods. In this way the relative sorption potentials of the two ions may be assessed, quickly and accurately.

5.2.3 Sample Preparation

All samples of building materials and clay minerals were wet ground in a M°Crone™ micronising mill for thirty minutes and analyzed in a particle sizer to determine particle size and size distribution. A mean particle size of 2-3μm was obtained in all cases, independent of the material being ground.

Samples were extracted, using a modified version of the technique of Scott and Reid [9], which replaced all exchangeable potassium ions with sodium ions. The ground sample was dispersed for four days in a solution 0.05M in sodium tetraphenylboron and 1M in NaCl.

The volume of solution was chosen such that there was approximately a five times excess of tetraphenylboron over the expected exchangeable potassium content in the sample. A precipitate of potassium tetraphenylboron was formed. An equivalent amount of acetone was added to the dispersion to dissolve the potassium tetraphenylboron precipitate. The mixture was then centrifuged, followed by successive washing and centrifuging with acetone/0.1M NaCl, 0.1M NaCl and finally, distilled water. Any potassium remaining in the mineral after extraction was effectively fixed - it could not be exchanged and so could not interfere with the caesium electrode, nor participate in ion exchange. Since the extraction procedure converts the materials to the sodium form, the sorbing cation will exchange exclusively with sodium cation. Selectivity coefficients K_{Na}^{M}, where M is the sorbing cation, were readily obtained. Using the "triangle" rule, K_{M2}^{M1} was obtained from measurements of K_{Na}^{M1} and K_{Na}^{M2}, where M1 and M2 are different cations.

A simplified method of conversion to the sodium form was established for rapid screening of the ion exchange properties of building materials. Samples were dispersed in a concentrated solution of NaCl (approximately 4M) for 24 hours, filtered and washed, redispersed in 1M NaCl for 24 hours, filtered, washed and air-dried. This method was found to be sufficient to convert the macrosites of the urban building materials studied to the sodium form. This simplified extraction method was efficient and produced samples which showed identical ion exchange properties to samples extracted with sodium tetraphenylboron. In future experiments only this simplified extraction method need be used.

5.2.4 Automatic Titration System

A fully automated system for performing titrations was developed at the Glasgow laboratory. This computer-controlled system enabled the user to perform a multi-ionic titration with a maximum of six syringes and to monitor the solution concentration of up to four different ions using ion-selective electrodes (ISEs). **Figure 5.2** shows schematically the connection between the central computer and the titration equipment on one hand and the output devices - VDU, plotter and printer - on the other. The electronic interfacing is achieved using the Biodata "Microlink"™ system.

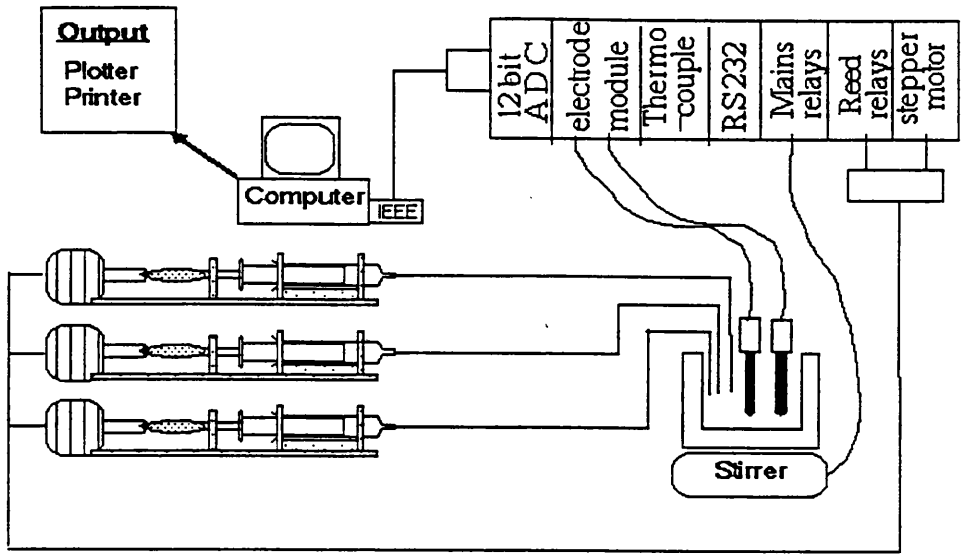

Figure 5.2 Schematic Representation of the Automatic Titration System

At the centre of the titration system lies the titration cell, which typically contained either a dispersion of the solid under study or a test solution. The titration cell consisted of a standard cylindrical polyethylene container within a 50 ml jacketed beaker, thermostatted at 25°C by recirculated water. In a titration these beakers were sealed with a perspex top which could hold up to four electrodes and the medical cannulae through which additions of reagents from the syringes were made. The cell was also fitted with a nitrogen inlet and outlet to maintain a carbon dioxide free system, in alkaline conditions. The syringes and electrodes used with this system were calibrated in independent experiments and their calibration parameters entered into controlling computer programmes. Micrometer syringes replaced conventional burettes in this system. The micrometers (Agla) were driven by stepper motors which advanced 1/200 rev per pulse received from the controller. The syringe outlet was via a medical cannula of internal diameter 0.03 cm, which was immersed in the test solution during titrations. The very fine capillary excluded the possibility of significant diffusion of reagent into the titrated solution/dispersion during use. Using this system, volume additions from a 10ml syringe could be made with an accuracy of $2 X10^{-5}$ ml. Ion concentrations in the titration cell were monitored by ion selective electrodes (ISE). By calculating the activity coefficient, the ion concentration in the cell can be determined. These calculations were performed automatically. Ion selective electrodes were calibrated before each titration over the concentration range and background conditions to be used in the titration itself. Standardised solutions were used for calibration.

The titration system was set up so that the user was able to choose operations from a menu. This facilitated choice and allowed the system to be used without further programming. In effect, the menu-driven options act as a high-level "language" for titration schemes. A full description of the system operation can be found in [2], [10].

Electrode calibrations were made by titrating the selected ion into a solvent or a solution of supporting electrolyte similar to that to be expected in the subsequent titration. These calibration techniques were conducted automatically by computer programmes similar to those used for the multi-electrode titrations of dispersions. Electrodes could be calibrated in pairs or individually, as required. During calibration, electrodes were automatically read and checked for stability after each addition of reagent and calibration displays were plotted. The software offered a curve fit option to obtain the best-fit curve, linear or second order polynomial least-squares curve fit through the data. Emf data (E) and p[ion] (actual) were compared with the estimates obtained by 1st and 2nd order curve fits. The percentage error produced from the 1st and 2nd order estimations was displayed. This is a direct estimate of the error on the ion activity (concentration) calculation, using the curve fit equations. All the ISEs employed in this work generally had errors less than 5% over the range of calibration. These results show that exceptional precision may be obtained using ISEs as concentration measuring devices under the most carefully controlled conditions. Glass pH electrode calibrations were performed using a range of buffers (pH range 1.5-12), made according to standard methods. The collected data were processed by a computer programme in the same manner as other ISE calibration data.

As previously constituted, the titration may be performed with up to six titrant solutions and a maximum of four electrodes can be used simultaneously. Prior to performing an automatic titration, the user was invited to define the reagents, concentrations and other vital statistics related to the dispersion and reagents, the ISE calibration data and a command format, in which the manner and range of the titration were defined. Once all the parameters were entered, the titration ran automatically, following exactly the options selected by the user. A range of screen displays are available to the user during the course of the titration, which are automatically updated as the titration proceeds. The selected display options may be altered at any time during the titration. The operator was therefore free to assess all aspects of the titration and computed results at all times during the experiment.

As described above, the automatic titration system allows the user to control all titration parameters, the manner and range of the titration and the monitor display during the course of the titration. The computer not only performs the experiment but also collects the raw (emf) data from each of the electrodes and records the volumes and concentrations of reagents. Data on ion sorption and ion release, pH and all other vital experimental data are collected, calculated and displayed as the titration proceeds. This flexibility of system usage enhances greatly the range of applications of the system.

For the dispersions, titrations were made over predetermined ranges of pH or pX (X - selected ion of the ISE) using acids, bases or salts as required. The major difference between a calibration titration and that of a dispersion titration is that with the dispersion, the electrode potentials were used to calculate the concentrations of the selected ions free in solution at each stage of the titration. Once these concentrations were known with confidence, it was a simple matter to calculate, by the principles of mass balance, the uptake or release of ions by the sample being titrated. These principles have been widely published in a series of papers, specifically on the ion exchange sorption of microcrystalline oxides **[11-15]**. After each addition of reagent, the dispersion was stirred for a specified period (typically 2 minutes), after which electrode reading commenced, each electrode being read in turn. The criteria for electrode stability (standard deviation, number of readings taken, gap between readings) were entirely at the control of the operator. Once the electrode was stable to within its predetermined tolerance (limits of tolerance having been inputted by the user), the reading was accepted. If one or more electrodes did not satisfy the predetermined criteria for its own stability after a set period (typically 15 minutes), a time-out bell was sounded and the titration was allowed to proceed. Unstable electrode data points were marked in the printouts.

In the particular application of the screening of the ion exchange properties of a given building material, the titration procedure would typically proceed as follows. A known weight of sample (0.5-1.5g), pretreated as described previously (i.e. in the sodium form), was dispersed for 24 hours in distilled water. As uptake is calculated by mass balance , it was generally found to be necessary to use larger weights if the sample has a small ion exchange capacity, in order to obtain precise results. The samples were then titrated with a standard solution of caesium chloride and the concentrations of caesium, sodium and hydrogen monitored using ISEs. Titrations proceeded until a plateau of Cs sorption was reached. From the titration the caesium uptake profile, cation exchange capacity, caesium distribution coefficients and Cs-Na selectivity coefficients were readily obtained, as described below.

By titrating with KCl, information on potassium sorption can be obtained. Using equivalent sets of data, selectivity data for Cs-K can be calculated, using the triangle rule.
With the titration system it is possible to obtain a wide range of ion exchange data, such as pH effects or the possibility of participation in the exchange process of other ions, such as calcium or chloride. This study concentrates mainly on caesium and potassium sorption onto samples in the sodium form. The flexibility of the system is of course one of the major advantages, together with the speed at which results may be obtained.

5.2.5 Processing of Data

Although the titration results are available continuously during the experiment, detailed analysis of the titration is printed out in tabular form by selecting the "Process Data" option from the main menu. The following information is available on printout:- Titration information - reagents, sample weights etc.; raw data - ISE readings (millivolts), reagent volumes added; concentrations, uptakes and distribution coefficients for each ion monitored; selectivity coefficients K_B^A, where A and B are exchanging ions; activity coefficients and ionic strength of solution; a significance factor S.F. which gives an estimate of the significance of the measured uptakes; probable uncertainties of uptake, based on electrode measurement error levels. The calculation of these parameters is discussed below.
Results are also presented graphically as X-Y plots. The user can choose from a number of ranges to plot. It is also possible to set measurement error margins and to view the resultant error bars produced by the set measurement error. As the ISEs used in this work consistently produced measurement errors of less than 5% on estimated concentrations in calibration and test procedures, the error margin was assumed to be a maximum of 5%.

The uptake or release of ions from an ion exchanger (ie. the clay mineral or building material under investigation) can be determined experimentally by considering solution mass balance. The units of uptake are expressed as milliequivalents (mmol) per gramme of exchanger. It is calculated for a given ion by the expression:-

$$X_{(uptake)} = \frac{mmoliinitally + mmoliadded - mmoliobserved}{weight\,of\,sample\,(exchanger)} \qquad (5.3)$$

Where i(initial) and i(observed) are measured by ISE and i(added) is a known quantity (standardised solutions used in titrations).

This means that the ionic uptake is the difference between the amount of ion known to be the whole dispersion system and the amount measured in the liquid phase. Uptake of ions by the exchanger is expressed as positive uptake and release of ions as negative uptake.

For all the substances examined, the cation uptake profile showed an increasing amount of cation sorbed as the titration proceeded, reaching a plateau beyond which there was no further uptake. The overall cation exchange capacity of the materials under investigation was taken to be equal to the plateau level of cation uptake (in mmol/g). For all samples, CECs were calculated using both caesium and potassium as the index cation.

Distribution coefficients for a given ion were calculated by dividing the ion uptake (per gram of sorbant) by the ion concentration in solution, giving a coefficient in units of litres/kg. This calculation was performed automatically during the titration.

Since the urban building materials and clay minerals used in this study are in the sodium form, the ion exchange process taking place is between sodium and the sorbing cation (usually caesium or potassium). Sodium is released by the exchanger as caesium or potassium is sorbed, preserving electroneutrality.

Selectivity coefficients K_B^A for the ion exchange process involving two ions (designated A and B) were calculated using the equation -

$$K_B^A = \frac{Z_A . S_B}{Z_B . S_A} \tag{5.6}$$

where Z is the equivalent fraction of the ion in the solid phase and S is the ion concentration in the aqueous phase. From the data obtained by titration, K_{Na}^{Cs} and K_{Na}^{K} were calculated using the above equation and, subsequently, K_K^{Cs} values were calculated using the triangle rule. As the error on K becomes large at both low and high loadings of the sorbing cation (i.e. when Z_A is in the ranges $0<Z_A<0.15$ and $0.75<Z_A< 1.0$), selectivity coefficients are recorded for the range $0.15<Z_A<0.75$.

5.3 Verification of Methodology using Well-Characterised Clay Minerals

Since the automated titrimetric technique is entirely new, the credibility of the method was established by titrating some well-characterised clay minerals - illite, montmorillonite and kaolinite - for which independent comparisons with literature data and the measurements of the Leuven Group are readily available. Using this new technique, the mechanism of

caesium sorption was established as ion exchange and the cation exchange capacities, ion exchange selectivity coefficients and distribution coefficients obtained were compared with those reported in the literature.

The hydrous mica, illite, is a widely distributed clay mineral commonly found in sedimentary rock. It has a non-expanding layer structure, with the interlayer charge balanced by alkali ions co-ordinated between the 2:1 layers. In this study, Fithian illite (Ward's Science Establishment cat.no.35) was used . Kaolinite , a member of the kaolin group, is a silicate mineral with uncharged 1:1 layers. Montmorillonite is a member of the smectite group, with charged 2:1 layers and interlayer cations. Beidellite montmorillonite (Ward's Science Establishment cat.no.23) from Arizona and Georgian kaolinite (Ward's Science Establishment cat.no.4) were used in this work.
The reasons for choosing illite as the main standard reference mineral were twofold. Firstly, data on the ion exchange properties of illite are quoted extensively in previously published literature. Additionally, the importance of micaceous minerals such as illite in the sorption of caesium is well documented **[16], [17].**

All minerals were converted to the sodium form, as described above, before use. Samples were titrated with both caesium chloride and potassium chloride. In each case the initial sodium concentration was 0.001M. The following information, for each mineral, was obtained :-
Cation exchange capacities (using both Cs and K as index (sorbing) cations)
Direct verification of the stoichiometry of the ion exchange process by monitoring sodium release from the exchanger simultaneously with cation sorption
Selectivity coefficients (K_{Na}^{Cs}, K_{Na}^{K}, K_{K}^{Cs})
Distribution coefficients for Cs and K

The results are presented below.

5.3.1 Cation Exchange Capacities

Cation exchange capacities (CECs) for illite have been quoted extensively.

Table 5.2 Cation Exchange Capacities for Illite

Ref No.	CEC (mmol/g)	Illite type
[16]	0.23	Morris illite
[18]	0.28	Fithian illite
[19]	0.28	illite 35
[20]	0.29	illite 35
[21]	0.24	-
[22]	0.25	illite 35
[23]	0.20	illite 35
Current study	0.27	illite 35

Figure 5.3 shows cation uptake, measured by the caesium selective electrode, with addition of cation (caesium and potassium) to the illite dispersion. Caesium sorption increased to a plateau of 0.27 mmol/g. This maximum is the cation exchange capacity for this illite sample and is in good agreement with the literature values, **Table 5.2.**. The lower levels of potassium uptake is indicative of the lower selectivity of potassium relative to caesium. This is discussed in detail below.

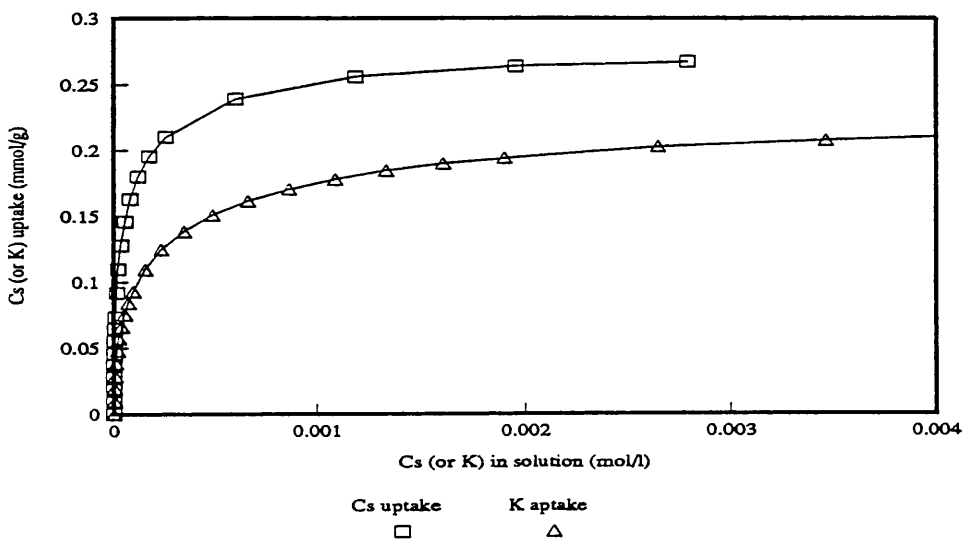

Figure 5.3 Caesium and Potassium Sorption on Illite.

Similarly, caesium uptakes were determined for kaolinite and montmorillonite. Results are summarised in **Table 5.3** and **Figures 5.4, 5.5.**

Table 5.3 Quoted Cation Exchange Capacities for Kaolinite and Montmorillonite

Mineral	Quoted Range (mmol/g)	Present Study (mmol/g)	Ref. No.
Kaolinite	0.01- 0.09	.014	[16],[21],[24], [25],[26]
Beidellite-Montmorillonite	0.50- 0.70	0.58	[18],[27]

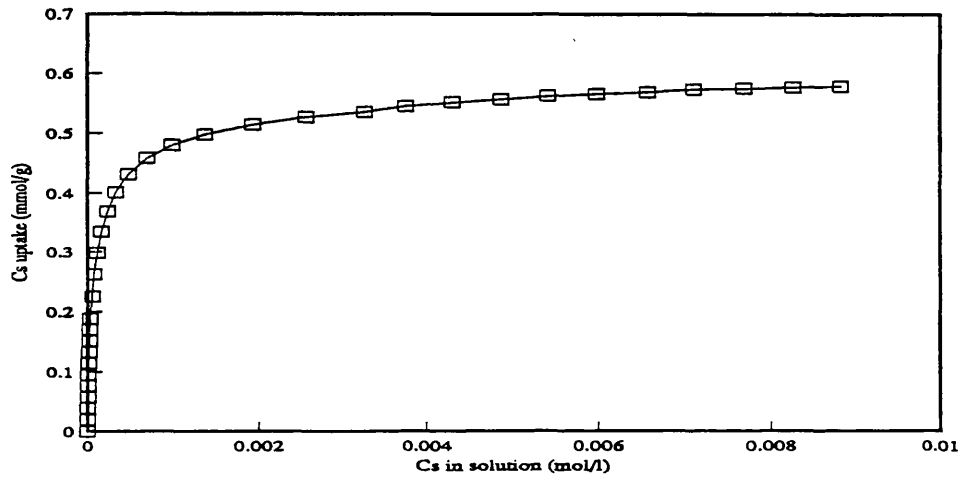

Figure 5.4 Caesium Sorption on Montmorillonite

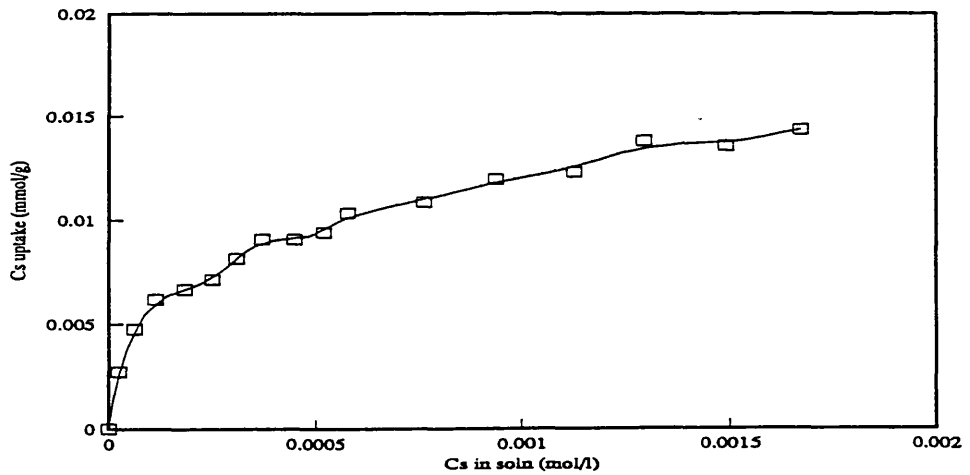

Figure 5.5 Caesium Sorption on Kaolinite

5.3.2 Verification of Ion Exchange Process

After sample pre-treatment, the material under investigation was in the sodium form and sodium was the only exchangeable cation. In this case equivalent release of sodium is

expected when another cation is sorbed. In **Figure 5.6** the symmetry of the two curves for caesium uptake and sodium release confirms the stoichiometry of the ion exchange process on illite and that the anionic sites occupied by sodium ion are the only ones involved. No additional sites are available to caesium ion. Similar results were obtained on the other minerals investigated.

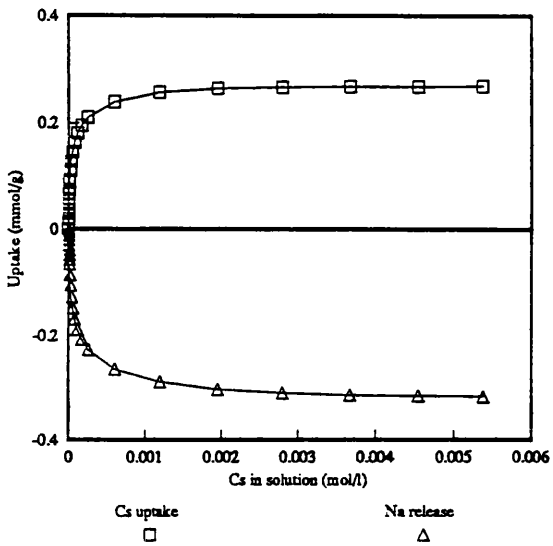

Figure 5.6 Simultaneous Sodium Release with Caesium Uptake on Illite

5.3.3 Selectivity Coefficients

From the isotherms the selectivity coefficients for Cs-Na and K-Na were calculated as described previously. Selectivity coefficients for Cs-K were calculated, using the triangle rule. In **Figure 5.7** these selectivity coefficients are shown as a function of the fractional loading of the sorbing cation.

In **Table 5.4** the average selectivity coefficients for illite obtained in this study agree well with published values over the same fractional loading range.

The same general pattern of selectivity is observed for montmorillonite, **Figure 5.8.**

Table 5.4 Selectivities on Illite over Fractional Loading Range 0.2-0.8

Ref No.	$\ln K_{Na}^{Cs}$	$\ln K_{Na}^{K}$	$\ln K_{K}^{Cs}$
[16]	-	-	1.6
[28]	4		1.4
Present Study	4.5-4.2	3.6-3.0	1.2-0.7

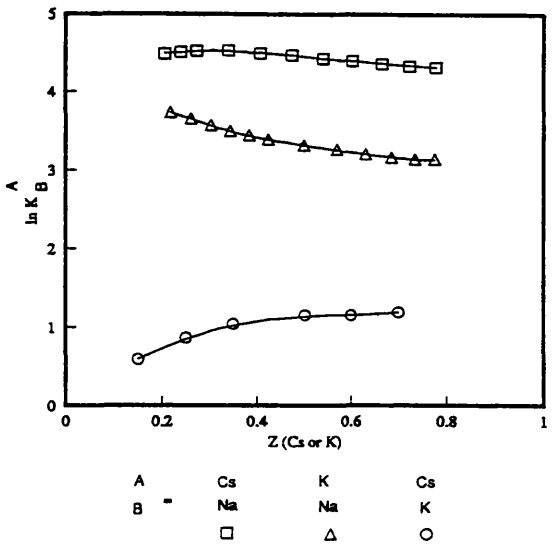

Figure 5.7 lnK for Cs-Na, K-Na and Cs-K Exchanges on Illite plotted against Fractional Occupancy of Sorbing Cation

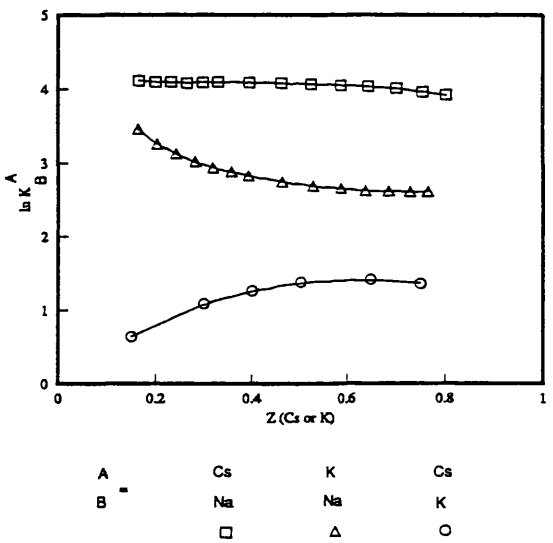

Figure 5.8 lnK for Cs-Na, K-Na and Cs-K Exchanges on Montmorillonite plotted against Fractional Occupancy of Sorbing Cation

5.3.4 Distribution Coefficients

Distribution coefficients are commonly measured to assess ion binding in environmental and nuclear studies. They may be obtained readily from titration curves.

Figures 5.9 and **5.10** plot distribution coefficients for caesium and potassium on sodium illite and sodium montmorillonite respectively, with initial equilibrium solution sodium concentration 0.001M. Again, these results are in agreement with published data **[19]**.

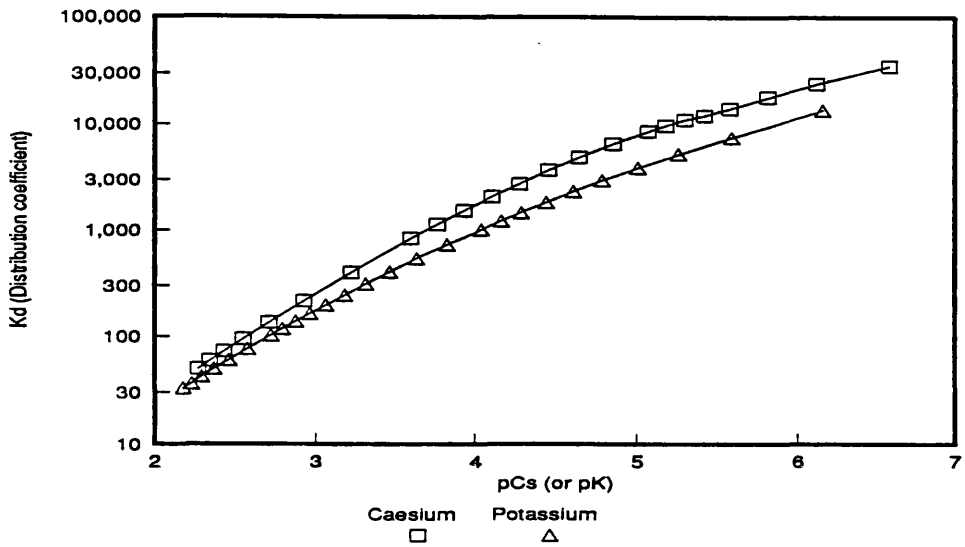

Figure 5.9 Caesium and Potassium Distribution Coefficients on Illite (Initial Sodium Concentration 0.001M)

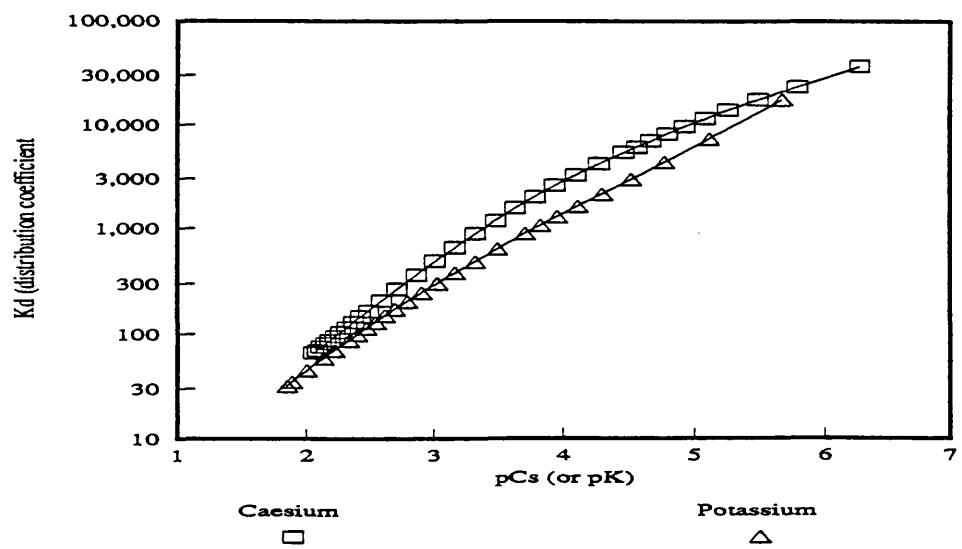

Figure 5.10 Caesium and Potassium Distribution Coefficients on Montmorillonite (Initial Sodium Concentration 0.001M)

5.3.5 Conclusions

The good agreement between the results obtained above and published results from a variety of sources validates the Glasgow titration methodology and the results obtained from its application. It also shows that the pretreatment of samples does not alter the ion exchange properties of the material examined. In the following section the methodology is applied to the examination of caesium sorption on urban building materials.

5.4 Caesium Binding Potentials of Urban Surfaces

5.4.1 Selection of Building Materials

An inventory of construction materials in the urban environment of the United Kingdom was compiled as part of the current programme. A representative selection of materials and their constituents was made for the purpose of screening the sorption and ion exchange characteristics of these materials. A number of materials from other parts of Europe were also examined, including a sample of clay rooftile from Leuven (which had been studied extensively by the Leuven laboratory **[16]**, **[17]**) and a clay tile from Gävle in Sweden, supplied by the Risø laboratory. This tile was of particular interest as significant Chernobyl fallout has been recorded at Gävle. To a large degree the methodology of uptake and preventive sorption of surfactants have concentrated on this symbolic sample of Chernobyl contaminated material.

Table 5.5 Codes for Materials

Material		Type		Manufacturer* (or Area)**	
A	Aggregate	-	-	Tar	Tarmac*
"	"	"	"	Til	Tilcon*
B	Brick	-	-	BB	Butterley Brick*
"	"	"	"	LB	London Brick*
"	"	"	"	SB	Scottish Brick*
P	Pigment	-	-	R	Redland*
S	Sandstone	-	-	-	-
T	Tile	Cl	Clay	Ri	Risø**
"	"	"	"	R	Rosemary**
"	"	"	"	L	Leuven**
"	"	"	"	B	Bavarian**
"	"	Co	Concrete	M	Marley*
"	"	"	"	R	Redland*
"	"	"	"	B	Bavarian**
"	"	S	Slate	-	-

* Manufacturers' full name and address are given in **Section 5.5**

** Areas are given for materials which were obtained from urban environments

Sorption data on other urban materials, including street dust, are presented in **Chapter 6**. All materials obtained for this research have been allocated unique codes. These codes contain, where appropriate, Material/Type/Manufacturer or Area/Number. The codes for the materials used in this section are described in **Table 5.5**. All samples will subsequently be referred to by their codes. **Table 5.6** lists the building materials examined, together with suppliers and source area.

Table 5.6 Building Materials Selected for Examination in this Study

Code	Material	Source Area	Supplier	Status	Source Material
ATil1	Aggregate (road)		Tilcon	Ex works	Greywacke
BBB1	Facing Brick	Glasgow	Butterley	Ex works	Carb. shale
BBB6	Facing Brick	London	Butterley	Ex works	Weald clay
BLB1	Fletton Brick	London	L.B.C.	Ex works	Oxford clay
BRi1	Brick	Gâvle		Field	Clay
BSB1	Facing Brick	Scotland	S.B.C.	Ex works	Carb. clay
PR1	Pigment (concrete)		Redland	Ex works	iron oxide
PTil1	Pigment (mortar)		Tilcon	Ex works	
TClB1	Tile	Bavaria		Field	Clay
TClL1	Tile	Leuven		Field	Clay
TClR1	Tile	Glasgow		Field	Clay
TClRi1	Tile	Gâvle		Field	Clay
TCoB	Tile	Bavaria		Field	Concrete
TCoM1	Tile	Mendip	Marley	Ex works	Concrete
TCoR1	Tile	Stirling	Redland	Ex works	Concrete
TS1	Tile	Stirling		Field	Slate
S1	Sandstone	Stirling		Field	Sandstone

All samples were ground to 2μ and extracted, as previously described. **Table 5.7** lists the ionic composition (in mmol/l) of aqueous extracts (0.5g of sample dispersed in 25 ml distilled water) of the building materials under investigation, prior to potassium extraction.

Table 5.7 Ionic Composition (in mmol/l) of Aqueous Extracts of Building Materials

Code *	L/S Ratio	pH	Na	K	Ca	Cl
BBB1	50	7.55	0.22	0.10	0.20	0.05
BBB6	50	7.92	0.005	0.09	1.04	0.16
BLB1	50	8.37	0.005	0.06	6.47	0.18
BRi1	50	7.98	0.64	0.37	8.88	0.04
BSB1	50	8.62	0.17	0.12	1.45	0.04
PR1	50	8.67	0.43	0.02	0.12	0.11
TClB1	50	7.80	0.20	0.12	1.11	0.06
TClL1	50	6.74	0.04	0.06	0.01	
TClR1	50	8.34	0.01	0.02	0.28	0.06
TClRi1	50	8.06	0.78	0.21	0.07	0.10
TCoB	50	11.10	0.39	0.76	5.14	0.12
TCoM1	50	11.55	0.02	0.05	7.60	0.06
TCoR1	50	11.16	0.04	0.20	6.20	0.40
TS1	50	7.19	0.04	0.14	0.01	

* See table 5.6 for explanation of code

5.4.2 Ion Exchange Processes

By the extraction process, all exchangeable ions are replaced by sodium ion. An equivalent release of sodium is expected when caesium is sorbed, as observed in the clay mineral titrations. In all titrations, in addition to the monitoring of caesium ion concentration, the concentration of sodium in the equilibrium solution was monitored, using a sodium electrode. It was found that there was a equivalent release of sodium (in units of millimoles per gram of exchanger) for cation uptake (caesium or potassium), within the limits of experimental error, in most cases (the exceptions being cementitious products with high integral calcium content). **Figure 5.11** is a typical example of the observed ion exchange process, on Leuven clay tile TClL1. Selectivity coefficients for these ions were consequently readily obtained, as described previously.

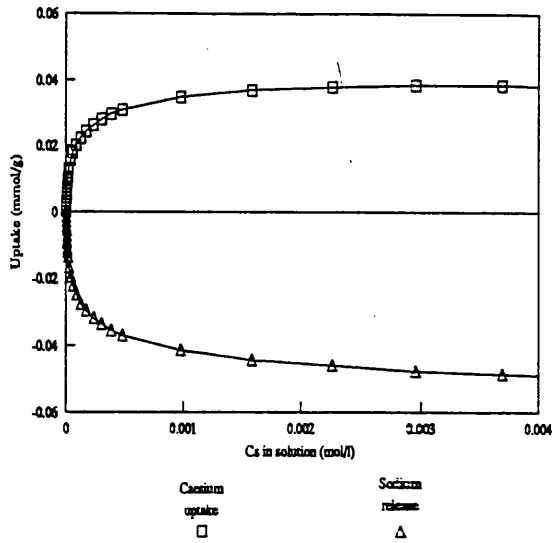

Figure 5.11 Simultaneous Release of Sodium with Caesium Uptake on Leuven Clay Tile TClL1

5.4.3 Surface Area and Ion Exchange

The relationship between sorptive capacity and surface area was examined by measuring caesium uptake on Leuven clay tile (TClL1) samples with three different particle sizes. The surface area of each sample was determined by nitrogen sorption (BET) (**Table 5.8**). The low surface areas for the 250μm and 200μm fractions (1,89 and 4.43 m^2/g respectively) are at the sensitivity limit for the nitrogen BET method - consequently the precision of these estimates is low. The surface area of the 2μ sample is, however, most reliable. Caesium uptake on each sample was determined by titration and the results are shown in **Figure 5.12.**

Table 5.8 shows that caesium capacity is directly proportional to the surface area of these samples and, within the credibility limits for surface area determination, the caesium binding capacity per unit area is constant. Using the surface area calculated on the 2-3 μm sample, the caesium exchange capacity per unit area is 2.94 $\mu mol/m^2$ (cf. results from Leuven laboratory for Cs sorption on same tile- app. 3.16 $\mu mol/m^2$ **[16]**). The surface area per anionic exchange site was calculated as 56.5 sq. $Å^2$, giving a site to site distance of 7Å.

The direct proportionality between surface area and sorption enables predictions to be made on sorption and capacities on whole samples of building materials in the environment, if the surface areas of the laboratory sample and the whole tile or brick are known.

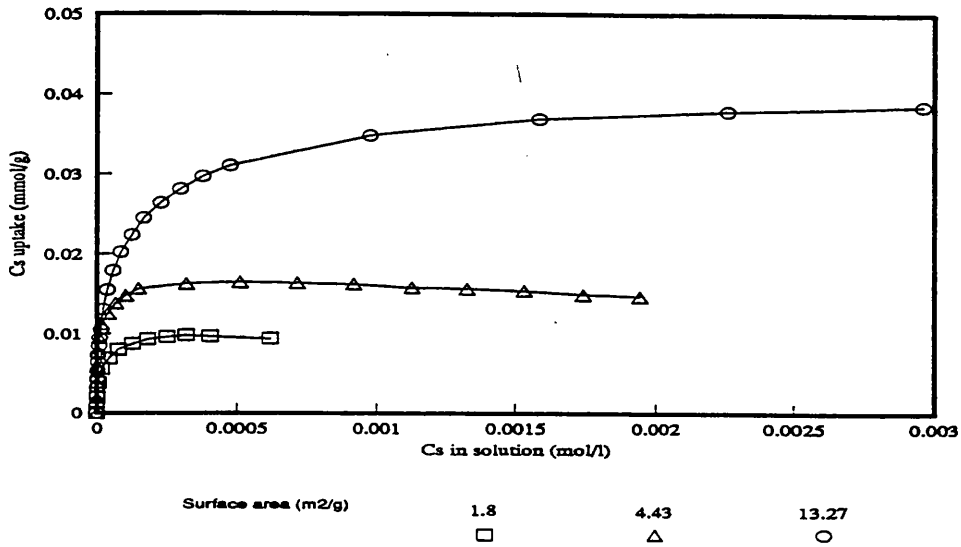

Figure 5.12 Caesium Sorption on Samples of Leuven Clay Tile TCIL1 at Varying Surface Area

Table 5.8 Leuven Clay Tile TCIL1- Capacities per Unit Area

Particle size µm	Surface Area m^2/g	Cs capacity mmol/g	Cs capacity $\mu mol/m^2$
2-3	13.27	0.039	2.94
<200	4.43	0.016	3.61
<250	1.89	0.009	4.76

5.4.4 Cation Exchange Capacities

Cation exchange capacities (CEC) of a range of building materials were determined using the titrimetric method as described previously, with caesium as the sorbing cation. All urban materials examined in this study bind caesium from aqueous solution by ion exchange. **Table 5.9** presents the measured cation exchange capacities for samples with particle size of 2µm. At this particle size, BET surface areas were $10m^2/g$ to $15m^2/g$ for all materials. The direct proportionality between surface area and sorptive capacity, as shown previously, enabled the calculation of the exchange capacity per unit area. This value is equivalent to the superficial surface capacities of urban materials, as they occur in the environment. Although present evidence is that caesium contamination is limited to the outer layers, any subsequent decontamination may make available the underlying sites, which can resorb caesium.

The total exchange capacity for a 1cm deep section of Gävle rooftile (TClRi1) has been calculated as 47 mmol per square metre of geometric surface exposed to the environment, giving a capacity increase of the order of 30 000 for a 1cm penetration. There is therefore a large reservoir of binding sites underlying the superficial surface.

Table 5.9 Cation Exchange Capacities of a Range of Urban Building Materials- 0.2μ Particle Size in All Cases

Code *	C.E.C. (mmol/g)	Capacity per unit area (μmol/m^2)
ATil1	0.075	6.25
BBB1	0.010	0.83
BBB6	0.010	0.83
BLB1	0.014	1.17
BRi1	0.023	1.92
BSB1	0.011	0.92
PR1	0.006	0.50
PTil1	0.006	0.50
TClB1	0.021	1.75
TClL1	0.038	2.94
TClR1	0.008	0.67
TClRi1	0.018	1.50
TCoB	0.025	2.08
TCoM1	0.042	3.50
TCoR1	0.066	5.50
TS1	0.035	2.92
S1	0.025	2.08

* See table 5.6 for explanation of code

Figures 5.13 to **5.15** are examples of plots of caesium uptake on a variety of materials against caesium equilibrium concentration in solution. Uptake increases with increasing equilibrium concentration until the cation exchange capacity is reached.

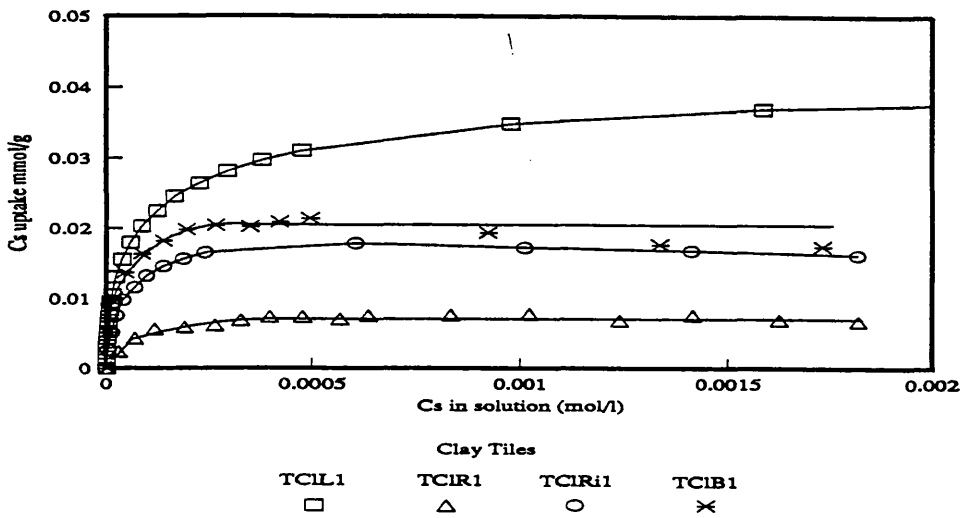

Figure 5.13 Caesium Uptake on Clay Tiles (Field) from Leuven (TClL1), Gävle (TClRi1), Glasgow (TClR1) and Bavaria (TClB1)

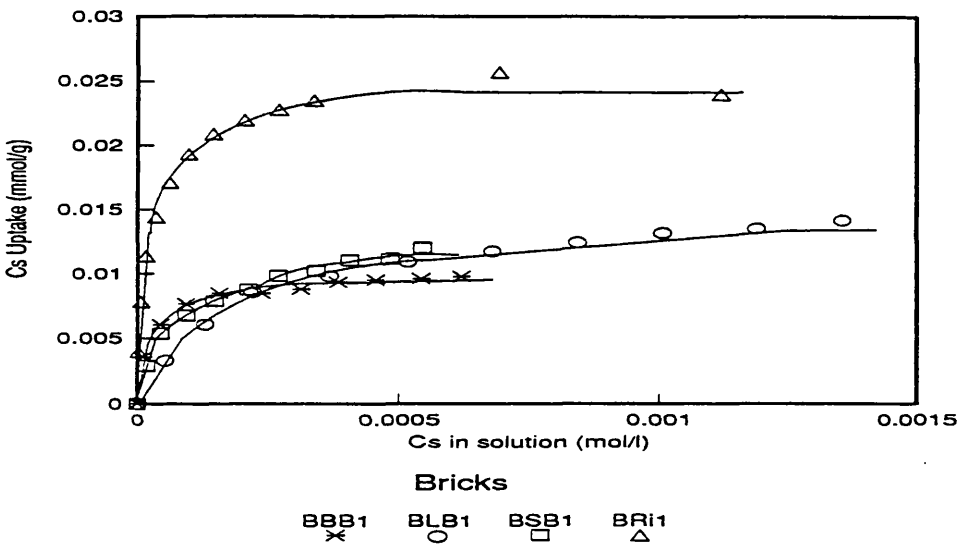

Figure 5.14 Caesium Uptake on Brick Samples (Ex-works) supplied by Butterley Brick (BBB1), Scottish Brick (BSB1), London Brick (BLB1) and Field sample from Gävle (BRi1)

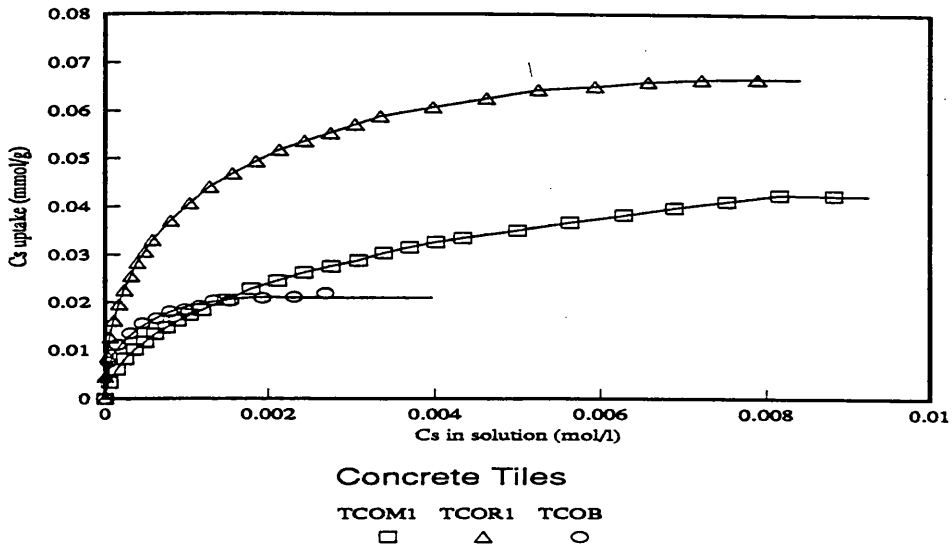

Figure 5.15 Caesium Uptake on Concrete Tiles Supplied by Marley (TCoM1), Redland (TCoR1) (both Ex-works) and Field sample from Bavaria (TCoB)

The magnitude of the sorption capacities for caesium observed on these building materials is considerably less than those of the clay minerals examined by the same methodology. The capacities of the materials examined are identical to those in parallel titrations with potassium as the sorbing cation. This shows that caesium occupies the same sites as the natural exchangeable cations (K^+, Ca^{2+}, Na^+). Caesium sorption on the macrosites of these materials is largely reversible, as evidenced by redispersion in 1.7M NaCl. In all cases, caesium was desorbed, the cation selectivity coefficient (see below) determining the degree of conversion back to the sodium form. For the highly active sites, different selectivity coefficients are applicable- these are studied in **Chapter 6.**

5.4.5 Cation Selectivities

Ion selectivity coefficients K_{Na}^{Cs} and K_{Na}^{K} for the building materials were calculated directly from titration data for caesium and potassium titrations respectively. K_{K}^{Cs} can be estimated from K_{Na}^{Cs} and K_{Na}^{K}, using the triangle rule. For the samples which did not show simple exchange with sodium, K_{K}^{Cs} were estimated from the ratios of distribution coefficients for Cs and K sorption respectively, but with less confidence. In all cases the background sodium concentration was approximately 10^{-3}M. **Table 5.10** lists the selectivity coefficients for these exchanges on the sample materials over the fractional loading range $0.15<Z^A<0.75$, where Z^A is the fractional occupancy of the sorbing cation, A.

The general order of selectivity is Cs>K>Na. The magnitude of selectivity varies considerably, for example the selectivity for caesium over sodium ranges from 1.3 times on sandstone (S1) to 55 times on aggregate (ATil1).

Table 5.10 Cation Selectivity Coefficients for a Range of Urban Building Materials

Code *	K_{Na}^{Cs}	K_{Na}^{K}	K_{K}^{Cs}
ATil1	55		
BBB1	25	10	2.5
BBB6			
BLB1	8	7	1.1
BRi1	22	18	1.2
BSB1	8	4	2
TClB1	26		
TClL1	35	25	1.4
TClR1	25	25	1
TClRi1	37	16	2
TCoB	5	1	5
TCoM1	-	-	0.69
TCoR1	-	-	2.5
TS1	30	25	1.5
S1	1.3	1	1.3

* See table 5.6 for explanation of code

5.4.6 Distribution Coefficients

Distribution coefficients (K_d) for caesium are readily obtained from titration data, as was observed in clay mineral studies. **Figures 5.16** to **5.18** present caesium K_d values, over a range of aqueous caesium concentrations, for various building materials, all in the sodium form and with a particle size of 2μm.

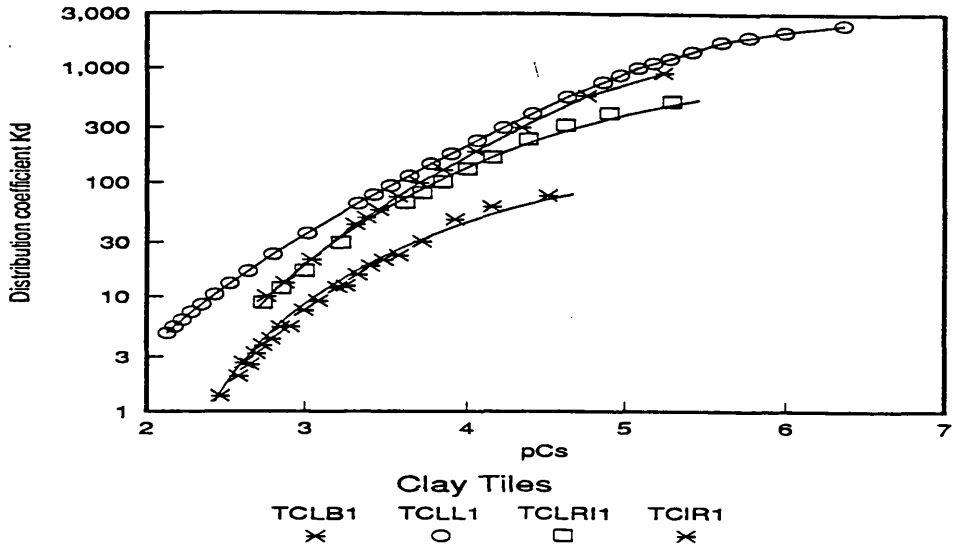

Figure 5.16 Distribution Coefficients for Caesium on Clay Tiles (Field) from Bavaria (TCLB1), Leuven (TCIL1), Gävle (TCIRi1) and Glasgow (TCIR1)

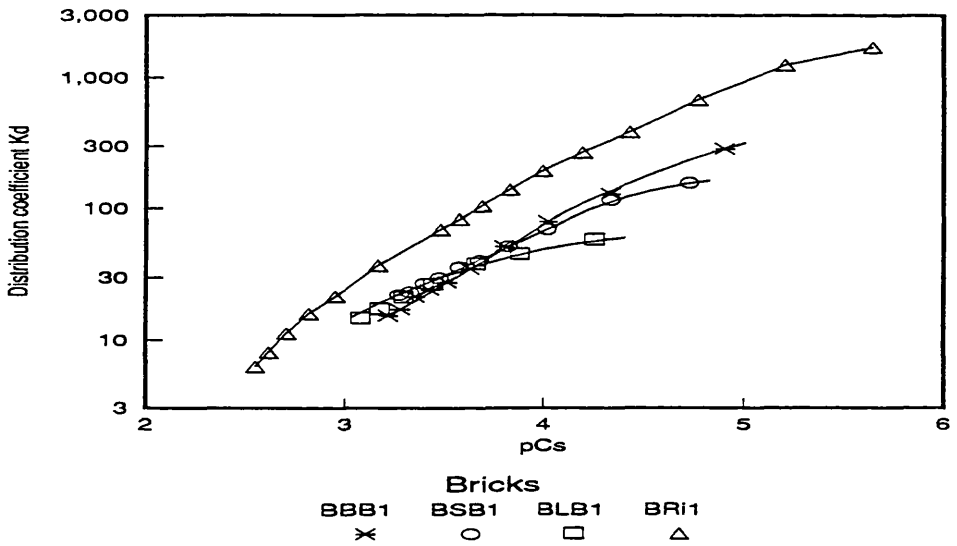

Figure 5.17 Distribution Coefficients for Caesium on Brick Samples supplied by Butterley Brick (BBB1), Scottish Brick (BSB1) and London Brick (BLB1) (Ex-works) and Field sample from Gävle (BRi1)

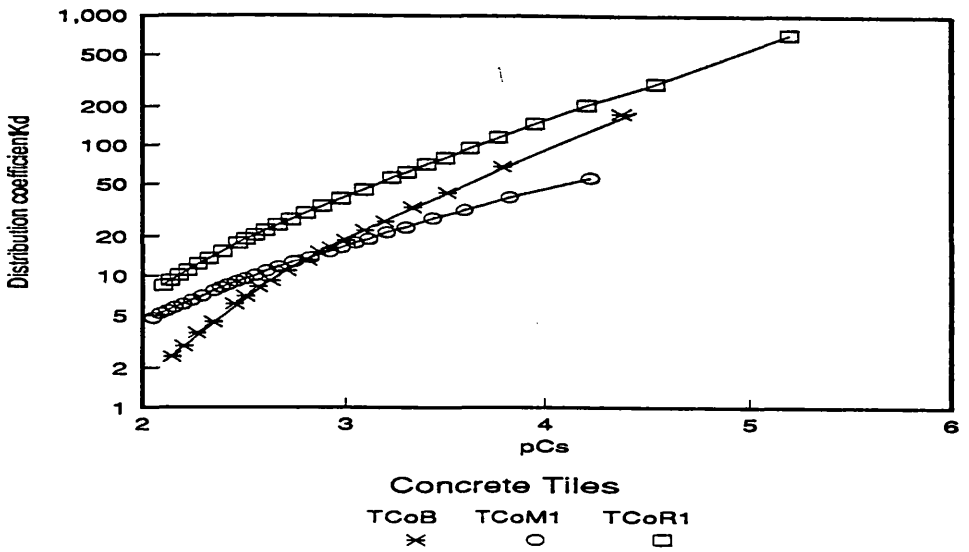

Figure 5.18 Distribution Coefficients for Caesium on Concrete Tiles Supplied by Marley (TCoM1), Redland (TCoR1) (both Ex-works) and Field sample from Bavaria (TCoB)

5.5 Conclusions

All materials examined in this study demonstrated capacity for sorbing caesium ions from aqueous solution. The mechanism of sorption was shown to be ion exchange by the observation of simultaneous release of sodium and sorption of caesium in all cases, apart from two concrete tile samples, where calcium, rather than sodium, was most probably the dominant exchanging cation.

CECs of the studied building materials were considerably lower than those of clay minerals, such as illite and montmorillonite. The observed cation exchange capacities of the urban materials (2μ fractions) varied over a range from 0.008 mmol/g (weathered clay rooftile, Glasgow) to 0.075 (ex-works road surfacing aggregate). The caesium capacities were identical to those in parallel titrations with potassium as the sorbing cation. This showed that sorbed caesium occupies the same sites as the natural exchangeable cations (K^+, Ca^{2+}, Na^+). Cation exchange capacity was shown to be directly proportional to surface area by determining caesium sorption on a clay tile at different BET surface areas. Cation exchange capacities per unit area were calculated, enabling the determination of the caesium binding capacity of the superficial surface area of building materials as they occur in the environment. The total exchange capacity of a 1cm deep section of Gävle clay rooftile was calculated to be around 30 000 times greater than that of the superficial surface exposed to the environment.

The relative selectivities of the exchange sites on building materials were observed for caesium, sodium and potassium ions. The order of selectivity observed was generally Cs>K>Na, with the magnitude of selectivity varying according to the nature of the material.

The ion exchange sites (the macrosites) examined in this study were seen to be reversible with respect to caesium sorption. The final destination of sorbed caesium is the high affinity sites (HAS), as determined by the Leuven laboratory. However, the much larger number of macrosites compared to the HAS means that initial sorption is statistically more probable on the macrosites. It is likely therefore that the macrosites act as intermediate binding sites, intercepting caesium from rainwater initially. The sorbed caesium can then find its way to the high affinity sites, thus being effectively irreversibly bound. A possible method of preventing or reducing caesium sorption on urban building materials, therefore, is to block sorption on the intermediate binding sites (the macrosites), thus making it statistically less likely that the caesium will find the high affinity sites. This approach is explored in **Chapter 8.**

5.6 References

[1] Paterson R. and Gallagher S., in preparation

[2] Paterson R. and Gallagher S., in preparation

[3] Kimura, K., Tamura, H. and Shono, T., (1979), J. Electroanal. Chem. Interfacial Electrochem., **105(2)**, 335-340

[4] Abdulrahman S. Attiyat et al., (1988), Microchem J., **37**, 122-128

[5] Wang, Da and Shih, Jeng Shang,(1985), Analyst, **110**, 635-638

[6] Johansson, G. and Risinger, L., (1980), Anal. Chim. Acta, **119**, 25-32

[7] Ajay K. Jain, Raj P. Singh and Chand Bala, (1984), J. Chem. Tech. Biotechnol., **34A,** 363-366

[8] Martin, C.R. and Freiser, H., (1981), Anal. Chem., **53**, 904-905

[9] Scott, A.D. and Reed, M.G., (1962), Soil Science of America Proceedings, **26**, 45-48

[10] Paterson R., Improvement of practical countermeasures against nuclear contamination

in the urban environment, Interim Report No. 2, for period Feb 1 1988 to Oct 31 1988, Contract No. B16-0270.UK(H)

[11] Paterson R. and Rahman H., (1983), Journal of Colloid and Interface Science **94** 60-69

[12] Paterson R. and Rahman H., (1984), Journal of Colloid and Interface Science **97** 423-427

[13] Paterson R. and Rahman H., (1984), Journal of Colloid and Interface Science **98** 494-499

[14] Paterson R. and Rahman H., (1985), Journal of Colloid and Interface Science **103** 106-111

[15] Paterson R. and Smith A., (1988), Journal of Colloid and Interface Science **124** 581-584

[16] Paterson ,R., Cremers,A., Improvement of practical countermeasures against nuclear contamination in the urban environment, Interim Report No.1, for period Aug 1 1987 to Feb 1 1988, Contract Nos. B16-0270.UK(H) & B16-0268-B(GDF)

[17] Cremers,A., Improvement of practical countermeasures against nuclear contamination in the urban environment, Interim Report No.2, for period Feb 1 1988 to Oct 31 1988, Contract No. B16-0268-B(GDF)

[18] Sawhney, B.L., (1970), Potassium and cesium ion selectivity in relation to clay mineral structure, Clays and Clay Minerals, **18**, p.47-52

[19] Wahlberg, J.S. et al., (1964), Exchange adsorption of strontium on clay minerals, U.S. Geol. Surv. Bull. 1140-D

[20] Tamura,T., (1963), Cesium sorption reactions as indicator of clay mineral structures , International Clay Conference Proceedings Stockholm, **1**, p.229-237

[21] Ganguly, A.K., Mukherjee, S.K.,(1951), The cation exchange behavior of heteroionic and homoionic clays of silicate minerals, Journal of Physical and Colloid Chemistry, **55**, p. 1429-1446

[22] Lewis, D.R., (1949), Analytical data on reference clay minerals, Reference, Clay Minerals: Am. Petroleum Inst. Research Proj. 49, p.92-97

[23] Beetem, W.A. et al., (1962), Use of Cesium-137 in the determination of Cation

Exchange Capacity, U.S. Geol. Surv. Bull. 1140-B

[24] Nishita,H. et al., (1956), Fixation and extractability of fission products contaminating various soils and clays, Soil Science, **89**, p.317-326

[25] Nishita,H. et al., (1962), Influence of stable Cs and K on the reactions of Cs137 and K42 in soils and clay minerals, Soil Science, **94**, p.187-197

[26] Tamura,T., Jacobs,D.G., (1960), Structural implications in cesium sorption, Health Physics, **2**, p.391-398

[27] Abdel-Gawad,A.S. et al., (1982), Column studies on the sorption of radioactive isotopes by some natural clay minerals, Isotopenpraxis, **18**, 355-358

[28] Brouwer,E., Baeyens,B., Maes,A., Cremers,A., (1983), Cesium and rubidium ion equilibria in illite clay, Journal of Physical Chemistry, **87**, p.1213-1219

5.7 Acknowledgements

Butterley Brick Limited, Mr.F.Lord, Regional Technical Director, Wellington Street, Ripley, Derby DE5 3DZ

Marley Roof Tile Company Limited, Mr.G.Eastcroft, Manufacturing Manager, Cadder, Bishopbriggs, Glasgow G64 2PY

London Brick Company Limited, Mr.R.Beard, Chief Technical Manager, Stewartby, Bedford MK43 9LZ

Redland Roof Tiles Limited, Mr.Kennedy, Technical Department, H.O. Reigate, Surrey RH2 0SJ

Scottish Brick Corporation Limited, Mr.Abram, Centurion Factory, Balmuildy Road, Glasgow G23

Tarmac Quarry Products, Mr.J.Cook, Technical Director, H.O. Roadstone House, P.O. Box 44, 50 Waterloo Road, Wolverhampton WV1 4RU

Tilcon Limited, Mr.J.Stewart, Area Director, 250 Alexandra Parade, Glasgow G31 3AX

SUMMARY

The ultimate aim of this research was to measure the caesium binding capacity of materials identified in the Urban Survey as being predominant in U.K. urban environments. The research was extended to other building materials obtained from various sites in Europe. The caesium binding capacities were rapidly characterised using a titrimetric methodology developed at the University of Glasgow. Ion exchange characteristics were measured for K^+/Na^+ and

Cs^+/Na^+ and selectivities were calculated for these ions. It was necessary to measure the binding sites as they could provide catchment for fallout caesium which could then migrate to highly active sites.

Ion Selective Electrodes were used to measure Cs^+, K^+, Na^+ and H^+ ion activities in the aqueous phase. The Cs^+ selective electrode was developed in Glasgow and has proved central to this research. The one limitation to its use is the interference caused by K^+, but using a well-developed method of replacing K^+ with Na^+, this interference was removed. The selectivity of this electrode for Cs^+ against Na^+ is very high.

The titrimetric system was automated. Multi-ionic titrations were performed using a computer-controlled system which allowed for additions of varying amounts of electrolytes, stirring times and graphic displays as the titrations progressed. Data on ion sorption, ion release, pH and other vital experimental data were collected, calculated and displayed. Uptake and release of ions from the materials under investigation were calculated by mass balance.
From the data collected, Cs^+ uptake, Cation Exchange Capacities, Cs^+ distribution coefficients, Cs^+/Na^+ selectivities and K^+/Na^+ selectivities were readily obtained. These last were then processed to obtain Cs^+/K^+ selectivity coefficients.

The results for the Cation Exchange Capacities of the clay minerals tested using the new titrimetric methodology were in close agreement to those figures obtained using the conventional method of batch equilibrations. The benefits of this new method were the ease of operation, the speed of obtaining and calculating results and the large quantity of data produced from one titration run.

The Cation Exchange Capacities (CEC) of the construction materials tested were considerably lower than those of the clay minerals. The range was from 0.008mmole/g for a clay roof tile to 0.075mmol/g for road surfacing aggregate.

The CEC's of these dispersions were shown to be proportional to the surface areas of the particle determined by nitrogen sorption, using the BET method. Ion exchange capacities per unit area of BET surface were constant. From BET surface area measurements on the whole tile or brick the Cs^+ binding capacities per square meter of superficial surface of these construction materials in the urban environment were obtained.

Selectivities were generally in the order $Cs^+ > K^+ > Na^+$ with the magnitudes varying according to the nature of the material. The maximum selectivity of Cs^+ over K^+ was 5 for

a concrete tile from Bavaria. It is clear that these relatively abundant "macrosites" have low selectivities for caesium and are not those responsible for the tenacity with which fallout radiocaesium is bound.

As further confirmation it was shown that the caesium bound to these sites can be easily and reversibly exchanged for potassium or sodium (or ammonium) ions. It is however most likely that these macrosites play an important role in the mechanism by which radiocaesium in rainwater is intercepted on these surfaces. In this mechanism, these poorly-selective but abundant ion exchange sites will serve as intermediate binding sites, facilitating the removal of radiocaesium present at hyper-dilute concentration in the fallout rain. The caesium thus sorbed can then find its way (slowly) by surface diffusion to the one percent or less of highly active sites (described in **Chapter 6**) where they become irreversibly bound and remain thereafter. This mechanism would explain the otherwise improbable fact that radiocaesium at extreme dilution is efficiently scavenged by the very small number of active sites which are present on each square meter of exposed surface. If these macrosites were to be blocked or to rendered inactive, then, it might be hypothesized that radiocaesium sorption might be significantly reduced. This concept of a preventative strategy (based on pretreatment with surfactants) is developed further in **Chapter 8**.

Proceedings of ICIM91
Montpellier, France, July 1991

ION EXCHANGE AND SORPTIVE PROPERTIES OF THE ACTIVE LAYERS OF CERAMIC MEMBRANES *

S. Gallagher and R. Paterson (a)

J. Etienne, A. Larbot and L. Cot (b)

(a) Colloid & Membrane Research Group., Chemistry Dept., University of Glasgow, U.K.

(b) Ecole Nationale Supérieure de Chimie de Montpellier, France

ABSTRACT

The ion exchange and sorptive properties of the oxide active layer of ceramic membranes were determined using new automated titration methods employing ion selective electrodes. pH and salt concentration effects were evaluated. Ion exchange properties were determined in the presence of a range of ions to which the ceramic membrane may be routinely exposed. The mechanisms for ion exchange were consistent with those previously determined on non-calcined oxides, with anion exchange a function of the activity of total acid (pA) and cation exchange a function of the activity of total base (pB) [1-6]. These results show that sign of the surface charge and the exchange capacities for each counterion may be altered in a predictive way, by changing the pH and the activity of the sorbing ion. On this basis, conditions of pH and ionic strength and to some degree the ionic composition of the feed may be selected with a view to optimising separation efficiency and minimising membrane fouling.

INTRODUCTION

Surface charge and ion sorption properties are major contributory factors to fouling by polar or ionic substrates, since surface sorption is often the first step in fouling leading to pore blocking within the membrane structure. By altering the surface charge density and changing its polarity, the opportunity exists for minimising fouling and optimising separation processes. Consequently, a fundamental understanding of the surface charge and sorptive properties within the pores of the active layers of ceramic membranes is essential to their efficient use. This is particularly true for reverse osmosis membranes, in which surface charge plays a dominant role in determining the degree of salt rejection through the Donnan potential.

In the manufacture of ceramic membranes, the sol-gel process provides the only generally applicable technique for producing thin ceramic active layers of controlled porosity on a wide range of macroporous substrates [7,8]. The active layer of operational ceramic membranes consists of oxide particles, typically 3-10μm thick in a commercial membrane. Although calcined, these oxides are still ion exchangers with fixed charges on their surfaces. Most oxides are amphoteric and surface and pore charges may be altered and even reversed as the pH of the solution is changed from acidic to alkaline. Ceramic membranes consisting of an oxide active layer on a support of α alumina

* The research presented in this paper was performed as part of an E.C. Twinning (Jumelage) of E.N.S.C.Montpellier, U.S.T.Languedoc and University of Glasgow.

were prepared and calcined by this method. From the gels used to prepare the membrane active layers, calcined oxides in powder form were obtained in gram quantities. These powders therefore present an identical surface to that of the active layer and are of near identical morphology. Aqueous dispersions of these materials were examined titrimetrically. Ceramic oxides examined by this method are listed in table 1.

Table 1 Physical characteristics of oxides of the active layers of ceramic membranes

Oxide	Structure	Specific Area (m^2/g)	Density (g/cm^3)	Avg. Particle Diameter (Å)
ZrO_2	Monoclinic	66	5.6	160
TiO_2	Tetragonal	25	3.9	600
SiO_2	Amorphous	135	2.2	200
γAl_2O_3	Cubic	250	3.2	80

EXPERIMENTAL

A fully automated computer-controlled system has been designed and constructed, which enabled the user to perform a multi-ionic titration with a maximum of six syringes and monitor the solution activity of up to four different ions simultaneously, using ion-selective electrodes (ISEs). Titrations were made over predetermined ranges of pH or pX (by X-ion ISE) using acids, bases or salts as required. At each titration point the equilibrium activities of hydrogen (pH) and those of a variety of ions (chloride, sodium, potassium, calcium) were determined using the relevant ion selective electrodes. From these data, the uptake and/or release of the monitored ions by the exchanger were determined from observed concentration changes in solution and calculated by mass balance. Uptake of ions by the exchanger, expressed as milliequivalents (meq) per gram of exchanger, is taken as positive and release as negative.

RESULTS AND DISCUSSION

The ion exchange properties of the (non-calcined) oxide precursors of ceramic membranes has been studied extensively previously [1-6]. Earlier work on dispersions of microcrystals, particularly of monoclinic zirconia [4] prepared by the method of Clearfield [9], proved to be particularly relevant. From these researches the pH dependent equilibria for exchange processes (with NaCl as the electrolyte) may be represented by equations 1 and 2.

$$M-OH_{pore} + H^+_{aq} + Cl^-_{aq} \rightleftharpoons M-OH^+_{2\,pore} + Cl^-_{pore} \quad (1)$$

$$M-OH_{pore} + OH^-_{aq} + Na^+_{aq} \rightleftharpoons M-O^-_{pore} + Na^+_{pore} + H_2O \quad (2)$$

(By the titration method H^+ uptake cannot be differentiated from OH^- release, or vice-versa. For a specifically adsorbed anion, ligand exchange of hydroxyl ion would be expected, rather than protonation, as in equation 1.)
The magnitude and sign of the surface charge is therefore sensitive to both pH and the activity of the counterion in solution (here, chloride in acid, sodium in alkaline solution). The mechanisms of equations 1 and 2 were validated by the observations that anion capacity is a single valued function of the negative logarithm of the total acid concentration, pA (= pH + pCl) and cation capacity is a single valued function of the negative logarithm of the total base concentration, pB (= pNa + pOH), below and above the zero point charge (zpc) respectively.
When a dispersion of active layer of calcined monoclinic zirconia was titrated the results were similar to those obtained with Clearfield samples previously [4,6] but capacities were considerably reduced. The dual effects of pH and salt concentration on the exchange capacity, are shown in figure 1 with zpc between pH 7 and 8, as before. In this case the titrating base was KOH (with salt additions of KCl), but similar results were obtained on titration

with NaOH (and NaCl). Figures 2 and 3 show that the monofunctional relationships between pA and anionic capacity and between pB and cationic capacity branches respectively, as predicted by the exchange mechanisms (equations 1 and 2) previously established for the oxide precursors of ceramic membranes, apply equally to calcined oxides. The enhanced precision of the automated titration method is readily apparent, with capacities of around 0.1 meq/g being resolved with confidence, an order of magnitude smaller than previously achieved.

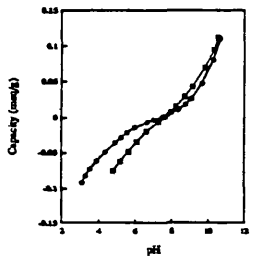
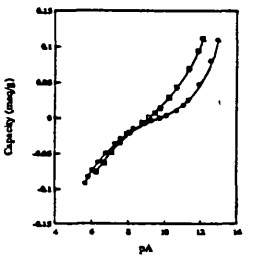
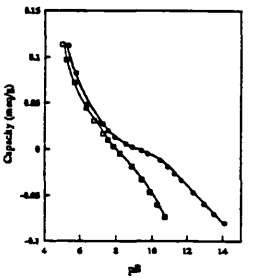

Figures 1,2,3 Exchange properties of calcined monoclinic zirconia. Capacities were obtained for a 1.4g zirconia sample dispersed in 25ml water. The dispersion was titrated with 0.1M HCl and 0.1M KOH (●). At pH 10.65, 2ml 0.5M KCl was added and the dispersion back-titrated with 0.1M HCl (□). In Figure 2 the capacity data from Figure 1 is shown as a function of pA (= pH + pCl) and in Figure 3 as a function of pB (= pK + pOH)

The unique dependence of anion exchange capacity on pA below the zpc and cation exchange capacity on pB above the zpc was observed with all calcined oxides studied in the course of this work. To illustrate further the universality of these relationships, capacity data on silica are presented. Silica was selected here because alumina and titania have ion exchange properties qualititatively similar to zirconia. Figures 4 and 5 show the exchange capacity of calcined silica as functions of pH and pB respectively. Once more it is clear that cation exchange capacity a single valued function of pB. (For silica, there is no corresponding pA relationship, since it has no anion exchange branch in this pH range. Figure 6 demonstrates a direct proof of the stoichiometry of the cation exchange process and absence of anionic exchange, with uptake data obtained from the H^+, Na^+ and Cl^- ion selective electrodes.

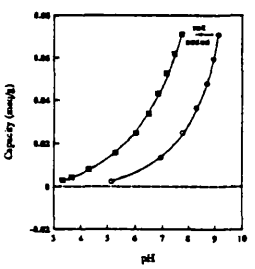
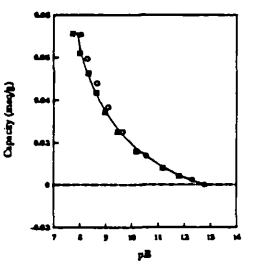
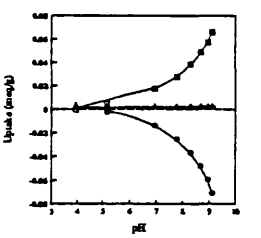

Figures 4,5,6 Exchange properties of calcined silica. Dispersions of silica were titrated with 0.12M NaOH, after an initial addition of 0.1ml 0.1M HCl (○). At pH 9, 1ml 1M NaCl was added and the dispersion back-titrated with 0.1M HCl (■). In Figure 5 the capacity data from Figure 4 is shown as a function of pB. Figure 6 plots uptake data for H^+ (○), Na^+ (□) and Cl^- (△), obtained directly from the respective ion selective electrodes.

The ion exchange capacities of a range of calcined oxides are summarised in table 2. Anion capacities (negative) are shown as functions of pA and cation capacities (positive) as functions of pB. Measured zpc values are given. In all cases, the oxides were titrated with HCl and NaOH, with additions of NaCl. Uptake (or release) of H^+, OH^-, Na^+ and Cl^- were determined by ion selective electrode. With silica dispersions, titrations were terminated below pH 10 to ensure that no significant dissolution of the solid took place. For the same reasons, alumina titrations were kept within the pH range 4-10.

All active layer oxides (with the exception of silica) were amphoteric, being positively charged below the zpc (anion exchange) and negatively charged above the zpc (cation exchange). The exchange capacities of titania are

markedly less than those of zirconia and γ alumina, which is perhaps a consequence of the lower specific surface area of this material (see table 1). Samples of α alumina support material were studied. Their exchange properties were qualitatively similar to active layer alumina but capacities were much smaller throughout the titration range.

Table 2 Anion capacities (with Cl^- as the sorbing ion) and cation capacities (with Na^+ as the sorbing ion) of active layer calcined oxides, as a function of total acid pA (= pH + pCl) and total base pB (= pNa + pOH) respectively

		pA						pB					
Oxide	**zpc**	**5**	**6**	**7**	**8**	**9**	**10**	**5**	**6**	**7**	**8**	**9**	**10**
ZrO_2	7-8		-0.074	-0.044	-0.018	-0.003	0	0.147	0.085	0.042	0.019	0.005	0
γAl_2O_3	8-9			-0.207	-0.104	-0.03	0			0.080	0.043	0	0
SiO_2	<3	0	0	0	0	0	0				0.067	0.035	0.020
TiO_2	6-7	-0.025	-0.020	-0.013	-0.005	0	0	0.053	0.036	0.021	0.010	0	0
		Anion capacity (meq/g)						**Cation capacity (meq/g)**					

Since the ion exchange properties are single valued functions of pA or pB, it is possible to estimate the exchange characteristics of any of these materials at a particular pH and salt concentrations.

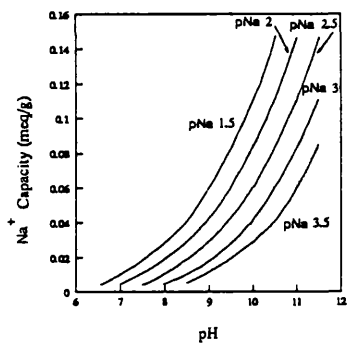

Figure 7 Variation of sodium capacities on zirconia as a function of pH, at fixed sodium ion activities.

The effect of changing pH and salt concentration on the sorption of sodium and chloride ion on calcined zirconia are shown in figures 7 and 8. Analogous plots have been obtained for all oxides studied [10]. The results show clearly that the sorptive properties of these oxides can be radically and predictively altered by adjusting the pH and/or the salt concentration in the solutions to which they are exposed. Distribution coefficients (in ml/g) for the sorbing ions on each oxide were also obtained. In the case of sodium sorption on zirconia, the ratio of adsorbed sodium ion to sodium ion in solution increases when the solution pH is raised, figure 9. Similarly, the ratio of adsorbed chloride ion to chloride ion in solution increases with decreasing pH. These results are characteristic of all amphoteric oxides studied in this research.

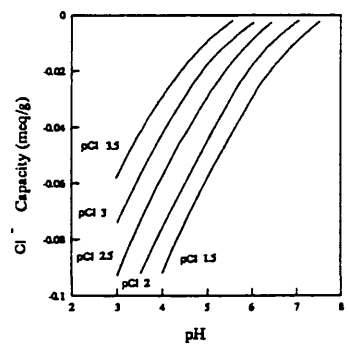

Figure 8 Variation of chloride capacities on zirconia as a function of pH, at fixed chloride ion activities.

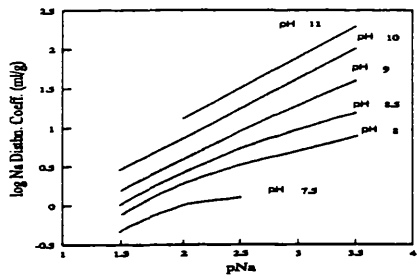

Figure 9 Distribution coefficients (in ml/g) for sodium ion on zirconia as a function of pNa at fixed pH.

Sorption and ion exchange studies on the calcined oxide active layers were extended to include a wider range of ions to which the membranes may be routinely exposed. The effect of the choice of cation on the exchange characteristics of the oxides were determined by changing the titrating base and the salt added and monitoring the cation uptake using the appropriate ion selective electrode. Titrations were performed with Na^+, K^+ and Ca^{2+} as the sorbing cations. In each case, cation capacities were single valued functions of pB (in the case of calcium, pB was defined as 1/2 pCa + pOH, to enable direct comparison with NaOH and KOH titration). At equivalent pH, calcium capacities were much larger than for Na^+ and K^+, figure 10. The calcium distribution coefficient (in ml/g) at pH 10 and pCa 4 is 1300, compared with a distribution coefficient of around 250 for sodium at equivalent pH and pNa. Calcium uptake commenced at around pH 6, one pH unit lower than potassium and sodium. Increased selectivity for calcium was observed in parallel titrations of titania and γ alumina dispersions. In contrast, silica did not show particular selectivity for calcium over sodium or potassium.

In an analogous manner to the cation sorption studies, the effect of the nature of the sorbing anion was determined. Sulphate sorption on zirconia was investigated by titration with H_2SO_4 and sulphate salts. The uptake of sulphate was much greater than that of chloride at equivalent pH values. An apparent degree of irreversibility was observed, with sulphate remaining bound to the exchanger above pH 9. Considerable overlap between cation and anion exchange was observed, with the zpc shifted to higher values. Increased sulphate ion concentration resulted in positive shifts in the zpc, to a maximum of pH 10. When titrations were performed in the presence of both calcium and sulphate, the shift in the zpc was slightly less than in the titrations with sodium and sulphate. These observations may be due to chemical adsorption of sulphate, by ligand displacement of hydroxyl groups. This appears to be supported by F.T.I.R. measurements which show lowering of the symmetry of adsorbed sulphate from T_d to C_{3v}, characteristic of sulphate as a monodentate ligand in inorganic complexes. It is clear, therefore, that the presence of sulphate ion has major effects on the sorptive properties of zirconia and may permanently alter its surface properties. It is expected that phosphate ion would create even larger effects, and this is being investigated currently.

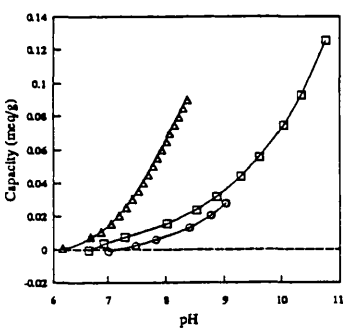

Figure 10 Cation capacities of calcined monoclinic zirconia with Na^+(□), K^+(○) and Ca^{2+}(△) as the sorbing cations.

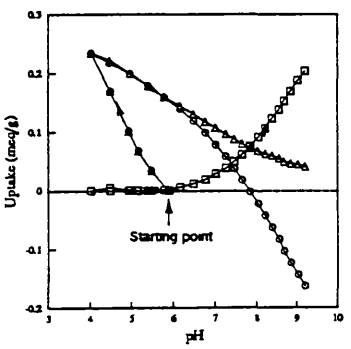

Figure 11 Sulphate sorption on calcined monoclinic zirconia. Dispersion was titrated with H_2SO_4 and $Ca(OH)_2$, with K_{sp} Ca_2SO_4 not reached throughout the titration. Uptakes for H^+ (○), Ca^{2+} (□) and SO_4^{2-} (△) are displayed.

CONCLUSIONS

The ion exchange and sorptive properties of the active layers of ceramic membranes have been characterised. The factors influencing these properties have been isolated and their influence explained in mechanistic terms. These mechanisms for ion exchange were shown to be the same as for those previously determined on non-calcined microcrystalline oxides, but ion exchange capacities are an order of magnitude smaller than observed previously for their non-calcined analogues. These were determined precisely using improved computer controlled titration methods.

The effects of calcium and sulphate ion on the surface charge and sorptive properties are considerably greater than those observed with monovalent sorbing ions.

The main factors affecting the membrane active layer sorptive properties are solution pH, the activity of the sorbing ion and the sorbing ion species. By changing these parameters, it has been demonstrated that it is possible to alter the membrane surface charge density and reverse the polarity in a predictable way. The ion exchange and sorption characteristics of the membrane are correspondingly altered. Irreversible sorption of specific substrates opens up the possibility of permanently modifying the surface characteristics of the active layer.

By manipulation of the operational parameters, it should be possible to optimise conditions for separation processes across UF/RO membranes. Similarly, optimisation of operating conditions and membrane surface modifications raise the possibility of reducing membrane fouling by charged substrates such as proteins, thus improving efficiency and increasing the membrane lifetime.

REFERENCES

[1] R. Paterson, H. Rahman, J. Coll. Int. Sci., 1983, 94 60
[2] R. Paterson, H. Rahman, J. Coll. Int. Sci., 1984, 97 423
[3] R. Paterson, H. Rahman, J. Coll. Int. Sci., 1985, 98 494
[4] R. Paterson, H. Rahman, J. Coll. Int. Sci., 1985, 103 106
[5] R. Paterson, A. Smith, J. Coll. Int. Sci., 1988, 124 581
[6] R. Paterson, 1st Int. Conference on Inorganic Membranes, Montpellier, July 1989, 127
[7] L. Cot, 1st Int. Conference on Inorganic Membranes, Montpellier, July 1989, 17
[8] A. Larbot, A. Julbe, J. Randon, C. Guizard, L. Cot, 1st Int. Conference on Inorganic Membranes, Montpellier, July 1989, 31
[9] A. Clearfield, Inorg. Chem., 1964, 3 146
[10] R. Paterson, S. Gallagher et al., in preparation

ACKNOWLEDGEMENTS

This research was supported by the E.C. as part of a joint project (Jumelage) between E.N.S.C Montpellier, Université des Sciences et Techniques du Languedoc and University of Glasgow, Contract No. SC 1 0178-C(EDB) and by the SERC as part of their programme on separation processes, Contract No. GR/F 64296.

SURFACE CHARGE AND ION SORPTION PROPERTIES INFLUENCING THE FOULING AND FLOW CHARACTERISTICS OF CERAMIC MEMBRANES

STEPHEN GALLAGHER and RUSSELL PATERSON
Colloid & Membrane Research Group,
Chemistry Dept.,
University of Glasgow, U.K.

JOCELYN ETIENNE, ANDRE LARBOT and LOUIS COT
Ecole Nationale Supérieure de Chimie de Montpellier,
France

ABSTRACT

Ion exchange and sorption characteristics of a range of calcined oxides which constitute the active layers of ceramic membranes have been determined using new automated titration methods employing ion selective electrodes. The effects of pH and salt concentration on exchange capacities have been evaluated and explained mechanistically. These were shown to be consistent with the exchange mechanisms of non-calcined oxides determined previously (1-6). The sign of the surface charge and the exchange capacities for each counterion may be altered in a predictive way, by changing the pH and the activity of the sorbing ion. The effects of altering pH and salt concentration on the flow characteristics of whole ceramic membranes have been determined. Studies on the minimisation of fouling by charged substrates on ceramic membranes have been initiated, with promising results.

INTRODUCTION

Surface charge and ion sorption properties are major contributory factors to fouling by polar or ionic substrates, since surface sorption is often the first step in fouling leading to pore blocking within the membrane structure. By altering the surface charge density and changing its polarity, the opportunity exists for minimising fouling and optimising separation processes. A fundamental understanding of the surface charge and sorptive properties within the pores of the active layers

of ceramic membranes is therefore essential to their efficient use.

This research was performed on the calcined oxide active layers of ceramic membranes, as prepared by the sol-gel process (7,8). From the gels used to prepare the membrane active layers, calcined oxides in powder form were obtained. These powders are identical to those of the active layers of the membrane. Aqueous dispersions of these materials were examined titrimetrically.

EXPERIMENTAL

A fully automated computer-controlled system was designed and constructed, enabling the performance of multi-ionic titrations with a maximum of six syringes and the monitoring of the solution activity of up to four different ions simultaneously, using ion-selective electrodes (ISEs) (9). Titrations were made over predetermined ranges of pH or pX (by X-ion ISE) using acids, bases or salts as required. At each titration point the equilibrium activities of hydrogen (pH) and those of a variety of ions (chloride, sodium, potassium, calcium) were determined using the relevant ion selective electrodes. From these data, the uptake and/or release of the monitored ions by the exchanger were determined from observed concentration changes in solution and calculated by mass balance. Uptake of ions by the exchanger, expressed as milliequivalents (meq) per gram of exchanger, is taken as positive and release as negative.

A traditional problem in the determination of pH or other p(ion) in colloidal solution, particularly in dilute solutions with highly charged colloidal particles, is the problem of the suspension effect, due to the potential of the electrical double layer surrounding charged particles (the suspension potential, Ψ). In the region of the double layer, the activity of counterions exceeds those of coions due to the influence of the electrical potential near the surface. From the condition of uniform electrochemical potential, it is shown that

$$p(ion)_{(\infty)} = p(ion)_{(x)} - \frac{z_i F \Psi_{sp}}{2.303RT} \qquad (1)$$

It is not possible to detect a suspension effect in a single electrode titration. However, it has been shown (10) that it is possible to determine and correct for suspension potentials

if all ions which participate in exchange processes are monitored by ISEs. These corrections were employed in the current research.

RESULTS AND DISCUSSION

Previous research (1-6) on the (non-calcined) oxide precursors of ceramic membranes showed that the pH dependent equilibria for exchange processes on monoclinic zirconia (with NaCl as the electrolyte) may be represented by equations 2 and 3.

$$M-OH_{pore}+H^{+}_{aq}+Cl^{-}_{aq} \rightleftharpoons M-OH^{+}_{2\,pore}+Cl^{-}_{pore} \qquad (2)$$

$$M-OH_{pore} + OH^{-}_{aq} + Na^{+}_{aq} \rightleftharpoons M-O^{-}_{pore} + Na^{+}_{pore} + H_2O \qquad (3)$$

The magnitude and sign of the surface charge is sensitive to both pH and the activity of the counterion in solution. The mechanisms of equations 2 and 3 were validated by the observations that anion capacity is a single valued function of pA (= pH + pCl) and cation capacity is a single valued function of pB (= pNa + pOH), below and above the zero point charge (zpc) respectively.

Titration of a dispersion of active layer calcined monoclinic zirconia gave similar results to those obtained previously (4,6), with capacities an order of magnitude lower (11). The dual effects of pH and salt concentration on the exchange capacity were seen, with zpc between pH 7 and 8. Monofunctional relationships between pA and anionic capacity and between pB and cationic capacity were observed. The exchange mechanisms (equations 2 and 3) for the oxide precursors of ceramic membranes therefore apply equally to calcined oxides. Figure 1 demonstrates the stoichiometry of the ion exchange processes. Below the zpc there is stoichiometric uptake of H^+ and Cl^- ions (negative capacity), with no cation uptake. Above the zpc there is cation uptake only (positive capacity), with a stoichiometric uptake of Na^+ and release of H^+.

Similar studies were performed on a range of active layer calcined oxides (γ alumina, silica, titania). All were amphoteric, being positively charged below the zpc and negatively charged above the zpc, with the exception of silica, which showed cation exchange behaviour throughout the pH range studied (Table 1). The mechanisms of equations 2 and 3 applied in all cases, with the observance of the dependency of anion exchange on pA and cation exchange on pB.

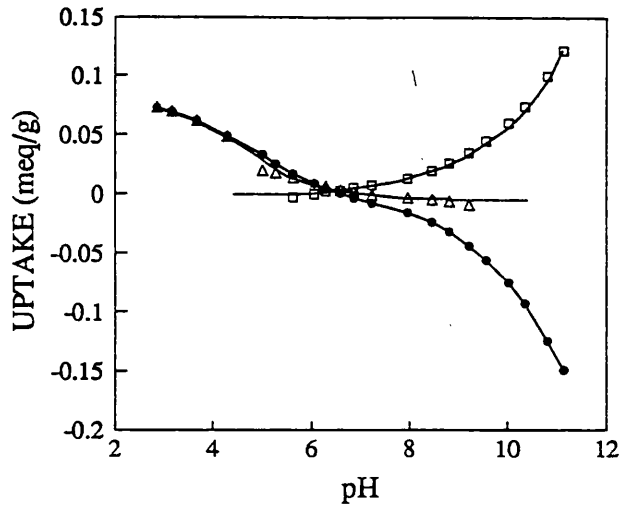

Figure 1. Ion uptakes for H^+ (●), Na^+ (□) and Cl^- (△) on titration of a dispersion of calcined monoclinic zirconia with HCl and NaOH. Data were obtained by mass balance calculations from ISE solution activity measurements, after correction for suspension potential.

Table 1 Anion capacities (with Cl^- as the sorbing ion) and cation capacities (with Na^+ as the sorbing ion) of active layer calcined oxides, as a function of total acid pA (= pH + pCl) and total base pB (= pNa + pOH) respectively.

		pA						pB					
Oxide	zpc	5	6	7	8	9	10	5	6	7	8	9	10
ZrO_2	7-8		-0.074	-0.044	-0.018	-0.003	0	0.147	0.085	0.042	0.019	0.005	0
γAl_2O_3	8-9			-0.207	-0.104	-0.03	0			0.080	0.043	0	0
SiO_2	<3	0	0	0	0	0	0				0.067	0.035	0.020
TiO_2	6-7	-0.025	-0.020	-0.013	-0.005	0	0	0.053	0.036	0.021	0.010	0	0
		Anion capacity (meq/g)						Cation capacity (meq/g)					

Ion sorption studies were extended to include a wider range of ions to which the membranes may be routinely exposed. For indifferent electrolytes (such as KCl), similar results to those obtained with NaCl electrolyte were observed. Specific sorption was observed when the oxides were exposed to multivalent ions (Ca^{2+}, SO_4^{2-}). In these cases considerably higher capacities were observed. Parallel research on the electrophoretic mobility of calcined oxides in the presence of Ca^{2+} and SO_4^{2-} confirmed that specific sorption was occurring.

The exchange characteristics of calcined oxides can therefore be determined precisely, if the pH and salt concentration in the solution phase are known. Figure 2 shows the ion exchange capacity of monoclinic zirconia at varying pH and NaCl concentrations, calculated from pA and pB relationships. From the exchange capacity and the specific surface area, the surface charge may be calculated.

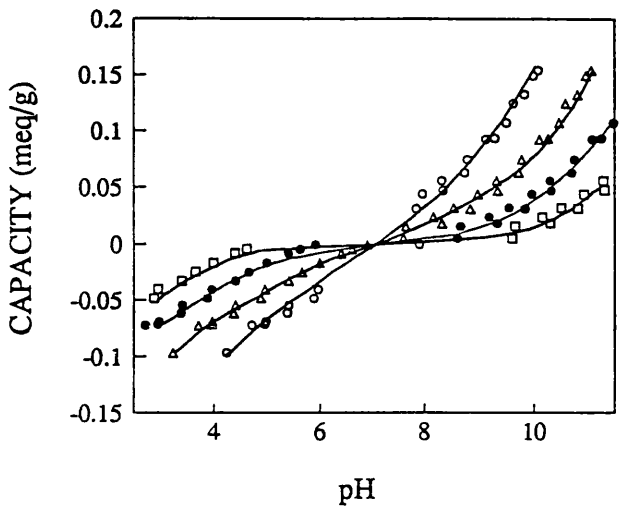

Figure 2. pH dependency of ion exchange capacity of calcined monoclinic zirconia at pNa (and pCl) = 4 (□); = 3 (●); = 2 (△); = 1 (○).

PRACTICAL APPLICATIONS

This research has led to a fundamental understanding of the operational factors which govern ceramic membrane function. The magnitude and sign of the surface charge may be manipulated by small changes in pH or salt concentration. The final stage of this research was concerned with the practical applications of this fundamental knowledge, with a view to optimising operating conditions and minimising membrane fouling.

The effects of varying the pH and salt concentration of feed solution on the filtration characteristics of ceramic membranes were investigated. The results discussed refer to an ultrafiltration membrane with an 4.5μm zirconia active layer on a 1 mm microporous alumina disc. Fluxes were measured at constant pressure of 2 bar and constant temperature of 25°C. Filtrations were performed until constant fluxes were reached

and permeate pH was similar to retentate pH. Figure 3 shows the influence of pH on fluxes across the zirconia membrane, at constant NaCl concentration (0.0051 M). Maximum flux was observed at the zpc of zirconia (pH 7-8), where interactions between the solution and the electrical double layer are at a minimum. When the pH of the feed solution was decreased (surface charge increased), there was a gradual decrease in the flux (relative to the maximum flux), with a flux reduction of almost 10% at pH 3.5. Similarly, by raising the pH, the relative flux decreased with increasing surface charge.

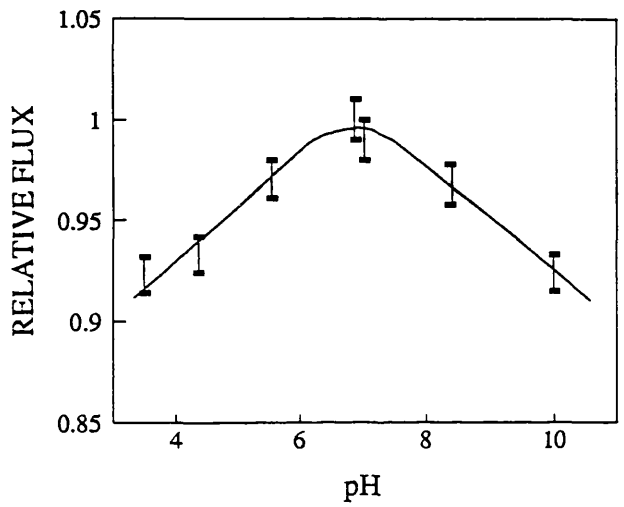

Figure 3. Influence of pH on filtration of 0.005M NaCl solutions, for a 4.5 μm thick zirconia ultrafiltration membrane. Fluxes are relative to the highest observed. Error bars correspond to fluxes at ±1%.

An increase in the ionic strength leads to a collapse of the double layer inside the pore, which reduces the interactions between the solution and the charged walls of the membrane. Higher fluxes were observed at high ionic strength (NaCl 0.1M), at equivalent pH (Figure 4). At high ionic strength, the effect of altering the surface charge on flux across the membrane is considerably less than with solutions of low ionic strength.

Studies on the effects of manipulation of surface charge (by changing pH and salt concentration) on membrane fouling by charged substrates were initiated. Preliminary studies were performed on the sorption of amino acids on active layer calcined oxides. Qualitative results showed that sorption

occurred only when the sign of the charge on the amino acid and on the oxide surface were opposite. An increase in the oxide surface charge caused an increase in the sorption of an oppositely charged amino acid. In this way it is possible to minimise amino acid sorption by selection of suitable pH and salt concentration (based on pA and pB relationships).

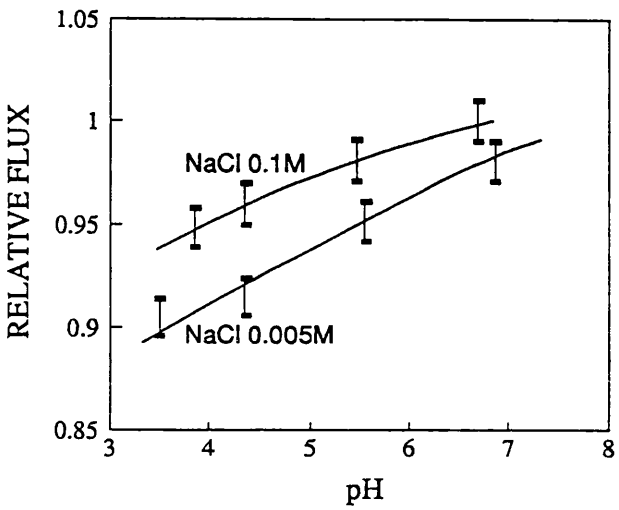

Figure 4. Influence of pH and ionic strength on measured fluxes for NaCl filtration (zirconia membrane).

CONCLUSIONS

The factors influencing the ion exchange and sorptive properties of the oxide active layers of ceramic membranes have been isolated and their influence explained in mechanistic terms. These mechanisms were shown to be the same as for those previously determined on non-calcined microcrystalline oxides, with lower capacities observed.

By changing the parameters influencing the sorption characteristics of oxide active layers (solution pH, salt concentration, nature of sorbing ion), it has been demonstrated that it is possible to alter the membrane surface charge density and reverse the polarity in a predictable way.

Studies on the effect of manipulation of surface charge on the filtration characteristics and on membrane fouling were initiated, with encouraging results. The effects of pH and salt concentration on fluxes and on membrane fouling by charged organic substrates were shown to be as predicted by the relationships determined in this research. By appropriate

selection of the membrane active layer material and manipulation of the operational parameters, it should be possible to optimise conditions for separation processes across UF/RO membranes. Similarly, optimisation of operating conditions and membrane surface modification raise the possibility of reducing membrane fouling by charged substrates such as proteins, thus improving efficiency and increasing the membrane lifetime.

NOMENCLATURE

F	Faraday's constant	C mol $^{-1}$
$pH_{(x)}$	pH at distance x (0 - ∞) from colloid surface	
R	Gas constant	J mol $^{-1}$ K $^{-1}$
T	Temperature	K
z_i	valency of ion i	
Ψ	electrical potential	V
Ψ_{sp}	suspension potential	V

REFERENCES

(1) Paterson R., Rahman H., J. Coll. Int. Sci., 1983, **94** 60
(2) Paterson R., Rahman H., J. Coll. Int. Sci., 1984, **97** 423
(3) Paterson R., Rahman H., J. Coll. Int. Sci., 1985, **98** 494
(4) Paterson R., Rahman H., J. Coll. Int. Sci., 1985, **103** 106
(5) Paterson R., Smith A., J. Coll. Int. Sci., 1988, **124** 581
(6) Paterson R., 1st Int. Conference on Inorganic Membranes, Montpellier, July 1989, 127
(7) Cot L., 1st Int. Conference on Inorganic Membranes, Montpellier, July 1989, 17
(8) Larbot A., Julbe A., Randon J., Guizard C., Cot L., 1st Int. Conference on Inorganic Membranes, Montpellier, July 1989, 31
(9) Gallagher S., Paterson R., Chapter 5 in: Improvement of Practical Countermeasures against Nuclear Contamination in the Urban Environment (ed. A. Cremers, R. Paterson, J. Roed, F.J. Sandalls), Commission of the European Communities, EUR 12555 EN, in press
(10 Etienne J., Gallagher S., Paterson R., in preparation
(11) Gallagher S., Paterson R., Etienne J., Larbot A., Cot L., 2nd Int. Conference on Inorganic Membranes, Montpellier, July 1991, in press